Heavy Quark Symmetry in the Soft Collinear Effective Theory

by

Gautam Mantry

Submitted to the Department of Physics
in partial fulfillment of the requirements for the degree of

Doctor of Philosophy in Physics

at the

MASSACHUSETTS INSTITUTE OF TECHNOLOGY

May 2005 [June 2005]

Author .....
Department of Physics
May 20, 2005

Certified by .....
Iain W. Stewart
Assistant Professor
Thesis Supervisor

Accepted by .....
Thomas Greytak
Chairman, Department Committee on Graduate Students

Heavy Quark Symmetry in the Soft Collinear Effective Theory

by

Gautam Mantry

Submitted to the Department of Physics
on May 20, 2005, in partial fulfillment of the
requirements for the degree of
Doctor of Philosophy in Physics

Abstract

We study strong interaction effects in nonleptonic decays of $\bar{B}$ mesons with energetic particles in the final state. An introduction to Soft Collinear Effective Theory(SCET), the appropriate effective field theory of QCD for such decays, is given. We focus on decays of the type $\bar{B} \to D^{(*)}M$ where M is a light energetic meson of energy E. The SCET formulates the problem as an expansion in powers of Λ_{QCD}/Q where $Q \sim \{m_b, m_c, E\}$. A factorization theorem is proven at leading order that separates the physics of the scales $\Lambda_{QCD} \ll \sqrt{E\Lambda_{QCD}} \ll Q$. In addition, the factorization theorem decouples energetic degrees of freedom associated with the light meson allowing us to derive heavy quark symmetry relations between the $\bar{B} \to DM$ and $\bar{B} \to D^*M$ type amplitudes. A new mechanism for the generation of non-perturbative strong phases is shown within the framework of factorization. Heavy quark symmetry relations are shown to apply for these strong phases as well. Furthermore, the strong phases for certain light mesons in the final state are shown to be universal. The analysis is extended to $\bar{B} \to D^{(*)}M_s$ and $\bar{B} \to D^{**}M$ type decays with isosinglet light mesons and excited charmed mesons in the final state respectively. A host of other phenomenological relations are derived and found to be in good agreement with available data.

Thesis Supervisor: Iain W. Stewart
Title: Assistant Professor

Acknowledgments

I thank C. Arnesen, B. Bistrovic, G. Carosi, M. Chan, E. Coletti, N. Constable, M. Forbes, S. Franco, A. Jain, P. Kazakopoulos, C. Kouvaris, J.D. Kundu, B. Lange, K. Lee, V. Mohta, J. Shelton, I. Sigalov, D. Tong, D. Vegh, and H. Yang for providing a friendly atmosphere to work in. I give special thanks to Profs. Eddie Farhi, Bob Jaffe, and Krishna Rajagopal for their continued support and encouragement during my time at MIT. I am thankful to my collaborators Andrew Blechman, Dan Pirjol, and Iain Stewart. It has been a pleasure working with them over the past two years and has led to the writing of this thesis. I am especially grateful to my advisor Prof. Iain Stewart for being an outstanding teacher and mentor. I am deeply indebted to him for his guidance, support, and encouragement. I thank my thesis committee members Profs. U. Becker, K. Rajagopal, and I. Stewart for their valuable input in the course of writing this thesis. I give special thanks my parents for their unconditional love and support.

Contents

List of Figures

List of Tables

Chapter 1

Introduction

1.1 Low Energy Symmetry and Power Counting

We are fortunate in that nature allows to investigate various phenomena independently of each other. For example we can study planetary motion without understanding atomic structure, atomic physics without knowing that nuclei are made up of protons and neutrons, and nuclear physics without solving quantum gravity. We then come to realize the world by unifying the physics of these different domains into a coherent picture of our universe.

In the modern language, we say that the world is described by a set of "Effective Theories" each describing the world as seen at some resolution. For example, in studying properties of an atom, we are investigating the world at a resolution of $\sim 10^{-10}$meters, roughly the size of the atom. At this resolution, the substructure of the nucleus(typically of size 10^{-15}meters) cannot be seen and effectively behaves as a point particle with some characteristic mass, charge, and spin. The relevant physics regarding the nucleons and their interactions that goes into making up the nucleus, is encoded in such parameters. We can directly measure these parameters from experiment and proceed with atomic physics to make quantitative predictions even if we lack an understanding of the underlying nuclear physics that goes into making the core of the atom. One can continue along this line and study the structure of the nucleus($\sim 10^{-15}$meters) in terms of nucleon and meson degrees of freedom

without a knowledge of the underlying quark-gluon dynamics($\sim 10^{-18}$meters). In this sense, the world can be viewed as a chain of effective theories starting at very large distance scales(low energy) on the order of the size of our universe all the way down to the Planck scale(high energy).

Furthermore, effective theories allow us to describe various phenomena by formulating the problem in the "appropriate" degrees of freedom. For example, even though the Standard Model gives a correct description of the strong, electromagnetic, and weak interactions down to distances of order 10^{-18} meters, it would be silly to study the hydrogen atom in terms of quark and gluon degrees of freedom interacting with the electron. Instead a simple and accurate description is given by an effective theory in which non-relativistic quantum mechanics is applied to an electron moving in the Coulomb field of a point particle whose mass is equal to that of the proton. The relevant physics of quark-gluon dynamics in the proton is absorbed into parameters of the effective theory such as the proton mass and charge. At very high precision, effects from phenomenon such as vacuum polarization, predicted only in a more fundamental theory such as the Standard Model, become important and can be treated perturbatively as corrections to the Hamiltonian of the effective theory.

Thus, even if the underlying theory of our universe is known, most likely it will be expressed in terms of inappropriate degrees of freedom for most problems. The fundamental question then becomes

> "What is the appropriate effective theory with the right degrees of freedom for the problem at hand?"

In the context of Quantum Field Theory(QFT), the problem of formulating the theory in the right degrees of freedom becomes more non-trivial. We define a low energy scale E at which we would like to construct an Effective Field Theory(EFT) entirely in terms of the low energy degrees of freedom. We also define an UltraViolet(UV) scale Λ_{UV} such that $\Lambda_{UV} \gg E$. The physics of the UV scale may or may not be understood. The problem in QFT is that the physics of the UV scale can significantly affect the formulation of a low energy theory. Heisenberg's uncertainty principle allows energy

non-conservation for short periods of time. Thus, even if we start out exclusively with low energy modes at the scale E, UV degrees of freedom show up in the form of large momenta in virtual loops and heavy particles ($m \sim \Lambda_{UV} \gg E$) far of their mass shell. A familiar example of this is muon ($m_\mu \sim 105\text{MeV}$) decay which proceeds through the exchange of a heavy virtual W ($M_W \sim 90\text{GeV} \gg m_\mu$) boson.

The challenge becomes to remove the UV degrees of freedom in the low energy EFT and still get the physics right. The key idea is that at low energies, the UV physics associated with heavy virtual particles and large momenta in loops looks local. All the relevant UV physics can be absorbed into a set of local operators in the EFT. More specifically, UV effects can be absorbed into the low energy theory by adjusting the coefficients of the EFT Lagrangian built entirely in terms of the low energy degrees of freedom. As we shall see, in the EFT, higher dimensional or non-renormalizable operators are suppressed by positive powers of E/Λ_{UV} allowing us to treat their effects perturbatively.

Here in lies the power of EFT. It allows us to express theories entirely in terms of the low energy degrees of freedom in such a manner, that corrections from the effects of UV modes, can be treated perturbatively in powers of (E/Λ_{UV}). The effective theory Lagrangians, will have the general form

$$\mathcal{L}_{EFT} = \mathcal{L}^{(0)} + \mathcal{L}^{(1)} + \mathcal{L}^{(2)} + \cdots \tag{1.1}$$

where the superscript denotes the order in power counting. Furthermore, we will find that the leading terms $\mathcal{L}^{(0)}$ in the power expansion exhibit symmetries that are in general broken by the power suppressed terms. In other words, in the low energy EFT we find additional approximate symmetries that are not manifest in the underlying UV theory and are broken in a controlled manner at higher powers in (E/Λ_{UV}). Thus, even if the underlying UV theory is understood, the low energy EFT can give us additional information by allowing us to exploit low energy approximate symmetries while providing a framework to systematically compute power corrections. The underlying theme of all our discussions is captured in two main ideas

- Low Energy Symmetry.
- Power Counting.

The low energy symmetries of EFTs combined with power counting can be exploited to make quantitative model independent phenomenological predictions.

1.2 An Example: $U(1)_{B-L}$ as a Low Energy Symmetry

To illustrate the above discussion, let's consider the familiar example of the Standard Model(SM) which is an $SU(3)_c \times SU(2)_L \times U(1)_Y$ gauge theory with quarks, leptons, gauge bosons, and a scalar Higgs field[1] as the relevant degrees of freedom at the electroweak scale (see Table 1.1). Any new physics beyond the standard model can be absorbed into higher dimensional operators that are suppressed by powers of the New Physics(NP) scale Λ_{NP} resulting in an effective Lagrangian of the form:

$$\mathcal{L}_{EFT} = \mathcal{L}_{SM} + \frac{1}{\Lambda_{NP}}\mathcal{L}_5 + \ldots \tag{1.2}$$

where $\mathcal{L}_{SM}$ denotes the Standard Model Lagrangian, $\mathcal{L}_5$ is a dimension five operator made out of Standard Model fields, and the ellipses denote possible higher dimensional operators. In the language of EFT, the SM is just the leading term in the expansion in powers of $\frac{1}{\Lambda_{NP}}$. Gauge symmetry and the particle content of the SM(or the relevant degrees of freedom at the electroweak scale) allow only one dimension five operator:

$$\mathcal{L}_5 = c^{ij} L_L^{iT} \epsilon \phi C \phi^T \epsilon L_L^j + h.c., \tag{1.3}$$

where ϵ is the constant $SU(2)_L$ antisymmetric tensor and C is the charge conjugation matrix acting on Dirac spinors in the notation of [98]. $\mathcal{L}_5$ and other higher

[1]The Higgs field which gives mass to the Standard Model fermions through Yukawa interactions has not yet been observed. However, in the spirit of effective field theories, the Higgs mechanism can be thought to parametrize the true nature of the UV physics responsible for fermion mass generation.

				$SU(3)_c$	$SU(2)_L$	$U(1)_Y$	$U(1)_{B-L}$
$Q_L^i =$	$\begin{pmatrix} u_L \\ d_L \end{pmatrix}$	$\begin{pmatrix} c_L \\ s_L \end{pmatrix}$	$\begin{pmatrix} t_L \\ b_L \end{pmatrix}$	3	2	$\frac{1}{6}$	$\frac{1}{3}$
$(u)_R^i =$	$(u)_R$	$(c)_R$	$(t)_R$	3	1	$\frac{2}{3}$	$\frac{1}{3}$
$(d)_R^i =$	$(d)_R$	$(s)_R$	$(b)_R$	3	1	$-\frac{1}{3}$	$\frac{1}{3}$
$L_L^i =$	$\begin{pmatrix} \nu_{eL} \\ e_L \end{pmatrix}$	$\begin{pmatrix} \nu_{\mu L} \\ \mu_L \end{pmatrix}$	$\begin{pmatrix} \nu_{\tau L} \\ \tau_L \end{pmatrix}$	1	2	$-\frac{1}{2}$	-1
$(e)_R^i =$	$(e)_R$	$(\mu)_R$	$(\tau)_R$	1	1	1	1
ϕ				1	2	$\frac{1}{2}$	0

Table 1.1: Summary of the Standard Model particle content and symmetries. The $SU(3)_c \times SU(2)_L \times U(1)_Y$ symmetry is required by gauge invariance and must be respected by any new physics beyond the electroweak scale. The global $U(1)_{B-L}$ symmetry is a low energy leading order accidental symmetry expected to be broken by power corrections in inverse powers of the new physics scale.

dimensional operators can be thought of as arising from integrating out[2] UV degrees of freedom associated with the scale Λ_{NP}. The leading order term in $\mathcal{L}_{EFT}$ or the SM Lagrangian possesses a global $U(1)_{B-L}$ symmetry that is broken by $\mathcal{L}_5$. Here B and L are the Baryon and Lepton numbers respectively. This $U(1)_{B-L}$ global symmetry of the Standard Model is "accidental" resulting from the specific particle content(see Table 1.1) of the SM, and is not required by any fundamental principle such as gauge symmetry which would forbid $\mathcal{L}_5$. In the effective field theory language, $U(1)_{B-L}$ is a low energy leading order symmetry[107] in the expansion in powers of $\lambda \equiv E/\Lambda_{NP} \ll 1$ where E is the low energy (electroweak) scale. We can use this low energy symmetry to predict vanishing rates for $B - L$ violating processes at leading order.

As an example, consider neutron decay in the channel $n \to e^-\pi^+$. Since this

[2]For example, in the see-saw mechanism [67] of neutrino mass generation, Λ_{NP} is of the order of the mass of a heavy right handed Majorana neutrino which when integrated out generates $\frac{1}{\Lambda_{NP}}\mathcal{L}_5$. When the Higgs field acquires a vacuum expectation value, it generates a small Majorana mass for the SM neutrino of order $\frac{v^2}{\Lambda_{NP}}$.

process violates $B - L$, one can predict that at leading order in m_n/Λ_{NP}

$$Br(n \to e^- \pi^+) \;=\; 0. \tag{1.4}$$

In fact, in this case the rate will vanish even at the next order in m_n/Λ_{NP}, since one needs at least a six dimensional operator for the decay to proceed[46]. This is of course a well known result. We were able to obtain this result even though our understanding of the non-perturbative QCD physics associated with the neutron and pion hadrons is rather limited. This was made possible by exploiting low energy symmetry combined with power counting. In this thesis we will consider many other examples where the presence of low energy symmetries is linked to the dynamics of the EFT in more complicated ways but the basic idea is the same.

1.3 $M_W \to \Lambda_{QCD}$: Electroweak Decay to Confinement

Our main interest is in studying electroweak decays of $\bar{B}$ mesons made up of a bottom(b) quark and a light antiquark. In particular, we are interested in controlling strong interaction effects in such decays. The goal [62] of the B-physics community is to test flavor physics and CP violation in the quark sector of the SM as determined by the Cabibbo-Kobayashi-Maskawa(CKM) quark mixing matrix. Any observed deviations from results predicted by the SM would signal the onset of new physics and provide much needed constraints on model building beyond the electroweak scale. Any hope of observing new physics depends on experimental precision and in addition the ability of theory to match this precision.

Attaining theoretical precision is complicated by the confining property of QCD at low energies. Testing the SM at the electroweak scale requires a precise extraction of the parameters of the CKM matrix which determine the strength with which quarks couple to the massive electroweak $W^{\pm}$ gauge bosons. However, QCD confinement does not allow free quarks to exist, trapping them inside hadrons of size $\sim 1/\Lambda_{QCD}$

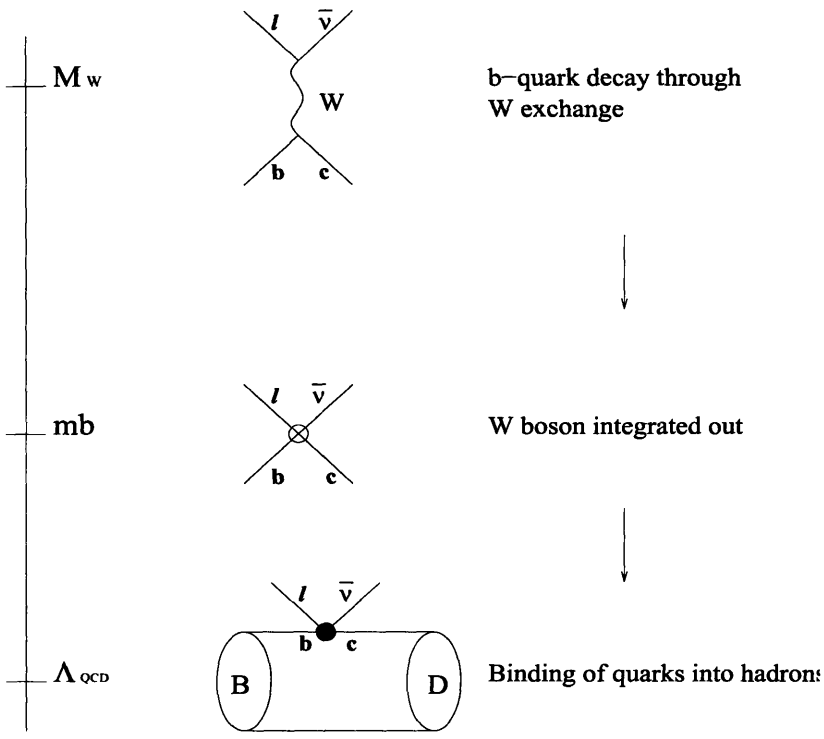

Figure 1-1: The relevant energy scales involved in the semileptonic decay $B \to Dl\bar{\nu}$. Quark level decay is determined by electroweak scale physics. At the characteristic energy scale m_b of the decay process, the electroweak physics of W exchange is described by a local effective four fermion operator. At the Λ_{QCD} scale, the electroweak decay vertex is hidden deep within the hadronic structure by the non-perturbative effects that go into binding quarks into hadrons .

where Λ_{QCD} is the confinement scale. These hadrons then become the observed asymptotic states in particle detectors. In other words, the flavor physics of the electroweak scale is hidden deep inside hadrons by strong interaction effects. The theoretical challenge is to bring these strong interaction effects under control in order to be able to extract electroweak scale physics to the desired precision. At the next generation of accelerators, the challenge will become the extraction of TeV scale physics in hadronic processes. In some scenarios, as suggested by Technicolor [54] models, we might discover new gauge interactions that confine near the TeV scale in which case all the machinery and understanding developed in studying the non-perturbative effects of QCD will become invaluable. Finally, our efforts in studying strong interaction effects will generally improve our ability to deal with QFTs when

they become strongly coupled.

We will tackle the problem of strong interaction effects in electroweak decays using the formalism of EFTs. We can immediately identify two relevant energy scales in this problem: the mass of the $W^{\pm}$ gauge bosons or the electroweak scale $M_W \sim 90GeV$ and the QCD confinement scale $\Lambda_{QCD} \sim 500MeV$. The SM electroweak scale physics that triggers the quark level decay process through W-exchange is theoretically on firm footing. It is the confining property of QCD at the Λ_{QCD} scale, responsible for hadronization, that poses the most difficulty. For the problem of B-decays, there is another relevant energy scale on the order of the b-quark mass $\Lambda_{QCD} \ll m_b \sim 5GeV \ll M_W$. This is the characteristic energy scale at which the quark level decay proceeds. To summarize, there are three widely disparate energy scales involved in B-decays. In keeping with the theme of low energy symmetry and power counting, we will begin at the electroweak scale and flow towards the low energy QCD confinement scale, removing irrelevant degrees of freedom along the way and obtain an effective field theory expanded in powers of ratios of the disparate energy scales. This idea is illustrated in Figure 1-1 for the semileptonic decay $\bar{B} \to Dl\bar{\nu}$ of a $\bar{B}$ meson into a charmed D meson. The color neutrality of the final lepton pair $l\bar{\nu}$ make semileptonic decays the simplest systems in which to study strong interactions effects in B-decays. As a result, semileptonic B-decays have been widely studied and a wealth of theoretical work can be found in the literature [91, 77].

Integrating out the electroweak scale physics to construct an effective at the m_b energy scale is well understood and is just the well known Fermi theory of weak decays. The decay amplitudes in Fermi theory involve non-perturbative matrix elements which cannot be analytically computed, limiting predictive power. In keeping with our theme of low energy symmetry and power counting, we need to proceed below the scale m_b towards Λ_{QCD} in hopes of finding additional symmetries that will allow us to relate the non-perturbative matrix elements of different processes. In other words, we need to find the appropriate EFT in terms of the right degrees of freedom for QCD at low energy.

There are in fact various low energy limits of QCD with the appropriate degrees

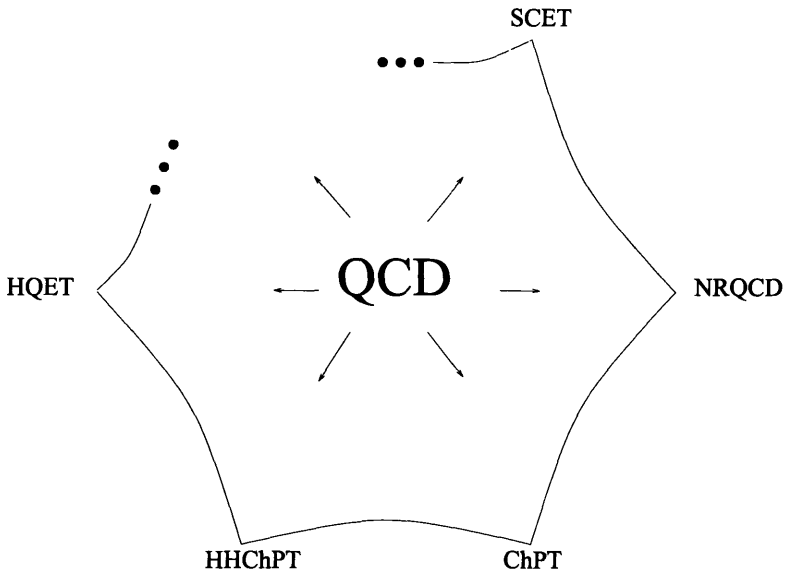

Figure 1-2: Some of the low energy EFTs of QCD. Each EFT is appropriate for a certain set of processes characterized by the relevant energy scales and degrees of freedom in the problem.

of freedom relevant for different processes. Some of these are shown in Fig. 1-2. For example, Chiral Perturbation Theory(ChPT) is an EFT with low momentum light mesons as the relevant degrees of freedom and chiral symmetry as the low energy approximate symmetry. Similarly, NonRelativistic QCD(NRQCD)[88, 87, 99, 37] is for heavy quark-antiquark systems, Heavy Quark Effective Theory(HQET)[92, 60, 59, 51, 91] is for systems with one heavy quark, and Soft Collinear Effective Theory(SCET)[16, 22, 26, 19] is for systems with the presence of energetic particles with momenta close to the light cone(collinear). A combination of HQET and ChPT, Heavy Hadron Chiral Perturbation theory(HHChPT) [91], allows a description of interactions of hadrons with one heavy quark with low momentum light mesons.

1.4 Objectives

Our main focus will be on the application of the Soft Collinear Effective Theory(SCET) which is appropriate for $\bar{B}$ decays into energetic hadrons. This EFT is a rather recent

development and has been applied to a host of processes with remarkable success. Some typical examples are $\bar{B} \to D\pi$ [?, 94], $\bar{B} \to \pi\pi$ [20, 6] , $\bar{B} \to \gamma l\bar{\nu}$, [74, 75] $\bar{B} \to X_u l\bar{n}u$ [76, 74, 75], and $\bar{B} \to X_s\gamma$ [16, 76, 74, 75]. SCET has also been applied to Deep Inelastic Scattering(DIS) [89] processes at large momentum transfer.

We will apply the SCET to nonleptonic B-decays with a charmed meson and a light energetic meson(M) in the final state. Typical examples of such decays are $\bar{B} \to D\pi$, $\bar{B} \to D^*\pi$, $\bar{B} \to D\rho$, $\bar{B} \to D^*\rho$, $\bar{B} \to DK$, $\bar{B} \to D^*K$, $\bar{B} \to DK^*$, $\bar{B} \to D^*K^*$, $\bar{B} \to D_sK^-$, $\bar{B} \to D_sK^{*-}$... [27, 50, 97, 36, 41, 101, 29, 83, 21, 109, 96, 14, 47, 110, 82]. In particular we will relate $\bar{B} \to D\pi$ and $\bar{B} \to D^*\pi$ type decays. Here the pseudoscalar and vector charmed mesons D and D^* respectively are ground state mesons related by Heavy Quark Symmetry(HQS) which will be explained in detail in subsequent chapters. This symmetry was first made manifest through the leading order term $\mathcal{L}^{(0)}_{HQET}$ in HQET and has been successfully used in semileptonic decays to relate the $\bar{B} \to Dl\bar{\nu}$ and $\bar{B} \to D^*l\bar{\nu}$ amplitudes through a single form factor called the Isgur-Wise function [64]. In other words, HQS was used to reduce six form factors, that appear in the $\bar{B} \to D^{(*)}l\bar{\nu}$ amplitudes, down to one!

We are tempted to ask if can use HQS in a similar manner to relate $\bar{B} \to D\pi$ and $\bar{B} \to D^*\pi$ type decays. In this case it is not so simple to use HQS directly. The problem arises from the presence of the energetic pion which introduces a new energy scale on the order of the pion energy $E_\pi \sim 2.3$ GeV. As we will explain in subsequent chapters, the presence of this new energy scale destroys the power counting of HQET. With the power counting no longer valid, the HQS breaking terms in HQET become large invalidating the use of HQS.

The SCET solves this problem through a factorization theorem [?, 94] that decouples the problematic energetic degrees of freedom associated with the pion allowing us to once again use HQS. A typical result that we show from the use of HQS in the SCET at leading order is of the type

$$\frac{Br(\bar{B}^0 \to D^{*0}\pi^0)}{Br(\bar{B}^0 \to D^0\pi^0)} = 1, \tag{1.5}$$

which is in remarkable agreement with the experimental value of 0.97 ± 0.21 [52].

The $\bar{B}^0 \to D^{*0}\pi^0$ type decays are often referred to as color suppressed decays. As we will show, proving factorization theorems for color suppresses modes, which is crucial to predictions of the type in Eq. (1.5), is a rather difficult task since the decay involves interactions with spectator quarks. SCET is used to deal with such spectator interactions through a systematic framework of EFTs. We will show that for color suppressed decays there are in fact four relevant energy scales

$$\Lambda_{QCD} \ll \sqrt{Q\Lambda_{QCD}} \ll Q \ll M_W, \tag{1.6}$$

where $Q \sim \{m_b, m_c, E_M\}$ and m_b, m_c, E_M are the bottom and charm quark masses and the light meson energy respectively. The SCET provides us with the appropriate EFTs at the two lowest energy scales which is where the relevant factorization theorems will be proven. In addition, we will show that the SCET provides a novel mechanism for generating non-perturbative strong phases to take into account final state interactions. A host of other phenomenological predictions also follow from SCET and are discussed in subsequent chapters.

1.5 Outline

In chapter 2 we briefly outline the basic terminology of EFTs and describe the Fermi theory for semileptonic decays. In chapter 3 we give an introduction to HQET and it's application to semileptonic decays and set up the transition to nonleptonic decays. In chapter 4, we give an introduction to SCET in preparation for it's applications to nonleptonic decays in chapter 5. We make concluding remarks in chapter 6.

Chapter 2

Effective Field Theory

2.1 The Basics

In this section we review the basic concepts of EFTs and in the process establish the relevant terminology that we will use throughout the manuscript. There are many excellent reviews on this subject and we refer the reader to the literature [102, 58] for further details.

An EFT is useful in the presence of widely disparate energy scales(see Fig. 2-1). Typically the low energy scale E, is the scale at which the experiment is performed and is determined by the characteristic energy of the process in question. The EFT is constructed exclusively in terms of degrees of freedom that are observable at the low energy scale E. These degrees of freedom all have momenta upto a typical size $p \sim E$. The high energy or UV scale Λ_{UV}, is the scale at which the effects of new degrees of freedom such as heavy particles with mass $m_H \sim \Lambda_{UV}$ become important. The theory at the UV scale that takes into account these new degrees of freedom is often referred to as the "full" theory. The EFT computes amplitudes for processes observed by the experimenter at the low energy scale E as a power expansion in $E/\Lambda_{UV} \ll 1$. We now outline the main steps in constructing an EFT at the low energy scale.

The fundamental question is "if we know the full theory, how can we use a EFT Lagrangian constructed entirely in terms of the relevant low energy degrees of freedom and still get the physics right?". The main idea is to calculate amplitudes in the full

and effective theories to a given order in E/Λ_{UV}, depending on our desired level of accuracy, and adjust the parameters of the EFT to reproduce the full theory result. This procedure is called "matching". For the problems we are interested in this matching will be perturbative in nature allowing us to find the appropriate adjustments of the EFT parameters through the use of Feyman diagrams. We now present the main steps involved in the matching procedure.

1. The matching calculation is done at some scale μ which is the scale we choose to renormalize the full and effective theories. The UV degrees of freedom in the full theory now fall into two categories

   - Heavy particle fields H with mass $m_H \sim \Lambda_{UV}$[1]
   - Hard momentum modes of light fields ϕ_L with virtuality $p^2 > \mu^2$ and with mass $m_L \sim E$.

   We divide the light fields ϕ_L into soft(ϕ_s) and hard modes(ϕ_h)

   $$\phi_L = \phi_s + \phi_h, \tag{2.1}$$

   such that

   $$\partial^2 \phi_s < \mu^2 \phi_s, \quad \partial^2 \phi_h > \mu^2 \phi_h. \tag{2.2}$$

2. The EFT Lagrangian at the scale μ is given by setting all heavy fields H and the hard modes of the light fields ϕ_h in the full theory to zero and adding a complete set of higher dimensional operators made exclusively out of the light soft fields ϕ_s to account for the effects of the UV degrees of freedom

   $$\begin{aligned} \mathcal{L}^{\mu}_{EFT}(\phi_s) &= \mathcal{L}_{full}(\phi_s, \phi_h = 0, H = 0, g_i(\mu)) \\ &+ \frac{1}{m_H} C_5 \left(\frac{m_H}{\mu}, g_i(\mu) \right) O_5(\mu) + \cdots, \end{aligned} \tag{2.3}$$

[1] We assume that there are no other heavy particles with mass between E and Λ_{UV}. If there were, we would construct an intermediate EFT at that scale.

where $O_5(\mu)$ denotes a dimension five operator made out of the light soft fields ϕ_s and the ellipses denote all other possible higher dimensional operators. The possible set of added higher dimensional operators is determined by the allowed symmetries of the full theory. The Wilson coefficients $C_i\left(\frac{m_H}{\mu}, g_i(\mu)\right)$ are to be determined in the matching calculation.

3. Calulate the amplitude A_{full} in the full theory and expand in powers of (E/m_H) upto a given order depending on the desired level of accuracy.

4. Next calculate the same amplitude in the EFT which will have the general form

$$A_{EFT} = \sum_i C_i\left(\frac{m_H}{\mu}, g_i(\mu)\right) \langle O_i(\mu)\rangle. \tag{2.4}$$

5. Compute the Wilson coefficients by requring the difference between the full and effective theory amplitudes to vanish.

6. Since, the EFT reproduces the infrared behavior of the full theory, any infrared divergences that may appear in loop calculations will cancel during matching. On the other hand, the structure of ultraviolet divergences in the full and effective theories will not agree in general. This to be expected since the UV degrees of freedom are different in the full and effective theories. One will find additional UV divergences in the EFT that can only removed by an additional operator renormalization

$$O_i^{(0)} = Z_{ij} O_j. \tag{2.5}$$

7. The operator renormalization in the EFT introduces the renormalization scale μ dependence in the EFT operators $O_i(\mu)$ and their evolution is given by

$$\mu\frac{d}{d\mu}O_i = -\gamma_{ji} O_i, \tag{2.6}$$

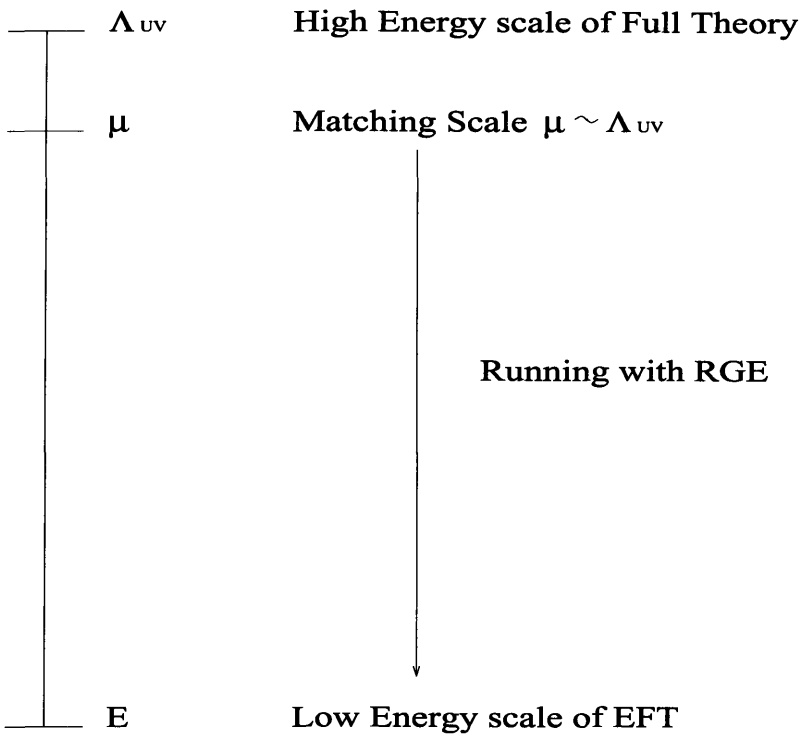

Figure 2-1: Full theory is matched onto EFT at $\mu \sim \Lambda_{UV}$. RGE equations of the EFT are used to lower the matching scale down to the scale of the EFT and summing large logs.

where γ is known as the anomalous dimension matrix

$$\gamma_{ji} = Z^{-1}_{jk}\left(\mu\frac{d}{d\mu}Z_{ki}\right). \tag{2.7}$$

The renormalization scale independence of the amplitudes in Eq. (2.4) determines the evolution of the Wilson coefficients through the Renormalization Group Equation(RGE)

$$\mu\frac{d}{d\mu}C_i(\mu) = -\gamma_{ji}C_j(\mu). \tag{2.8}$$

The disparity in energy scales between effective theories can give rise to large logarithms in the Wilson coefficients when matching onto the EFT at the low energy scale. The standard procedure to deal with the presence of large logarithms is to perform the matching at the scale $\mu \sim \Lambda_{UV}$ so that the logarithms in the Wilson

coefficients are small $\text{Log}(\mu/\Lambda_{UV}) \ll 1$. However, now large logarithms appear in the matrix elements $\langle O_i(\mu)\rangle$ of the form $\text{Log}(\mu/E) \gg 1$. The RGE Eq. (2.6) is used to lower μ to $\mu \sim E$ eliminating the large logs from the matrix element and Eq. (2.8) is used to sum the large logarithms [39] that now appear in the Wilson coefficients.

2.2 Fermi Theory for Semileptonic Decays

In this section, we review Fermi theory for semileptonic decays. This is an EFT at the scale $\sim m_b$ where the decay of the b-quark through W exchange is described by a four fermion effective operator. In the next chapter we will match Fermi theory onto HQET which is an EFT near the Λ_{QCD} scale. We remind the reader that we want to keep matching onto EFTs at lower energy in hopes of finding additional symmetries.

As shown in Figure 1-1, the bottom quark decay into a charmed quark is determined by electroweak scale physics and involves the exchange of a W boson. The tree level amplitude for this quark level decay is given by

$$\begin{aligned} iM &= \left(\frac{ig_W^2 V_{cb}}{2}\right) l_L \gamma^\mu \nu_L \frac{-ig_{\mu\nu}}{q^2 - M_W^2} \bar{c}_L \gamma^\nu b_L \\ &= \left(\frac{4G_F V_{cb}}{\sqrt{2}}\right) \left(1 + q^2/M_W^2 + \cdots\right) l_L \gamma^\mu \nu_L \bar{c}_L \gamma_\mu b_L, \end{aligned} \tag{2.9}$$

where $G_F = \sqrt{2} g_W^2/8M_W^2$ is the Fermi Constant and we have Taylor expanded in powers of $q^2/M_W^2 \sim m_b^2/M_W^2 \ll 1$. To leading order in q^2/M_W^2, we can reproduce this tree level amplitude through the matrix element of an effective four fermion operator

$$H_{eff} = \left(\frac{4G_F V_{cb}}{\sqrt{2}}\right) \bar{l}_L \gamma^\mu \nu_L \bar{c}_L \gamma_\mu b_L. \tag{2.10}$$

Note that H_{eff} is a dimension 6 operator and is suppressed by two powers of the electroweak scale M_W. One can reproduce the amplitude at higher orders in q^2/M_W^2 by adding higher derivative effective operators that will be suppressed by higher powers of the electroweak scale. Thus, at the energy scale $E \sim m_b \ll M_W$ characterizing the bottom quark decay, we can write down an EFT for semileptonic B-decays without

the massive W gauge boson as dynamical degree of freedom, incorporating it's effects into the local operator H_{eff}(see Figure 1-1)

$$\mathcal{L}_{EFT} = \mathcal{L}_{QCD} - \left(\frac{4G_F V_{cb}}{\sqrt{2}}\right) \bar{l}_L \gamma^\mu \nu_L \bar{c}_L \gamma_\mu b_L + \cdots \tag{2.11}$$

where the ellipses denote higher dimensional derivative operators. We arrived at the above result by "matching" the full theory(SM) onto the EFT. In other words, the above Lagrangian contains only the degrees of freedom relevant well below the electroweak scale and can still reproduce the amplitudes of the full theory to a given order in powers of $1/M_W$. The matching above was performed only at tree level. In general, being able to reproduce the amplitudes of the full theory at higher loops can change the coefficients(Wilson coefficients) of the effective operators and can even require the addition of new operators whose Wilson coefficients vanish at tree level. However, for the case of semileptonic decays, QCD loop effects will not affect the coefficient of H_{eff} or induce new operators. This is because QCD does not affect the leptonic bilinear $l_L \gamma^\mu \nu$, but only the quark bilinear $\bar{c}_L \gamma^\mu b_L$ which is a conserved current and has vanishing anomalous dimension.

We note that $\mathcal{L}_{EFT}$ has an expansion in G_F. We can write the amplitude for semileptonic decay to leading order in G_F as

$$\begin{aligned} A^{(*)}_{EFT} &= \left(\frac{4G_F V_{cb}}{\sqrt{2}}\right) \langle D^{(*)} l\bar{\nu} | \bar{l}_L \gamma^\mu \nu_L \bar{c}_L \gamma_\mu b_L | B \rangle \\ &= \left(\frac{4G_F V_{cb}}{\sqrt{2}}\right) \bar{l}_L \gamma^\mu \nu_L \langle D^{(*)} | \bar{c}_L \gamma_\mu b_L | B \rangle, \end{aligned} \tag{2.12}$$

where in the second line, the color neutrality of the lepton pair was used to factorize and evaluate the leptonic matrix element $\langle l\bar{\nu} | \bar{l}_L \gamma^\mu \nu_L | 0 \rangle = \bar{l}_L \gamma^\mu \nu_L$. We have included the possibilty of decay into a pseudoscalar D or vector D^* meson which are related by heavy quark symmetry as we will show in the next chapter.

We now return to our theme of low energy symmetry and power counting, to see if we can simplify the amplitude Eq. (2.12). We see that the leading order term $\mathcal{L}_{QCD}$ in the G_F expansion of $\mathcal{L}_{EFT}$ in Eq. (2.11), possesses the symmetries of parity(P) and

charge conjugation(C) which are broken by the suppressed H_{eff} operator. We can use the leading order parity symmetry to immediately simplify the matrix element in Eq. (2.12). To leading order in G_F, the physics of the $B \to D^{(*)}$ matrix element in Eq. (2.12) is completely determined by $\mathcal{L}_{QCD}$ which respects parity. In particular, QCD doesn't care if the left-handed quarks in the operator insertion $\bar{c}_L \gamma^\mu b_L$ are replaced by right-handed quarks. This implies an equality between the $B \to D$ matrix element and it's parity transformed version. The quark bilinear operator $\bar{c}_L \gamma_\mu b_L$ can be written as a linear combination of a vector operator $V_\mu = \bar{c}\gamma_\mu b$ and an axial vector operator $A_\mu = \bar{c}\gamma_\mu\gamma_5 b$ which have well defined parity transformations. In this basis, the parity invariance of QCD implies

$$\begin{aligned}
\langle D(p')|V_\mu|B(p)\rangle &= (-1)^\mu \langle D(p'_P)|V_\mu|B(p_P)\rangle \\
\langle D(p')|A_\mu|B(p)\rangle &= -(-1)^\mu \langle D(p'_P)|A_\mu|B(p_P)\rangle \\
\langle D^*(p',\epsilon)|V_\mu|B(p)\rangle &= -(-1)^\mu \langle D(p'_P,\epsilon_P)|V_\mu|B(p_P)\rangle \\
\langle D^*(p',\epsilon)|A_\mu|B(p)\rangle &= (-1)^\mu \langle D(p'_P,\epsilon_P)|A_\mu|B(p_P)\rangle
\end{aligned} \tag{2.13}$$

where $(-1)^\mu = 1$ for $\mu = 0$ and $(-1)^\mu = -1$ for $\mu = 1,2,3$ and the subscript P on the momenta denotes the parity transformation. The only four vectors available at our disposal to parametrize the $\bar{B} \to D$ matrix elements are the four momenta p^μ and p'^μ of the B and D mesons respectively. The $\bar{B} \to D^*$ matrix element must be linear in the polarization vector ϵ^* and can also depend on the four momenta p^μ and p'^μ. Given that p^μ, p'^μ, and ϵ^* all tranform like vectors and the property $p' \cdot \epsilon = 0$, the conditions of Eq. (2.13) lead to a general form for the matrix elements

$$\begin{aligned}
\langle D(p')|V_\mu|B(p)\rangle &= f_+(q^2)(p+p')^\mu + f_-(q^2)(p-p')^\mu, \\
\langle D(p')|A_\mu|B(p)\rangle &= 0, \\
\langle D^*(p',\epsilon)|V_\mu|B(p)\rangle &= g(q^2)\epsilon^{\mu\nu\alpha\tau}\epsilon^*_\nu (p+p')_\alpha (p-p')_\tau, \\
\langle D^*(p',\epsilon)|A_\mu|B(p)\rangle &= -\imath f(q^2)\epsilon^{*\mu} - \imath\epsilon^* \cdot p[a_+(q^2)(p+p')^\mu + a_-(q^2)(p-p')^\mu].
\end{aligned} \tag{2.14}$$

Thus, the $\bar{B} \to Dl\bar{\nu}$ amplitude has been reduced to two form factors $f_+(q^2)$ and $f_-(q^2)$ where $q^2 = (p - p')^2$. On the other hand, there was no further simplification for $\bar{B} \to D^* l\bar{\nu}$ which is still parameterized in terms of four form factors. All together we have six form factors describing the $\bar{B} \to Dl\bar{\nu}$ and $\bar{B} \to D^* l\bar{\nu}$ amplitudes. Can we further reduce the number of form factors? As we will discuss in the next chapter, matching onto HQET reduces the total number of form factors down to one!

Chapter 3

Heavy Quark Symmetry

In the last chapter, we saw that integrating out electroweak scale physics and arriving at the Fermi theory of weak decays, the EFT at the m_b energy scale, led to simplifications in the structure of the weak decay amplitudes. We would like to continue along this line and construct an EFT near the Λ_{QCD} scale in hopes of finding additional symmetries which can further simplify the structure of the amplitudes and enhance our predictive power. However, the scale of the experiment, determined by the characteristic energy in the process, is $E \sim m_b$. Proceeding toward Λ_{QCD} means that we will be investigating the process below this experimental energy scale. Thus, the experimental energy scale $\mu \sim m_b$ becomes the UV scale while the low energy EFT scale becomes Λ_{QCD} and is the scale at which we choose to "observe" the process(see Fig. 3-1). In other words, we want to observe the process with a resolution of order $1/\Lambda_{QCD}$ at which the order m_b fluctuations become invisible. However, we cannot simply integrate out the b quark even though $m_b \gg \Lambda_{QCD}$ since we want to study b quark decay. So we must somehow integrate out the hard fluctuations $p^2 \sim m_b^2 \gg \Lambda_{QCD}$ without actually removing the b quark field. This situation is rather different from the more familiar EFTs such as Fermi theory, where the low energy scale is just the scale of the experiment. Proceeding below the scale of the experiment leads to a rather different and much richer structure for the EFT as we will see for HQET and SCET. In this chapter we describe the formalism of HQET and apply it to the case of semileptonic decays. The tools we develop along the way

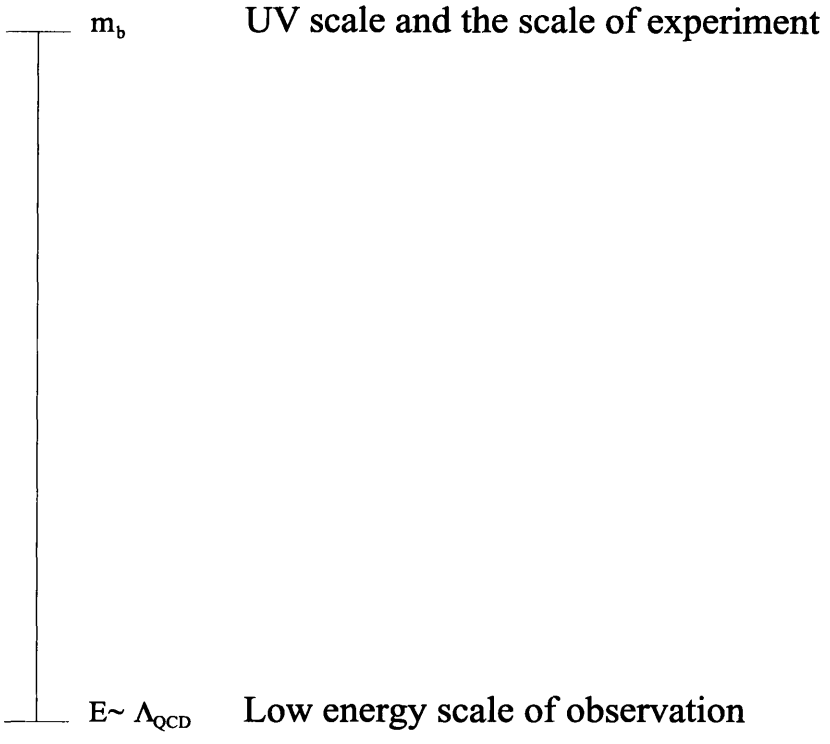

Figure 3-1: For the EFT below the scale m_b which is the characteristic energy of the decay process, the UV scale is m_b and the resolution scale($\sim 1/E$) at which we choose to observe the process determines the low energy scale E.

will be useful for our study of non-leptonic decays for which the appropriate EFT is SCET.

The characteristic energy scale of B-decays is $m_b \gg \Lambda_{QCD}$ and Λ_{QCD} is the scale of nonperturbative QCD dynamics responsible for hadronization. HQET separates these widely disparate energy scales and reformulates the theory through an expansion in powers of Λ_{QCD}/m_b. The leading terms in the expansion make manifest additional symmetries, collectively called Heavy Quark Symmetry(HQS). In the limit $m_b \to \infty$, the HQS violating subleading terms vanish and HQS becomes an exact symmetry. Before going over the formalism of HQET [53, 65, ?], we first give a brief intuitive explanation of HQS.

Consider a $Q\bar{q}$ meson where $Q = b, c$ is a heavy quark $m_Q \gg \Lambda_{QCD}$ and $\bar{q}$ is a light antiquark. Imagine investigating such a system using a "microscope"(the low energy scale of observation) with a maximum resolution of $\sim 1/\Lambda_{QCD}$, the typical size of the

meson. The heavy quark Q, interacts with degrees of freedom that have momenta typically of size Λ_{QCD}, which we collectively call the light degrees of freedom and includes the light antiquark $\bar{q}$, light quark-antiquark pairs, and gluons.

The disparity between the large mass m_Q and the nonperturbative scale Λ_{QCD} leads to interesting consequences. The on-shell momentum of the heavy quark is defined by $p^\mu = m_Q v^\mu$ so that $v^2 = 1$. The momentum of the heavy quark interacting with the light degrees of freedom can now be written as

$$p_Q^\mu = m_Q v^\mu + k^\mu, \tag{3.1}$$

where $k \sim \Lambda_{QCD}$. In other words, the heavy quark will be off-shell by an amount Λ_{QCD} due to it's interaction with the light degrees of freedom. As a result, the typical change in the velocity of the heavy quark is of order

$$\Delta v^\mu \sim \frac{\Lambda_{QCD}}{m_Q} \ll 1. \tag{3.2}$$

The velocity of the heavy quark is almost unchanged and the light degrees of freedom view the heavy quark as a static color source. This picture becomes exact in the heavy quark limit $m_Q \to \infty$. Furthermore, in this limit the flavor of the heavy quark, made manifest in QCD through it's mass, can no longer be distinguished by the light degrees of freedom. This leads to a Heavy Quark Flavor Symmetry(HQFS). N_h heavy quark flavors leads to a global $U(N_h)$ flavor symmetry with $N_h = 2$ in the real world corresponding to the bottom and charm quarks. In reality, this symmetry is only approximate and will receive corrections due to the finite masses of the bottom and charm quarks.

Furthermore, the static heavy quark can only interact with the light degrees of freedom via it's chromoelectric charge. The spin dependent interactions of the light degrees of freedom with the chromomagnetic moment $\mu \sim g/2m_Q$ of the heavy quark vanish in the heavy quark limit where $\mu \to 0$. The light degrees of freedom are oblivious to the spin state of the heavy quark leading to a $SU(2)$ Heavy Quark Spin Symmetry(HQSS).

Putting all this together, the $U(N_h)$ flavor symmetry and the $SU(2)$ spin symmetry can be embedded in to a larger $U(2N_h)$ symmetry. The N_h flavor states with spin up and down transform in the fundamental representation of the $U(2N_h)$ spin-flavor symmetry

$$\begin{pmatrix} Q_1(\uparrow) \\ Q_1(\downarrow) \\ \cdot \\ \cdot \\ Q_{N_h}(\uparrow) \\ Q_{N_h}(\downarrow) \end{pmatrix} \to U(2N_h) \times \begin{pmatrix} Q_1(\uparrow) \\ Q_1(\downarrow) \\ \cdot \\ \cdot \\ Q_{N_h}(\uparrow) \\ Q_{N_h}(\downarrow) \end{pmatrix}. \tag{3.3}$$

The above heavy quark spin-flavor symmetry relates different states in the heavy meson spectrum. This in turn will allow us to relate nonperturbative matrix elements appearing in different $\bar{B}$-decay channels leading to enhanced predictive power.

For future reference, we note that the propagator of the heavy quark with momentum given by Eq. (3.1) simplifies in the heavy quark limit

$$i\frac{\not{p}_Q + m_Q}{p_Q^2 - m_Q^2 + i\epsilon} \to \left(\frac{1+\not{v}}{2}\right)\frac{i}{v\cdot k + i\epsilon}, \tag{3.4}$$

where corrections to this form are of order $k/m_Q \sim \Lambda_{QCD}/m_Q \ll 1$. In the next section we describe the formalism of HQET which makes the above described heavy quark symmetry manifest within a systematic EFT framework.

3.1 Heavy Quark Effective Theory

We would like to continue our journey toward the Λ_{QCD} scale to exploit heavy quark symmetry as described in the previous section. At this point we are faced with a problem. We want to construct an EFT by integrating out hard fluctuations $p^2 \sim m_b \gg \Lambda_{QCD}$ but without actually integrating out the b quark, whose decay we are trying to study in the first place. How can we do this?

First let's consider the light degrees of freedom. The argument for heavy quark symmetry depends crucially on the light degrees of freedom interacting with the heavy quark, having momentum fluctuations on the order of $k^2 \sim \Lambda_{QCD}^2 \ll m_b^2$. Thus, a description of the light degrees of freedom in the EFT must be given exclusively in terms of "soft" fields ϕ_s characterized by momentum fluctuations of order Λ_{QCD}

$$\partial^2 \phi_s \sim \Lambda_{QCD}^2 \phi_s. \tag{3.5}$$

The effects of the hard modes ϕ_h with fluctuations $p^2 \gg \Lambda_{QCD}^2$, will be absorbed into higher dimensional operators made out of the soft fields.

Now let's turn to the heavy quark field. The momentum of the heavy quark fluctuates about it's on-shell value $m_Q v^\mu$ by an amount $k \sim \Lambda_{QCD}$ as shown in Eq. (3.1). So, for the heavy quark field Q we have

$$\partial^2 Q \;=\; (m_Q v + k)^2 Q \sim m_Q^2 Q. \tag{3.6}$$

But this is a problem since we want our EFT to be free of hard fluctuations so that we might expand the theory in powers of Λ_{QCD}/m_Q. We cannot simply divide the heavy quark field into soft and hard modes as in Eq. (2.1) and set the hard modes to zero since keeping only the soft modes ($p^2 \sim \Lambda_{QCD}^2$) would mean that the heavy quark is far offshell due to it's large mass $m_Q \gg \Lambda_{QCD}$. As we saw in the previous section, the heavy quark is offshell only by a small amount $k \sim \Lambda_{QCD}$. What we really need is a soft field that describes $\sim \Lambda_{QCD}$ fluctuations that are centered about the onshell momentum $\sim m_Q$.

In order to do this, we introduce new fields $h_v(x)$ and $B_v(x)$

$$Q(x) \;=\; e^{-im_Q v\cdot x}[h_v(x) + B_v(x)] \tag{3.7}$$

where,

$$h_v(x) = e^{im_Q v\cdot x}\left(\frac{1+\not{v}}{2}\right)Q(x), \quad B_v(x) = e^{im_Q v\cdot x}\left(\frac{1-\not{v}}{2}\right)Q(x) \tag{3.8}$$

We note that in the rest frame of the heavy quark, $\frac{1+\not{v}}{2}$ projects onto particle components of Q. Notice that the two fields h_v and B_v are labeled by a velocity v corresponding to the exponential factor $e^{im_Q v\cdot x}$ in Eq. (3.8), which precisely subtracts the on-shell part of the momentum of a heavy quark with velocity v form the heavy quark field Q

$$\begin{aligned}\partial^\mu h_v(x) &= (p_Q - m_Q v)^\mu h_v(x) \sim \Lambda_{QCD} h_v(x),\\ \partial^\mu B_v(x) &= (p_Q - m_Q v)^\mu B_v(x) \sim \Lambda_{QCD} h_v(x).\end{aligned} \tag{3.9}$$

Thus, as desired, the fields h_v and B_v describe precisely the soft fluctuations centered about the on-shell momentum $m_Q v$ and motivates the label v which characterizes the on-shell momentum. Recall that since the velocity of the heavy quark is essentially constant, the label v will take on different values corresponding to heavy quarks with different velocity vectors. Let's press on and write the QCD Lagrangian for the heavy quark field Q in terms of h_v and B_v. After some computation, we find

$$\begin{aligned}\mathcal{L} &= \bar{Q}\left(i\not{D} - m_Q\right)Q\\ &= \bar{h}_v\left(iv\cdot D\right)h_v - \bar{B}_v\left(iv\cdot D + 2m_Q\right)B_v + \bar{h}_v i\not{D} B_v + \bar{B}_v i\not{D} h_v,\end{aligned} \tag{3.10}$$

where we have used the the following properties of the h_v and B_v fields

$$\not{v} h_v = h_v, \quad \not{v} B_v = -B_v, \tag{3.11}$$

which follow from Eq. (3.8) and $v^2 = 1$. The form of the Lagrangian in Eq. (3.10) makes it clear on how to proceed in constructing the EFT. We note that the first term in the Lagrangian along with the property $\frac{1+\not{v}}{2} h_v = h_v$, implies a propagator for the h_v field given by the right side of Eq. (3.4). Just what we need! The propagator of a heavy quark interacting with soft degrees of freedom as seen at a resolution of $1/\Lambda_{QCD}$. At the same time we have succeeded in removing the hard fluctuations by introducing the field h_v as seen in Eq. (3.9).

What about the B_v field? From it's equation of motion

$$B_v = \frac{1}{iv \cdot D + 2m_Q} i\not{D}_\perp h_v, \tag{3.12}$$

we see that it is suppressed relative to the field h_v by one power of Λ_{QCD}/m_Q since the derivatives acting of h_v are of order Λ_{QCD}. In other words, the antiparticle component of the heavy quark field Q is small in the heavy quark limit. This motivates us to integrate out B_v so that we can obtain a power expansion in Λ_{QCD}/m_Q. Substituting Eq. (3.12)in Eq. (3.10) and expanding in powers of $iv \cdot D/2m_Q$ we get the HQET Lagrangian

$$\mathcal{L}_{HQET} = \bar{h}_v (iv \cdot D) h_v - \bar{h}_v \frac{D_\perp^2}{2m_Q} h_v - a(\mu) g \bar{h}_v \frac{\sigma_{\mu\nu} G^{\mu\nu}}{4m_Q} h_v + \cdots, \tag{3.13}$$

where $a(\mu)$ will be different from 1 beyond tree level [91][1]. The ellipses denote terms with higher powers of $iv \cdot D/2m_Q$ and the perpendicular derivatives are given by

$$D_\perp^\mu = D^\mu - v \cdot D v^\mu. \tag{3.14}$$

The HQET Lagrangian in Eq. (3.13) is the main result of this section. We now have the Lagrangian for an EFT describing the interaction of a heavy quark with soft partons and have succeeded in removing the hard fluctuations associated with the Q quark field.

3.2 Power Counting

We notice several interesting aspects about the HQET Lagrangian in Eq. (3.13). The first term is independent of the heavy quark mass and has a trivial spin(Dirac) structure. In other words, it possesses a $U(N_h)$ Heavy Quark Flavor Symmetry(HQFS) and a $SU(2)$ Heavy Quark Spin Symmetry(HQSS) which can be embedded together into a global $U(2N_h)$ symmetry. The second term in the HQET Lagrangian violates

[1]The coefficient of the second term is fixed to one due to reparameterization invariance which we will discuss in a later section.

the HQFS through it's dependence on the heavy quark mass. The third term violates both HQFS and HQSS through it's dependence on the heavy quark mass and a non-trivial spin structure. Similarly, the remaining terms in the HQET Lagrangian also violate heavy quark symmetry. These ideas are summarized below for the first three terms

$$\begin{array}{lccc} & \bar{h}_v\,(iv\cdot D)\,h_v & -\bar{h}_v\frac{D_\perp^2}{2m_Q}h_v & -a(\mu)g\bar{h}_v\frac{\sigma_{\mu\nu}G^{\mu\nu}}{4m_Q}h_v \\ & \downarrow & \downarrow & \downarrow \\ \text{Symmetries:} & HQFS & HQFS & - \\ & HQSS & - & - \end{array} \tag{3.15}$$

If we want to exploit the heavy quark symmetry of the first term in the HQET Lagrangian, we must show that the remaining terms which violate this symmetry are suppressed. Of course in this case the suppression is made evident by the powers of $1/m_Q$ accompanying the HQS violating terms. It will however be useful to establish a systematic power counting scheme. The language for power counting developed here will directly carry over to SCET where the power counting is more subtle.

We will set the first kinetic term to be of zeroth order in the power counting since we are only interested in a "relative" suppression for the remaining terms. As we will see, this constraint allows us to determine a power counting for the fields themselves which makes power counting of the terms in the Lagrangian quite transparent. The action of the kinetic term in HQET is

$$\begin{array}{cccc} \int d^4x & \left[\bar{h}_v\right. & iv\cdot\partial & \left.h_v\right] \\ \downarrow & \downarrow & \downarrow & \downarrow \\ \Lambda_{QCD}^{-4} & \Lambda_{QCD}^{\alpha} & \Lambda_{QCD} & \Lambda_{QCD}^{\alpha} \end{array} \tag{3.16}$$

where we have also indicated the scaling of the various pieces in powers of Λ_{QCD}. As of now, the scaling of the HQET field is not known and is denoted as some power α of Λ_{QCD} which needs to be determined. Since there are no hard fluctuations in the theory, any derivative acting on the HQET fields will scale like one power of Λ_{QCD}(see

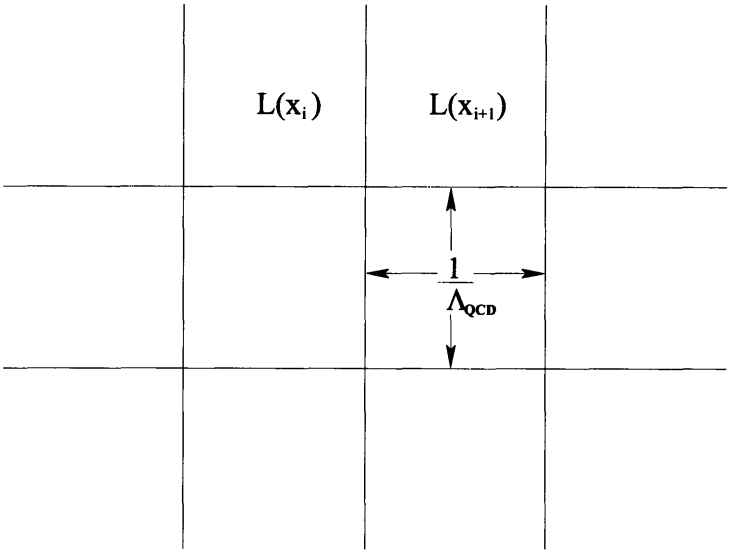

Figure 3-2: For momentum fluctuations of size Λ_{QCD}, a significant variation in the integrand of the HQET Lagrangian will only occur over distances of size $1/\Lambda_{QCD}$. As a result, the HQET action can be computed using the average value $\mathcal{L}_{HQET}(x_i)$ of the integrand over the ith four dimensional box of volume $1/\Lambda_{QCD}^4$ as in Eq. (3.17).

Eq. (3.9)). The scaling of the integration measure can be roughly understood as follows. Since the dynamical momentum fluctuations in theory are of order Λ_{QCD}, a significant variation in the integrand of the action will only occur over distances of order $1/\Lambda_{QCD}$(see Fig. 3.2). As a result the action can be approximated as

$$\int d^4x \mathcal{L}_{HQET}(x) \approx \sum_i \mathcal{L}_{HQET}(x_i)\Delta^4 x_i, \tag{3.17}$$

where $\Delta^4 x_i$ is a four dimensional box of volume Λ_{QCD}^{-4} implying the scaling for the measure indicated in Eq. (3.16). Requiring the overall action of the kinetic term to scale as an order one quantity implies $\alpha = 3/2$ and a scaling for the HQET field $h_v \sim \Lambda_{QCD}^{3/2}$. Similarly, requiring the kinetic term of the soft gluon field to be of zeroth order gives a scaling $A_s \sim \Lambda_{QCD}$. We can now easily compute the scaling of any term in the HQET Lagrangian. We show this for the three terms in Eq. (3.13)

$$\bar{h}_v \, (iv \cdot D) \, h_v \;\; \sim \;\; \Lambda_{QCD}^4$$

Field	Fluctuations	Scaling
h_v	$\partial h_v \sim \Lambda_{QCD}$	$\lambda^{3/2}$
A_s^μ	$\partial A_s \sim \Lambda_{QCD}$	λ

Table 3.1: A summary of the HQET fields, the characteristic size of their fluctuations, and their scaling in powers of $\lambda = \Lambda_{QCD}/Q$.

$$\begin{aligned} \bar{h}_v \frac{D_\perp^2}{2m_Q} h_v &\sim \Lambda_{QCD}^4 \frac{\Lambda_{QCD}}{m_Q} \\ g\bar{h}_v \frac{\sigma_{\mu\nu} G^{\mu\nu}}{4m_Q} h_v &\sim \Lambda_{QCD}^4 \frac{\Lambda_{QCD}}{m_Q} \end{aligned} \tag{3.18}$$

where we have ignored the scaling of the measure which is common to all terms. We now see that the HQS violating terms are indeed suppressed by a factor of $\Lambda_{QCD}/m_Q \ll 1$. It becomes convenient to define a power counting parameter

$$\lambda \equiv \frac{\Lambda_{QCD}}{m_Q}, \tag{3.19}$$

in terms of which we get the scalings $h_v \sim (m_Q\lambda)^{3/2}$ and $A_s \sim m_Q\lambda$. We can set $m_Q \to 1$ so that we can talk about scalings exclusively in terms of λ and the appropriate powers of m_Q can always be inserted in the end using dimensional analysis. We summarize the situation so far in Table (3.1).

We can now write the HQET Lagrangian as an expansion in powers of λ

$$\mathcal{L}_{HQET} = \mathcal{L}^{(0)} + \mathcal{L}^{(1)} + \mathcal{L}^{(2)} + \cdots \tag{3.20}$$

where the superscript denotes the order in λ. From Eqs. (3.18) and (3.19) we see that

$$\begin{aligned} \mathcal{L}^{(0)} &= \bar{h}_v \left(iv \cdot D\right) h_v, \\ \mathcal{L}^{(1)} &= -\bar{h}_v \frac{D_\perp^2}{2m_Q} h_v - a(\mu) g\bar{h}_v \frac{\sigma_{\mu\nu} G^{\mu\nu}}{4m_Q} h_v. \end{aligned} \tag{3.21}$$

Thus, the leading order term $\mathcal{L}^{(0)}$ possess heavy quark symmetry which is broken by the subleading term $\mathcal{L}^{(1)} \sim \lambda$. We can now clearly see heavy quark symmetry

emerging as a low energy symmetry. In the EFT near the low energy scale Λ_{QCD}, the absence of hard fluctuations associated with the UV scale $p^2 \sim m_Q^2 \gg \Lambda_{QCD}^2$, allows us to expand in powers of Λ_{QCD}/m_Q and the leading term in this power expansion exhibits heavy quark symmetry.

3.3 Heavy Meson Spectroscopy

We how explore some of the consequences of heavy quark symmetry. We first look at the implications of HQSS which will be most useful for our purposes and then comment on HQFS.

The total spin $\vec{J}$ of the heavy quark meson is a conserved quantity and is given by the sum of the heavy quark spin $\vec{S}_Q$ and the spin of the light degrees of freedom $\vec{S}_l$

$$\vec{J} = \vec{S}_Q + \vec{S}_l. \tag{3.22}$$

The HQSS of $\mathcal{L}^{(0)}$ implies that at leading order in λ, the heavy quark spin S_Q is conserved. i.e. at leading order, the interaction of the heavy quark with the light degrees of freedom is spin independent. Combined with the conservation of $\vec{J}$, the spin of the light degrees of freedom $\vec{S}_l$ is also a conserved quantity. The spin of the light degrees of freedom in turn is given by the sum of the light antiquark spin $\vec{S}_{\bar{q}}$ and the relative orbital angular momentum $\vec{L}$

$$\vec{S}_l = \vec{L} + \vec{S}_{\bar{q}}. \tag{3.23}$$

Thus, we can characterize the heavy meson states in terms of two good quantum numbers j and s_l for the total heavy meson spin and the spin of the light degrees of freedom respectively. The HQSS of $\mathcal{L}^{(0)}$ implies a degeneracy in the coupling of the heavy quark spin $s_Q = 1/2$ to the spin of the light degrees of freedom s_l. In other words, we can expect to find heavy quark mesons of similar mass to appear in the

heavy quark spin symmetry doublets

$$j_{\pm} = s_l \pm 1/2. \tag{3.24}$$

For example, in ground state charmed mesons which have zero orbital angular momentum $l = 0$, the spin of the light degrees of freedom is just $s_l = 1/2$ corresponding to the light antiquark spin and Eq. (3.24) implies a spin doublet $j = (0, 1)$ corresponding to the charmed mesons (D, D^*). At leading order, HQET predicts equal masses for the D and D^* mesons

$$\begin{aligned} m_D &= m_c + \bar{\Lambda} + O(1/m_c), \\ m_{D^*} &= m_c + \bar{\Lambda} + O(1/m_c) \end{aligned} \tag{3.25}$$

where[2] $\bar{\Lambda} = \langle D|\mathcal{H}^{(0)}|D\rangle = \langle D^*|\mathcal{H}^{(0)}|D^*\rangle$ as a consequence of HQSS and $\mathcal{H}^{(0)}$ is the leading order HQET Hamiltonian obtained from $\mathcal{L}^{(0)}$. $\bar{\Lambda}$ is the leading order effective meson mass in HQET since the charm quark mass m_c has been subtracted from all energies. A difference in the D and D^* masses comes in at the next order in λ from the spin dependent interaction term in $\mathcal{L}^{(1)}$. Experimentally, the $D - D^*$ mass difference is $\sim$ 100MeV which is tiny compared to the typical mass of a charmed meson $\sim$ 2GeV. Heavy quark symmetry works quite well! The lowest lying heavy quark spin doublets for the charmed mesons are listed in Table (3.2) where the mass of each doublet is averaged over all the spin states [77]. Similar heavy quark spin doublets also exist for the bottom mesons [91]

$$\begin{aligned} m_B &= m_b + \bar{\Lambda} + O(1/m_b), \\ m_{B^*} &= m_b + \bar{\Lambda} + O(1/m_b), \end{aligned} \tag{3.26}$$

where once again a $\bar{B} - \bar{B}^*$ mass splitting comes in at the next order in λ through the spin dependent interaction in $\mathcal{L}^{(1)}$. Experimentally, $\bar{B} - \bar{B}^*$ mass difference [91]

[2]The heavy meson states appearing in the matrix elements are actually HQET states which differ from the full QCD states by a normalization and Λ

Charm Doublets	l	s_l	$j_\pm^P$	Mass(GeV)
(D, D^*)	0	$\frac{1}{2}$	$(0^-, 1^-)$	1.971
(D_0^*, D_1^*)	1	$\frac{1}{2}$	$(0^+, 1^+)$	2.40
(D_1, D_2^*)	1	$\frac{3}{2}$	$(1^+, 2^+)$	2.445

Table 3.2: The first three heavy quark spin symmetry doublets for charmed mesons along with their quantum numbers. The last column gives the mass averaged over all the spin states in the doublet [77].

is $\sim$ 46 MeV which is smaller than the $D - D^*$ mass difference. This reflects the fact that heavy quark expansion works better for bottom mesons compared to charm mesons since $\Lambda_{QCD}/m_b < \Lambda_{QCD}/m_c$.

Note that the same $\bar{\Lambda}$ appears in Eqs. (3.25) and (3.26) as a consequence of HQFS. In fact, combining the HQFS and HQSS of $\mathcal{H}^{(0)}$ we have

$$\bar{\Lambda} = \langle D|\mathcal{H}^{(0)}|D\rangle = \langle D^*|\mathcal{H}^{(0)}|D^*\rangle = \langle \bar{B}|\mathcal{H}^{(0)}|\bar{B}\rangle = \langle \bar{B}^*|\mathcal{H}^{(0)}|\bar{B}^*\rangle, \tag{3.27}$$

resulting in the leading order mass relations

$$\begin{aligned} m_D = m_{D^*} \qquad & m_B = m_{B^*}, \\ m_B - m_D = m_B - m_{D^*} \quad = \quad & m_{B^*} - m_D = m_{B^*} - m_{D^*}. \end{aligned} \tag{3.28}$$

We refer the interested reader to [92] for further details on this type of heavy meson spectroscopy.

3.4 Isgur-Wise Functions

We have just witnessed the power of low energy symmetry and power counting. Simply by observing the HQSS of the leading order term in the HQET Lagrangian and without doing any detailed calculations we were able to make quantitative predictions of mass relations between heavy mesons. So, far the predictions we have explored have to do with the static properties (spectroscopy) of heavy mesons. Can we exploit

heavy quark symmetry for decay rates? Let's come back to the case of semileptonic decays $\bar{B}$-decays. Now that we know that the charmed D and D^* mesons sit in a heavy quark symmetry doublet, can we relate the $\bar{B} \to Dl\bar{\nu}$ and $\bar{B} \to D^* l\bar{\nu}$ amplitudes?

Before addressing this question, it will be useful to introduce a formalism in which the heavy quark spin symmetry doublet (D, D^*) can be treated as a single object that transforms linearly under heavy quark symmetry. We treat this subject briefly with just enough detail to establish the necessary language and allow us to proceed with our investigation of semileptonic decays. A more complete treatment can be found in [91].

The ground state $Q\bar{q}$ mesons can be represented by a bilinear field $H_v^{(Q)}$ that transforms under Lorentz transformations as

$$H_{v'}^{(Q)'}(x') = D(\Lambda) H_v^{(Q)}(x) D(\Lambda)^{-1}, \tag{3.29}$$

where $v' = \Lambda v$ and $x' = \Lambda x$ and $D(\Lambda)$ is the spinor representation matrix of the Lorentz group. The introduction of the field $H_v^{(Q)}$ with the Lorentz transformation property above is motivated by the transformation of the product of spinors $Q\bar{q}$. Since the ground state heavy quark charmed mesons (D, D^*) involve a pseudoscalar and a vector, we would like the field $H_v^{(Q)}$ to be a linear combination of a pseudoscalar field $P_v^{(Q)}(x)$ and a vector field $P_{v\mu}^{*(Q)}$

$$H_v^{(Q)} = \frac{1+\not{v}}{2}[\not{P}_v^{*(Q)} + \imath P_v^{(Q)}\gamma_5], \tag{3.30}$$

where the projector $\frac{1+\not{v}}{2}$ picks out only the large particle component of the heavy quark field Q ignoring corrections from the small antiparticle component B_v in Eq. (3.7). Thus, the meson states destroyed by $H_v^{(Q)}$, which we call the HQET states, will differ from the full QCD states due to subleading corrections to Q coming from substituting Eq. (3.12) in Eq. (3.7). We will always work with these leading order HQET states and include subleading corrections through matrix elements of time ordered products with insertions of subleading operators. The definition of $H_v^{(Q)}$ is consistent with $P_v^{*(Q)}$ transforming as a vector and $P_{v\mu}^{(Q)}$ transforming as a pseudoscalar. The vector

particles have a polarization vector ϵ_μ, with $\epsilon \cdot \epsilon = -1$ and $v \cdot \epsilon = 0$ and are destroyed by $P^{*(Q)}_{v\mu}$ with an amplitude of ϵ_μ.

$H^{(Q)}_v$ transforms in the $(1/2, 1/2)$ representation under $S_Q \otimes S_l$, the spin operators for the heavy quark and light degrees of freedom. In particular, under heavy quark spin transformations

$$H^{(Q)}_v \longrightarrow D(R)_Q H^{(Q)}_v. \tag{3.31}$$

We now have a field that destroys mesons in the ground state heavy quark spin symmetry doublet with a well defined heavy quark spin transformation. The HQET states destroyed by $H^{(Q)}_v$ are labeled by their velocity v and and are related to the QCD states as

$$|H(p)>^{QCD} = \sqrt{m_H}[\ |H(v)> + \mathcal{O}(1/m_Q)\ ], \tag{3.32}$$

where the details of the normalizations, etc. can be found in [91].

Matching onto HQET

We now have enough tools to apply HQET for semileptonic decays. As seen in the last chapter in Eq. (2.14), Fermi theory at the scale $\mu \sim m_b$ gives an effective operator that appears in the hadronic matrix element between the bottom and charmed mesons, of the form $\bar{c}\Gamma b$ where $\Gamma = \gamma_\mu\gamma_5, \gamma_\mu$. The next step is to match this operator onto HQET at the scale $\mu \sim m_b$. At tree level matching and leading order in $1/m_{b,c}$ there is only HQET operator available

$$\bar{c}\,\Gamma\, b \quad \longrightarrow \quad \bar{h}^{(c)}_{v'}\,\Gamma\, h^{(b)}_v. \tag{3.33}$$

We can now use heavy quark symmetry to write $\bar{h}^{(c)}_{v'}\,\Gamma\, h^{(b)}_v$ directly in terms of the meson fields H^b_v and $H^c_{v'}$. This must we done in such way that all quantum numbers and transformation properties are preserved in going to the new operator in terms of the meson field. We use the standard trick and note that $\bar{h}^{(c)}_{v'}\,\Gamma\, h^{(b)}_v$ is invariant under

heavy quark spin transformations if we assign to Γ the transformation rule

$$\Gamma \to D(R)_c \Gamma D(R)_b^{-1}. \tag{3.34}$$

The problem now becomes to write $\bar{h}^{(c)}_{v'} \Gamma h^{(b)}_v$ as some combination the meson fields H^b_v and $H^c_{v'}$ which is invariant under heavy quark spin transformations combined with the rule of Eq. (3.34). From Eq. (3.31) and the requirement that the operator be linear in H^b_v and $H^c_{v'}$ we are led to the combination $\bar{H}^c_{v'} \Gamma H^b_v$. Finally, Lorentz covariance requires this to be a trace

$$\bar{h}^{(c)}_{v'} \, \Gamma \, h^{(b)}_v = Tr X \bar{H}^{(c)}_{v'} \Gamma H^{(b)}_v, \tag{3.35}$$

where X is the most general bispinor that can be constructed using the available variables v, v'

$$X = X_0 + X_1 \not{v} + X_2 \not{v}' + X_3 \not{v} \not{v}', \tag{3.36}$$

where the coefficients are functions of the invariant $w = v \cdot v'$. However, the relations $\not{v} H^{(b)}_v = H^{(b)}_v$ and $\not{v}' H^{(c)}_{v'} = -H^{(c)}_{v'}$ make all the terms above proportional to the first so that we can write

$$\bar{h}^{(c)}_{v'} \, \Gamma \, h^{(b)}_v = -\xi(w) Tr \bar{H}^{(c)}_{v'} \Gamma H^{(b)}_v. \tag{3.37}$$

Evaluating the above trace between the HQET states $|H^{(b)}(v)>$ and $|H^{(c)}(v')>$ gives us the relations

$$\begin{aligned}
\langle D(v')|\bar{h}^{(c)}_{v'} \, \gamma_\mu \, h^{(b)}_v|\bar{B}(v)\rangle &= \xi(w)[v_\mu + v'_\mu], \\
\langle D^*(v')|\bar{h}^{(c)}_{v'} \, \gamma_\mu \gamma_5 \, h^{(b)}_v|\bar{B}(v)\rangle &= -i\xi(w)[(1+w)\epsilon^*_\mu - (\epsilon^* \cdot v) v'_\mu], \\
\langle D^*(v')|\bar{h}^{(c)}_{v'} \, \gamma_\mu \, h^{(b)}_v|\bar{B}(v)\rangle &= \xi(w)[(1+w)\epsilon_{\mu\nu\alpha\beta}\epsilon^*_\nu v'^\alpha v^\beta].
\end{aligned} \tag{3.38}$$

Note that only one form factor $\xi(w)$ relates all the above matrix elements. This is the Isgur-Wise function. We see that the low energy heavy quark symmetry of HQET has allowed us to go from six from factors in Eq. (2.14) down to just one significantly enhancing our predictive power. We point the interested reader to [91] for the phenomenological implications in semileptonic B-decays.

What would happen if we were to replace the lepton pair $l\bar{v}$ in the semileptonic decays with a pion? Could we also relate the amplitudes for $\bar{B} \to D\pi$ and $\bar{B} \to D^*\pi$ by heavy quark symmetry? In this case it becomes much more difficult to make heavy quark symmetry manifest. The problem is that the pion introduces a new hard scale in the problem due to it's large energy $E_\pi \sim m_b$. In particular, the presence of energetic degrees of freedom related to the pion destroy the power counting scheme of HQET. For example, the subleading terms in HQET which usually are of order $\Lambda_{QCD}/m_b \ll 1$ can now scale like $E_\pi/m_b \sim 1$ due to the presence of hard fluctuations introduced by the pion degrees of freedom. We need a new EFT that takes into account this new hard scale and expands in powers of Λ_{QCD}/E_π. The theory which does this is Soft Collinear Effective Theory(SCET) and is the subject of the next chapter.

Chapter 4

Soft Collinear Effective Theory

The Soft Collinear Effective Theory(SCET) is an effective theory describing the interactions of soft particles with energetic collinear particles defined to be close to their light cone. This effective theory is appropriate for the $\bar{B} \to D^{(*)}\pi$ type decays that we are interested in. The $\bar{B}$ and $D^{(*)}$ mesons are treated as soft and the pion is treated as collinear. The Fermi theory Hamiltonian for such decays gives the amplitude

$$\begin{aligned} iA &= \frac{G_F}{\sqrt{2}} V_{cb} V_{ud}^* \{ \; C_1(\mu) \langle D^{(*)}\pi | \, (\bar{c}b)_{V-A} (\bar{d}u)_{V-A} \, | \bar{B} \rangle \\ &+ \; C_2(\mu) \langle D^{(*)}\pi | \, (\bar{c}_i b_j)_{V-A} (\bar{d}_j u_i)_{V-A} \, | \bar{B} \rangle \; \}. \end{aligned} \tag{4.1}$$

The nonperturbative matrix elements that appear in the amplitude, limit our predictive power and as seen in the previous chapter, the presence of the energetic pion even forbids us to use heavy quark symmetry to make a relative prediction for the D and D^* rates. Once again we will proceed below the scale of experiment $\mu \sim m_b$ toward Λ_{QCD}, integrating out hard fluctuations along the way but without actually removing the relevant fields, in hopes of finding new symmetries to enhance our predictive power. The relevant EFT below the $\mu \sim m_b$ scale is the SCET and it will help us do the following:

- In addition to the hard scales m_b and m_c(as for HQET), an additional hard scale E_π appears due to the energy of the pion. The SCET takes this additional hard scale into account and expands the theory in powers of Λ_{QCD}/Q where

$Q \sim \{m_b, m_c, E_\pi\}$.

- The SCET allows us to factorize the nonperturbative matrix elements into a product of soft and collinear matrix elements. This factorization permits us to use the formalism of HQET on the soft matrix elements and relate the D and D^* rates through heavy quark symmetry. A host of other phenomenological predictions also follow from factorization.

- From a theoretical point of view, a clear separation of physics coming from the different scales $Q \gg \sqrt{E\Lambda_{QCD}} \gg \Lambda_{QCD}$ is achieved. Furthermore a systematic framework to sum large logarithms between Q and $\sqrt{E\Lambda_{QCD}}$, although we will not address the latter in this thesis and leave it as possible future work. The relevance of the intermediate scale $\sqrt{E\Lambda_{QCD}}$ will become apparent as we try to construct the SCET near the Λ_{QCD} scale.

4.1 Degrees of Freedom: $\mathrm{SCET_I}$ and $\mathrm{SCET_{II}}$

The presence of light energetic particles makes it convenient to introduce the light cone coordinate system. The basis vectors in this coordinate system are given by

$$\begin{aligned} n^\mu &= (1,0,0,-1), \qquad \bar{n}^\mu = (1,0,0,1), \\ \hat{x}_\perp^{1\mu} &= (0,1,0,0), \qquad \hat{x}_\perp^{2\mu} = (0,0,1,0), \end{aligned} \tag{4.2}$$

with a normalization for the light cone vectors given by $\bar{n} \cdot n = 2$, and $n^2 = \bar{n}^2 = 0$. Any four vector can be decomposed in this basis as

$$p^\mu = \frac{n \cdot p}{2} \bar{n}^\mu + \frac{\bar{n} \cdot p}{2} n^\mu + p_\perp^\mu, \tag{4.3}$$

where the components in the $x_\perp^{i\mu}$ direction are collectively labeled as $p_\perp^\mu$. We will denote momentum vector components using the compact notation

$$(p^+, p^-, p_\perp) \equiv (n \cdot p, \bar{n} \cdot p, p_\perp), \tag{4.4}$$

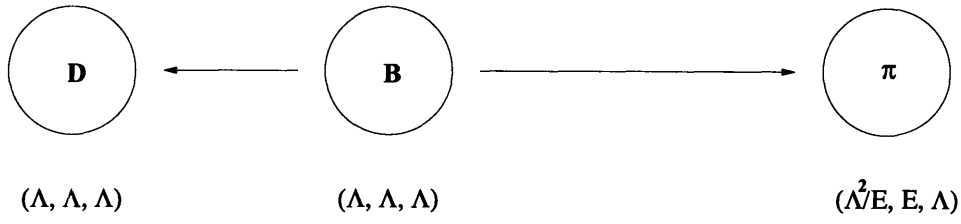

Figure 4-1: The two body $\bar{B} \to D\pi$ decay in the rest frame of the $\bar{B}$ meson. The typical scaling of the momentum components $(p^+, p^-, p_\perp)$ for the partons in the $\bar{B}$, D, and π mesons are shown where E_π is the pion energy. The bottom and charm quarks are described by HQET fields with the hard part of their momenta removed as described in the previous chapter. The momenta that scale as $(\Lambda_{QCD}, \Lambda_{QCD}, \Lambda_{QCD})$ and $(\Lambda^2_{QCD}/E_\pi, E_\pi, \Lambda_{QCD})$ correspond to soft and collinear degrees of freedom respectively. The SCET describes the interaction dynamics of these relevant degrees of freedom in terms of soft and collinear effective theory fields introduced explicitly at the level of the Lagrangian.

so that p^+ and p^- denote components along the $\bar{n}^\mu$ and n^μ directions respectively.

Having established a coordinate system let's look at the $\bar{B} \to D\pi$ decay channel in the rest frame of the $\bar{B}$ meson(see Fig. 4.1). The momentum of the $\bar{B}$ meson is $p_B^\mu = m_B v^\mu$ where $v^\mu = (1, 0, 0, 0)$ in the rest frame. The momentum of the D meson is denoted by $p_D^\mu = m_B v'^\mu$ where v' denotes it's four velocity. Solving the kinematics of this two body problem, we find that the D meson has an energy on the order of it's mass $E_D \sim m_D$ allowing us to treat the light degrees of freedom in the D meson as soft $p_s \sim (\Lambda_{QCD}, \Lambda_{QCD}, \Lambda_{QCD})$ and describe the relevant dynamics using the formalism of HQET. Of course the same holds true for the light degrees of freedom in the $\bar{B}$ meson which is at rest. On the other hand, the momentum of the pion is found to be collinear, close to the light cone, to a very good approximation $p_\pi^\mu = (2.310GeV, 0, 0, -2.306GeV) \approx E_\pi n^\mu$. The partons in the pion will also have a large momentum component along the n^μ direction but in addition will have smaller dynamically generated components in the $\bar{n}^\mu$ and $x_\perp^{i\mu}$ directions. The momentum scaling of the collinear partons are given by $p_c \sim (\Lambda^2_{QCD}/E_\pi, E_\pi, \Lambda_{QCD})$. One can understand this scaling as the result of boosting from the pion from it's rest frame in which the partons have a soft momentum scaling $p_s \sim (\Lambda_{QCD}, \Lambda_{QCD}, \Lambda_{QCD})$ to the rest frame of the $\bar{B}$ meson in which the pion travels close to the light cone. Since the boost

is in the light cone direction orthogonal to the $x_\perp^{i\mu}$ directions, the $p_\perp^\mu$ momenta are unaffected. The p^- component just becomes $p^- \sim E_\pi$ corresponding to the observed momentum of the pion in the $\bar{B}$ rest frame. The scaling of the p^+ component then follows by the requirement that the partons have a virtuality $p_c^2 \sim \Lambda_{QCD}^2$.

In addition to the hard scales m_b and m_c that we encountered in semileptonic decays, there is a new hard scale $E_\pi \sim 2.31 GeV$ in this problem. We will not distinguish between these hard scales and will collectively refer to a hard scale $Q \sim \{m_b, m_c, E_\pi\}$. We introduce the power counting parameter $\eta = \Lambda_{QCD}/Q$ in terms of which we can write the scaling of the soft and collinear momenta as

$$\begin{aligned} p_s &\sim Q(\eta, \eta, \eta), \qquad p_s^2 \sim Q^2\eta^2 \\ p_c &\sim Q(\eta^2, 1, \eta), \qquad p_c^2 \sim Q^2\eta^2. \end{aligned} \tag{4.5}$$

We notice that the interactions of the soft and collinear modes are non-local. The sum of the soft and collinear momenta produce an offshell state of momentum κ^μ

$$p_s^\mu + p_c^\mu = \kappa^\mu \sim Q(\eta, 1, \eta), \qquad \kappa^2 \sim Q^2\eta \gg Q^2\eta^2, \tag{4.6}$$

whose virtuality is much larger than Λ_{QCD}. Even after removing all the hard fluctuations $p^2 \gg \Lambda_{QCD}^2$, the soft and collinear infrared degrees of freedom of the EFT, through their interactions, generate an intermediate hard scale $\mu \sim \kappa \sim \sqrt{Q\Lambda_{QCD}}$. This is a consequence of the inhomogeneous scaling of the collinear momentum components. In other words, even though the collinear modes have a soft virtuality $p^2 \sim \Lambda_{QCD}^2$, they contain a hard momentum component $p^- \sim Q$. In order to construct an EFT in terms of the soft and collinear infrared degrees of freedom, we must integrate out the far offshell modes $\kappa \sim Q(\eta, 1, \eta)$ [22, 63].

An alternative is to construct an intermediate EFT at the scale $\mu \sim \sqrt{Q\Lambda_{QCD}}$ for these offshell modes and then match onto the EFT of soft and collinear modes. We will use the latter method and it's advantages will become clear as we proceed. We refer to this intermediate EFT at $\mu \sim \sqrt{Q\Lambda_{QCD}}$ as SCET$_{\rm I}$ and the EFT at $\mu \sim \Lambda_{QCD}$

as $\mathrm{SCET_{II}}$. We will use a two step matching procedure [100] to go from the Fermi theory of b quark decay to $\mathrm{SCET_{II}}$

$$\text{Fermi Theory + QCD} \longrightarrow \mathrm{SCET_I} \longrightarrow \mathrm{SCET_{II}}\,, \tag{4.7}$$

where we match onto $\mathrm{SCET_I}$ at $\mu \sim Q$, use the renormalization group to run in $\mathrm{SCET_I}$ down to $\mu \sim \sqrt{Q\Lambda_{QCD}}$, and then match onto $\mathrm{SCET_{II}}$.

We introduce a new power counting parameter λ for $\mathrm{SCET_I}$ such that $\lambda = \sqrt{\eta} = \sqrt{\Lambda_{QCD}/Q}$. The relevant modes for $\mathrm{SCET_I}$ are ultrasoft(usoft) and hard-collinear with momenta denoted as p_{us} and p_{hc} respectively

$$\begin{aligned} p_{us} &\sim Q(\lambda^2, \lambda^2, \lambda^2), \qquad p_{us}^2 \sim Q^2\lambda^4 \\ p_{hc} &\sim Q(\lambda^2, 1, \lambda), \qquad p_{hc}^2 \sim Q^2\lambda^2, \end{aligned} \tag{4.8}$$

with all other modes integrated out. What is the physical relevance of these modes? From the relation $\lambda = \sqrt{\eta}$ we see that the usoft modes of $\mathrm{SCET_I}$ have the same scaling as the soft modes of $\mathrm{SCET_{II}}$. In fact these two modes are identical with momentum scaling $(\Lambda_{QCD}, \Lambda_{QCD}, \Lambda_{QCD})$. The different names "usoft" and "soft" correspond to the scaling of these modes in terms of the $\mathrm{SCET_I}$ power counting parameter λ and the $\mathrm{SCET_{II}}$ power counting parameter η respectively. In other words, the $(\Lambda_{QCD}, \Lambda_{QCD}, \Lambda_{QCD})$ modes have a usoft scaling in $\mathrm{SCET_I}$ and a soft scaling in $\mathrm{SCET_{II}}$. On the other hand, the hard-collinear modes of $\mathrm{SCET_I}$ have a virtuality $p_{hc}^2 \sim Q\Lambda_{QCD} \gg \Lambda_{QCD}^2$ and correspond to the far offshell modes of $\mathrm{SCET_{II}}$ of momentum κ^μ produced by the interactions of the soft and collinear modes. In matching $\mathrm{SCET_I}$ onto $\mathrm{SCET_{II}}$, the usoft states match onto the soft states and the hard-collinear states will match onto the collinear states. We summarize the degrees of freedom in $\mathrm{SCET_I}$ and $\mathrm{SCET_{II}}$ in Table 4.1.

EFT	Scale of EFT	Power counting Parameter	Degrees of Freedom	Momenta Scalings
SCET_I	$\mu \sim \sqrt{Q\Lambda_{QCD}}$	$\lambda = \sqrt{\frac{\Lambda_{QCD}}{Q}}$	hard-collinear usoft	$Q(\lambda^2, 1, \lambda)$ $Q(\lambda^2, \lambda^2, \lambda^2)$
SCET_II	$\mu \sim \Lambda_{QCD}$	$\eta = \frac{\Lambda_{QCD}}{Q}$	collinear soft	$Q(\eta^2, 1, \eta)$ $Q(\eta, \eta, \eta)$

Table 4.1: A summary of the relevant degrees of freedom in SCET_I and SCET_II .

4.2 SCET_I : Leading Order

4.2.1 The Lagrangian

We need to write down a Lagrangian for SCET_I in terms of hard-collinear and usoft fields. There are several pieces to the Lagrangian

$$\mathcal{L}_{SCET_I} = \mathcal{L}_{hc} + \mathcal{L}_{us} + \mathcal{L}^h_{us} + \mathcal{L}^g_{hc} + \mathcal{L}^g_{us} + \mathcal{L}_{hc,us}, \tag{4.9}$$

where $\mathcal{L}_{hc}$ has only hard-collinear quarks and their interactions with usoft and hard-collinear gluons, $\mathcal{L}_{us}$ has only light usoft quark fields and their lowest order interactions with usoft gluons, $\mathcal{L}^h_{us}$ has only heavy bottom and charm quarks and their lowest order interaction with usoft gluons, $\mathcal{L}^g_{hc}$ is the kinetic term for hard-collinear gluons, $\mathcal{L}^g_{us}$ is the kinetic term for usoft gluons , and $\mathcal{L}_{hc,us}$ includes the remaining terms involving hard-collinear and usoft modes in general. In keeping with our theme of low energy symmetry and power counting, our ultimate goal will be to expand the SCET_I Lagrangian in powers of λ and identify as many leading order symmetries as possible.

We start with the Lagrangian for the hard-collinear quarks. Before working out the details, let's look at what we should expect. What will be the form of the hard-collinear free quark propagator in SCET_I ? We can find this out by expanding the

QCD propagator for a massless hard-collinear quark in powers of λ

$$\begin{aligned}\frac{\imath \not{p}}{p^2+\imath\epsilon} &= \frac{\imath \not{n}}{2}\frac{\bar{n}\cdot p}{\bar{n}\cdot p n\cdot p + p_\perp^2 + \imath\epsilon} + \cdots \\ &= \frac{\imath \not{n}}{2}\frac{1}{n\cdot p + \frac{p_\perp^2}{\bar{n}\cdot p} + \imath\epsilon sign(\bar{n}\cdot p)} + \cdots \end{aligned} \tag{4.10}$$

where we have used the momentum scaling for the hard-collinear momenta given in Table(4.1) and the ellipses denote higher order terms in λ. Thus, we expect the leading order term of the $\mathrm{SCET_I}$ hard-collinear Lagrangian to reproduce this propagator and will provide a consistency check.

The massless collinear field of QCD Ψ_n which creates a hard-collinear parton with large momentum in the n^μ direction can be decomposed as

$$\Psi_n = \xi_n + \xi_{\bar{n}}, \tag{4.11}$$

where

$$\xi_n \equiv \frac{\not{n}\not{\bar{n}}}{4}\Psi, \qquad \xi_{\bar{n}} \equiv \frac{\not{\bar{n}}\not{n}}{4}\Psi, \tag{4.12}$$

and satisfy the relations

$$\frac{\not{n}\not{\bar{n}}}{4}\xi_n = \xi_n, \qquad \frac{\not{\bar{n}}\not{n}}{4}\xi_{\bar{n}} = \xi_{\bar{n}}. \tag{4.13}$$

We have used the identity

$$1 = \frac{\not{n}\not{\bar{n}}}{4} + \frac{\not{\bar{n}}\not{n}}{4}, \tag{4.14}$$

to achieve the decomposition in Eq. (4.11). The above decomposition of the hard-collinear QCD field is a projection onto the components ξ_n and $\xi_{\bar{n}}$ which create momenta in the n^μ and $\bar{n}^\mu$ directions respectively. This evident from the properties

of ξ_n and $\xi_{\bar{n}}$ fields

$$\not{n}\xi_n = 0, \qquad \not{\bar{n}}\xi_{\bar{n}} = 0, \tag{4.15}$$

which follow from the $n^2 = \bar{n}^2 = 0$ property of the light cone vectors combined with Eq. (4.12). These conditions just correspond to the equations satisfied by massless fermion spinors with momentum in the n^μ and $\bar{n}^\mu$ direction respectively. We point out that the above decomposition does not require the QCD spinor to have hard-collinear momentum and can be done for any type of spinor field. However, as we shall see, this decomposition is most useful for hard-collinear spinor fields. Since Ψ_n creates a parton with large momentum in the n^μ direction we expect the $\xi_{\bar{n}}$ component to be small relative to ξ_n and we will use this to our advantage. This idea will become precise shortly. Let us substitute Eq. (4.11) into the QCD Lagrangian to obtain

$$\begin{aligned} \bar{\Psi}_c \imath\not{D}\Psi_c &= \left(\bar{\xi}_n + \bar{\xi}_{\bar{n}}\right)\left[\imath\frac{\not{n}}{2}\bar{n}\cdot D + \imath\frac{\not{\bar{n}}}{2}n\cdot D + \imath\not{D}_\perp\right](\xi_n + \xi_{\bar{n}}) \\ &= \bar{\xi}_n\imath\frac{\not{\bar{n}}}{2}n\cdot D\xi_n + \bar{\xi}_{\bar{n}}\imath\frac{\not{n}}{2}\bar{n}\cdot D\xi_{\bar{n}} + \bar{\xi}_n\imath\not{D}_\perp\xi_{\bar{n}} + \bar{\xi}_{\bar{n}}\imath\not{D}_\perp\xi_n, \end{aligned} \tag{4.16}$$

where additional possible terms vanish by the property in Eq. (4.15). The gluon field in the covariant derivative is a sum of usoft A_{us} and hard-collinear A_n gluon fields

$$\imath D^\mu = \imath\partial^\mu + A^\mu_{us} + A^\mu_n, \tag{4.17}$$

which are the relevant modes for SCET_I . The presence of two types of gluon fields will lead to a rich structure of gauge symmetry which we will explore in some detail in the next section. But for the moment, let us look at the equation of motion that follows for $\xi_{\bar{n}}$

$$\xi_{\bar{n}} = \frac{1}{\imath\bar{n}\cdot D}\imath\not{D}_\perp\frac{\bar{n}}{2}\xi_n. \tag{4.18}$$

From the scaling of the hard-collinear momenta in Table(4.1), we see that in the above

equation the derivatives scale like $D_\perp \sim Q\eta$ and $\bar{n}\cdot D \sim Q$[1] implying that $\xi_{\bar{n}}$ is in fact suppressed relative to ξ_n by one power of λ as we suspected. So, we can integrate out the $\xi_{\bar{n}}$ field to get an expansion in powers of λ. At tree level we substitute the result of Eq.(4.18) in Eq.(4.16) to obtain the hard-collinear Lagrangian

$$\mathcal{L}_\xi = \bar{\xi}_n \left(in\cdot D + i\not{D}_\perp \frac{1}{i\bar{n}\cdot D} i\not{D}_\perp \right) \frac{\not{\bar{n}}}{2} \xi_n. \tag{4.19}$$

We see that the above Lagrangian does in fact reproduce the hard-collinear propagator of Eq. (4.10). In other words, by integrating out the small $\xi_{\bar{n}}$ field, we have made the expansion of the massless hard-collinear propagator in Eq. (4.10) manifest in the EFT Lagrangian itself. We can further expand the above Lagrangian in powers of λ. We postpone this for the moment and will do so in a later section.

We can assign a power counting to the hard-collinear field by requiring it's kinetic term to be of order λ^0. Recall that we would like to establish a power counting scheme relative to the kinetic terms of the relevant degrees of freedom which will count as zeroth order. We illustrate the power counting for the kinetic term of the hard-collinear quark obtained by setting all gluon fields in the covariant derivatives of Eq. (4.19) to zero

$$\begin{array}{ccccccccccc} \int dx^+ & dx^- & d^2x_\perp & \left[\bar{\xi}_n \right. & in\cdot\partial & + & i\not{\partial}_\perp & \frac{1}{i\bar{n}\cdot\partial} & i\not{\partial}_\perp & \left. \right] \frac{\not{\bar{n}}}{2}\xi_n. \\ \downarrow & \downarrow & \downarrow & \downarrow & \downarrow & & \downarrow & \downarrow & \downarrow & \downarrow & \\ \lambda^0 & \lambda^{-2} & \lambda^{-2} & \lambda^\alpha & \lambda^2 & & \lambda & \lambda^0 & \lambda & \lambda^\alpha & \end{array} \tag{4.20}$$

Here we have used the scaling of hard-collinear momenta in Table(4.1) for the derivatives and the measure and have set $Q \to 1$ since the appropriate powers of Q can always be restored in the end by dimensional analysis. Both the terms above are of the same order and the requirement that they be of zeroth order gives $\alpha = 1$. Thus, the hard-collinear quark fields scale as $\xi_n \sim \lambda$.

Similarly, there will be EFT fields for the usoft light quarks q_{us}. The EFT La-

[1] We will show that the gluon fields A_{us} and A_n appearing in the covariant derivative scale in the same way as the usoft and hard-collinear momenta respectively, implying the scaling $D_\perp \sim Q\eta$ and $\bar{n}\cdot D \sim Q$.

grangian for the usoft quarks has the same form as in QCD

$$\mathcal{L}_{us} = \bar{q}_{us}\,(\imath \not{D}_{us})\,q_{us}, \tag{4.21}$$

but with the covariant derivative D_{us} involving only usoft gluons since a hard-collinear gluon will turn a usoft quark into a hard-collinear quark

$$\imath D^{\mu}_{us} \equiv \imath\partial^{\mu} + gA^{\mu}_{us}. \tag{4.22}$$

We see that the form of the usoft quark propagator is the same as in QCD since all the momentum components of a usoft quark scale in the same way. In the next section we will discuss the absence of a hard-collinear gluon in the covariant derivative in more detail. Once again, by requiring the kinetic term for the usoft quark to be of zeroth order we obtain a scaling relation $q_{us} \sim \lambda^3$.

The heavy usoft bottom and charm quarks are created by the usoft EFT fields $h^{b}_{v,us}$ and $h^{c}_{v',us}$ which are identical to the HQET soft fields $h^{b}_{v}, h^{c}_{v'}$. The Lagrangian will be the same as in HQET

$$\mathcal{L}^{h}_{us} = \bar{h}^{(b)}_{v}\,(\imath v\cdot D_{us})\,h^{(b)}_{v} + \bar{h}^{(c)}_{v'}\,(\imath v'\cdot D_{us})\,h^{(c)}_{v'}, \tag{4.23}$$

and once again no hard-collinear quarks enter in the covariant derivative.

The kinetic term for the usoft gluon takes the usual form as in QCD

$$\mathcal{L}^{g}_{us} = -\frac{1}{2}\,\mathrm{tr}\left\{G^{\mu\nu}_{us}G^{us}_{\mu\nu}\right\}, \tag{4.24}$$

where $G^{\mu\nu} = \imath[D^{\mu}_{us}, D^{\nu}_{us}]/g$ and the kinetic term for the hard-collinear gluon is

$$\mathcal{L}^{(g)}_{hc} = \frac{1}{2g^2}\,\mathrm{tr}\left\{\left[\imath\partial^{\mu} + gA^{\mu}_{us} + gA^{\mu}_{n}\,,\imath\partial^{\mu} + gA^{\mu}_{us} + gA^{\nu}_{n,q'}\right]\right\}^2, \tag{4.25}$$

which is also identical to the form in QCD except that the usoft gluon appears as a "background" field. We will discuss this point in the next section. We have ignored the gauge fixing and ghost field terms [?] since they will not be essential for our

Type	Momenta $p^\mu = (p^+, p^-, p^\perp)$	Fields	Field Scaling
hard-collinear	$p^\mu \sim Q(\lambda^2, 1, \lambda)$	ξ_n $(A_n^+,\ A_n^-,\ A_n^\perp)$	λ $(\lambda^2,1,\lambda)$
usoft	$p^\mu \sim Q(\lambda^2, \lambda^2, \lambda^2)$	q_{us}	λ^3
		$h_{v,us}$	λ^3
		A^μ_{us}	λ^2

Table 4.2: Power counting for the SCET_I quark and gluon fields.

purposes.

All that remains are the terms for $\mathcal{L}_{hc,us}$. As we shall see later on, these terms will be power suppressed relative to the kinetic terms of the hard-collinear and usoft modes. For any physical process only a small number of terms from $\mathcal{L}_{hc,us}$ will contribute at any given order. We postpone the derivation of the relevant terms in $\mathcal{L}_{hc,us}$ until section??.

As we did for the hard-collinear quark field, one can obtain scalings for the usoft light and heavy quarks, usoft gluons, and hard-collinear gluons as $q_{us} \sim \lambda^3, h_{v,us} \sim \lambda^3$, $A^\mu_{us} \sim (\lambda^2, \lambda^2, \lambda^2)$, and $A^\mu_{us} \sim (\lambda^2, 1, \lambda)$. The field content of SCET_I along with their scalings are summarized in Table(4.2).

4.2.2 Ultrasoft and Hard-Collinear Gauge Symmetry

As we briefly mentioned in the previous section, there are two types of gluon fields A_{us} and A_n corresponding to usoft and hard-collinear gluons of the EFT. The difference in the momentum scaling of the hard-collinear and usoft modes leads to a rich structure of gauge symmetry. Corresponding to the usoft and hard-collinear gluons we define usoft and hard-collinear gauge transformations denoted by U_{hc} and U_{us} respectively such that

$$\partial^\mu U_{hc}(x) \sim Q(\lambda^2, 1, \lambda), \qquad \partial^\mu U_{us}(x) \sim Q(\lambda^2, \lambda^2, \lambda^2). \tag{4.26}$$

The above scalings of U_{hc} and U_{us} correspond to the scalings of the hard-collinear and usoft momenta respectively. In the EFT only the subset of usoft and hard-collinear gauge transformations of the full gauge symmetry of QCD are relevant. The usoft and hard-collinear quarks will not transform under "harder" gauge transformations which introduce large phases in the integrand and their rapid oscillations set the variations to zero. This is also true for HQET for which only soft gauge symmetry corresponding to the soft gluons is relevant. However, in HQET since all the degrees of freedom have the same soft scaling in momenta, only one type of gluon(soft) is needed, and the form of the gauge transformations are identical to that in QCD. This is not the case for SCET. For example, a usoft field does not transform under a hard-collinear gauge transformation. Intuitively, this is apparent since a hard-collinear gauge transformation will turn a usoft field into a hard-collinear field. One can see this more explicitly through the effect of large phase oscillations, by looking at the variation of the kinetic term of a usoft quark under a hard-collinear transformation $q_{us}(x) \to U_{hc}(x) q_{us}(x)$

$$\begin{aligned}
\delta \int d^4x\, \bar{q}_{us}(x) \imath \not{\partial} q_{us}(x) &= \int d^4x \bar{q}_{us}(x) \left[U_{hc}^\dagger \imath \not{\partial} U_{hc}(x) \right] q_{us}(x) \\
&= \int d^4x \int \frac{dp^-}{2\pi} e^{-\imath p^- \cdot x^+} \bar{q}_{us}(x) \left[\mathcal{U}_{hc}^\dagger \imath \not{\partial} \mathcal{U}_{hc}(p^-, x^-, x_\perp) \right] q_{us}(x) \\
&= 0, \qquad (4.27)
\end{aligned}$$

where in the second line $\left[\mathcal{U}_{hc}^\dagger \imath \not{\partial} \mathcal{U}_{hc}(p^-, x^-, x_\perp) \right]$ was obtained by Fourier transforming $\left[U_{hc}^\dagger \imath \not{\partial} U_{hc}(x) \right]$ in the x^+ coordinate. The last equality was obtained after performing the integration over the x^+ coordinate and noting that the quantity $\left[\mathcal{U}_{hc}^\dagger \imath \not{\partial} \mathcal{U}_{hc}(p^-, x^-, x_\perp) \right]$ has support only over large $p^- \sim Q \gg Q\lambda^2$. In this region the rapid oscillation of the large phase $e^{-\imath p^- \cdot x^+}$ compared to the usoft fields $q_{us}(x)$ gives a vanishing integral over x^+. So, we see that the kinetic derivative term of the usoft quark does not transform under a hard-collinear gauge transformation. This implies that the covariant derivative for the usoft quark will not have a hard-collinear gluon field. Equivalently, the interaction of a usoft quark with a hard-collinear gluon will vanish $\int d^4x\, g \bar{q}_{us}(x) \not{A}_n(x) q_{us}(x) = 0$ due to rapid oscillations of the hard-collinear

gluon. It was in anticipation of this result that we first wrote Eq. (4.21) for the usoft quark Lagrangian without a hard-collinear gluon. By the same argument as above, the usoft gluon also does not transform under a hard-collinear gauge transformation. We summarize the hard-collinear and usoft gauge transformations below [30]

$$\begin{aligned}
&\text{hard-collinear:} && A_c \to U_c A_c U_c^\dagger + \frac{i}{g} U_c \left[D_{\text{us}}, U_c^\dagger\right], && \xi \to U_c \xi, \\
& && A_{\text{us}} \to A_{\text{us}}, && q \to q, \\
&\text{ultrasoft:} && A_c \to U_{\text{us}} A_c U_{\text{us}}^\dagger, && \xi \to U_{\text{us}} \xi, \\
& && A_{\text{us}} \to U_{\text{us}} A_{\text{us}} U_{\text{us}}^\dagger + \frac{i}{g} U_{\text{us}} \left[\partial, U_{\text{us}}^\dagger\right], && q \to U_{\text{us}} q.
\end{aligned} \tag{4.28}$$

One can check that due to the fact that the usoft gluons do not transform under hard-collinear gauge transformations, hard-collinear gauge invariance of the hard-collinear quark Lagrangian[2] requires the replacement $\frac{i}{g} U_{hc} \partial^\mu U_{hc}^\dagger \to \frac{i}{g} U_{hc} \left[D_{\text{us}}, U_{hc}^\dagger\right]$ in the second term of the usual transformation of the hard-collinear gluon field. This is seen in the first line of Eq. (4.28). In this sense the usoft gluon field plays the role of a "background" field under hard-collinear gauge transformations. Once again it was in anticipation of this result, that we included A_{us} in $\mathcal{L}_{hc}^g$ in Eq. (4.25). Conversely, a usoft gauge transformation is effectively global for the hard-collinear quarks and gluons as seen in the third line of Eq. (4.28).

4.2.3 Label Operators

Altough we have a Lagrangian for the usoft and hard-collinear particles, we have not yet managed to remove all the hard fluctuations $p \gg \sqrt{Q\Lambda_{QCD}}$

$$\partial^\mu \phi_n = Q(\lambda^2, 1, \lambda)\phi_n, \tag{4.29}$$

as can be seen from the $p^- \sim Q$ momentum fluctuations of the hard-collinear field ϕ_n. Here ϕ_n represents either a hard-collinear quark or gluon. In fact, unlike in

[2]This is most clear for the hard-collinear quark Lagrangian $\Psi_n[in\!\!\!/ \cdot \partial_{us} + g A\!\!\!/_n]\Psi_n$ before integrating out the $\xi_{\bar{n}}$ field in order to obtain an expansion in powers of λ and here $\Psi_n = \xi_n + \xi_{\bar{n}}$.

HQET, we will not entirely succeed in removing these hard fluctuations. In HQET, the hard part of the heavy quark momentum remained static since it's interactions with the light degrees of freedom involved momenta exchange of order $\Lambda_{QCD} \ll m_Q v$. In this sense, the hard part of the heavy quark momentum was no longer dynamical in HQET. As a result, we were able to formulate the dynamics of the heavy quark exclusively in terms of fluctuations of order Λ_{QCD} centered about the hard part of it's momentum.

The situation for SCET_I (and also SCET_II) is rather different. In this case the hard part of the hard-collinear momentum is dynamical. The interactions of hard-collinear particles amongst themselves involves the exchange of order Q momenta for the p^- component. But we want to construct an EFT at the scale $\mu \sim \sqrt{Q\Lambda_{QCD}}$. Physically, this means that we are looking at the system using a "microscope" with a maximum resolution of distances or order $1/\sqrt{Q\Lambda_{QCD}}$ and we will not be able to resolve the $p^- \sim Q$ momentum fluctuations. So, we would still like to construct the EFT using fields with the hard fluctuations removed. How can we do this considering that there are dynamical hard $p^- \sim Q$ momenta present in this problem?

We can do this by generalizing the method of separating out the hard momenta in HQET. In HQET there was one heavy quark field h_v corresponding to order Λ_{QCD} fluctuations about the hard on-shell momentum $m_Q v$. Similarly, in SCET_I we can introduce a hard-collinear field $\phi_{n,p}$ with a label p, corresponding to small fluctuations about the hard momentum component $p^- \sim Q$ of the hard-collinear particle. However, in this case there will be one such field for each hard-collinear particle and a hard momentum exchange will be taken into account by a corresponding change in the label momentum. We now make this idea precise.

Before proceeding, we point out that unlike in HQET, from the scaling of the hard-collinear momenta we see that there are actually two low energy scales $Q\lambda, Q\lambda^2 \ll Q$. In this situation, it becomes convenient to absorb the order $Q\lambda$ momentum along with the order Q momentum into the label, and let the $\phi_{n,p}$ field have only order $Q\lambda^2$ fluctuations. As we will see, with all the effective theory fields now having uniform order $Q\lambda^2$ fluctuations the power counting in this "label" formalism will be much

more transparent. Continuing along, we separate the momenta as

$$P^\mu = p^\mu + k^\mu, \tag{4.30}$$

so that $p^{-\mu} \sim Q$ and $p_\perp^\mu \sim Q\lambda$ get absorbed into the label momentum p and the $k \sim Q\lambda^2$ momenta become the "residual" momenta corresponding to fluctuations of the field $\phi_{n,p}$. We write the hard-collinear field ϕ_n as

$$\phi_n = \sum_p e^{-ip\cdot x}\phi_{n,p}, \tag{4.31}$$

so that

$$\partial^\mu \phi_{n,p} \sim Q(\eta^2, \eta^2, \eta^2). \tag{4.32}$$

In other words, the field ϕ_n has Fourier components to create all hard-collinear particles with momenta that scale as indicated in Table (4.1) and Eq. (4.31) just divides up this momentum space into bins corresponding to each label p and each bin is of size $k \sim Q\lambda^2$(see Fig.4.2.3)

$$\int d^4P \to \sum_p \int d^4k. \tag{4.33}$$

In each bin corresponding to the label p there sits a field $\phi_{n,p}$ that creates momentum fluctuations of size $k \sim Q\eta^2$ centered about the label momentum p. In this language, in SCET_I one can think of two hard-collinear particles with label momenta p_1 and p_2, as being particles with global "charges" p_1 and p_2 and are created by the fields ϕ_{n,p_1} and ϕ_{n,p_2} respectively. The conservation of these label momenta in the EFT corresponds to the conservation of global charges. Note that a separate conservation for the label and residual momenta is required since the label momenta are harder than the residual momenta.

To keep track of the changes in label momenta due to hard momentum exchange among hard-collinear particles, it becomes convenient to introduce the label opera-

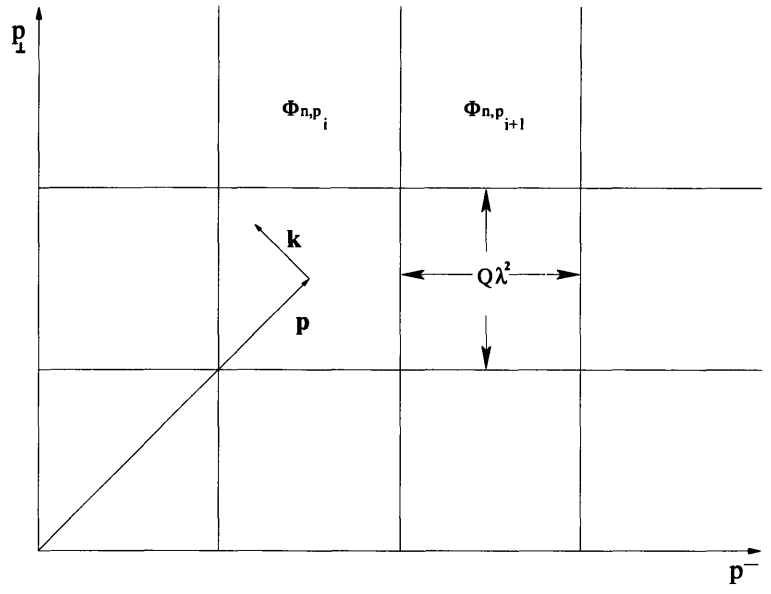

Figure 4-2: The separation of momenta into "label" and "residual" components. The SCET fields $\phi_{n,p}$ describe $k \sim Q\lambda^2$ fluctuations centered about the label momentum p.

tors [26]

$$\bar{\mathcal{P}}\phi_{n,p} = \bar{n}\cdot p\phi_{n,p}, \qquad \mathcal{P}_\perp^\mu \phi_{n,p} = p_\perp^\mu \phi_{n,p}, \tag{4.34}$$

so that $\bar{\mathcal{P}}$ and $\mathcal{P}_\perp^\mu$ operators pick out the $\bar{n}\cdot p$ and $p_\perp^\mu$ components of the label respectively. We define their action on a product of fields as

$$\mathcal{P}^\mu\left(\phi_{q_1}^\dagger \cdots \phi_{q_m}^\dagger \phi_{p_1}\cdots\phi_{p_n}\right) = (p_1^\mu + \ldots + p_n^\mu - q_1^\mu - \ldots - q_m^\mu)\left(\phi_{q_1}^\dagger \cdots \phi_{q_m}^\dagger \phi_{p_1}\cdots\phi_{p_n}\right) \tag{4.35}$$

where we have defined $\mathcal{P}^\mu = \frac{n^\mu}{2}\bar{\mathcal{P}} + \mathcal{P}_\perp^\mu$. Note that these label operators always act in the forward direction. The hermitian conjugate of these operators acts in the backward direction so that

$$\left(\phi_{q_1}^\dagger \cdots \phi_{q_m}^\dagger \phi_{p_1}\cdots\phi_{p_n}\right)\mathcal{P}^{\mu\dagger} = (q_1^\mu + \ldots + q_n^\mu - p_1^\mu - \ldots - p_m^\mu)\left(\phi_{q_1}^\dagger \cdots \phi_{q_m}^\dagger \phi_{p_1}\cdots\phi_{p_n}\right). \tag{4.36}$$

The introduction of these label operators allows us to write

$$i\partial^\mu \left(e^{-ip\cdot x}\phi_{n,p}(x)\right) = e^{-ip\cdot x}\left(\mathcal{P}^\mu + i\partial^\mu\right)\phi_{n,p}(x), \tag{4.37}$$

so that all the derivatives $i\partial^\mu$ in $\mathrm{SCET_I}$ scale like $Q\lambda^2$

$$i\partial^\mu \sim Q\lambda^2 \tag{4.38}$$

and all the large phases get pulled out in front of the operator. The rapid oscillation of the large phase relative to the slowly varying $\phi_{n,p}$ type fields in position space, ensures conservation of label momenta

$$\begin{aligned}\int d^4x \quad e^{-i(p_1+p_2+\cdots p_n)\cdot x} \quad \phi_{n,p_1}(x)\cdots\phi_{n,p_n}(x) &\longrightarrow (2\pi)^3\delta^2(p_{1_\perp}+p_{2_\perp}+\cdots p_{n_\perp}) \\ \times \quad \delta(p_1^- + p_2^- + \cdots p_n^-)\int d^4x\phi_{n,p_1}(x)\cdots\phi_{n,p_n}(x).\end{aligned} \tag{4.39}$$

When the above property is combined with the sum over momentum labels that will appear in the Lagrangian due to the substitution of Eq. (4.31), the delta functions over the momentum labels can be removed with the implicit understanding that the sum of the labels in a product of hard-collinear fields must add up to zero. This leads to four rules regarding our label notation:

1. There is always an implicit sum over all label momenta unless otherwise stated.

2. For any interaction involving a product of fields with momentum labels $p_1, \cdots, p_n$, there is an implicit conservation of label momenta $p_1 + \cdots + p_n = 0$. This conservation of label momenta will also carry over to the Feynman diagrams.

3. The implicit sum over label momenta allows a change of variables on the labels since the original summation variable is a dummy index.

4. In general $\mathcal{P}\mathcal{O} = [\mathcal{P}\mathcal{O}] + \mathcal{O}\mathcal{P}$ where the square bracket indicates that the label operator $\mathcal{P}$ acts only on terms within the bracket.

What will the hard-collinear gauge transformations look like in the label formalism? Consider a hard-collinear gauge transformation $U_{hc}(x) = e^{i\alpha^A(x)T^A}$ with all of it's support over hard-collinear momenta as in Eq. (4.26). Just as we did for the hard-collinear fields, we can remove the hard momenta by a redefinition

$$U_{hc}(x) \;=\; \sum_Q e^{-iQ\cdot x}\mathcal{U}_Q, \tag{4.40}$$

such that $\partial^\mu \mathcal{U}_Q \sim Q\lambda^2$. We can extract the transformation of the hard-collinear quark field $\xi_{n,p}$ by looking at the transformation of the full hard-collinear field $\xi_n(x) = \sum_p e^{-iQ\cdot x}\xi_{n,p}$

$$\xi_n = \sum_q e^{-iq\cdot x}\xi_{n,q} \longrightarrow \qquad U_{hc}\phi_n \;=\; \sum_{Q,q} e^{-i(Q+p)\cdot x}\mathcal{U}_Q\xi_{n,p}. \tag{4.41}$$

For clarity, in the above equation we make the summation over labels explicit. Using the orthogonality property of the phases[3] $\int d^+x d^2x_\perp e^{-i(q-k)\cdot x} \propto \delta(q^- - k^-)\delta^2_\perp(q_\perp - k_\perp)$, we arrive at the transformation of the hard-collinear label fields

$$\xi_{n,q} \longrightarrow \sum_p \mathcal{U}_{q-p}\xi_{n,p}, \tag{4.42}$$

where in the above equation there is no sum over q. One can similarly derive the transformation for the hard-collinear gluon label fields $A_{n,q}$. However, we postpone this result until later in the section after we have discussed how to incorporate the label formalism for covariant derivatives.

We now apply the full power of the label formalism to separate out the hard parts of momenta in the EFT and make power counting as transparent as possible. We can break up the covariant derivatives of SCET_I into terms characterized by their scaling in powers of λ just like the decomposition of the ordinary derivative in Eq. (4.37).

[3] We remind the reader that the label momenta p have non-zero components only for p^- and $p_\perp$.

For the $in\cdot D$ and $iD_\perp$ components, the decomposition is given by

$$\begin{array}{lllll} in\cdot D & = in\cdot D_{hc} & + in\cdot D_{us}, & iD_\perp^\mu & = iD_{hc\perp}^\mu & + iD_{us\perp}^\mu \\ & \downarrow & \downarrow & & \downarrow & \downarrow \\ & \lambda^0 & \lambda^2 & & \lambda & \lambda^2 \end{array} \tag{4.43}$$

where iD_{us} was defined in Eq. (4.22) and

$$in\cdot D_{hc} \equiv \bar{\mathcal{P}} + g\bar{n}\cdot A_{n,q}, \qquad iD_{hc\perp}^\mu \equiv \mathcal{P}_\perp^\mu + gA_{n,q\perp}^\mu. \tag{4.44}$$

No such decomposition is required for the $in\cdot D$ component since all it's term have a homogeneous scaling in λ

$$\begin{array}{lll} in\cdot D & = in\cdot D_{us} & + in\cdot A_{n,q}. \\ & \downarrow & \downarrow \\ & \lambda^2 & \lambda^2 \end{array} \tag{4.45}$$

As promised we now state the leading order transformation of hard-collinear gluon label fields under hard-collinear gauge transformations

$$A_{n,q}^\mu \to \sum_{Q,R} \mathcal{U}_Q\, A_{n,R}^\mu \mathcal{U}_{Q+R-q}^\dagger + \frac{i}{g}\mathcal{U}_Q\left[\mathcal{D}^\mu, \mathcal{U}_{Q-q}^\dagger\right], \tag{4.46}$$

which can be derived in the same way as we did for the hard-collinear quarks and once again there is no sum over q. Here we have defined

$$\mathcal{D}^\mu \equiv \frac{n^\mu}{2}\bar{\mathcal{P}} + \mathcal{P}_\perp^\mu + \mathcal{P}_\perp^\mu + \frac{\bar{n}^\mu}{2} in\cdot D_{us}, \tag{4.47}$$

which is obtained after dropping the order λ^2 terms in the equations of (4.43). It is interesting to note from this example that hard-collinear gauge transformations will in general relate the coefficients of terms of different order in the EFT Lagrangian [24, ?]. It is possible to use redefined fields so that the gauge transformations do not mix terms of different order in power counting. This was shown in [24, 32]. We simply state

the result that is relevant to us. In terms of the redefined fields the n^μ and perp components of the total covariant derivatives get modified

$$in\cdot D = in\cdot D_{hc} + W_{hc} in\cdot D_{us} W_{hc}^\dagger, \qquad iD_\perp^\mu = iD_{hc\perp}^\mu{}^\mu + W_{hc} iD_{us\perp}^\mu W_{hc}^\dagger, \quad (4.48)$$

where the W_{hc} are Wilson lines that will be defined in the next section.

We now have all the pieces needed to rewrite the hard-collinear Lagrangian $\mathcal{L}_{hc}$ of Eq. (4.19) in label notation. In fact, with the power counting of the various terms in the covariant derivatives made explicit by Eqs. (4.43) and (4.45), we can obtain a power expansion of $\mathcal{L}_{hc}$

$$\mathcal{L}_{hc} \;=\; \mathcal{L}_{hc}^{(0)} + \mathcal{L}_{hc}^{(1)} + \cdots \quad (4.49)$$

where the superscripts denote the order in λ. Ignoring the order λ^2 terms in Eq. (4.43), we obtain the leading order hard-collinear Lagrangian [18]

$$\mathcal{L}_{hc}^{(0)} = \bar\xi_{n,p'}\Big[in\cdot D_{us} + gn\cdot A_{n,q} + (i\mathcal{P}_\perp + g\mathcal{A}_{\perp n,r}^\mu)\frac{1}{i\bar n\cdot\mathcal{P} + g\bar n\cdot A_{n,s}}(i\mathcal{P}_\perp + g\mathcal{A}_{\perp n,t}^\mu)\Big]\frac{\bar{\not n}}{2}\xi_{n,p}, \quad (4.50)$$

where as discussed earlier there is an implied sum over all momentum labels and an implicit conservation of the label momenta in each term of the sum. The leading order hard-collinear Lagrangian of the above equation is the main result of this section.

The homogeneous scaling of the D_{us} as seen in Eq. (4.45) implies that all the terms in the light and heavy usoft quark Lagrangians $\mathcal{L}_{us}$ and $\mathcal{L}_{us}^h$, defined in Eqs. (4.21) and (4.23) respectively, have the same scaling and can be checked to be of zeroth order

$$\mathcal{L}_{us} \sim \mathcal{L}_{us}^h \sim \lambda^0. \quad (4.51)$$

As a result there is no expansion for the light and heavy usoft quark Lagrangians $\mathcal{L}_{us}$ and $\mathcal{L}_{us}^h$ similar to Eq. (4.49) for the hard-collinear Lagrangian. Subleading terms

involving the usoft quarks will appear in $\mathcal{L}_{hc,us}$ defined through Eq. (4.9).

4.2.4 Wilson Lines

As we saw in section 4.2.2, SCET_I has hard-collinear and usoft gauge symmetries as the relevant subset of gauge symmetries in QCD. However, the hard-collinear gauge symmetry is not manifest in the current form of the leading order hard-collinear Lagrangian $\mathcal{L}_{hc}^{(0)}$ in Eq. (4.50). We would like to recast $\mathcal{L}_{hc}^{(0)}$ in a form that will make hard-collinear gauge invariance manifest at leading order and is the main goal of this section. In the course of doing so we will be led to the introduction of Wilson lines.

We introduce a order λ^0 object W which is a function of $\bar{n}\cdot A_{n,q}$

$$W = \Big[\sum_{perms} exp\Big(-g\frac{1}{\bar{\mathcal{P}}}\bar{n}\cdot A_{n,q}\Big)\Big], \qquad W^\dagger = \Big[\sum_{perms} exp\Big(-g\bar{n}\cdot A^*_{n,q}\frac{1}{\bar{\mathcal{P}}^\dagger}\Big)\Big], \quad (4.52)$$

and satisfies $W^\dagger W = 1$. In the expansion of the exponential we sum over all permutations of the gluon fields and in the Feynman rules the $\frac{1}{n}!$ in this expansion cancels the $n!$ from the permutation of the gluon fields. It is easy to show that W satisfies

$$\bar{n}\cdot D_{hc} W = \Big[\Big(\bar{\mathcal{P}} + g\bar{n}\cdot A_{n,q}\Big) W\Big] = 0. \quad (4.53)$$

We note that the above equation looks a lot like the equation for a Wilson line along a path in the n^μ direction. We will come back to this point and make the connection clearer later in the section. For now let us proceed and try to figure out the transformation of W under a hard-collinear gauge transformation. We will show that the correct transformation of W is given by

$$W \to \mathcal{U}_T W, \quad (4.54)$$

as follows. We note that for a given boundary condition, Eq. (4.53) has a unique solution and that $\mathcal{U}_T W$ satisfies Eq. (4.53) with $\Big(\bar{\mathcal{P}} + g\bar{n}\cdot A_{n,q}\Big)$ transformed using

Eq. (4.46)

$$
\begin{aligned}
&\Big[\Big(\bar{\mathcal{P}} + g\Big\{\mathcal{U}_Q\,\bar{n}\cdot A_{n,R}\,\mathcal{U}^\dagger_{Q+R-q} + \frac{1}{g}\mathcal{U}_Q\big[\bar{\mathcal{P}}\,\mathcal{U}^\dagger_{Q-q}\big]\Big\}\Big)\mathcal{U}_T W\Big] \\
&= \Big[\Big(\mathcal{U}_T\,\{\bar{n}\cdot T + \bar{\mathcal{P}}\} + g\mathcal{U}_Q\,\bar{n}\cdot A_{n,R}\mathcal{U}^\dagger_{-q}\mathcal{U}_T + \bar{n}\cdot(q-Q)\,\mathcal{U}_Q\mathcal{U}^\dagger_{Q-q}\mathcal{U}_T\Big)W\Big] \\
&= \Big[\Big(\mathcal{U}_T\,\{\bar{n}\cdot T + \bar{\mathcal{P}}\} + g\mathcal{U}_Q\,\bar{n}\cdot A_{n,R} - \bar{n}\cdot Q\,\mathcal{U}_Q\mathcal{U}^\dagger_{-q}\mathcal{U}_T\Big)W\Big] \qquad (4.55)\\
&= \Big[\mathcal{U}_T(\bar{\mathcal{P}} + g\bar{n}\cdot A_{n,R})W\Big] = 0\,.
\end{aligned}
$$

In the second line we have used (for fixed p) $\bar{\mathcal{P}}\phi_{n,p} = [\bar{\mathcal{P}}\phi_{n,p}] + \phi_{n,p}\bar{\mathcal{P}} = \phi_{n,p}(\bar{n}\cdot p + \bar{\mathcal{P}})$. To obtain the third and fourth lines unitarity of the gauge transformation $\mathcal{U}^\dagger_{P+r}\,\mathcal{U}_{P+r'} = \delta_{r,r'}$ (with fixed r, r') was used. Thus, we see that $\mathcal{U}_T$ is a solution of the linear equation with $(\bar{\mathcal{P}} + g\bar{n}\cdot A_{n,q})$ transformed using Eq. (4.46). Thus, from uniqueness the transformation is given by Eq. (4.54). This immediately allows us to write a hard-collinear gauge invariant combination

$$
W^\dagger\xi_{n,p}, \qquad (4.56)
$$

which can be used as one of building blocks for constructing gauge invariant operators. We will see examples of this later on. Similarly, one can write down another building block using the perpendicular hard-collinear covariant derivative

$$
W^\dagger \not{D}^\perp_{hc}\xi_{n,p}, \qquad (4.57)
$$

which is suppressed by one power of λ relative to the building block of Eq. (4.56). The corresponding building block using $\imath\bar{n}\cdot D_{hc}$ can always be rewritten to arrive at the form in Eq. (4.56) as we now show. Using unitarity $WW^\dagger = 1$ and Eq. (4.53),

$$
\begin{aligned}
0 &= \big[\bar{\mathcal{P}}\left(WW^\dagger\right)\big] \\
&= \big[\bar{\mathcal{P}}WW^\dagger\big] + \big[W\bar{\mathcal{P}}W^\dagger\big] \\
&= -g\bar{n}\cdot A_{n,p} + \big[W\bar{\mathcal{P}}W^\dagger\big], \qquad (4.58)
\end{aligned}
$$

which combined with $W\bar{\mathcal{P}}W^\dagger = \left[W\bar{\mathcal{P}}W^\dagger\right] + \bar{\mathcal{P}}$ gives

$$\imath\bar{n}\cdot D_{hc} \;=\; W\bar{\mathcal{P}}W^\dagger. \tag{4.59}$$

Thus, the building block $W^\dagger \imath\bar{n}\cdot D_{hc}\xi_{n,p}$ can be rewritten as

$$\begin{aligned} W^\dagger\imath\bar{n}\cdot D_{hc}\xi_{n,p} &= \left(W^\dagger\imath\bar{n}\cdot D_{hc}W\right)\left(W^\dagger\xi_{n,p}\right) \\ &= \bar{\mathcal{P}}W^\dagger\xi_{n,p}, \end{aligned} \tag{4.60}$$

which is of the same form given in Eq. (4.56). In fact, by replacing $\bar{\mathcal{P}}$ with any function $f(\bar{\mathcal{P}})$ in Eq. (4.58), we can show

$$f(\imath\bar{n}\cdot D_{hc}) \;=\; Wf(\bar{\mathcal{P}})W^\dagger. \tag{4.61}$$

In particular, we can write $1/\imath\bar{n}\cdot D_{hc}$ as $W\frac{1}{\bar{\mathcal{P}}}W^\dagger$ in the second term of the hard-collinear Lagrangian $\mathcal{L}_{hc}^{(0)}$ in Eq. (4.50) to arrive at the form

$$\mathcal{L}_{hc}^{(0)} = \bar{\xi}_{n,p'}\left[\imath n\cdot D_{us} + gn\cdot A_{n,q} + (\imath\mathcal{P}_\perp + g\mathcal{A}^\mu_{\perp n,r})W\frac{1}{\bar{\mathcal{P}}}W^\dagger(\imath\mathcal{P}_\perp + g\mathcal{A}^\mu_{\perp n,t})\right]\frac{\bar{n}\!\!\!/}{2}\xi_{n,p}. \tag{4.62}$$

We now see that hard-collinear gauge invariance is made manifest. The first two terms together are easily checked to be invariant while the last term is now written as a product of the hard-collinear gauge invariant building blocks of Eq. (4.57). Since the hard-collinear gauge transformations don't commute with label operators, the $1/\bar{\mathcal{P}}$ operator in the second term sits between gauge invariant products and appears in the denominator by dimensional analysis. In fact using the constraints of power counting, gauge invariance, and dimensional analysis, we the above form of the leading order hard-collinear Lagrangian $\mathcal{L}_{hc}^{(0)}$ can be uniquely determined. The terms in $\mathcal{L}_{hc}^{(0)}$ are protected from acquiring anamolous dimensions by normalizing the hard-collinear quark kinetic term and imposing gauge invariance. Expanding the factors of W gives an infinite set of leading order couplings of hard-collinear quarks to $\bar{n}\cdot A_{n,q}$ gluons.

We now turn to an interpretation of these objects W which from the point of view

of SCET$_{\rm I}$ are just functions of $\bar{n}\cdot A_{n,q}$ gluons. It can be shown that the object W is the fourier transform of the position space Wilson line

$$W(x,-\infty) \;=\; Pexp\left(\imath g\int_{-\infty}^{0} ds\bar{n}\cdot A(x^+ + sn^+)\right), \tag{4.63}$$

along the n^μ direction. We can see this by fourier transforming the exponential in Eq. (4.52)

$$\begin{aligned}
-g\int dq^- e^{-iq^-x^+}\frac{\bar{n}\cdot A_{n,q}}{q^+ + \imath\epsilon} &= \frac{-g}{2\pi}\int_{-\infty}^{\infty} dy^+ \int dq^- \frac{e^{iq^-(y^+-x^+)}}{n\cdot q + i\epsilon}\bar{n}\cdot A_n(y^+) \\
&= \frac{-g}{2\pi}\int_{-\infty}^{\infty} dy^+(-2\pi\imath\theta(x^+-y^+))\bar{n}\cdot A_n(y^+) \\
&= \imath g\int_{-\infty}^{x^+} dy^+\,\bar{n}\cdot A_n(y^+) \\
&= \imath g\int_{-\infty}^{0} ds\,\bar{n}\cdot A_n(x^+ + sn^+).
\end{aligned} \tag{4.64}$$

For brevity in notation we have used $\bar{n}\cdot q = q^-$, etc. The $+\imath\epsilon$ prescription was used while integrating over q^- to close the countour in the bottom half of the complex q^- plane giving rise to the step function $\theta(x^+ - y^+)$ in the second line. In the last line we changed the integration variable $y^+ \to sn^+ = y^+ - x^+$ to obtain the form of the exponential for the position space Wilson line in Eq. (4.63). Finally, it can be shown that the $+\imath\epsilon$ prescription enforces path ordering and we refer the reader to [43] for an illustration of this point at order g^2.

We should not be suprised at the appearance of Wilson lines along the n^μ direction. Recall that the interactions of hard-collinear particles among themselves involve the exchange of order $Q \gg Q\lambda$ momenta in the n^μ direction. Thus, in our effective theory at the scale $Q\lambda$, such interactions will be non-local giving rise to Wilson lines. However, in our formulation of SCET$_{\rm I}$ using label operators we have removed these hard fluctuations through field redefinitions like the one in Eq. (4.31). However these field redefinitions simply relate the label fields $\phi_{n,p}$ to the position space fields $\phi_n(x)$ through a fourier transform over the label momenta. As a result in our label formulation of SCET$_{\rm I}$, we see the presence of the "momentum space" Wilson lines

W which can be thought of as connecting hard-collinear particles in different p^- label bins(see fig. 4.2.3).

The transformation of the momentum space Wilson line W, shown in Eq. (4.54), under a hard-collinear gauge transformation is consistent with that of the position space Wilson line $W(x, -\infty)$

$$W(x, -\infty) \longrightarrow U_{hc}(x) W(x, -\infty) U_{hc}^\dagger(x - \infty \bar{n}^\mu), \tag{4.65}$$

with $U_{hc}^\dagger(x - \infty \bar{n}^\mu) = 1$. In other words, the hard-collinear gauge transformations have no support at $n \cdot x \to -\infty$. But this follows immediately from the scaling of the hard-collinear momenta

$$\phi_n(x) = \int dp^- d^2 p_\perp e^{(-ip^- \cdot x^+ - ip_\perp \cdot x_\perp)} \phi_{n,p} \longrightarrow 0, \tag{4.66}$$

as $x^+ \to \infty, -\infty$ due to rapid oscillations of the exponential $e^{(-ip^- \cdot x^+)}$ over the smooth function $\phi_{n,p}$ in the region of large p^-. For clarity we have switched from our usual convention of denoting the integral over label momenta by a summation symbol, and have made the integral explicit. So, all hard-collinear particles are effectively confined to a bin near $n \cdot x \approx 0$(see fig. 4-3). More intuitively, this just corresponds to the fact that

$$n \cdot x = t - z \approx 0, \tag{4.67}$$

for hard-collinear particles close to their light cone direction n^μ. Thus, with all hard-collinear gluons confined to be near the $n \cdot x \approx 0$ bin, the gauge transformation $U_{hc}(x)$ has no support for large $n \cdot x$ which is consistent with the transformation of the momentum space Wilson line W shown in Eq. (4.54).

4.2.5 Hard-Collinear and Ultrasoft Decoupling

Now that we have a manifestly gauge invariant leading order Lagrangian $\mathcal{L}_{hc}^{(0)}$ for hard-collinear quarks, we could go ahead and write down the leading order Feynman

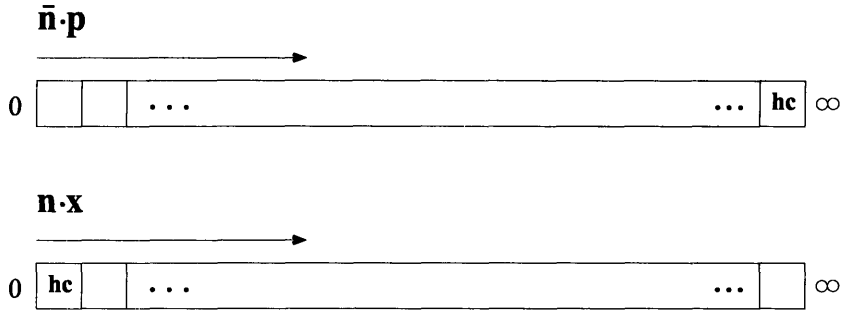

Figure 4-3: The hardcollinear particles with a large momentum component $\bar{n} \cdot p \sim Q$ are effectively confined to bins near $n \cdot x \approx 0$.

rules for SCET_I . However, we momentarily postpone this to the end of this section and first discuss another important property of the hard-collinear Lagarangian. This property called Ultrasoft-Hard-Collinear decoupling [22], is at the heart of factorization theorems in SCET and has a huge impact in our ability to make phenemenological predictions. In fact, it is this property of SCET_I that will allow us to implement heavy quark symmetry in $\bar{B} \to D^{(*)}\pi$ type decays which cannot not be done in HQET alone.

The idea of ultrasoft-hard-collinear decoupling is to reformulate SCET_I in terms of new fields such that there are no interactions between hard-collinear and usoft particles at leading order λ^0. We see that in it's current form in Eq. (4.62), $\mathcal{L}_{hc}^{(0)}$ involves the interaction of a hard-collinear quark with a usoft gluon through D_{us}. Ultrasoft-hard-collinear decoupling uses redfined fields such that this interaction disappears at leading order. In this new formulation one can factorize amplitudes for appropriate physical processes at leading order and then systematically compute power corrections to it. We will show how this works in detail for the $\bar{B} \to D^{(*)}\pi$ type decays in later chapters.

We now show how decoupling works. Just as we introduced hard-collinear momentum space Wilson lines W in the previous section, we can define a usoft momentum space Wilson line

$$Y = 1 + \sum_{m=1}^{\infty} \sum_{\text{perms}} \frac{(-g)^m}{m!} \frac{n\cdot A_{us}^{a_1} \cdots n\cdot A_{us}^{a_m}}{n\cdot k_1\, n\cdot(k_1+k_2)\cdots n\cdot(\sum_{i=1}^{m} k_i)} T^{a_m} \cdots T^{a_1}, \qquad (4.68)$$

where $n \cdot k_i$ denotes the $\bar{n}^\mu$ momentum component of the ith fourier transformed usoft

gluon $A^i_{us}(k_i)$ and the a_i denote color indices. It is related to the fourier transform of the position space Wilson line

$$Y(x) \;=\; \mathrm{P}\exp\left(ig\int_{-\infty}^{x} \mathrm{d}s\, n\cdot A^a_{us}(ns)T^a\right). \tag{4.69}$$

In a manner similar to the proof of Eq. (4.61), we can show

$$Y^\dagger\, n\cdot D_{us}\, Y = n\cdot\partial. \tag{4.70}$$

Next we perform field redefinitions which introduce new fields denoted by the superscript (0)

$$\xi_{n,p} \;=\; Y\,\xi^{(0)}_{n,p}, \qquad A^\mu_{n,p} = Y A^{(0)\mu}_{n,p}\, Y^\dagger, \qquad c_{n,p} = Y c^{(0)}_{n,p}\, Y^\dagger. \tag{4.71}$$

The field redefinition for the hard-collinear gluon implies a redfinition for the hard-collinear Wilson line

$$W \;=\; \Big[\sum_{\text{perms}} \exp\Big(-g\,\frac{1}{\bar{\mathcal{P}}}\; Y\,\bar{n}\cdot A^{(0)}_{n,q}\, Y^\dagger\Big)\Big] = Y\, W^{(0)}\, Y^\dagger. \tag{4.72}$$

In Eq. (4.71) we have also included the field redefinition for the ghost fields $c_{n,p}$. For the hard-collinear Lagrangian $\mathcal{L}^{(0)}_{hc}$, the above field redefinitions give

$$\begin{aligned}
\mathcal{L}^{(0)}_{hc} \;&=\; \bar{\xi}^{(0)}_{n,p'} Y^\dagger \Big\{ in\cdot D_{us} + gYn\cdot A^{(0)}_{n,q} Y^\dagger + \left(\not{\mathcal{P}}_\perp + Yg\not{A}^{(0)\perp}_{n,q} Y^\dagger\right) YW^{(0)}Y^\dagger\,\frac{1}{\bar{\mathcal{P}}} \\
&\qquad \times YW^{(0)\dagger}Y^\dagger\left(\not{\mathcal{P}}_\perp + Yg\not{A}^{(0)\perp}_{n,q'} Y^\dagger\right)\Big\}\frac{\bar{\not{n}}}{2}\, Y\xi^{(0)}_{n,p}\Big\} \qquad (4.73) \\
&= \bar{\xi}^{(0)}_{n,p'}\Big\{ Y^\dagger in\cdot D_{us} Y + gn\cdot A^{(0)}_{n,q} + \left(\not{\mathcal{P}}_\perp + g\not{A}^{(0)\perp}_{n,q}\right) W^{(0)}\,\frac{1}{\bar{\mathcal{P}}}\, W^{(0)\dagger}\left(\not{\mathcal{P}}_\perp + g\not{A}^{(0)\perp}_{n,q'}\right)\Big\}\frac{\bar{\not{n}}}{2}\,\xi^{(0)}_{n,p} \\
&= \bar{\xi}^{(0)}_{n,p'}\Big\{ in\cdot\partial + gn\cdot A^{(0)}_{n,q} + \left(\not{\mathcal{P}}_\perp + g\not{A}^{(0)\perp}_{n,q}\right) W^{(0)}\,\frac{1}{\bar{\mathcal{P}}}\, W^{(0)\dagger}\left(\not{\mathcal{P}}_\perp + g\not{A}^{(0)\perp}_{n,q'}\right)\Big\}\frac{\bar{\not{n}}}{2}\,\xi^{(0)}_{n,p}. \qquad (4.74)
\end{aligned}$$

We see in the last line above that in terms of the new fields there are no usoft-hard-collinear interactions. We have, at leading order, decoupled the usoft gluons

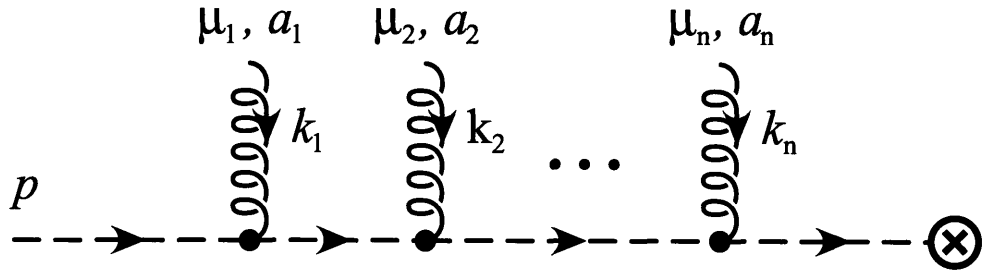

Figure 4-4: The interactions of usoft gluons with hardcollinear quarks can be summed into a Wilson line along the path of the hardcollinear quark. [22]

from the hard-collinear quarks at the level of the Lagrangian itself. Similarly, we the hard-collinear gluon Lagrangian becomes

$$\begin{aligned}\mathcal{L}^{(0)}_{g,hc} &= \frac{1}{2g^2}\,\mathrm{tr}\left\{\left[iD^{\mu}_{(0)}+gA^{(0)\mu}_{n,q}\,,iD^{\nu}_{(0)}+gA^{(0)\nu}_{n,q'}\right]\right\}^2+\frac{1}{\alpha}\,\mathrm{tr}\left\{\left[iD^{(0)}_{\mu}\,,A^{(0)\mu}_{n,q}\right]\right\}^2\\ &\quad +2\,\mathrm{tr}\Big\{\bar{c}^{(0)}_{n,p'}\left[iD^{(0)}_{\mu},\left[iD^{\mu}_{(0)}+gA^{(0)\mu}_{n,q}\,,c^{(0)}_{n,p}\right]\right]\Big\}\,, \qquad (4.75)\end{aligned}$$

where

$$iD^{\mu}_{(0)}=\frac{n^{\mu}}{2}\,\bar{\mathcal{P}}+\mathcal{P}^{\mu}_{\perp}+\frac{\bar{n}^{\mu}}{2}\,in\cdot\partial\,. \qquad (4.76)$$

The result in Eq. (4.75) shows that the new hard-collinear gluon and ghost fields $A^{(0)}_{n,q}$ and $c^{(0)}_{n,p}$ also decouple from usoft gluons. From now on we will work in this new formulation in terms of the redefined fields and drop the superscript (0) for notational simplicity.

From the form of the field redefinitions in Eq. (4.71), we can interpret this result of decoupling as the statement that the interactions of hard-collinear particles with usoft gluons can be summed into Wilson lines Y along the n^{μ} direction at leading order. This idea is shown pictorially in Fig. 4.2.5. We stress that decoupling is only a leading order property of SCET. Beyond leading order, there will be interactions between hard-collinear and usoft gluons that cannot be summed into Wilson lines.

Finally, we end this section by giving the Feynman rules for the leading order interactions between hard-collinear quarks and gluons as determined by $\mathcal{L}^{(0)}_{hc}$ in Eq. (4.73).

Figure 4.2.5 gives the Feyman rules for the first few terms of $\mathcal{L}_{hc}^{(0)}$.

4.3 $\mathrm{SCET_I}$: Beyond Leading Order

In the previous section we derived the leading order Lagrangian for $\mathrm{SCET_I}$ which involved no interactions between usoft and hard-collinear particles. However heavy hadron decays cannot proceed without usoft-hard-collinear transitions. Such transitions occur at subleading order in $\mathrm{SCET_I}$. To go beyond leading order it becomes convenient to establish a set of constraints that will allow us to write down a complete set of operators onto which we can match QCD plus Fermi theory which was the relevant the EFT at $\mu \sim Q$.

4.3.1 Operator Constraints and Symmetries

There are three main guiding principles for the construction of operators in $\mathrm{SCET_I}$

1. Power counting.
2. Hard-collinear and usoft gauge invariance.
3. Reparameterization invariance(RPI).

We have already discussed the first two principles in some detail. In addition. SCET also contains a kinematical reparameterization invariance [90] analogous to HQET which we now discuss.

Reparameterization Invariance

$\mathrm{SCET_I}$ is an EFT constructed in a frame of reference in which the degrees of freedom have usoft or hard-collinear momenta. In a different frame of reference these same degrees of freedom will in general have very different looking momentum scalings for which $\mathrm{SCET_I}$ is not appropriate. However, the appropriate frame of reference for $\mathrm{SCET_I}$ is not absolute. $\mathrm{SCET_I}$ will be invariant under the subset of Lorentz transformations that do not alter the momentum scalings of the usoft and hard-collinear

particles. The invariance of SCET_I under this subset of Lorentz transformations is what we call the RPI symmetry of SCET_I . In particular, due to the vectors $n, \bar{n}$, Lorentz invariance is broken by the generators $n^\mu M_{\mu\nu}, \bar{n}^\mu M_{\mu\nu}$ but preserved under $\epsilon_\perp^{\mu\nu} M_{\mu\nu}$.

In HQET, RPI is the result of the freedom to make small changes to the heavy quark four velocity label v^μ without changing the scaling of the soft momenta and preserving the on-shell condition $v^2 = 1$ for the heavy quark. In SCET, RPI manifests itself as the freedom to make changes to the light cone vector label n^μ without changing the scaling of the hard-collinear momenta and preserving the normalization conditions $n^2 = \bar{n}^2 = 0, n \cdot \bar{n} = 2$. There are three types of RPI transformations allowed

$$\begin{aligned}
&\text{type I:} && n \to n + \Delta_\perp, && \Delta_\perp \sim \lambda. \\
&\text{type II:} && \bar{n} \to \bar{n} + \epsilon_\perp, && \epsilon_\perp \sim \lambda^0. \\
&\text{type III:} && n \to e^\alpha n, \ \bar{n} \to e^{-\alpha} \bar{n}, && \alpha \sim \lambda^0.
\end{aligned} \tag{4.77}$$

The scaling of the transformation parameters $\Delta_\perp, \epsilon_\perp, \alpha$ given above are determined by the requirement the scaling of the hard-collinear momenta remain unchanged. For example, under a type I RPI transformation, the hard-collinear momentum $p^\mu = (n \cdot p, \bar{n} \cdot p, p_\perp) \sim (\lambda^2, \lambda^0, \lambda)$ transforms as

$$\begin{array}{rccccc}
p^\mu \to & \left(\frac{n\cdot p}{2} + \frac{\Delta_\perp \cdot p_\perp}{2}\right) \bar{n}^\mu + & \frac{\bar{n}\cdot p}{2} n^\mu + & \left(p_\perp^\mu + \frac{\bar{n}\cdot p}{2} \Delta_\perp\right), \\
& \downarrow & \downarrow & \downarrow \\
& \lambda^2 & \lambda^0 & \lambda
\end{array} \tag{4.78}$$

where the last line shows the required scaling for the hard-collinear momentum components and implies that $\Delta_\perp \sim \lambda$.

RPI transformations also affect the hard-collinear fields due to the requirement of preserving Eqs. (4.13), (4.15), and (4.53). We refer the reader to [90] for further

details. We point out that just as in HQET, RPI transformations in SCET_I connect operators at different orders which provides severe constraints on the Wilson coefficients of subleading terms. In fact we will exploit this property in the next section to derive the order λ usoft-hard-collinear coupling using tree level equations of motion.

4.3.2 Ultrasoft-Hard-Collinear Transitions

In this section we derive the form of subleading usoft-hard-collinear interactions using tree level equations of motion. In principle there are two problems with this approach. The first is that we may miss non-trivial Wilson coefficients that may arise during matching beyond tree level and the second is that we may miss operators whose tree level Wilson coefficients vanish. However, it was shown in [100], that using RPI invariance along with gauge symmetry and power counting, neither of these problems arise up to order λ^2. We will assume this result and derive the usoft-hard-collinear Lagrangian at order λ using tree level equations of motion.

For simplicity of notation we drop label fields in the following and will put them back in the final result. Furthermore, in what follows we will be starting at the very beginning before having made the ultrasoft-hard-collinear decoupling transformation. We will make the decoupling transformation after we arrive at the final result.

We simply generalize our procedure for obtaining the leading order hard-collinear Lagrangian by including the usoft quark field in the decomposition of the quark field into SCET_I fields

$$\Psi = \xi_n + \xi_{\bar{n}} + q_{us}. \tag{4.79}$$

Starting with the action $\mathcal{L} = \bar{\Psi} i \not{D} \Psi$ we get

$$\begin{aligned} \mathcal{L} &= \bar{\xi}_n \frac{\not{\bar{n}}}{2} in\cdot D\, \xi_n + \bar{\xi}_n i \not{D}^\perp \xi_{\bar{n}} + \bar{\xi}_n g \not{A}_c\, q_{us} + \bar{q}_{us}\, g \not{A}_c\, \xi_n + \bar{q}_{us}\, g \not{A}_c\, \xi_{\bar{n}} + \bar{q}_{us}\, i \not{D}_{us}\, q_{us} \\ &\quad + \left[\bar{\xi}_{\bar{n}} i \not{D}^\perp \xi_n + \bar{\xi}_{\bar{n}} \frac{\not{n}}{2} i\bar{n}\cdot D \xi_{\bar{n}} + \bar{\xi}_{\bar{n}} g \not{A}_c q_{us} \right], \end{aligned} \tag{4.80}$$

where $D \equiv D_{us} + D_{hc}$. The equation of motion for $\xi_{\bar{n}}$ is given by

$$\xi_{\bar{n}} = -\frac{1}{i\bar{n}\cdot D}\frac{\bar{n}\!\!\!/}{2}\left[i\not{D}_\perp \xi_n + g\mathcal{A}_n\, q_{us}\right], \qquad \bar{\xi}_{\bar{n}} = \left[\bar{q}_{us} g\mathcal{A}_n - \bar{\xi}_n i\overleftarrow{\not{D}}_\perp\right]\frac{\bar{n}\!\!\!/}{2}\frac{1}{i\bar{n}\cdot\overleftarrow{D}}. \quad (4.81)$$

Substituting Eq. (4.81) in Eq. (4.80) and only keeping mixed usoft-hard-collinear terms(since this is the additional piece we want) we get

$$\mathcal{L}_{\xi q} = \left[\bar{\xi}_n g\mathcal{A}_n\, q_{us} + \bar{\xi}_n \frac{\bar{n}\!\!\!/}{2} i\not{D}_\perp \frac{1}{i\bar{n}\cdot D} g\mathcal{A}_n\, q_{us}\right] + \left[\bar{q}_{us}\, g\mathcal{A}_n\, \xi_n + \bar{q}_{us}\, g\mathcal{A}_n \frac{1}{i\bar{n}\cdot D} i\not{D}_\perp \frac{\bar{n}\!\!\!/}{2}\xi_n\right]. \quad (4.82)$$

Next we use the power counting scheme of $\mathrm{SCET_I}$ to expand the above Lagrangian in powers of λ. The terms up to first order in λ are given by [100]

$$\mathcal{L}^{(1)}_{\xi q} = \bar{\xi}_n\Big(g\mathcal{A}^c_\perp - i\not{D}^c_\perp \frac{1}{i\bar{n}\cdot D_c}\, g\bar{n}\cdot A_c\Big) q_{us} + \text{h.c.}, \quad (4.83)$$

$$(4.84)$$

where as always the superscript denotes the order in λ. For the purposes of phenomenology which we discuss in later chapters, it is enough to keep only $\mathcal{L}^{(1)}_{\xi q}$ and we will not worry about the further suppressed terms [100]. We can write $\mathcal{L}^{(1)}_{\xi q}$ in the more compact form

$$\mathcal{L}^{(1)}_{\xi q} = \bar{\xi}_n \frac{1}{i\bar{n}\cdot D_c}\, ig\bar{n}\!\!\!/ B^\perp_c W q_{us} + \text{h.c.}, \quad (4.85)$$

by introducing the field strength

$$igB^{\perp\mu}_c \equiv [i\bar{n}\cdot D^c, iD^{\perp\mu}_c]. \quad (4.86)$$

Finally, we perform the decoupling transformation of Eq. (4.71) to arrive at

$$\mathcal{L}^{(1)}_{\xi q} = \bar{\xi}_n \frac{1}{i\bar{n}\cdot D_c}\, ig\bar{n}\!\!\!/ B^\perp_c W Y^\dagger q_{us} + \text{h.c.}, \quad (4.87)$$

as our final result for the order λ usoft-hard-collinear interaction. In the above expres-

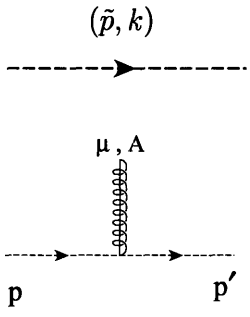

$$= i\frac{\not{n}}{2}\frac{\bar{n}\cdot p}{n\cdot k\,\bar{n}\cdot p + p_\perp^2 + i\epsilon}$$

$$= igT^A\left[n_\mu + \frac{\gamma_\mu^\perp \not{p}_\perp}{\bar{n}\cdot p} + \frac{\not{p}'_\perp \gamma_\mu^\perp}{\bar{n}\cdot p'} - \frac{\not{p}'_\perp \not{p}_\perp}{\bar{n}\cdot p\,\bar{n}\cdot p'}\bar{n}_\mu\right]\frac{\not{n}}{2}$$

$$= \frac{ig^2 T^A T^B}{\bar{n}\cdot(p-q)}\left[\gamma_\mu^\perp\gamma_\nu^\perp - \frac{\gamma_\mu^\perp \not{p}_\perp}{\bar{n}\cdot p}\bar{n}_\nu - \frac{\not{p}'_\perp\gamma_\nu^\perp}{\bar{n}\cdot p'}\bar{n}_\mu + \frac{\not{p}'_\perp\not{p}_\perp}{\bar{n}\cdot p\,\bar{n}\cdot p'}\bar{n}_\mu\bar{n}_\nu\right]\frac{\not{n}}{2}$$

$$+ \frac{ig^2 T^B T^A}{\bar{n}\cdot(q+p')}\left[\gamma_\nu^\perp\gamma_\mu^\perp - \frac{\gamma_\nu^\perp \not{p}_\perp}{\bar{n}\cdot p}\bar{n}_\mu - \frac{\not{p}'_\perp\gamma_\mu^\perp}{\bar{n}\cdot p'}\bar{n}_\nu + \frac{\not{p}'_\perp\not{p}_\perp}{\bar{n}\cdot p\,\bar{n}\cdot p'}\bar{n}_\mu\bar{n}_\nu\right]\frac{\not{n}}{2}$$

Figure 4-5: Order λ^0 Feynman rules: collinear quark propagator with label $\tilde{p}$ and residual momentum k, and collinear quark interactions with one soft gluon, one collinear gluon, and two collinear gluons respectively. [22]

sion the hard-collinear fields are the redefined fields of Eq. (4.71) with the superscript (0) dropped. In other words the hardcollinear fields in the above expression do not transform under usoft gauge transformations. Usoft gauge invariance in made manifest through the invariant combination $Y^\dagger q_{us}$. To see the gauge invariance note that under a hard-collinear gauge transformation U_{hc} we have $\xi_n \to U_{hc}\xi_n$, $W \to U_{hc}W$, $\not{B}_\perp \to U_c \not{B}_\perp U_c^\dagger$, and $(\bar{n}\cdot D_c)^{-1} \to U_c\,(\bar{n}\cdot D_{hc})^{-1}\,U_{hc}^\dagger$ so all factors of U_{hc} cancel.

The usoft-hard-collinear transition $\mathcal{L}_{\xi q}^{(1)}$ will play a crucial role for color suppressed decays of the type $\bar{B} \to D^{(*)}\pi$ in which soft spectator quarks in the $\bar{B}, D^{(*)}$ mesons end up in the energetic collinear pion. We will discuss this at length in subsequent chapters. In Fig. 4-6 we show the Feynman rule for the first term in $\mathcal{L}_{\xi q}^{(1)}$ which involves one hard-collinear gluon.

4.4 Matching

The previous sections were devoted to the development of SCET_I as the EFT near the $\mu \sim \sqrt{Q\Lambda_{QCD}}$ entirely in terms of usoft and hard-collinear degrees of freedom. We are now in a position to match Fermi theory onto SCET_I . However, the peculiar nature of SCET_I due to the presence of three different scales in the hard-collinear momenta leads to non-trivialities in the matching procedure which we explore in this section. In fact we will find that matching simplifies dramatically due to all the symmetries of SCET_I discussed in previous sections.

4.4.1 Operator Wilson Coefficients

In matching from Fermi theory at the scale $\mu \sim Q$ onto SCET_I at $\mu \sim \sqrt{Q\Lambda_{QCD}}$, the Wilson coefficients will depend on the hard scale Q. In other words, the physics of the hard scale is captured by the Wilson coefficients and SCET_I describes the dynamics at the scale $\mu \sim \sqrt{Q\Lambda_{QCD}}$. However, as we have discussed before the hard-collinear modes with virtuality $\mu \sim \sqrt{Q\Lambda_{QCD}}$ possess a hard momentum component $\bar{n}\cdot p \sim Q \gg \sqrt{Q\Lambda_{QCD}}$ making this separation of scales more difficult.

To get a better idea of the interplay between the different scales associated with hard-collinear momenta, let's consider the example of heavy to light semileptonic decay. Consider the matching [18] of the weak Hamiltonian of Fermi theory for heavy to light semileptonic decays

$$H_{eff} = \frac{G_F}{\sqrt{2}}\, V\, C^{\text{full}}(\mu)\, J_{\text{had}}\, J\,, \tag{4.88}$$

where J is the leptonic current and J_{had} is a heavy to light hadronic current of the form

$$J_{had} = \bar{q}\Gamma b \tag{4.89}$$

for the decay of a b quark into a light quark q. The Wilson Coefficient $C^{\text{full}}(\mu)$ has been run down from $\mu \sim M_W$ to μ_{m_b}. Finally, Γ represents the general Dirac structure

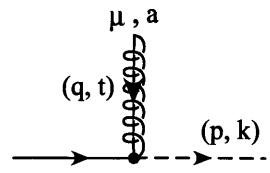

$$= \quad ig\,T^a\,[\gamma_\mu^\perp - \bar{n}_\mu \frac{\not{q}_\perp}{\bar{n}\cdot q}\,]$$

Figure 4-6: Feynman rules for the subleading usoft-collinear Lagrangian $\mathcal{L}_{\xi q}^{(1)}$ with one and two collinear gluons (springs with lines through them). The solid lines are usoft quarks while dashed lines are collinear quarks. For the collinear particles we show their (label,residual) momenta. (The fermion spinors are suppressed.)

of the operator and it's details will not be relevant for our discussion.

The tree level matching of J_{had} onto the SCET_I operator $J_{\text{had}}^{\text{eft}}$ is shown pictorially in Fig. (4-7) [18]. On the left we show hard-collinear gluons interacting with a usoft heavy b quark in the full theory. Each hard-collinear gluon knocks the b quark far offshell and this offshell mode must be integrated out to match onto SCET_I which only contains a b quark that is offshell by a small amount $\sim \Lambda_{QCD}$. Note that it is the hard $\bar{n}\cdot p \sim m_b$ component of the hard-collinear gluon responsible for knocking the b quark far offshell. As a result the Wilson coefficient will depend on $\bar{n}\cdot p$. However, at the same time, the hard momentum component $\bar{n}\cdot p$ is still dynamical in SCET_I due to the exchange of $\bar{n}\cdot p$ momentum components among hard-collinear modes. In other words, the hard component $\bar{n}\cdot p$ appears both in the Wilson coefficients and in the EFT at the same time!

In the label formalism introduced in the previous sections, we introduced EFT fields $\phi_{n,p}$ such that the hard momentum component $\bar{n}\cdot p \sim Q$ gets absorbed into the label and the dynamical momenta now have fluctuations $\partial^\mu \phi_{n,p} \sim (\lambda^2, \lambda^2, \lambda^2)\phi_{n,p}$. In this way we managed to seperate the hard scale Q from the EFT at the scale $\mu \sim \sqrt{Q\Lambda_{QCD}}$. But from our discussion above this implies that the Wilson coefficients in SCET_I will depend on the hard-collinear field labels. In particular, we can express the Wilson coefficients as functions of the label operators

$$C = C(\bar{\mathcal{P}}, \bar{\mathcal{P}}^\dagger). \tag{4.90}$$

In this sense, the Wilson coefficients become operators that act on the labels of the $\mathrm{SCET_I}$ operators. When this formalism is combined with the gauge symmetries and power counting framework of $\mathrm{SCET_I}$, matching calculations can simplify dramatically. We now illustrate this for the matching of the heavy to light operator J_{had} onto $\mathrm{SCET_I}$. We use two guiding principles

- Write down all possible operators in $\mathrm{SCET_I}$ consistent with power counting, gauge symmetry, and RPI.
- Operator Wilson coefficients for $\mathrm{SCET_I}$ operators are inserted only between gauge invariant blocks.

To avoid confusion, we first work with fields of $\mathrm{SCET_I}$ defined before the ultrasoft-hard-collinear decoupling redefinition. We will rewrite the $\mathrm{SCET_I}$ operators in terms of the redefined fields as the very last step. At leading order in $\mathrm{SCET_I}$, there is only one gauge invariant heavy to light operator and J_{had} matches onto $\mathrm{SCET_I}$ as

$$J_{had} = \left[C(\bar{\mathcal{P}})\bar{\xi}_{n,p}W\right]\Gamma\, h_v^b. \tag{4.91}$$

We note that the Wilson coefficient $C(\bar{\mathcal{P}})$ can only be placed in front of the hard-collinear gauge invariant block [4] $\bar{\xi}_{n,p}W$. Thus, we see that hard-collinear gauge invariance relates the Wilson coefficients of the various terms obtained after expanding out the hard-collinear Wilson line W. In other words, if we were unaware of hard-collinear gauge symmetry and we attempted to match diagrammatically as in figure 4-7, our matching equation would look like

$$\begin{aligned} J_{\rm had}^{\rm eft} \;=\; & c_0(\bar{n}\cdot p,\mu)\,\bar{\xi}_{n,p}\,\Gamma\, h_v \;+ c_1(\bar{n}\cdot p,\bar{n}\cdot q_1,\mu)\,\bar{\xi}_{n,p}\,(g\,\bar{n}\cdot A_{n,q_1})\Gamma\, h_v \\ & + c_2(\bar{n}\cdot p,\bar{n}\cdot q_1,\bar{n}\cdot q_2,\mu)\,\bar{\xi}_{n,p}\,(g\,\bar{n}\cdot A_{n,q_1})(g\,\bar{n}\cdot A_{n,q_2})\Gamma\, h_v + \ldots \quad , \end{aligned} \tag{4.92}$$

where the ellipsis stand for terms of the same order with more powers of $\bar{n}\cdot A_{n,q}$. We would not expect the Wilson coefficients c_i to be related in any way since in general

[4] Hence the Wilson coefficient is independent of $\bar{\mathcal{P}}^\dagger$ which only acts in the backward direction.

they would be expected to evolve independently through the RGE equations down to lower scales. But hard-collinear gauge invariance tells us that this is not the case.

In terms of the redefined fields of Eq. (4.71) with the superscript (0) dropped, the SCET_I heavy to light operator becomes

$$J_{had} = \left[C(\bar{\mathcal{P}})\bar{\xi}_{n,p}W\right] \Gamma\, Y^\dagger h_v^b, \tag{4.93}$$

and we remind the reader that in the above expression the hard-collinear fields are decoupled from the usoft fields and do not transform under usoft gauge transformations. So, we see that this SCET_I operator is just a product of hard-collinear and usoft gauge invariant blocks with a Wilson coefficient operator acting on the hard-collinear block.

Finally we end this section by introducing notation that will make the separation of the hard scale manifest. We define

$$\left(\bar{\xi}_{n,p}W\right)_\omega \equiv \bar{\xi}_{n,p}W\delta(\omega - \bar{\mathcal{P}}^\dagger), \tag{4.94}$$

in terms of which we can write Eq. (4.93) as a convolution

$$J_{had} = \int d\omega \Big\{\, C(\omega)\ \left(\bar{\xi}_{n,p}W\right)_\omega\, \Gamma\, Y^\dagger h_v^b \,\Big\}, \tag{4.95}$$

and all the physics of the hard scale is now contained in $C(\omega)$. In other words, we have "factorized" the hard scale physics.

4.4.2 $\text{SCET}_\text{I} \to \text{SCET}_\text{II}$

SCET_II

We are now ready to match SCET_I onto SCET_II . Recall that SCET_II is the appropriate EFT of soft and collinear degrees of freedom near the Λ_{QCD} scale. The form of SCET_II is similar to that of SCET_I . Recall that the soft modes of SCET_II are

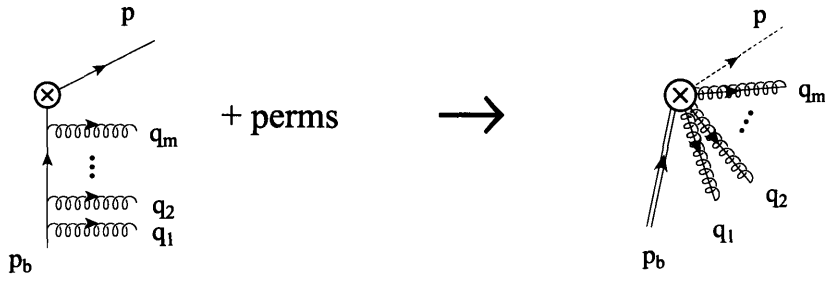

Figure 4-7: Matching for the order λ^0 Feynman rule for the heavy to light current with n collinear gluons. All permutations of crossed gluon lines are included on the left. [18]

identical to the usoft modes of SCET_I . The collinear modes of SCET_II are contained in the hard-collinear modes of SCET_I and correspond to subset of "softer" fluctuations ($p^2 \sim \Lambda^2_{QCD}$) of the hard-collinear modes in the sense of Eq. (2.1). Thus, the SCET_II Lagrangian is obtained from SCET_I by identifying the usoft fields with the soft fields and keeping only the "softer" fluctuations[5] of the hard-collinear fields which are identified with the collinear fields of SCET_II . The physics that is missed by setting the "harder" hard-collinear fields to zero will be captured by the Wilson coefficients or "jet functions" of higher dimensional or non-renormalizable operators of SCET_II . But these higher dimensional operators are power suppressed. Thus, to leading order SCET_I and SCET_II have identical Lagrangians with the usoft and soft fields and hard-collinear and collinear fields identified respectively. We summarize the content of SCET_I and SCET_II in Table **??**.

All the arguments for gauge symmetry and RPI invariance of SCET_I carry over to SCET_II . In particular, SCET_II will have Soft and Collinear gauge symmetry and one can construct gauge invariant objects as products of soft and collinear gauge invariant blocks.

We summarize the two step matching procedure[25] $(QCD{+}Fermi) \to \text{SCET}_\text{I} \to \text{SCET}_\text{II}$ below

- Match QCD+Fermi theory onto SCET_I at the scale $\mu \sim Q$. Here the hard-

[5]We mean this in the sense of Eq. (2.3), where we set ϕ_h to zero since $\partial^2\phi_h \sim Q\Lambda_{QCD}$ and only the ϕ_s modes are kept such that $\partial^2\phi_h \sim \Lambda^2_{QCD}$.

collinear fields of SCET_I have virtuality $p_{hc}^2 \sim Q\Lambda_{QCD}$.

- Factorize the usoft-hard-collinear interactions with the field redefinitions of the ultrasoft-hard-collinear decoupling.

$$\xi_{n,p} = Y\,\xi^{(0)}_{n,p}, \qquad A^\mu_{n,p} = Y\,A^{(0)\mu}_{n,p}\,Y^\dagger,$$

followed by a renaming of the $\xi^{(0)}_{n,p}, A^{(0)\mu}_{n,p}$ fields in which the superscripts (0) are dropped. Run down to the scale $\mu \sim \sqrt{Q\Lambda_{QCD}}$ using the RGE equations in SCET_I .

- Match SCET_I onto SCET_II at the scale $\mu \sim \sqrt{Q\Lambda_{QCD}}$. At leading order, since the SCET_I and SCET_II Lagrangians are identical, all time ordered products will exactly agree. Thus, the leading order matching amounts to identifying usoft fields with soft fields and hard-collinear fields with collinear fields($p_c^2 \sim \Lambda_{QCD}^2$). Run down towards $\mu \sim \Lambda_{QCD}$ using the RGE equations in SCET_II .

We illustrate this matching sequence by continuing with our example of heavy to light semileptonic decays from the previous section. We only consider matching at tree-level which will allow us to ignore the RGE running between scales altough this can be included in a straightforward manner. We have already performed the first two steps in the matching procedure

1. Match QCD+Fermi theory onto SCET_I :

$$J_{had} = \bar{q}\Gamma b \to \left[C(\bar{\mathcal{P}})\bar{\xi}_{n,p}W\right]\Gamma\, h_v^b.$$

2. Perform decoupling field redefinition:

$$\left[C(\bar{\mathcal{P}})\bar{\xi}_{n,p}W\right]\Gamma\, h_v^b = \left[C(\bar{\mathcal{P}})\bar{\xi}^{(0)}_{n,p}W^{(0)}\right]\Gamma\, Y^\dagger h_v^b,$$

followed by a renaming of the new decoupled hard-collinear fields by dropping

the superscript (0)

$$\left[C(\bar{\mathcal{P}})\bar{\xi}^{(0)}_{n,p}W^{(0)}\right]\Gamma\, Y^\dagger h_v^{(b)us} \longrightarrow \left[C(\bar{\mathcal{P}})\bar{\xi}_{n,p}W\right]\Gamma\, Y^\dagger h_v^b.$$

3. Match onto SCET_{II} at leading order by identifying usoft and hard-collinear fields with the soft and collinear fields of SCET_{II} respectively:

$$\left[C(\bar{\mathcal{P}})\bar{\xi}_{n,p}W\right]\Gamma\, Y^\dagger h_v^b \longrightarrow \left[C(\bar{\mathcal{P}})\bar{\xi}^{II}_{n,p}W^{II}\right]\Gamma\, S^\dagger h_v^b, \tag{4.96}$$

where we have denoted the SCET_{II} collinear fields with numeral II for clarity but is coventionally dropped. Note that we have identified the usoft Wilson line Y of SCET_{I} becomes the soft Wilson line S of SCET_{II} under the identification of the usoft and soft fields.

We note that one could have arrived at the above result by considering a direct matching from QCD onto SCET_{II} without using the intermediate theory SCET_{I} . We can write down a set of gauge and RPI invariant leading operators in SCET_{II} onto which QCD will be matched. Doing this we will immediately arrive at the SCET_{II} operator $\bar{\xi}_{n,p}W\ \Gamma\ S^\dagger h_v^b$. However, neither gauge invariance nor power counting can tell us the exact path of the Wilson line S from $-\infty$ to x since all the components of the soft fields A_s^μ scale the same way. The only way to determine this path of the soft Wilson line is through an explicit matching calculation which integrates out the $p^2 \sim Q\Lambda_{QCD}$ [63, 26] fluctuations generated from the soft-collinear interactions.

The procedure described above in which one goes through SCET_{I} as an intermediate step is a simpler alternative. In particular, the path of the Wilson line S is determined by the path of Y which was introduced in the field redefinitions of Eq. (4.71) in order to decouple hard-collinear and usoft modes in SCET_{I} .

Going through SCET_{I} becomes especially useful at subleading order where time ordered products in SCET_{I} and SCET_{II} can differ. In particular, time ordered products in SCET_{I} can induce non-trivial jet functions in SCET_{II} containing the physics of effects at the $\mu \sim \sqrt{Q\Lambda_{QCD}}$ scale. In this case matching directly from QCD to

$\mathrm{SCET_{II}}$ can become even more diffcult. On the other hand $\mathrm{SCET_I}$ gives well defined Feyman rules along with a power counting scheme for computing these non-trivial jet functions. We will explore such situations in detail in the next chapter when we apply SCET to color suppressed B-decays which proceed only at subleading order.

Chapter 5

Color Suppressed Decays

We are finally ready to consider applications of the SCET discussed in the last chapter. We focus on two body nonleptonic decays of $\bar{B}$ mesons. Typical decays of this kind are $\bar{B} \to D\pi$, $\bar{B} \to D^*\pi$, $\bar{B} \to D\rho$, $\bar{B} \to D^*\rho$, $\bar{B} \to DK$, $\bar{B} \to D^*K$, $\bar{B} \to DK^*$, $\bar{B} \to D^*K^*$, $\bar{B} \to D_sK^-$, $\bar{B} \to D_sK^{*-}$, ... and will be generically referred to as $\bar{B} \to D\pi$ decays. Since these decays are the simplest of a complicated array of hadronic channels a great deal of theoretical work has been devoted to their understanding [27, 50, 97, 5, 45, 36, 61, 41, 101, 29, 83, 21, 109, 96, 14, 47, 110, 82]. In subsequent chapters we also consider the color suppressed decays $\bar{B} \to D^{(*)}\{\eta, \eta', \phi, \omega\}$ where the light meson is an isosinglet and $\bar{B} \to D^{**}\pi$ type decays where the charmed meson is in an orbitally excited stated.

5.1 Color Allowed and Color Suppressed Decays

After integrating out the W-boson the weak Hamiltonian for $\bar{B} \to D\pi$ decays is

$$\mathcal{H}_W = \frac{G_F}{\sqrt{2}} V_{cb}V_{ud}^*[C_1(\mu)(\bar{c}b)_{V-A}(\bar{d}u)_{V-A} + C_2(\mu)(\bar{c}_i b_j)_{V-A}(\bar{d}_j u_i)_{V-A}]\,, \qquad (5.1)$$

where i, j are color indices, and for $\mu_b = 5\,\mathrm{GeV}$, $C_1(\mu_b) = 1.072$ and $C_2(\mu_b) = -0.169$ at NLL order in the NDR scheme [40]. For the Cabibbo suppressed $\mathcal{H}_W$ we replace $\bar{d} \to \bar{s}$ and $V_{ud}^* \to V_{us}^*$. It is convenient to categorize the decays into three classes [27],

depending on the role played by the spectator in the B meson (where "spectator" is a generic term for the flavor structure carried by the light degrees of freedom in the B). Class I decays receive contributions from graphs where the pion is emitted at the weak vertex (Fig. 5-1T), while in class II decays the spectator quark ends up in the pion (Figs. 5-1C,5-1E). Finally, class III decays receive both types of contributions. Many of these channels have been well studied experimentally [52, 4, 48, 2, 49, 103], see Table 5.1. Another method to categorize these decays makes use of amplitudes corresponding to the different Wick contractions of flavor topologies. These can be read off from Fig. 5-1 and are denoted as T (tree), C (color-suppressed), and E (W-exchange or weak annihilation).

5.1.1 Theoretical Status

Long ago, it was observed that approximating the matrix elements by the factorized product $\langle D|(\bar{c}b)_{V-A}|B\rangle\langle\pi|(\bar{d}u)_{V-A}|0\rangle$ gives an accurate prediction for the branching fractions of type-I decays, and a fair prediction for type-III decays. For all class-I and -II amplitudes a similar procedure was proposed [27]. In terms of two phenomenological parameters $a_{1,2}$,

$$iA(\bar{B}^0 \to D^+\pi^-) = \frac{G_F}{\sqrt{2}} V_{cb}V_{ud}^*\, a_1(D\pi)\, \langle D^+|(\bar{c}b)_{V-A}|\bar{B}^0\rangle\langle\pi^-|(\bar{d}u)_{V-A}|0\rangle\,, \quad (5.2)$$
$$iA(\bar{B}^0 \to D^0\pi^0) = \frac{G_F}{\sqrt{2}} V_{cb}V_{ud}^*\, a_2(D\pi)\, \langle\pi^0|(\bar{d}b)_{V-A}|\bar{B}^0\rangle\langle D^0|(\bar{c}u)_{V-A}|0\rangle\,.$$

Type-III amplitudes are related by isospin to linear combinations of type-I and II decays. Naive factorization[1] predicts the universal values $a_1 = C_1 + C_2/N_c$ and $a_2 = C_2 + C_1/N_c$. Phenomenological analyses testing the validity of the factorization hypothesis have been presented in [97], where typically contributions from E are not included. These contributions can be modeled using the vacuum insertion approximation which gives the $D \to \pi$ form factor at a large time-like momentum transfer

[1] We will use the phrase naive factorization to refer to factoring matrix elements of four quark operators even though this may not be a justified procedure, and will use the phrase factorization for results which follow from a well-defined limit of QCD.

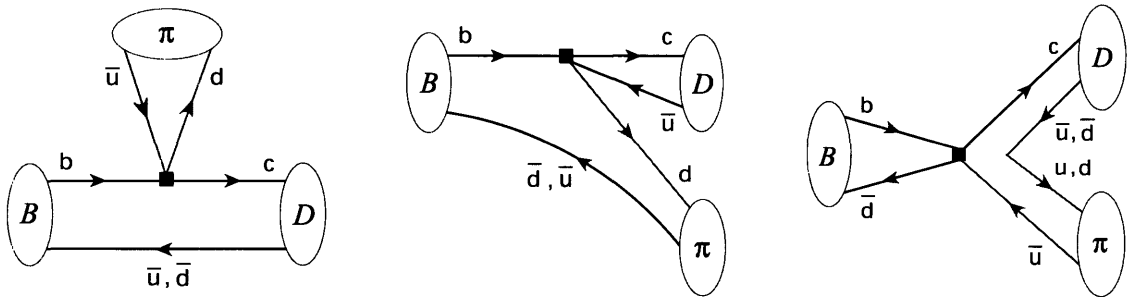

T: $\bar{B}^0 \to D^+\pi^-$, $B^- \to D^0\pi^-$ C: $B^- \to D^0\pi^-$, $\bar{B}^0 \to D^0\pi^0$ E: $\bar{B}^0 \to D^+\pi^-$, $\bar{B}^0 \to D^0\pi^0$

Figure 5-1: Decay topologies referred to as tree (T), color-suppressed (C), and W-exchange (E) and the corresponding hadronic channels to which they contribute.

$q^2 = m_B^2$. For this reason, they are often estimated to be suppressed relative to the T amplitudes by $\Lambda_{\rm QCD}^2/m_b^2$ [29].

One rigorous method for investigating factorization in these decays is based on the large N_c limit of QCD. In this limit the amplitudes for type-I decays start at $O(N_c^{1/2})$ while type-II decays are suppressed by $1/N_c$ (whence the name color-suppressed). The type-I amplitudes have a form similar to Eq. (5.2) since non-factorizable diagrams are suppressed, while type-II decays simultaneously receive contributions from factorized and non-factorizable diagrams. For a typical class-II decay, a Fierz transformation puts the amplitude into the form

$$\begin{aligned} iA(\bar{B}^0 \to D^0\pi^0) \;=\; & \frac{G_F}{\sqrt{2}} V_{cb}V_{ud}^*\Big\{\Big(C_2 + \frac{C_1}{N_c}\Big)\langle D^0\pi^0|(\bar{d}b)(\bar{c}u)|\bar{B}^0\rangle \\ & +2C_1\langle D^0\pi^0|(\bar{d}T^a b)(\bar{c}T^a u)|\bar{B}^0\rangle\Big\}. \end{aligned} \tag{5.3}$$

where the $(V-A)\otimes(V-A)$ structure is implicit. The two matrix elements have expansions in $1/N_c$ which start with terms of order $N_c^{1/2}$ and $N_c^{-1/2}$, respectively

$$\begin{aligned} &\frac{1}{N_c^{1/2}}\langle D^{(*)0}\pi^0|(\bar{d}b)(\bar{c}u)|\bar{B}^0\rangle = F_0^{(*)} + \frac{1}{N_c^2}F_2^{(*)} + \cdots \\ &\frac{1}{N_c^{1/2}}\langle D^{(*)0}\pi^0|(\bar{d}T^a b)(\bar{c}T^a u)|\bar{B}^0\rangle = \frac{1}{N_c}G_1^{(*)} + \frac{1}{N_c^3}G_3^{(*)} + \cdots, \end{aligned} \tag{5.4}$$

where $F_i^{(*)} \sim N_c^0$, $G_i^{(*)} \sim N_c^0$. The Wilson coefficients in Eq. (5.1) can be assigned

scalings with N_c following from their perturbative expansions $C_1 \sim O(1)$, $C_2 \sim N_c^{-1}$, which roughly corresponds to the hierarchy in their numerical values at μ_b. The leading terms are the matrix elements $F_0^{(*)}$, which factor in terms of large N_c form factors and decay constants

$$N_c^{1/2} F_0^{(*)} \sim \langle D^{(*)0}|\bar{c}u|0\rangle\langle\pi^0|\bar{d}b|\bar{B}^0\rangle + \langle D^{(*)0}\pi^0|\bar{c}u|0\rangle\langle 0|\bar{d}b|\bar{B}^0\rangle\,, \tag{5.5}$$

plus the matrix elements $G_1^{(*)}$ which are nonfactorizable. The naive factorization assumption would keep only $F_0^{(*)}$ and neglect $G_1^{(*)}$. This approximation is not justified in the $1/N_c$ expansion since $G_1^{(*)}$ is enhanced by the large Wilson coefficient C_1. In either case, no prediction is obtained for the ratio of the $\bar{B} \to D\pi$ and $\bar{B} \to D^*\pi$ amplitudes,

$$R_0^\pi \equiv \frac{A(\bar{B}^0 \to D^{*0}\pi^0)}{A(\bar{B}^0 \to D^0\pi^0)} = \frac{(C_2 + C_1/N_c)F_0^* + (2C_1/N_c)G_1^*}{(C_2 + C_1/N_c)F_0 + (2C_1/N_c)G_1}\,. \tag{5.6}$$

Heavy quark symmetry does not operate with large N_c factorization because for C and E it is broken by the allowed exchange of energetic hard gluons between the heavy quarks and the quarks in the pion. In contrast, we will show that expanding about the limit $E_\pi \gg \Lambda$ this ratio is predicted to be 1 at leading order in Λ/Q. Here $\Lambda \sim \Lambda_{\rm QCD}$ is a typical hadronic scale.

Another rigorous approach to factorization becomes possible in the limit $E_\pi \gg \Lambda_{\rm QCD}$ which corresponds to having an energetic light hadron in the final state. In this thesis we analyze type-II decays using QCD and an expansion in $\Lambda_{\rm QCD}/m_b$, $\Lambda_{\rm QCD}/m_c$, and $\Lambda_{\rm QCD}/E_\pi$ (or generically $\Lambda_{\rm QCD}/Q$ where $Q = \{m_b, m_c, m_b - m_c\}$). We derive a factorization theorem and show that E and C appear at the same order in the power counting, and are suppressed by $\Lambda_{\rm QCD}/Q$ relative to T. Arguments for the suppression of C by $(\Lambda_{\rm QCD}/Q)^1$ and E by $(\Lambda_{\rm QCD}/Q)^{1,2}$ appear in the literature [29], but we are unaware of a derivation that is model independent. Our leading order result disagrees with the a_2-factorization result. Instead the amplitudes for $\bar{B}^0 \to D^{(*)0}\pi^0$ and $\bar{B}^0 \to D^{(*)0}\rho^0$ are determined by the leading light-cone wavefunctions $\phi_{\pi,\rho}$, and two new universal $\bar{B} \to D^{(*)}$ distribution functions. Long distance contributions also

occur at this order in $\Lambda_{\rm QCD}/Q$, but are shown to be suppressed relative to the short distance contributions by an additional $\alpha_s(Q)/\pi$.

For type-I decays a color transparency [35] argument given by Bjorken suggested $A(\bar{B}^0 \to D^+\pi^-) \simeq (C_1 + C_2/N_c) f_\pi F_0^{BD}(m_\pi^2) + O(\alpha_s(Q))$. In Ref. [50] it was argued that this factorization is the leading order prediction in the large energy limit $E_\pi \gg \Lambda_{\rm QCD}$, and in Refs. [101, 29] that α_s corrections can be rigorously included. This factorization was extended to all orders in α_s with the proof of a factorization theorem using the soft-collinear effective theory [21]

$$A(B \to D^{(*)}\pi) = N^{(*)}\, \xi(w_0,\mu) \int_0^1 dx\, T^{(*)}(x, m_c/m_b, \mu)\, \phi_\pi(x,\mu) + \dots\,, \tag{5.7}$$

where the ellipses denote power suppressed terms. This result is similar to predictions obtained from the hard exclusive scattering formalism of Brodsky-Lepage [80], except for the presence of the Isgur-Wise function, $\xi(\omega_0,\mu)$. The normalization factor is given by [2]

$$N^{(*)} = \frac{G_F V_{cb} V_{ud}^*}{\sqrt{2}}\, E_\pi f_\pi \sqrt{m_{D^{(*)}} m_B}\, \Big(1 + \frac{m_B}{m_{D^{(*)}}}\Big)\,. \tag{5.8}$$

The proof of Eq. (5.7) uses the heavy quark limit, so $m_D = m_{D^*}$ and $N = N^*$. In Eq. (5.7), $\phi_\pi(x,\mu)$ is the non-perturbative pion light-cone wave function, and $\xi(w_0,\mu)$ is evaluated at maximum recoil $v\cdot v' \to w_0 = (m_B^2 + m_{D^{(*)}}^2)/(2 m_B m_{D^{(*)}})$. The hard coefficient $T^{(*)}(x,\mu) = C_{L\pm R}^{(0)}((4x-2)E_\pi, \mu, m_b)$, where the $\pm$ correspond to the D and D^* respectively, and $C_{L\pm R}^{(0)} = C_L^{(0)} \pm C_R^{(0)}$ is the calculable Wilson coefficient of the operators defined in Eq. (5.19) below. The renormalization scale dependence of the hard scattering function $T(x,\mu)$ cancels the μ dependence in the Isgur-Wise function and pion wave function. In this framework [29] there is no longer a need to identify by hand a factorization scale.[3] In the language of SCET [21], the scale dependence

[2] Note for longitudinal D^*, $n\cdot\varepsilon_{D^*} = n\cdot v'$. Production of transverse ρ's is suppressed by Λ/Q.

[3] In naive factorization the hadronic matrix elements in Eq. (5.2) are independent of the scale that separates hard and soft physics. The scale dependence in a_1 and a_2 then causes the physical amplitudes to become scale dependent. The parameters a_1 and a_2 were therefore assumed to be evaluated at a specific scale called the "factorization scale". In other words, the non-factorizable effects were accounted for by allowing a_1 and a_2 to be free parameters that are fit to data. The

is understood from the matching and running procedure.

Eq. (5.7) implies equal rates for $\bar{B}^0 \to D^+\pi^-$ and $\bar{B}^0 \to D^{*+}\pi^-$ up to the $\alpha_s(m_b)$ corrections in $T^{(*)}$ and power corrections. This prediction is in good agreement with the observed data for type-I and III decays to π, ρ, K and K^* as shown in Tables I and II. For two-body type-I decays both the large N_c and large energy mechanisms make similar phenomenological predictions. However, these mechanisms can be distinguished with $B \to DX$ decays where X is a multi-hadron state [14].

So far, no results of comparable theoretical rigor exist for the color-suppressed type-II decays. In fact existing results in $B \to D\pi$ and $B \to \psi K^{(*)}$ do not support naive factorization with a universal coefficient a_2 [96]. Furthermore, it has been argued that in general factorization will not hold for type-II decays [29].

Using the soft-collinear effective theory (SCET) [16, 22], we prove a factorization theorem for color-suppressed (type-II) $\bar{B} \to DM$ decays, $M = \{\pi^0, \rho^0, \ldots\}$. These decays are power suppressed relative to the type I decays, and our results are valid at leading nonvanishing order in Λ/Q. The main results of our analysis are

- The color suppressed (C) and exchange (E) contributions to $B^0 \to D^{(*)0}\pi^0$ are both suppressed by Λ/Q relative to the amplitude (T). The C and E amplitudes are found to be of comparable size since the factorization theorem relates them to the same perturbative and non-perturbative quantities. Our result is incompatible with the naive a_2 type factorization.

- When our result is combined with heavy quark symmetry it predicts the equality of the amplitudes for $\bar{B}^0 \to D^0\pi^0$ and $\bar{B}^0 \to D^{*0}\pi^0$ (in fact for any DM and D^*M). This prediction is in good agreement with existing data and will be tested by future measurements.

- Our result gives a new mechanism for generating non-perturbative strong phases for exclusive decays within the framework of factorization. For DM and D^*M it implies the equality of the strong phases δ between isospin amplitudes. Furthermore, certain cases with different light mesons M are predicted to also have

factorization scale can then be extracted from the scale dependence of a_1 and a_2 [97].

a universal non-perturbative strong phase ϕ in their isospin triangle.

- The power suppressed amplitudes for all color suppressed $\bar{B} \to D^{(*)}M$ decays are factorizable into two types of terms, which we refer to as short distance ($\mu^2 \sim E_M\Lambda$) and long distance ($\mu^2 \sim \Lambda^2$) contributions. The short distance contributions depend on complex soft $B^0 \to D^{(*)0}$ distribution functions, $S^{(0,8)}_{L,R}(k_+, \ell_+)$, which depend only on the direction of M (the superscripts indicate that two color structures contribute). For $M = \pi, \rho$ the long distance contributions vanish at lowest order in $\alpha_s(Q)/\pi$.

Combined with Eq. (5.7) the results here give a complete leading order description of the $B \to D\pi$ isospin triangles.

In Section 5.1.2 we review the current data for $B \to D\pi$ decays. The derivation of a factorization theorem for the color suppressed channels $\bar{B}^0 \to D^{(*)0}\pi^0$ and $\bar{B}^0 \to D^{(*)0}\rho^0$ is carried out in section 5.1.3 using SCET. Then in section 5.1.4 the formalism is applied to decays with kaons, $\bar{B}^0 \to D^{(*)0}K^0$, $\bar{B}^0 \to D^{(*)0}K^{*0}$, $\bar{B}^0 \to D_s^{(*)}K^-$, and $\bar{B}^0 \to D_s^{(*)}K^{*-}$. In section 5.1.5 we contrast our results with the large N_c limit of QCD and prior theoretical expectations. Readers only interested in final results can safely skip sections 5.1.3, 5.1.4, and 5.1.5. In section 5.1.6 we discuss the phenomenological predictions that follow from our new formalism for color suppressed channels. Conclusions are given in 5.1.7. In Appendix 9.1 we prove that for π^0 and ρ^0 the long distance contributions are suppressed. Finally in Appendices B and C we elaborate on the properties of the jet functions and our new soft $B \to D^{(*)}$ distribution functions respectively.

5.1.2 Data

We start by reviewing existing data on the $\bar{B} \to D^{(*)}\pi$ decays. The branching ratios for most of these modes have been measured and the existing results are collected in Table 5.1. Taking into account that the $D^{(*)}\pi$ final state can have isospin $I = 1/2, 3/2$,

these decays can be parameterized by 2 isospin amplitudes $A_{1/2}$, $A_{3/2}$:

$$\begin{aligned} A_{+-} = A(\bar{B}^0 \to D^+\pi^-) &= \frac{1}{\sqrt{3}}A_{3/2} + \sqrt{\frac{2}{3}}A_{1/2} = T + E\,, \\ A_{0-} = A(B^- \to D^0\pi^-) &= \sqrt{3}A_{3/2} = T + C\,, \\ A_{00} = A(\bar{B}^0 \to D^0\pi^0) &= \sqrt{\frac{2}{3}}A_{3/2} - \frac{1}{\sqrt{3}}A_{1/2} = \frac{1}{\sqrt{2}}(C - E)\,. \end{aligned} \tag{5.9}$$

Similar expressions can be written for the decay amplitudes of $B \to D^*\pi$, $B \to D\rho$, $B \to D^*\rho$ with well defined helicity of the final state vector mesons. Eq. (5.9) also gives the alternative parameterization of these amplitudes in terms of the amplitudes T, C, E.

Using the data in Table 5.1, the individual isospin amplitudes A_I and their relative phase $\delta = \arg(A_{1/2}A^*_{3/2})$ can be extracted using

$$\mathrm{Br}(\bar{B} \to D^{(*)}M) = \tau_B\Gamma(\bar{B} \to D^{(*)}M) = \frac{\tau_B|\mathbf{p}|}{8\pi m_B^2}\sum_{\mathrm{pol}}|A(\bar{B} \to D^{(*)}M)|^2\,. \tag{5.10}$$

with $\tau_{\bar{B}^0} = 2.343 \times 10^{12}\,\mathrm{GeV}^{-1}$ and $\tau_{B^-} = 2.543 \times 10^{12}\,\mathrm{GeV}^{-1}$. We find

$$\begin{aligned} |A^D_{1/2}| &= (4.33 \pm 0.47) \times 10^{-7}\ \mathrm{GeV}\,, \qquad \delta^{D\pi} = 30.5^{\circ}{}^{+7.8}_{-13.8}\,, \\ |A^D_{3/2}| &= (4.45 \pm 0.17) \times 10^{-7}\ \mathrm{GeV}\,, \\ |A^{D^*}_{1/2}| &= (4.60 \pm 0.36) \times 10^{-7}\ \mathrm{GeV}\,, \qquad \delta^{D^*\pi} = 30.2 \pm 6.6^{\circ}\,, \\ |A^{D^*}_{3/2}| &= (4.33 \pm 0.19) \times 10^{-7}\ \mathrm{GeV}\,. \end{aligned} \tag{5.11}$$

The ranges for δ correspond to 1σ uncertainties for the experimental branching ratios. A graphical representation of these results is given in Fig. 5-6, where we show contour plots for the ratios of isospin amplitudes $R_I = A_{1/2}/(\sqrt{2}A_{3/2})$ for both $D\pi$ and $D^*\pi$ final states. For $\bar{B} \to D\pi$ an isospin analysis was performed recently by CLEO [4] including error correlations among the decay modes; we used their analysis in quoting errors on $\delta^{D\pi}$.

Decay	Br(10^{-3})	$\|A\|$ (10^{-7} GeV)	Decay	Br(10^{-3})	$\|A\|$ (10^{-7} GeV)
$\bar{B}^0 \to D^+\pi^-$	2.68 ± 0.29 [a]	5.89 ± 0.32	$\bar{B}^0 \to D^{*+}\pi^-$	2.76 ± 0.21	6.05 ± 0.23
$B^- \to D^0\pi^-$	4.97 ± 0.38 [a]	7.70 ± 0.29	$B^- \to D^{*0}\pi^-$	4.6 ± 0.4	7.49 ± 0.33
$\bar{B}^0 \to D^0\pi^0$	0.292 ± 0.045 [b]	1.94 ± 0.15	$\bar{B}^0 \to D^{*0}\pi^0$ [b]	0.25 ± 0.07	1.82 ± 0.25
$\bar{B}^0 \to D^+\rho^-$	7.8 ± 1.4	10.2 ± 0.9	$\bar{B}^0 \to D^{*+}\rho^-$	6.8 ± 1.0 [c]	9.08 ± 0.68 [†]
$B^- \to D^0\rho^-$	13.4 ± 1.8	12.8 ± 0.9	$B^- \to D^{*0}\rho^-$	9.8 ± 1.8 [c]	10.5 ± 0.97 [†]
$\bar{B}^0 \to D^0\rho^0$	0.29 ± 0.11 [d]	1.97 ± 0.37	$\bar{B}^0 \to D^{*0}\rho^0$	< 0.56	< 2.77

Table 5.1: Data on $B \to D^{(*)}\pi$ and $B \to D^{(*)}\rho$ decays from [a]Ref.[4], [b]Ref.[48, 2], [c]Ref.[49], [d]Ref.[103], or if not otherwise indicated from Ref.[52]. [†]For $\bar{B} \to D^*\rho$ the amplitudes for longitudinally polarized ρ's are displayed. The above data is as of June 2003.

For later convenience we define the amplitude ratios

$$R_0^M \equiv \frac{A(\bar{B}^0 \to D^{*0}M^0)}{A(\bar{B}^0 \to D^0M^0)}, \qquad R_0^{M/M'} \equiv \frac{A(\bar{B}^0 \to D^{(*)0}M^0)}{A(\bar{B}^0 \to D^{(*)0}M'^0)}, \tag{5.12}$$

$$R_I \equiv \frac{A_{1/2}}{\sqrt{2}A_{3/2}} = 1 - \frac{3}{2}\frac{C-E}{T+C}, \qquad R_c \equiv \frac{A(\bar{B}^0 \to D^{(*)+}M^-)}{A(B^- \to D^{(*)0}M^-)} = 1 - \frac{C-E}{T+C},$$

where the ratios R_I and R_c are defined for each $D^{(*)}M$ mode. Predictions are obtained for the ratios in Eq. (5.12), including the leading power corrections to R_I and R_c. The relation $R_I = 1 + \mathcal{O}(\Lambda/Q)$ can be represented graphically by a triangle with base normalized to 1 (see Fig. 5-6 in section 5.1.6). The two angles adjacent to the base are the strong isospin phase δ, and another strong phase ϕ. The usual prediction is that $\delta \sim 1/Q^k$ [29, 96], and that there is no constraint on the strong phase ϕ which can be large. In section 5.1.6 we show that at lowest order the angle ϕ is predicted to be the same for all channels in Table 5.1, and that δ can be dominated by a constrained non-perturbative strong phase. From R_I in Eq. (5.12) we note that for a leading order prediction of δ it is not necessary to know the power corrections to the T amplitude.

A similar analysis can be given for the Cabibbo suppressed $\bar{B} \to DK^{(*)}$ decays. Although several of these modes had been seen for some time, it is only recently that some of the corresponding class-II decays have been seen by the Belle Collaboration [72] (see Table II). For this case the final $D^{(*)}K^{(*)}$ states can have isospins $I = 0, 1$, so these decays are parameterized in terms of 2 isospin amplitudes $A_{I=0,1}$ (for given

Decay	Br(10^{-5})	$\|A\|$ (10^{-7} GeV)	Decay	Br(10^{-5})	$\|A\|$ (10^{-7} GeV)
$\bar{B}^0 \to D^+K^-$	20.0 ± 6.0	1.62 ± 0.24	$\bar{B}^0 \to D^{*+}K^-$	20 ± 5	1.64 ± 0.20
$B^- \to D^0K^-$	37.0 ± 6.0	2.11 ± 0.17	$B^- \to D^{*0}K^-$	36 ± 10	2.11 ± 0.29
$\bar{B}^0 \to D^0\bar{K}^0$	$5.0^{+1.1}_{-1.2} \pm 0.6$ [72]	0.81 ± 0.11	$\bar{B}^0 \to D^{*0}\bar{K}^0$	–	–
$\bar{B}^0 \to D^+K^{*-}$	37.0 ± 18.0	2.24 ± 0.54	$\bar{B}^0 \to D^{*+}K^{*-}$	38 ± 15	$2.30 \pm 0.45^\dagger$
$B^- \to D^0K^{*-}$	61.0 ± 23.0	2.76 ± 0.52	$B^- \to D^{*0}K^{*-}$	72 ± 34	$3.03 \pm 0.72^\dagger$
$\bar{B}^0 \to D^0\bar{K}^{*0}$	$4.8^{+1.1}_{-1.0} \pm 0.5$ [72]	0.81 ± 0.11	$\bar{B}^0 \to D^{*0}\bar{K}^{*0}$	–	–

Table 5.2: Data on Cabibbo suppressed $\bar{B} \to DK^{(*)}$ decays. Unless otherwise indicated, the data is taken from Ref.[52]. †Since no helicity measurements for D^*K^* are available we show effective amplitudes which include contributions from all three helicities.The above data is as of June 2003.

spins of the final particles)

$$\begin{aligned} A_{+-} = A(\bar{B}^0 \to D^+K^-) &= \frac{1}{2}A_0 + \frac{1}{2}A_1 = T\,, \\ A_{0-} = A(B^- \to D^0\,K^-) &= A_1 = T + C\,, \\ A_{00} = A(\bar{B}^0 \to D^0\,K^0) &= \frac{1}{2}A_1 - \frac{1}{2}A_0 = C\,. \end{aligned} \tag{5.13}$$

Isospin symmetry implies the amplitude relation among these modes $A_{+-} + A_{00} = A_{0-}$, which can be used to extract the isospin amplitudes $A_{0,1}$ and their relative phase $\delta = \arg(A_0 A_1^*)$. Using Gaussian error propagation we obtain

$$\begin{aligned} |A_0^{DK}| &= (1.45 \pm 0.62) \times 10^{-7}\ \text{GeV}, \qquad \delta^{DK} = 49.9 \pm 9.5^\circ \\ |A_1^{DK}| &= (2.10 \pm 0.17) \times 10^{-7}\ \text{GeV}, \end{aligned} \tag{5.14}$$

$$\begin{aligned} |A_0^{DK^*}| &= (1.93 \pm 1.49) \times 10^{-7}\ \text{GeV}, \qquad \delta^{DK^*} = 34.9 \pm 19.4^\circ \\ |A_1^{DK^*}| &= (2.76 \pm 0.52) \times 10^{-7}\ \text{GeV}. \end{aligned} \tag{5.15}$$

However, note that scanning the amplitudes A_{+-}, A_{00}, A_{0-} in their 1σ allowed regions still allows a flat isospin triangle [47].

5.1.3 SCET Analysis: Factorization

Observing the decay in the rest frame of the B meson, one can identify two types of degrees of freedom with offshellness $p^2 \sim \Lambda_{QCD}^2$ that are responsible for binding the hadrons. These are the collinear $(p^+, p^-, p_\perp) \sim Q(\eta^2, 1, \eta)$ and soft $(p^+, p^-, p_\perp) \sim Q(\eta, \eta, \eta)$ degrees of freedom where $\eta \sim \Lambda_{QCD}/Q$. The formalism of SCET allows us to construct an effective theory of this process directly in terms of these relevant soft and collinear modes with all other offshell modes integrated out. This effective theory at the hadronic scale is given the name SCET_{II} [4].

The $\bar{B} \to D^{(*)}M$ processes receive contributions from various effects occuring at different distance scales. A complete description of these decays requires us to flow between effective theories from the electroweak scale down to the hadronic scale. Each effective theory along the way contributes the neccessary mechanism for the decay to proceed. These mechanisms are encoded as effective operators with appropriate Wilson coefficients in the next effective theory on our way down to SCET_{II} at the hadronic scale.

The $b \to c$ quark flavor changing process occurs at the electroweak scale ($p^2 \sim m_W^2$) through a W-exchange process. The W boson is then integrated out to give the effective Hamiltonian of Eq. (5.1). This Hamiltonian gives rise to the three distinct topologies through which the decay can proceed as shown in Fig. 5-1.

Next we would like to match H_W onto operators in SCET_{II} with soft and collinear degrees of freedom. However, the soft-collinear interactions produce offshell modes $p^2 \sim Q\Lambda_{QCD}$ that are not present in SCET_{II} . These modes have momentum scalings $(p^+, p^-, p_\perp) \sim Q(\eta, 1, \eta)$ and have to be integrated out [22]. Instead, as discussed in the last chapter, it is more convenient to go through an intermediate effective theory SCET_{I} [23] at the scale $Q\Lambda_{QCD}$ and do the matching in two steps. SCET_{I} is a theory of ultrasoft $(p^+, p^-, p_\perp) \sim Q(\lambda^2, \lambda^2, \lambda^2)$ and hard-collinear $(p^+, p^-, p^\perp) \sim Q(\lambda^2, 1, \lambda)$ modes where $\lambda = \sqrt{\eta} = \sqrt{\frac{\Lambda_{QCD}}{Q}}$. The ultrasoft modes are identical to the soft modes

[4] The soft-collinear messenger modes of Ref. [28] could play a role in subleading corrections which we will not consider. The nature of these messenger modes is still unclear due to their dependence on the choice of infrared regulator [33, 15].

Theory	Scale	Wilson Coefficients	Physics Effect
SM	$\mu^2 \sim m_W^2$	-	$b \to c$ quark flavor transition
H_W	$\mu^2 \sim Q^2$	C_1, C_2	W boson integrated out
SCET_I	$\mu^2 \sim Q\Lambda_{QCD}$	C_L, C_R	soft-collinear transitions
SCET_II	$\mu^2 \sim \Lambda_{QCD}^2$	J	binding of hadrons

Table 5.3: The effective theories at different distance scales and the effects they provide for the $B \to DM$ process to occur. The Wilson coefficients that show up in each theory are also given.

and the hard-collinear modes play the role of the offshell modes produced by the soft-collinear interactions in SCET_II . The hard-collinear modes are eventually matched onto the collinear modes of SCET_II . This two step matching procedure allows us to avoid dealing directly with non-local interactions, altough it is also possible to construct SCET_II directly from QCD [63]. In summary, one arrives at the effective theory SCET_II at the hadronic scale through a series of matching and running procedures starting with the Standard Model(SM)

$$SM \to H_W \to \text{SCET}_\text{I} \to \text{SCET}_\text{II} .$$

In the above chain of effective theories, each matching calculation introduces Wilson coefficients which encode the physics of harder scales. These ideas are summarized in Table 5.3 and are illustrated in Fig. 3. We now briefly review the details of the procedure just discussed.

We start by reviewing type-I decays. Using SCET, the factorization of the leading amplitude for type-I decays has been proven in Ref. [21] at leading order in $1/Q$ (and non-perturbatively to all orders in α_s). The operators in Eq. (5.1) are matched onto effective operators at a scale $\mu_Q \simeq Q$

$$\sum_{1,2} C_i O_i \to 4 \sum_{j=L,R} \int d\tau_1 d\tau_2 [C_j^{(0)}(\tau_1,\tau_2) \mathcal{Q}_j^{(0)}(\tau_1,\tau_2) + C_j^{(8)}(\tau_1,\tau_2) \mathcal{Q}_j^{(8)}(\tau_1,\tau_2)] . \quad (5.16)$$

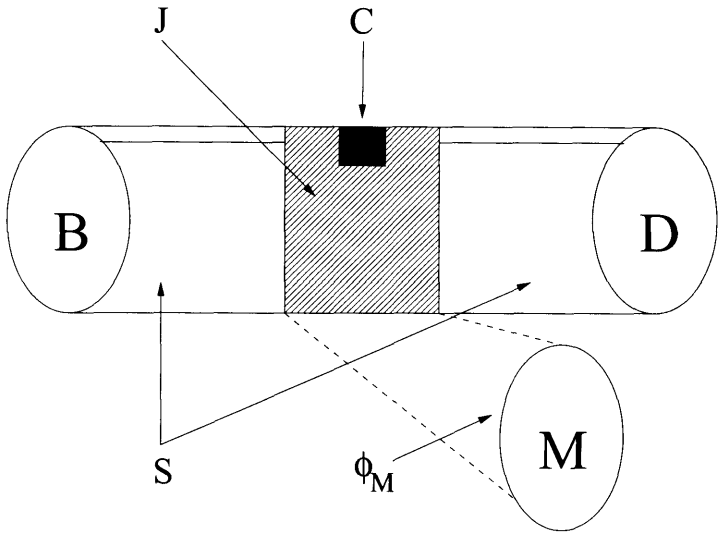

Figure 5-2: A schematic representation of the $B \to DM$ process and the contributions it receives from effects at different distance scales. The shaded black box is the weak vertex where the $b \to c$ transition takes place, the shaded grey region is where soft spectator quarks are converted to collinear quarks that end up in the light meson, and the unshaded regions are where non-perturbative processes responsible for binding of hadrons take place. These regions correspond to the functions C, J, S, and ϕ_M as labeled in the figure. For the color allowed modes, where the light meson is produced directly at the weak vertex and no soft-collinear transitions involving the spectator quarks are required, the jet function J is trivially just one.

At leading order in $\mathrm{SCET_I}$ there are four operators $[j = L, R]$

$$\begin{aligned} \mathcal{Q}_j^{(0)}(\tau_1,\tau_2) &= [\bar{h}_{v'}^{(c)}\Gamma_j^h h_v^{(b)}][(\bar{\xi}_n^{(d)}W)_{\tau_1}\Gamma_n(W^\dagger\xi_n^{(u)})_{\tau_2}]\,, \\ \mathcal{Q}_j^{(8)}(\tau_1,\tau_2) &= [\bar{h}_{v'}^{(c)}Y\Gamma_j^h T^a Y^\dagger h_v^{(b)}][(\bar{\xi}_n^{(d)}W)_{\tau_1}\Gamma_n T^a(W^\dagger\xi_n^{(u)})_{\tau_2}]\,. \end{aligned} \tag{5.17}$$

The superscript $(0,8)$ denotes the $1 \otimes 1$ and $T^a \otimes T^a$ color structures. The Dirac structures on the heavy side are $\Gamma_{L,R}^h = \not{v} P_{L,R}$ with $P_{R,L} = \frac{1}{2}(1 \pm \gamma_5)$, while on the collinear side we have $\Gamma_n = \not{\bar{n}} P_L/2$. The momenta labels are defined by $(W^\dagger\xi_n)_{\omega_2} = [\delta(\omega_2 - \bar{\mathcal{P}})\, W^\dagger\xi_n]$.

The matching conditions for the Wilson coefficients at tree level at $\mu = E_\pi$ are

$$C_L^{(0)}(\tau_i) = C_1 + \frac{C_2}{N_c}\,, \qquad C_L^{(8)}(\tau_i) = 2C_2\,, \qquad C_R^{(0,8)}(\tau_i) = 0\,. \tag{5.18}$$

Matching corrections of order $\mathcal{O}(\alpha_s)$ can be found in Ref. [29].

The operators in Eq. (5.17) are written in terms of collinear fields which do not couple to usoft particles at leading order. This was achieved by a decoupling field redefinition [22] on the collinear fields $\xi_n \to Y\xi_n$ etc. The operators in Eq. (5.17) are then matched onto $\mathrm{SCET_{II}}$ to give $[\omega_i = \tau_i]$

$$\begin{aligned} \mathcal{Q}_j^{(0)}(\omega_1,\omega_2) &= [\bar{h}_{v'}^{(c)}\Gamma_j^h h_v^{(b)}][(\bar{\xi}_n^{(d)}W)_{\omega_1}\Gamma_n(W^\dagger\xi_n^{(u)})_{\omega_2}]\,, \\ \mathcal{Q}_j^{(8)}(\omega_1,\omega_2) &= [\bar{h}_{v'}^{(c)}S\Gamma_j^h T^a S^\dagger h_v^{(b)}][(\bar{\xi}_n^{(d)}W)_{\omega_1}\Gamma_n T^a(W^\dagger\xi_n^{(u)})_{\omega_2}]\,, \end{aligned} \tag{5.19}$$

where the collinear and soft Wilson lines W and S are defined in Eq. (9.15) of Appendix 9.3. At leading order in $1/Q$ only the operators $\mathcal{Q}_{L,R}^{(0)}$ and the leading order collinear and soft Lagrangians ($\mathcal{L}_c^{(0)}$, $\mathcal{L}_s^{(0)}$), contribute to the $B^- \to D^{(*)0}\pi^-$ and $\bar{B}^0 \to D^{(*)+}\pi^-$ matrix elements. The matrix elements of $\mathcal{Q}_{L,R}^{(8)}$ vanish because they factorize into a product of bilinear matrix elements and the octet currents give vanishing contribution between color singlet states [21].

Note that we take the pion state or interpolating field to be purely collinear and the B and $D^{(*)}$ states to be purely soft. Power corrections to these states are included as time ordered products. This includes asymmetric configurations containing one soft and one collinear quark which involve T-products with subleading Lagrangians [23].

Next we consider type-II decays. The matrix elements of the leading order operators vanish, $\langle D^0\pi^0|Q_j^{(0,8)}|\bar{B}^0\rangle = 0$. This occurs due to a mismatch between the type of quarks produced by $\mathcal{Q}_j^{(0,8)}$ and those required for the light meson state, where we need two collinear quarks of the same flavor. The operator $\mathcal{Q}_j^{(0,8)}$ produces collinear quarks with (du) flavor. Therefore it can not produce a π^0 since the leading order SCET Lagrangian only produces or annihilates collinear quark pairs of the same flavor. For this reason the leading contributions to $\bar{B}^0 \to D^{(*)0}\pi^0$ are power suppressed.

In $\mathrm{SCET_I}$ there are several sources of power suppressed contributions obtained by including higher order four quark operators, higher order contributions from the Lagrangians, or both. However, there is only a *single type of $SCET_I$ operator* which contributes to $\bar{B}^0 \to D^{(*)0}M^0$ decays at leading order. They are given by T-ordered

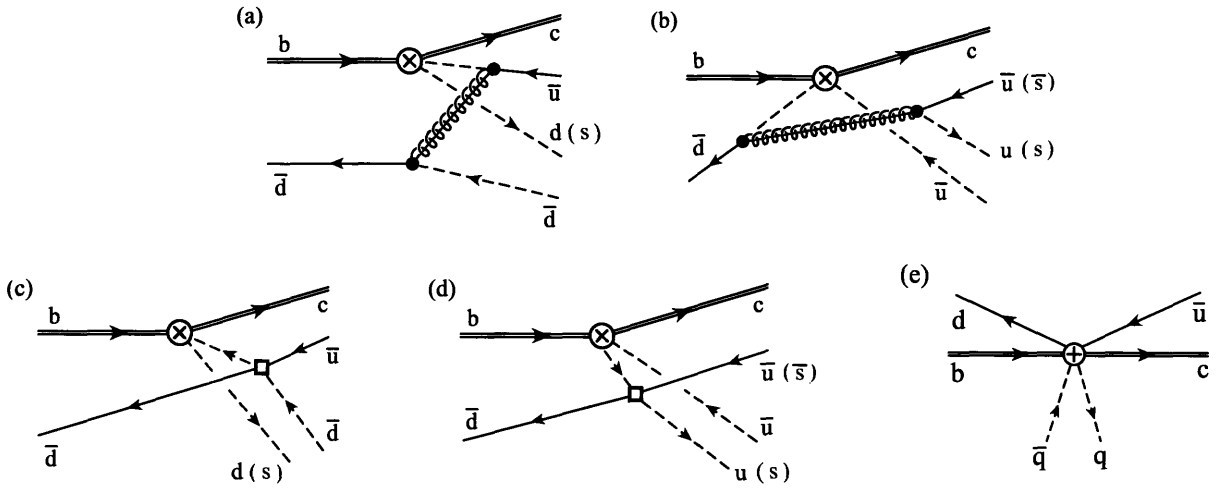

Figure 5-3: Graphs for the tree level matching calculation from $\mathrm{SCET_I}$ (a,b) onto $\mathrm{SCET_{II}}$ (c,d,e). The dashed lines are collinear quark propagators and the spring with a line is a collinear gluon. Solid lines in (a,b) are ultrasoft and those in (c,d,e) are soft. The $\otimes$ denotes an insertion of the weak operator, given in Eq. (5.17) for (a,b) and in Eq. (5.19) in (c,d). The $\oplus$ in (e) is a 6-quark operator from Eq. (5.27). The two solid dots in (a,b) denote insertions of the mixed usoft-collinear quark action $\mathcal{L}^{(1)}_{\xi q}$. The boxes denote the $\mathrm{SCET_{II}}$ operator $\mathcal{L}^{(1)}_{\xi\xi qq}$ in Eq. (5.24).

products of the leading operators in Eq. (5.17) with two insertions of the usoft-collinear Lagrangian $\mathcal{L}^{(1)}_{\xi q}$:

$$T_j^{(0,8)} = \frac{1}{2}\int d^4x\, d^4y\; T\{\mathcal{Q}_j^{(0,8)}(0)\,, i\mathcal{L}^{(1)}_{\xi q}(x)\,, i\mathcal{L}^{(1)}_{\xi q}(y)\}\,. \tag{5.20}$$

Here the subleading Lagrangian is [31, 23]

$$\mathcal{L}^{(1)}_{\xi q} = (\bar\xi_n W)\Big(\frac{1}{\bar{\mathcal{P}}}\, W^\dagger ig\, \not{B}^c_\perp W\Big) q_{us} - \bar q_{us}\Big(W^\dagger ig\, \not{B}^c_\perp W \frac{1}{\bar{\mathcal{P}}^\dagger}\Big)(W^\dagger \xi_n)\,, \tag{5.21}$$

where $ig\not{B}^c_\perp = [i\bar n\cdot D^c, i\not{D}^c_\perp]$. The two factors of $i\mathcal{L}^{(1)}_{\xi q}$ in Eq. (5.20) are necessary to swap one u quark and one d quark from ultrasoft to collinear. In contrast to the tree amplitude, for this case both the $\mathcal{Q}_j^{(0)}$ and $\mathcal{Q}_j^{(8)}$ operators can contribute. By power counting, the $T_j^{(0,8)}$'s are suppressed by $\lambda^2 = \Lambda/Q$ relative to the leading operators. They will give order Λ/Q contributions in $\mathrm{SCET_{II}}$, in agreement with our earlier statements.

In Fig. 6-2 we show graphs contributing to the matching of $\mathrm{SCET_I}$ operators (a,b) onto operators in $\mathrm{SCET_{II}}$ (c,d,e). In Figs. 6-2a,b the gluon always has offshellness $p^2 \sim E_M\Lambda$ due to momentum conservation, and is shrunk to a point in $\mathrm{SCET_{II}}$. However, the collinear quark propagator in (a,b) can either have $p^2 \sim E_M\Lambda$ giving rise to the short distance $\mathrm{SCET_{II}}$ contribution in Fig. 6-2e, or it can have $p^2 \sim \Lambda^2$ which gives the long distance $\mathrm{SCET_{II}}$ contribution in Figs. 6-2c,d. To match onto the short distance contribution in Fig. 6-2e we subtract the $\mathrm{SCET_{II}}$ diagrams (c,d):

$$(a) + (b) - (c) - (d) = (e)\,. \tag{5.22}$$

The operators in Figs. 6-2a,b are from the T-products $T_j^{(0,8)}$ in Eq. (5.20), while Figs. 6-2c,d involve the $\mathrm{SCET_{II}}$ T-products $\overline{O}_j^{(i)}$ in Eq. (6.15), and Fig. 6-2e involves $O_j^{(i)}$ in Eq. (5.27).

To generate connected $\mathrm{SCET_I}$ diagrams from the time-ordered product in Eq. (5.20) requires at least two contractions, of which the minimum basic possibilities can be grouped as follows:

1) Contraction of $\xi_n^{(u)}\,\bar\xi_n^{(u)}$ and the $\perp$ gluon in $B_\perp^\mu B_\perp^\nu$ (C-topology, Fig. 6-2a),

2) Contraction of $\xi_n^{(d)}\,\bar\xi_n^{(d)}$ and the $\perp$ gluon in $B_\perp^\mu B_\perp^\nu$ (E-topology, Fig. 6-2b),

3) Contraction of $\xi_n^{(u)}\,\bar\xi_n^{(u)}$ and $\xi_n^{(d)}\,\bar\xi_n^{(d)}$ (topology with two external collinear gluons and no external collinear quarks, not shown).

All more complicated contractions have one of these three as a root. Case 3) only contributes for light mesons with an isosinglet component (η, η', ω, ϕ), which we will consider in the next chapter.

Each of the $\mathrm{SCET_I}$ T-products is matched onto $\mathrm{SCET_{II}}$ operators at scale $\mu = \mu_0$, and

$$\begin{aligned}
&\int d\tau_1\, d\tau_2\, C_j^{(0,8)}\, T_j^{(0,8)} \to [T_j^{(0,8)}]_{\rm short} + [T_j^{(0,8)}]_{\rm long}\,, \qquad (5.23)\\
&[T_{L,R}^{(0,8)}]_{\rm short} = \int\! {\rm d}\tau_i\, {\rm d}k_\ell^+\, {\rm d}\omega_k\, C_{L,R}^{(0,8)}(\tau_i,\mu_0)\, J^{(0,8)}(\tau_i,k_\ell^+,\omega_k,\mu_0,\mu)\, O_{L,R}^{(0,8)}(k_\ell^+,\omega_k,\mu)\,,\\
&[T_{L,R}^{(0,8)}]_{\rm long} = \int\! {\rm d}k^+\, {\rm d}\omega_1\, {\rm d}\omega_2\, {\rm d}\omega\, C_{L,R}^{(0,8)}(\omega_i,\mu_0)\, \overline{J}^{(0,8)}(k^+\omega,\mu_0,\mu)\, \overline{O}_{L,R}^{(0,8)}(\omega_i,k^+,\omega,\mu)\,,
\end{aligned}$$

where the subscripts i, ℓ, k run over values 1, 2. Here J, $\overline{J}$ are jet functions containing effects at the $p^2 \sim E_M \Lambda$ scale and are Wilson coefficients for the $\mathrm{SCET_{II}}$ operators O and $\overline{O}$. The $[T_{L,R}^{(0,8)}]_{\mathrm{short}}$ and $[T_{L,R}^{(0,8)}]_{\mathrm{long}}$ terms are respectively Fig. 6-2e and Fig. 6-2c,d (after they are dressed with all possible gluons). The μ_0 and μ dependence in Eq. (5.23) signifies the scale dependence in $\mathrm{SCET_I}$ and $\mathrm{SCET_{II}}$ respectively. The jet functions are generated by the contraction of intermediate collinear fields with couplings $\alpha_s(\mu_0)$ (where $\mu_0^2 \sim E_\pi \Lambda$). In general the jet functions depend on the large light-cone momenta τ_i coming out of the hard vertex, the large light-cone momenta ω_k of the external collinear $\mathrm{SCET_{II}}$ fields, and the k_j^+ momenta of the external soft $\mathrm{SCET_{II}}$ fields. No other soft momentum dependence is possible since the leading $\mathrm{SCET_I}$ collinear Lagrangian depends on only $n\cdot\partial_{us}$.

The difference between the time-ordered products $T_{L,R}^{(0,8)}$ and the time-ordered products $\overline{O}_{L,R}^{(0,8)}$ gives the six quark $\mathrm{SCET_{II}}$ operator $O_{L,R}^{(0,8)}$, whose coefficients are the jet functions $J^{(0,8)}$. In this $\mathrm{SCET_I} \to \mathrm{SCET_{II}}$ matching calculation the $\overline{O}_{L,R}^{(0,8)}$ graphs subtract long distance contributions from the $T_{L,R}^{(0,8)}$ graphs so that $J^{(0,8)}$ are free of infrared singularities. In general the matrix elements for color suppressed decays then include both short and long distance contributions as displayed in Eq. (5.23). However, for the isotriplet π and ρ a dramatic simplification occurs at leading order in $C_J^{(i)}$. In this case it can be proven that the long distance contributions $[T_j^{(i)}]_{\mathrm{long}}$ *vanish* to all orders in the α_s couplings in $\mathrm{SCET_I}$, and with the α_s couplings in $\mathrm{SCET_{II}}$ treated non-perturbatively. The proof of this fact uses the G-parity invariance of QCD and is carried out in Appendix 9.1. At leading order in the coefficients $C_{L,R}^{(0,8)}$ the $M = \pi, \rho$ factorization theorem is therefore more predictive since possible long-distance contribution from $\overline{O}_j^{(i)}$ are absent. Most of the following discussion will focus on $O_j^{(i)}$, but $\overline{O}_j^{(i)}$ is fully included in the final factorization theorem.

In the $\mathrm{SCET_{II}}$ diagrams in Fig. 6-2c,d a power suppressed four quark Lagrangian appears. It is similar to an operator introduced in Ref. [63], and can be obtained from $T\{i\mathcal{L}_{\xi q}^{(1)}, i\mathcal{L}_{\xi q}^{(1)}\}$ in $\mathrm{SCET_I}$ by a simple matching calculation [25]. Summing over

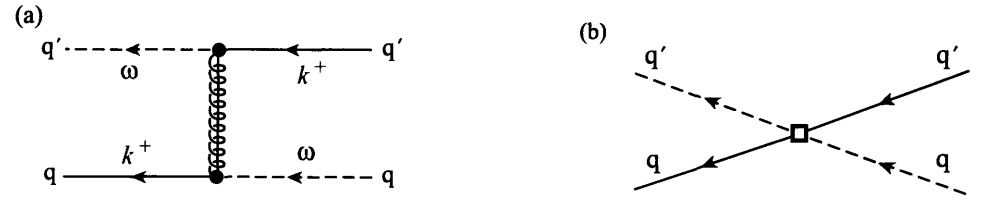

Figure 5-4: Tree level matching calculation for the $L^{(0,8)}_{L,R}$ operators, with (a) the T-product in $\mathrm{SCET_I}$ and (b) the operator in $\mathrm{SCET_{II}}$. Here q, q' are flavor indices and $\omega \sim \lambda^0$ are minus-momenta.

flavors q, q' we find

$$\begin{aligned}
\mathcal{L}^{(1)}_{\xi\xi qq} &= \sum_{j=L,R} \sum_{\omega} \sum_{k^+} \Big[\bar{J}^{(0)}(\omega k^+) L^{(0)}_j(\omega, k^+, x) + \bar{J}^{(8)}(\omega k^+) L^{(8)}_j(\omega, k^+, x) \Big] , \\
L^{(0)}_j(\omega, k^+, x) &= \sum_{q,q'} \Big[(\bar{\xi}^{(q)}_n W)_\omega \bar{n}\!\!\!/ P_j (W^\dagger \xi^{(q')}_n)_\omega \Big] \Big[(\bar{q}' S)_{k^+} n\!\!\!/ P_j (S^\dagger q)_{k^+} \Big](x) . \qquad (5.24)
\end{aligned}$$

In Eq. (5.24) the soft momenta labels are defined by $(S^\dagger q)_{k^+} = [\delta(k^+ - n\cdot P)\, S^\dagger q]$, and the positions $(x^+, x^-, x_\perp) \sim (1/\Lambda, Q/\Lambda^2, 1/\Lambda)$. For the soft fields the x^- coordinates encode small residual plus-momenta, and for the collinear fields the x^+ coordinates encode small residual minus-momenta. Thus, we used the summation/integration notation for label/residual momenta from Ref. [86]. The operator $L^{(8)}_j(\omega, k^+, x)$ has the same form as Eq. (5.24) except with color structure $T^a \otimes T^a$. At tree level the coefficient functions are given by the calculation in Fig. 5-4

$$\bar{J}^{(0)}(\omega k^+) = -\frac{C_F}{2N_c} \frac{4\pi\alpha_s(\mu)}{\omega k^+} , \qquad \bar{J}^{(8)}(\omega k^+) = \frac{1}{2N_c} \frac{4\pi\alpha_s(\mu)}{\omega k^+} . \qquad (5.25)$$

Beyond tree level they obtain contributions from loop diagrams with additional $\mathcal{L}^{(0)}_{\xi\xi}$ vertices. In terms of the operator in Eq. (5.24) the $\mathrm{SCET_{II}}$ operators that contribute to $[T^{(i)}_j]_{\mathrm{long}}$ in the factorization theorem are

$$\overline{O}^{(0,8)}_j(\omega_i, k^+, \omega, \mu) = \int \mathrm{d}^4x\, T\, \mathcal{Q}^{(0,8)}_j(\omega_i, x=0)\; iL^{(0,8)}(\omega, k^+, x) . \qquad (5.26)$$

The operators $\overline{O}$ generate the diagrams (c) and (d) in Fig. 6-2.

At any order in perturbation theory the jet functions J from the C–topology and E–topology generate one spin structure, and two color structures for the $\mathrm{SCET_{II}}$ operators.

For the six quark operators we find

$$
\begin{aligned}
O_j^{(0)}(k_i^+,\omega_k) &= \left[\bar h_{v'}^{(c)}\Gamma_j^h\, h_v^{(b)}\,(\bar d\, S)_{k_1^+}\not{n}P_L\,(S^\dagger u)_{k_2^+}\right]\left[(\bar\xi_n W)_{\omega_1}\Gamma_c(W^\dagger\xi_n)_{\omega_2}\right], \qquad (5.27)\\
O_j^{(8)}(k_i^+,\omega_k) &= \left[(\bar h_{v'}^{(c)}S)\Gamma_j^h\, T^a\,(S^\dagger h_v^{(b)})\,(\bar d\, S)_{k_1^+}\not{n}P_L T^a(S^\dagger u)_{k_2^+}\right]\left[(\bar\xi_n W)_{\omega_1}\Gamma_c(W^\dagger\xi_n)_{\omega_2}\right],
\end{aligned}
$$

where here the d, u, $h_{v'}^{(c)}$, and $h_v^{(b)}$ fields are soft, and the ξ_n fields are collinear isospin doublets, $(\xi_n^{(u)},\xi_n^{(d)})$. In Eq. (5.27) $\Gamma_{L,R}^h = \not{n}P_{L,R}$ as in Eq. (5.17), while for the collinear isospin triplet $\Gamma_c = \tau^3\not{\bar n}P_L/2$.[5] We do not list operators with a T^a next to Γ_c since they will give vanishing contribution in the collinear matrix element. For light vector mesons the spin structure Γ_c only produces the longitudinal polarization. This result follows from the quark helicity symmetry of $\mathcal{L}_{\xi\xi}^{(0)}$ and is discussed in further detail in Appendix 9.2.

In position space the $O_j^{(i)}$ are bilocal operators, with the two soft light quarks aligned on the n_μ light cone direction ($x^- = \frac{1}{2}n_\mu\bar n\cdot x, y^- = \frac{1}{2}n_\mu\bar n\cdot y$) passing through the point $x=0$

$$
\begin{aligned}
&(\bar h_{v'}^{(c)}S)\Gamma_h(S^\dagger h_v^{(b)})\,(\bar d\, S)_{r^+}\Gamma_q(S^\dagger u)_{\ell^+} = \qquad (5.28)\\
&\quad\int\frac{dx^-dy^-}{(4\pi)^2}\,e^{i/2(r^+x^- - \ell^+y^-)}[\bar h_{v'}^{(c)}\Gamma_h h_v^{(b)}](0)[\bar d(x^-)S_n(x^-,0)\Gamma_q S_n(0,y^-)u(y^-)]\,.
\end{aligned}
$$

The gluon interactions contained in matrix elements of $O_j^{(0,8)}$ include attachments to the light quarks q, to the heavy quarks $h_{v,v'}$, and to the Wilson lines S_n as shown in Fig. 5-5. The interactions with $h_{v,v'}$ have been drawn as Wilson lines $S_{v,v'}$ along v, v' [71]. Even though we have factored the collinear and soft degrees of freedom in the two final state hadrons, the presence of the soft Wilson lines bring in information about the vector n^μ. This allows the soft operators $O_j^{(i)}$ to be non-trivial functions of $n\cdot k_j$, $n\cdot v$, and $n\cdot v'$, and this information gives rise to a *complex phase* in the soft functions $S_{L,R}^{(0,8)}$ as shown in Appendix 9.3. Thus, the S_n Wilson lines are directly responsible for producing final state interactions, and the soft fields in $O_j^{(0,8)}$ encode non-perturbative rescattering information.[6] This makes good sense given that the

[5] There are also isosinglet contributions with $\Gamma_c = \not{\bar n}P_L/2$.

[6] Note that in semi-inclusive processes a different mechanism is responsible for the phases in

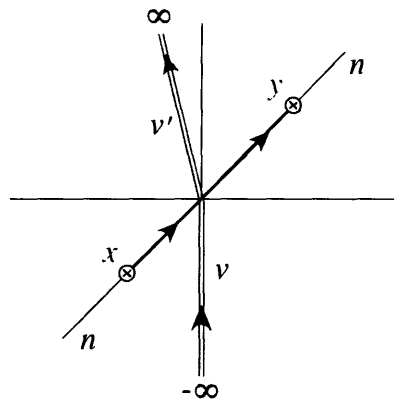

Figure 5-5: Non-perturbative structure of the soft operators in Eq. (5.28) which arise from $O_j^{(0,8)}$. Wilson lines are shown for the paths $S_n(x,0)$, $S_n(0,y)$, $S_v(-\infty,0)$ and $S_{v'}(0,\infty)$, plus two interacting QCD quark fields inserted at the locations x and y. The S_v and $S_{v'}$ Wilson lines are from interactions with the fields h_v and $h_{v'}$ fields, respectively. The non-perturbative structure of soft fields in $\overline{O}_j^{(0,8)}$ is similar except that we separate the single and double Wilson lines by an amount $x_\perp$.

soft gluons in the S_n's were originally generated by integrating out attachments to the collinear quarks and gluons making up the light energetic hadron.

The above procedure provides a *new* mechanism for generating non-perturbative strong phases for exclusive decays within factorization. In the soft $B \to D^{(*)}$ matrix elements the information about the light energetic meson is limited to its direction of motion n^μ. Since these matrix elements know nothing further about the nature of the light meson, these strong phases are universal. In particular the same strong phase ϕ is generated for the decays $\bar{B} \to D^{(*)}\pi$ and $\bar{B} \to D^{(*)}\rho$. (We caution that this is not the isospin strong phase, but rather a different angle in the triangle.) The same mechanism produces another universal strong phase for color suppressed decays to $D\bar{K}^{(*)0}$, and a third for decays to $D_s K^{(*)-}$. The different phases in the three classes arise in part due to the appearance of different moments of the matrix elements of the soft operators. However, for the kaons there are additional long distance contributions to the strong phases from $[T]_{\rm long}$, which make the universality of the phase ϕ from $[T]_{\rm short}$ hard to test. A more complete set of phenomenological predictions is given in Section 5.1.6, including a comparison with existing data. Further details on the

single-spin asymmetries which has to do with the boundary conditions on Wilson lines [38].

properties of the soft functions $S^{(0,8)}$ are given in the Appendix 9.3.

The matrix elements of the short distance operators $O_j^{(i)}$ in Eq. (5.27) factor into products of soft and collinear parts, respectively. The collinear part of the matrix elements are simply given in terms of the light cone wave function of the light meson. For the π and ρ the definitions are [we suppress pre-factors of $\int_0^1 dx\,\delta(\omega_1 - x\,\bar{n}\cdot p_M)\,\delta(\omega_2 + (1-x)\bar{n}\cdot p_M)$ on the RHS][7]

$$\begin{aligned}
\langle \pi_n^0 | (\bar{\xi}_n W)_{\omega_1} \bar{n}\!\!\!/ \gamma_5 \tau_3 (W^\dagger \xi_n)_{\omega_2} | 0 \rangle &= -i\sqrt{2}\, f_\pi\, \bar{n}\cdot p_\pi\, \phi_\pi(\mu, x)\ , \\
\langle \rho_n^0(\varepsilon) | (\bar{\xi}_n W)_{\omega_1} \bar{n}\!\!\!/ \tau_3 (W^\dagger \xi_n)_{\omega_2} | 0 \rangle &= i\sqrt{2}\, f_\rho\, m_\rho\, \bar{n}\cdot \varepsilon^*\, \phi_\rho(\mu, x) \\
&= i\sqrt{2}\, f_\rho\, \bar{n}\cdot p_\rho\, \phi_\rho(\mu, x)\ .
\end{aligned} \tag{5.29}$$

In the last equality we have used the fact that at this order the collinear operator only produces longitudinal ρ's, for which $m_\rho \bar{n}\cdot\varepsilon_L^* = \bar{n}\cdot p_\rho$.

Since it no longer contains couplings to energetic gluons, the soft part of the matrix elements of $\mathcal{O}_j^{(0,8)}$ can be constrained using heavy quark symmetry. In other words, heavy quark symmetry relations can be derived for matrix elements of soft fields. The constraints can be implemented most compactly using the trace formalism of the HQET [91]. First consider the matrix element of the soft fields in $O_j^{(0,8)}$. For $O_j^{(0)}$ we have

$$\frac{\langle D^{(*)0}(v') | (\bar{h}_{v'}^{(c)} S)\Gamma\, (S^\dagger h_v^{(b)})\, (\bar{d}\, S)_{k_1^+} \bar{n}\!\!\!/ P_L\, (S^\dagger u)_{k_2^+} | \bar{B}^0(v) \rangle}{\sqrt{m_B m_D}} = \mathrm{Tr}\,[\overline{H}_{v'}^{(c)} \Gamma H_v^{(b)} X^{(0)}]\,, \tag{5.30}$$

where $X^{(0)} = X^{(0)}(k_j^+, n, v, v')$ and we use the standard relativistic normalization for the states (and note that the LHS is independent of $m_{b,c}$ in the heavy quark limit). An identical equation holds for $O_j^{(8)}$ with an $X^{(8)}$. In writing the trace formula in Eq. (7.11) we have used the fact that the d and u quarks must end up in the $\bar{B}$ and $D^{(*)}$ states.[8] The heavy mesons (D, D^*) and (B, B^*) are grouped together into

[7] Our vector meson states are defined with an extra minus sign relative to the standard convention.

[8] The matrix element of the analogous soft operators with $(\bar{u}u) + (\bar{d}d)$ would contain a second term in Eq. (7.11) of the form $\mathrm{Tr}\,[\overline{H}_{v'}^{(c)} \Gamma H_v^{(b)} X]\mathrm{Tr}\,[Y]$, which arises from contracting the light quarks in the operator. These types of traces also show up for power corrections to $\bar{B}^0 \to D^{(*)+} M^-$ and $B^- \to D^{(*)0} M^-$.

superfields [91], defined as

$$H_v = \frac{1+\not{v}}{2}(P_v^{*\mu}\gamma_\mu + P_v\gamma_5)\,. \tag{5.31}$$

Now $X^{(0,8)}$ are the most general structures compatible with the symmetries of QCD. They involve 4 functions $a_{1-4}^{(0,8)}(k_1^+, k_2^+, v\cdot v', n\cdot v, n\cdot v')$

$$X^{(0,8)} = a_1^{(0,8)}\not{n}P_L + a_2^{(0,8)}\not{n}P_R + a_3^{(0,8)}P_L + a_4^{(0,8)}P_R\,, \tag{5.32}$$

Structures proportional to $\not{v}$ and $\not{v}'$ can be eliminated by using $H_v\not{v} = -H_v$, etc.

The presence of four functions in Eq. (5.32) would appear to restrict the predictive power of heavy quark symmetry. However, using the properties of H_v and $\bar{H}_{v'}$ and the fact that the two-body kinematics relates n to v and v' via $m_B v = m_D v' + E_M n$, it is easy to see that the four functions a_i appear only in two distinct combinations. (Note that we are taking $m_M/m_B \sim \Lambda/m_B \ll 1$.) For $\Gamma_{L,R}^h$ they give soft functions $S_{L,R}$ defined as $S_L = (n\cdot v')(a_1 - a_3/2) - a_4/2$, $S_R = (n\cdot v')(a_2 - a_4/2) - a_3/2$ and

$$\begin{aligned}
\frac{\langle D^0(v')|(\bar{h}_{v'}^{(c)}S)\not{n}P_{L,R}(S^\dagger h_v^{(b)})(\bar{d}S)_{k_1^+}\not{n}P_L(S^\dagger u)_{k_2^+}|\bar{B}^0(v)\rangle}{\sqrt{m_B m_D}} &= S_{L,R}^{(0)}(k_j^+)\,, \\
\frac{\langle D^{*0}(v',\varepsilon)|(\bar{h}_{v'}^{(c)}S)\not{n}P_{L,R}(S^\dagger h_v^{(b)})(\bar{d}S)_{k_1^+}\not{n}P_L(S^\dagger u)_{k_2^+}|\bar{B}^0(v)\rangle}{\sqrt{m_B m_{D^*}}} &= \pm\frac{n\cdot\varepsilon^*}{n\cdot v'}\,S_{L,R}^{(0)}(k_j^+)\,,
\end{aligned} \tag{5.33}$$

where the $\pm$ for the D^* refers to the choice of P_L or P_R. Identical definitions hold for the matrix elements of the color-octet operators which give $S_{L,R}^{(8)}(k_j^+)$. We will see in section 5.1.6 that the result in Eq. (6.5) relates decay amplitudes and strong phases for $\bar{B}^0 \to D^0 M^0$ and $\bar{B}^0 \to D^{*0} M^0$ at leading order in the power expansion, and up to terms suppressed by $\alpha_s(Q)/\pi$. If one takes $n\cdot v = 1$, then $n\cdot v' = m_B/m_D^{(*)}$, $v\cdot v' = (m_B^2 + m_{D^{(*)}}^2)/(2m_B m_{D^{(*)}})$. The D, D^* variables are equal in the heavy quark limit.

For the long distance operators $\overline{O}_j^{(i)}$ the same set of arguments in Eqs. (7.11–6.5) can be applied except that now we must add terms $a_5^{(0,8)}\not{x}_\perp P_L + a_6^{(0,8)}\not{x}_\perp P_R$ to $X^{(0,8)}$, and the a_i's can also depend on $x_\perp^2$. The functions analogous to $S_{L,R}^{(0,8)}$ are defined as

$\Phi^{(0,8)}_{L,R}(k^+, x_\perp, \varepsilon^*_{D^*})$. In this case the D and D^* decompositions are no longer related since the matrix element involves both $n\cdot\varepsilon^*$ and $x_\perp\cdot\varepsilon^*$ terms for the D^*. Thus, due to the long distance contributions for light vector meson we must restrict ourselves to the longitudinal polarization in order to have equality for the D and D^* amplitudes. In the case of the ρ this restriction is not important since the long distance contributions vanish (see Appendix 9.1). However this observation does have phenomenological implications for decays to K^*'s.

We are now in a position to write down the most general factorized result for the amplitude for the decays $\bar{B}^0 \to D^{(*)0}M^0$. Combining all the factors, this formula contains the soft functions $S^{(0,8)}(k_1^+, k_2^+)$ from Eq. (6.5), the jet functions $J^{(i)}$ from Eq. (5.23), and the Wilson coefficients $C^{(0,8)}_{L,R}$ from Eq. (5.16). In $J^{(i)}(\tau_i, k_\ell^+, \omega_k)$ we can pull out a factor of $\delta(\tau_1 - \tau_2 - \omega_1 + \omega_2)$ by momentum conservation. This leaves the variables $\tau_1 + \tau_2 = 2E_M(2z-1)$ and $\omega_1 + \omega_2 = 2E_M(2x-1)$ unconstrained, which give convolutions with the momentum fractions z and x respectively. In defining $J^{(i)}(z, x, k_\ell^+)$ we multiply $J^{(i)}(\tau_i, k_\ell^+, \omega_k)$ by $\omega_1 - \omega_2 = \bar{n}\cdot p_M$. All together the result for the $\bar{B}^0 \to D^{(*)0}M^0$ amplitude is

$$\begin{aligned} A_{00}^{D^{(*)}} &= N_0^M \int_0^1 dx\, dz \int dk_1^+ dk_2^+ \Big[C_L^{(i)}(z)\, J^{(i)}(z, x, k_1^+, k_2^+)\, S_L^{(i)}(k_1^+, k_2^+)\, \phi_M(x) \\ &\qquad \pm C_R^{(i)}(z)\, J^{(i)}(z, x, k_1^+, k_2^+)\, S_R^{(i)}(k_1^+, k_2^+)\, \phi_M(x)\Big] \\ &\quad + A_{\text{long}}^{D^{(*)}M}\,, \end{aligned} \tag{5.34}$$

where we sum over $i = 0, 8$ and the μ_0, μ dependence is as in Eq. (5.23). The $A_{\text{long}}^{D^{(*)}M}$ in Eq. (5.34) denotes the contributions from the matrix elements of the SCET_{II} time-ordered products $[T]_{\text{long}}$. Also the $\pm$ refer to D/D^*, $C^{(i)}_{L,R}(z) = C^{(i)}_{L,R}(\tau_1 + \tau_2, E_M, m_b, m_c, \mu)$, and

$$N_0^M = \frac{G_F V_{cb} V_{ud}^*}{2}\, f_M \sqrt{m_B m_{D^{(*)}}}\,. \tag{5.35}$$

The normalization factor is common since $m_D = m_D^*$ and $n\cdot\varepsilon^{(D^*)} = n\cdot v'$. This follows since the M's produced by $O_j^{(0,8)}$ are longitudinally polarized.

The long distance amplitudes also obey a factorization theorem which can be derived by examining the matrix elements of the $\overline{O}_{L,R}^{(0,8)}$ operators in Eq. (6.15). First factorize the collinear fields into the matrix element with the M and the soft fields into the matrix element with the $B, D^{(*)}$. The independence of the collinear propagators on the residual soft minus-momenta leads to a $\delta(x^+)$ and the independence of the soft propagators on the residual collinear plus-momenta leads to a $\delta(x^-)$ (somewhat similar to the calculation for $B \to X_s\gamma$ as described in Ref. [22]). The result is

$$\begin{aligned} A_{\rm long}^{D^{(*)}M} &= N_0^M \int_0^1 dz \int dk^+ d\omega \int d^2x_\perp \Big[C_L^{(i)}(z)\, \bar{J}^{(i)}(\omega k^+)\, \Phi_L^{(i)}(k^+, x_\perp, \varepsilon_{D^*}^*) \Psi_M^{(i)}(z, \omega, x_\perp, \varepsilon_M^*) \\ &\quad \pm C_R^{(i)}(z)\, \bar{J}^{(i)}(\omega k^+)\, \Phi_R^{(i)}(k^+, x_\perp, \varepsilon_{D^*}^*) \Psi_M^{(i)}(z, \omega, x_\perp, \varepsilon_M^*) \Big] . \end{aligned} \tag{5.36}$$

where the $\pm$ is for D and D^* and we defined the non-perturbative functions in a way which gives the same prefactor as in Eq. (5.34). Here $C_{L,R}^{(i)}$ are the Wilson coefficients of the weak operators in Eq. (5.19), and the jet functions $\overline{J}^{(0,8)}$ are the coefficients of the $\text{SCET}_{\rm II}$ Lagrangian in Eq. (5.24). The $\Phi_{L,R}^{(i)}$ and $\Psi_M^{(i)}$ are soft and collinear matrix elements from the operators $\overline{O}$ and are given by [with prefactor $\int_0^1 dz\, \delta(\omega_1 - z\bar{n}\cdot p_M)\delta(\omega_2 + (1-z)\bar{n}\cdot p_M)$ for $\Psi_M^{(0)}$]

$$\begin{aligned} &\Big\langle M^0(p_M, \epsilon_M) \Big| \Big[(\bar{\xi}_n^{(d)} W)_{\omega_1} \bar{n}\!\!\!/ P_L (W^\dagger \xi_n^{(u)})_{\omega_2} \Big](0_\perp) \Big[(\bar{\xi}_n^{(u)} W)_{\omega} \bar{n}\!\!\!/ P_L (W^\dagger \xi_n^{(d)})_{\omega} \Big](x_\perp) \Big| 0 \Big\rangle \\ &\quad = i f_M/\sqrt{2}\, \Psi_M^{(0)}(z, \omega, x_\perp, \varepsilon_M^*) , \\ &\Big\langle D^{(*)0}(v', \epsilon_{D^*}) \Big| \Big[(\bar{h}_{v'}^{(c)} S) \Gamma_{L,R}^h (S^\dagger h_v^{(b)}) \Big](0_\perp) \Big[(\bar{d} S)_{k^+} \bar{n}\!\!\!/ P_L (S^\dagger u)_{k^+} \Big](x_\perp) \Big| \bar{B}^0 \Big\rangle \\ &\quad = \pm \sqrt{m_B m_{D^{(*)}}}\, \Phi_{L,R}^{(0)}(k^+, x_\perp, \varepsilon_{D^*}^*) , \end{aligned} \tag{5.37}$$

and $\Psi_M^{(8)}$ and $\Phi_{L,R}^{(8)}$ are defined by analagous equations with color structure $T^a \otimes T^a$. The $\pm$ is for P_L and P_R respectively. In a more traditional language the $A_{\rm long}^{D^{(*)}M}$ contributions might be referred to as "non-factorizable" since they involve an direct $x_\perp$ convolution between non-perturbative functions. Eqs. (5.34) and (5.36) are the main results of our work. Additional details about the derivation of Eq. (5.36) will be presented in Ref. [?].

Using the $\text{SCET}_{\rm II}$ power counting in $\eta = \Lambda/Q$ we can verify that the short and

long distance contributions to the factorization theorem are indeed the same order. The coefficients $C_{L,R}^{(i)} \sim \eta^0$. The results in Eqs. (5.25) and (5.41) for the jet functions imply $J^{(i)} \sim 1/\Lambda^2$ and $\overline{J}^{(i)} \sim 1/(Q\Lambda)$. Furthermore, $\phi_M \sim \eta^0$ from the definitions in Eq. (5.29). For the soft function in Eq. (6.5) we get $(\eta^{3/2})^4$ from the fields, η^{-3} from the states, times η^{-2} from the delta functions indicated by the momentum subscripts. This gives $S(k_1^+, k_2^+) \sim \eta$, ie. $S(k_1^+, k_2^+) \sim \Lambda$. A similar calculation for the collinear and soft long distance matrix elements in Eq. (6.16) gives $\Psi_M^{(0,8)} \sim \Lambda^2/Q$ and $\Phi_{L,R}^{(0,8)} \sim \Lambda$. In the factorization theorem the measures have scaling $(dk_1^+ dk_2^+) \sim \Lambda^2$ and $(dk^+ d^2x_\perp) \sim 1/\Lambda$. Combining all the factors for the short distance amplitude gives $(\Lambda)(\Lambda^2)(1/\Lambda^2)(\Lambda)(\Lambda^0) = \Lambda^2$, while for the long distance amplitude we find $(\Lambda)(1/\Lambda)(1/\Lambda)(\Lambda)(\Lambda^2) = \Lambda^2$ also. Therefore, both terms in $A_{00}^{D^{(*)}}$ are the same order in the power counting. They also give the complete set of contributions at this order.

For numerical results with $M = \pi, \rho$ the $A_{\rm long}^{D^{(*)}M}$ contributions are very small since taking $C_{L,R}^{(i)}(z)$ independent of z gives $A_{\rm long}^{D^{(*)}M} = 0$ as shown in Appendix 9.1. This implies that $A_{\rm long}^{D^{(*)}M}/A_{00} \sim \alpha_s(Q)/\pi$, and together with the helicity structure of the jet function discussed in Appendix 9.2 implies that the production of transverse ρ mesons is suppressed. In Section 5.1.6 we explore further phenomenological implications.

Next tree level results are presented for the jet functions $J^{(0,8)}$. The $\mathrm{SCET_I}$ graphs in Fig. 6-2 are computed with insertions of $\mathcal{Q}_j^{(0,8)}$ and taking momenta $-k_1$ and $-k_2$ for the initial and final light soft antiquarks, together with momenta p_1 and p_2 for the collinear quark and antiquark. The diagrams in Fig. 6-2a,b with insertions of $\{\mathcal{Q}_j^{(0)}, \mathcal{Q}_j^{(8)}\}$ are

$$\begin{aligned}
\text{C:}\quad & g^2\,\frac{(\bar{u}_{v'}^{(c)}\gamma^\nu P_L\{1,T^B\}u_v^{(b)})(\bar{u}_n^{(d)}\gamma_\nu P_L \bar{n}\!\!\!//2\{1,T^B\}T^A\gamma_\perp^\mu v_s^{(u)})(\bar{v}_s^{(d)}T^A\gamma_\mu^\perp v_n^{(d)})}{[n\cdot(k_1-k_2)+i\epsilon][\bar{n}\cdot p_2\, n\cdot k_1+i\epsilon]}\,, \\
\text{E:}\quad & -g^2\,\frac{(\bar{u}_{v'}^{(c)}\gamma^\nu P_L\{1,T^B\}u_v^{(b)})(\bar{u}_n^{(u)}T^A\gamma_\perp^\mu v_s^{(u)})(\bar{v}_s^{(d)}T^A\{1,T^B\}\gamma_\mu^\perp \bar{n}\!\!\!//2\gamma_\nu P_L v_n^{(u)})}{[n\cdot(k_1-k_2)+i\epsilon][-\bar{n}\cdot p_1\, n\cdot k_2+i\epsilon]}
\end{aligned} \tag{5.38}$$

Adding these contributions with factors of $C_L^{(0)}$ and $C_L^{(8)}$ to distinguish the two color

structures, and then Fierzing gives

$$
\begin{aligned}
&C_L^{(0)}\Big[\bar u_{v'}^{(c)}\not{\bar n}P_L u_v^{(b)}\;\bar v_s^{(d)}\not{\bar n}P_L v_s^{(u)}\Big] \\
&\times\frac{2\pi\alpha_s C_F}{N_c}\left(\frac{\bar u_n^{(d)}\not{\bar n}P_L v_n^{(d)}}{[n\cdot(k_1-k_2)+i\epsilon][\bar n\cdot p_2 n\cdot k_1+i\epsilon]}-\frac{\bar u_n^{(u)}\not{\bar n}P_L v_n^{(u)}}{[n\cdot(k_1-k_2)+i\epsilon][-\bar n\cdot p_1 n\cdot k_2+i\epsilon]}\right) \\
&-C_L^{(8)}\Big[\bar u_{v'}^{(c)}\not{\bar n}P_L T^a u_v^{(b)}\;\bar v_s^{(d)}\not{\bar n}P_L T^a v_s^{(u)}\Big] \\
&\times\frac{\pi\alpha_s}{N_c^2}\left(\frac{\bar u_n^{(d)}\not{\bar n}P_L v_n^{(d)}}{[n\cdot(k_1-k_2)+i\epsilon][\bar n\cdot p_2 n\cdot k_1+i\epsilon]}-\frac{\bar u_n^{(u)}\not{\bar n}P_L v_n^{(u)}}{[n\cdot(k_1-k_2)+i\epsilon][-\bar n\cdot p_1 n\cdot k_2+i\epsilon]}\right).
\end{aligned}
\tag{5.39}
$$

where $C_F=(N_c^2-1)/(2N_c)$ and we set $C_R^{(0,8)}=0$. The first term in each round bracket originates from the $C-$type graph (Fig. 6-2a) and the second term from the $E-$type graph (Fig. 6-2b). It is convenient to group the result into isosinglet and isotriplet terms for the collinear spinors. Since the π^0 and ρ^0 have definite charge conjugation we can freely interchange the positive momenta $\bar n\cdot p_1\leftrightarrow\bar n\cdot p_2$, so a factor of $1/\bar n\cdot p_1$ can be pulled out front. For the terms in round brackets we find

$$
\left(\frac{1}{2}\,\frac{[\bar u_n^{(d)}\not{\bar n}P_L v_n^{(d)}-\bar u_n^{(u)}\not{\bar n}P_L v_n^{(u)}]}{[n\cdot k_1+i\epsilon][-n\cdot k_2+i\epsilon]}-\frac{1}{2}\,\frac{[[\bar u_n^{(d)}\not{\bar n}P_L v_n^{(d)}+\bar u_n^{(u)}\not{\bar n}P_L v_n^{(u)}]\;n\cdot(k_2+k_1)}{[n\cdot(k_1-k_2)+i\epsilon][n\cdot k_1+i\epsilon][-n\cdot k_2+i\epsilon]}\right) \tag{5.40}
$$

For $\bar B^0\to D^{(*)0}\pi^0$ and $\bar B^0\to D^{(*)0}\rho^0$ where we have isotriplet M^0's the contributions from the $\mathrm{SCET_{II}}$ diagrams in Figs. 6-2c,d cancel. Thus, the denominator in Eq. (5.40) directly gives the tree level isotriplet jet functions

$$
\begin{aligned}
J^{(0)}(z,x,k_1^+,k_2^+) &= -\frac{4\pi\alpha_s(\mu)C_F}{N_c}\,\frac{\delta(z-x)}{x\,[n\cdot k_1+i\epsilon][-n\cdot k_2+i\epsilon]}\,, \\
J^{(8)}(z,x,k_1^+,k_2^+) &= \frac{2\pi\alpha_s(\mu)}{N_c^2}\,\frac{\delta(z-x)}{x\,[n\cdot k_1+i\epsilon][-n\cdot k_2+i\epsilon]}\,,
\end{aligned}
\tag{5.41}
$$

where $\bar n\cdot p_1=x\,\bar n\cdot p_M$. These jet functions are non-singular given that the non-perturbative soft function $S(k_1^+,k_2^+)$ vanishes for $k_1^+=0$ or $k_2^+=0$, and that $\phi_{\pi,\rho}(x)$ vanishes at $x=0$ and $x=1$. On the other hand for isosinglet M^0's the result in Eq. (5.40) has a singular denominator $1/[n\cdot(k_1-k_2)+i\epsilon]$. The singularity occurs when the collinear quark propagators in Figs. 6-2a,b get too close to their mass shells, ie. when $n\cdot(k_1-k_2)\Lambda^2/Q$. This singularity is exactly what is canceled by subtracting

the $\mathrm{SCET_{II}}$ diagrams in Figs. 6-2c,d, which then gives a non-singular isosinglet jet function.

Next we consider the result for the factorization theorem for $M = \pi, \rho$ with these tree level jet functions. Taking the matrix elements of the $O_L^{(0,8)}$ operators, the collinear part factors from the soft operators as explained above. Their matrix elements are given in terms of the M^0 light cone wave function, and the $S^{(0,8)}(k_+, l_+)$ functions, respectively. This gives the explicit result for the $\bar{B}^0 \to D^{(*)0}\pi^0$ and $\bar{B}^0 \to D^{(*)0}\rho^0$ decay amplitudes, at lowest order in the matching for C and J

$$\begin{aligned} A(\bar{B}^0 \to D^{(*)0}\pi^0) &= N_0^\pi \left\{ -\frac{4\pi\alpha_s(\mu_0) C_F}{N_c}\, C_L^{(0)}\; s^{(0)} + \frac{2\pi\alpha_s(\mu_0)}{N_c^2}\, C_L^{(8)}\; s^{(8)} \right\} \langle x^{-1}\rangle_\pi \,, \\ A(\bar{B}^0 \to D^{(*)0}\rho^0) &= N_0^\rho \left\{ -\frac{4\pi\alpha_s(\mu_0) C_F}{N_c}\, C_L^{(0)}\; s^{(0)} + \frac{2\pi\alpha_s(\mu_0)}{N_c^2}\, C_L^{(8)}\; s^{(8)} \right\} \langle x^{-1}\rangle_\rho \end{aligned} \tag{5.42}$$

We choose to evaluate $C_L^{(0,8)}$, $s^{(0,8)}$, and $\langle x^{-1}\rangle$ at the common scales $\mu = \mu_0 \sim \sqrt{E_\pi \Lambda}$ since one of the hard scales m_c^2 is not much different than $E_\pi \Lambda$. In Eq. (5.42) the convolutions of the soft and collinear matrix elements are defined by

$$\begin{aligned} s^{(0,8)} &= |s^{(0,8)}| e^{i\phi^{(0,8)}} = \int \mathrm{d}k_1^+ \mathrm{d}k_2^+ \, \frac{S_L^{(0,8)}(k_1^+, k_2^+, \mu)}{(k_1^+ + i\epsilon)(-k_2^+ + i\epsilon)} \,, \\ \langle x^{-1}\rangle_M &= \int_0^1 dx \, \frac{\phi_M(x,\mu)}{x} \,. \end{aligned} \tag{5.43}$$

¿From Eq. (5.43) we can immediately verify the result of the power counting for operators described earlier. Since $\langle x^{-1}\rangle_M \sim \langle x^0\rangle_M \sim \lambda^0$, comparing Eqs. (5.7,5.8) and (5.42) we see that

$$\frac{A(\bar{B}^0 \to D^0\pi^0)}{A(\bar{B}^0 \to D^+\pi^-)} \sim 4\pi\alpha_s(\mu_0)\, \frac{N_0\, s^{(0)}}{N\, E_\pi} \sim 4\pi\alpha_s(\mu_0)\, \frac{s^{(0)}}{E_\pi} \sim 4\pi\alpha_s(\mu_0)\, \frac{\Lambda_{\mathrm{QCD}}}{E_\pi} \,, \tag{5.44}$$

where we have used the standard HQET power counting for the soft matrix elements to determine that $s^{(0,8)} \sim \Lambda_{\mathrm{QCD}}$. Thus, the ratio of type-II to type-I amplitudes scales as Λ/Q just as predicted. Due to the factor of 4π the suppression by α_s does not have much effect numerically. The 4π arises because the α_s is generated at tree level. It is expected that perturbative corrections to the matching for C and J will

be suppressed by factors of $\alpha_s(Q)/\pi$ and $\alpha_s(\sqrt{E_\pi \Lambda})/\pi$ respectively. In Eq. (5.44) grouping $g^2 N_c \sim 1$ gives an extra factor of $1/N_c$, so with this counting the ratio is color suppressed as expected.

5.1.4 Adding strange quarks

In this section we consider how the factorization theorem derived in section 5.1.3 is modified in the case of color suppressed decays involving kaons, which include $\bar{B}^0 \to D_s^{(*)} K^-$, $\bar{B}^0 \to D_s^{(*)} K^{*-}$, as well as the Cabbibo suppressed decays $\bar{B}^0 \to D^{(*)0} K^0$ and $\bar{B}^0 \to D^{(*)0} K^{*0}$.

If strange quarks are included in the final state then operators with different flavor structure appear. In the exchange topology we can have the production of an $s\bar{s}$ pair (as shown by the s-quarks in brackets in Fig. 6-2b). This gives $\mathrm{SCET_{II}}$ six-quark operators

$$
\begin{aligned}
O_j^{(0)}(k_i^+, \omega_k) &= \Big[\bar{h}_{v'}^{(c)} \Gamma_j^h \, h_v^{(b)} \, (\bar{d}\, S)_{k_1^+} \not{n} P_L \, (S^\dagger s)_{k_2^+}\Big] \Big[(\bar{\xi}_n^{(s)} W)_{\omega_1} \Gamma_c (W^\dagger \xi_n^{(u)})_{\omega_2}\Big] , \qquad (5.45) \\
O_j^{(8)}(k_i^+, \omega_k) &= \Big[(\bar{h}_{v'}^{(c)} S) \Gamma_j^h \, T^a \, (S^\dagger h_v^{(b)}) \, (\bar{d}\, S)_{k_1^+} \not{n} P_L T^a (S^\dagger s)_{k_2^+}\Big] \Big[(\bar{\xi}_n^{(s)} W)_{\omega_1} \Gamma_c (W^\dagger \xi_n^{(u)})_{\omega_2}\Big] ,
\end{aligned}
$$

which mediate $\bar{B}^0 \to D_s^{(*)} K^{(*)-}$. For the long distance contribution we take flavors $q' = d$ and $q = s$ in the Lagrangian in Eq. (5.24), which leads to s,$\bar{s}$ quarks replacing u, $\bar{u}$ quarks in $\overline{O}_{L,R}^{(i)}$. The result for the factorization theorem is then identical to Eqs. (5.34) and (5.36), except that only the E-topology contributes. For this case the long distance contribution is not suppressed, and serves to regulate the singularity when matching onto the E-topology jet functions $J^{(0,8)} = J_E^{(0,8)}$. Further discussion of the singularities is left to Ref. [?]. The hard coefficients $C_{L,R}^{(0,8)}$ are the same as in the previous section.

The remaining difference for $\bar{B}^0 \to D_s^{(*)} K^{(*)-}$ are the non-perturbative functions. The light-cone wavefunctions for K^-, $\bar{K}^0$, K^{*-}, and $\bar{K}^{*0}$ are [with $q = u, d$, $\omega_1 = \bar{n}p x_s$, $\omega_2 = -\bar{n}\cdot p x_q$, and a prefactor as in Eq. (5.29)]

$$
\langle K_n | (\bar{\xi}_n^{(s)} W)_{\omega_1} \not{\bar{n}} \gamma_5 (W^\dagger \xi_n^{(q)})_{\omega_2} | 0 \rangle = -2 i f_K \, \bar{n}\cdot p_K \, \phi_K(\mu, x_s) , \qquad (5.46)
$$

$$\begin{aligned}\langle K_n^*(\epsilon)|(\bar{\xi}_n^{(s)}W)_{\omega_1}\bar{n}\!\!\!/(W^\dagger\xi_n^{(q)})_{\omega_2}|0\rangle &= -2if_{K^*}\, m_{K^*}\, \bar{n}\cdot\epsilon^*\, \phi_{K^*}(\mu, x_s) \\ &= -2if_{K^*}\, \bar{n}\cdot p_{K^*}\, \phi_{K^*}(\mu, x_s)\ .\end{aligned}$$

The collinear functions $\Psi_M^{(0,8)}$ also depend on the light meson M. The non-perturbative soft functions involve strange quarks and are also different from section 5.1.3, $S \to \tilde{S}_{L,R}^{(i)}$ and $\Phi_{L,R}^{(0,8)} \to \tilde{\Phi}_{L,R}^{(0,8)}$. The non-perturbative functions are related to those in the previous section in the $SU(3)$ flavor symmetry limit. However, the jet functions are not related in this limit, they differ since different topologies contribute. This leads to different convolutions over the non-perturbative functions.

Next consider the Cabibbo suppressed $b \to cs\bar{u}$ transition with the color suppressed topology (as shown by the brackets in Fig. 6-2a). For the six quark operators we have[9]

$$\begin{aligned}O_j^{(0)}(k_i^+, \omega_k) &= \left[\bar{h}_{v'}^{(c)}\Gamma_j^h\, h_v^{(b)}\, (\bar{d}\,S)_{k_1^+}\bar{n}\!\!\!/P_L\, (S^\dagger u)_{k_2^+}\right]\left[(\bar{\xi}_n^{(s)}W)_{\omega_1}\Gamma_c(W^\dagger\xi_n^{(d)})_{\omega_2}\right], \qquad (5.47)\\ O_j^{(8)}(k_i^+, \omega_k) &= \left[(\bar{h}_{v'}^{(c)}S)\Gamma_j^h\, T^a\, (S^\dagger h_v^{(b)})\, (\bar{d}\,S)_{k_1^+}\bar{n}\!\!\!/P_L T^a (S^\dagger u)_{k_2^+}\right]\left[(\bar{\xi}_n^{(s)}W)_{\omega_1}\Gamma_c(W^\dagger\xi_n^{(d)})_{\omega_2}\right],\end{aligned}$$

which mediate the decays $\bar{B}^0 \to D^{(*)0}\bar{K}^{(*)0}$. In this case the $\mathrm{SCET_{II}}$ Lagrangian in Eq. (5.24) has the same flavor structure as in section 5.1.3. Since only the C-topology contributes the long distance contribution is not suppressed in the factorization theorem, and the jet function $J^{(0,8)} \to J_C^{(0,8)}$. For both the short and long distance non-perturbative functions the change of flavor appears only through the collinear quarks in the weak operator, so the collinear functions depend on the $K^{(*)0}$ but the soft functions $S_{L,R}^{(0,8)}$ and $\Phi_{L,R}^{(0,8)}$ are identical to those in section 5.1.3. (However, now $J_C^{(0,8)}$ appears, so the moments over the soft function $S_{L,R}^{(0,8)}$ will be different.) Finally note that if we allow a strange quark in the initial state (for B_s-decays) then the E-topology can also contribute and more operators are generated.

Due to the non-negligible long distance contributions the number of model independent phenomenological predictions for kaons are more limited. The main predictions are the equality of branching fractions and strong phase shifts for decays to

[9]Note that the flavor structure was not distinguished in naming the operators in Eqs. (5.27,6.4,5.47). This should not cause confusion since they always contribute to different decays.

D versus D^*. For $M = K^0, K^-$ an identical proof to the one for π^0 and ρ^0 can be used. For the vector mesons the proof can also be used if we restrict our attention to longitudinal polarizations, so the final states $D^{(*)}K_{\|}^{*0}$ are related, and so are $D^{(*)}K_{\|}^{*-}$. The factorization theorem allows for transversely polarized kaons at the same order in the power counting, but only through the long distance contribution.

5.1.5 Discussion and comparison with the large N_c limit

It is instructive to compare the N_c scaling of the different terms in the SCET result Eq. (5.34) (or Eq. (5.42)) with that expected from QCD before expanding in $1/Q$ given in Eq. (5.3). Combining the matrix elements in Eq. (5.3) written in a form similar to Eq. (5.42) gives the decay amplitude at leading order in $1/Q$ as

$$\begin{aligned} A(\bar{B}^0 \to D^0 M^0) &= N_0^M \left(C_1 + \frac{C_2}{N_c}\right)\left[\frac{1}{N_c}(F_0 + 2G_1) + \cdots\right] \\ &+ N_0^M\, C_2 \left[F_0 + \frac{1}{N_c^2}(-F_0 + F_2 - 2G_1) + \cdots\right] \cdots . \end{aligned} \tag{5.48}$$

The ellipses denote power suppressed terms. This reproduces the $1/N_c$ expansion of the SCET amplitude in Eq. (5.42) with the identification

$$F_0 = 0\,, \qquad G_1 = -\pi\alpha_s C_F\, s^{(0)}\big|_{N_c\to\infty}\,, \qquad F_2 - 2G_1 = 2\pi\alpha_s\, s^{(8)}\big|_{N_c\to\infty}\,, \tag{5.49}$$

where $s^{(0)} \sim N_c^0$ and $s^{(8)} \sim N_c$. This implies that the factorizable term F_0 is power suppressed in the limit of an energetic pion relative to the leading order amplitude in Eq. (5.42).

The naive factorization approach in Eq. (5.2) keeps only the F_0 term, which is expressed in terms of the $\bar{B} \to \pi$ form factor in the large N_c limit. We comment here on the form of this contribution in the effective theory. They appear in the matching of the $(\bar{d}b)_{V-A}(\bar{c}u)_{V-A}$ operator onto SCET$_{\rm I}$ $T-$products such as

$$T_1^{(4)} = T\{\mathcal{Q}_0^{(2)}, i\mathcal{L}_{q\xi}^{(2)}\}\,, \qquad T_2^{(4)} = T\{\mathcal{Q}_{1a,1b}^{(3)}, i\mathcal{L}_{q\xi}^{(1)}\}\,, \tag{5.50}$$

where the operators $\mathcal{Q}^{(2,3)}$ contain one usoft light quark. From the leading order operators in Eq. (5.19) they can be constructed by switching $\xi_n \to q$ to give $\mathcal{Q}^{(2)}$, and adding a further $W^\dagger i D_\perp W$ to get $\mathcal{Q}^{(3)}$. Their precise form is different depending on whether they are introduced by matching from the color-suppressed (C) or the W-exchange (E) graph. Schematically

$$\begin{aligned}
\text{C-type:} \qquad \mathcal{Q}_0^{(2)} &= [(\bar\xi_n^{(d)} W)_\omega \Gamma_c h_v^{(b)}][\bar h_{v'}^{(c)} \Gamma_h u] \qquad (5.51)\\
\mathcal{Q}_{1a}^{(3)} &= [(\bar\xi_n^{(d)} \frac{\bar{n}\!\!\!/}{2} i D\!\!\!/_{\perp c} W)_\omega \frac{1}{\bar n\cdot \mathcal{P}^\dagger} \Gamma_c h_v^{(b)}][\bar h_{v'}^{(c)} \Gamma_h u]\\
\mathcal{Q}_{1b}^{(3)} &= \frac{1}{m_c}[(\bar\xi_n^{(d)} W)_{\omega_1} \Gamma_c h_v^{(b)}][\bar h_{v'}^{(c)} [W^\dagger i D\!\!\!/_{\perp c} W]_{\omega_2} \Gamma_h u]\\
\text{E-type:} \qquad \mathcal{Q}_0^{(2)} &= [\bar d \Gamma_h h_v^{(b)}][\bar h_{v'}^{(c)} \Gamma_c (W^\dagger \xi_n^{(u)})_\omega] \qquad (5.52)\\
\mathcal{Q}_{1a}^{(3)} &= [\bar d \Gamma_h h_v^{(b)}][\bar h_{v'}^{(c)} \Gamma_c \frac{1}{\bar n\cdot \mathcal{P}} (W^\dagger i D\!\!\!/_{\perp c} \frac{\bar{n}\!\!\!/}{2} \xi_n^{(u)})_\omega]\\
\mathcal{Q}_{1b}^{(3)} &= \frac{1}{m_c}[\bar d \Gamma_h h_v^{(b)}][\bar h_{v'}^{(c)} [W^\dagger i D\!\!\!/_{\perp c} W]_{\omega_1} \Gamma_c (W^\dagger \xi_n^{(u)})_{\omega_2}]\,.
\end{aligned}$$

The presence of the usoft quark field q in these operators introduces an additional suppression factor of λ^2, such that the $T-$products $T_{1,2}^{(4)}$ are $O(\lambda^4) \sim \Lambda^2/Q^2$ down relative to the operators $\mathcal{Q}_{L,R}^{(0,8)}$ in Eq. (5.19). (Note that since the form factors enter as time ordered products we do not expect a different α_s suppression for $T_{1,2}^{(4)}$ relative to those in Eq. (5.20) [23].) This explains the absence of the F_0 contributions at order Λ/Q, as noted in (5.49). Although F_0 is part of the leading order result in the large N_c limit, it is subleading in the $1/Q$ expansion.

After soft-collinear factorization, the T-products (5.50) match onto factorizable operators in SCET_II . For example, the $C-$type time-ordered product containing $Q_{1a}^{(3)}$ gives (schematically)

$$T_2^{(4)} \to \int d\omega_1 d\omega_2\, \mathcal{J}(\omega_i, k_1^+) \Big[(\bar d S)_{k_1} \Gamma (S^\dagger h_v^{(b)})\Big] [\bar h_{v'}^{(c)} \Gamma_h u][(\bar\xi_n^{(u)} W)_{\omega_1} \Gamma_c (W^\dagger \xi_n^{(u)})_{\omega_2}] \qquad (5.53)$$

Apart from the $(\bar c u)$ soft bilinear, this is similar to a factorizable operator contributing to the $B \to \pi$ form factor [23]. The presence of the D meson in the final state implies that the matrix element of the soft operator in Eq. (5.53) is different from that

appearing in $\bar{B} \to \pi$. Therefore, naive factorization of type-II decay amplitudes, as written in Eq. (5.2), does not follow in general from the large energy limit. Still, in the large N_c limit, the matrix element of $T_1^{(4)}$ above can be indeed expressed in terms of the $B \to \pi$ form factor, as required by Eq. (5.5)

Recently an analysis of color-suppressed decays was performed using the "pQCD" approach working at leading order in an expansion in $m_{D^{(*)}}/m_B$ and $\Lambda_{\rm QCD}/m_{D^{(*)}}$ [68]. This differs from the expansion used here in that we do not expand in $m_{D^{(*)}}/m_B$. The non-perturbative functions in their proposed factorization formula include the light-cone wavefunctions $\phi_\pi^{(p)}(x_3)$, $\phi_D(x_2)$ and a B light-cone wavefunction that depends on a transverse coordinate $\phi_B(x_1, b_1)$. This differs from our result which involves a $B \to D$ function $S(k_1^+, k_2^+)$ and also has additional long distance contributions, $A_{\rm long}^{D^{(*)}M}$, at the same order in our power counting. Our long distance contributions are "non-factorizable" in the sense that the non-perturbative functions $\Phi_{L,R}^{(i)}(k^+, x_\perp)$ and $\Psi_M^{(i)}(z, \omega, x_\perp)$ communicate directly through their $x_\perp$ dependence without going through a hard kernel. In Ref. [68] strong phases only occur from the perturbative $\mu_0^2 \simeq E_M \Lambda$ scale, whereas we also find non-perturbative strong phases from the Λ^2 scale (in $S(k_1^+, k_2^+)$). The non-perturbative phases are expected to dominate in our result. Finally, the results in Ref. [68] do not manifestly predict the equality of the D and D^* amplitudes since at the order they are working contributions from different $B \to M$ form factors show up. For example their pQCD prediction $Br(\bar{B}^0 \to D^{*0}\rho^0)/Br(\bar{B}^0 \to D^0\rho^0) = 2.7$ is much different than the prediction of 1.0 that we obtain in the next section using heavy quark symmetry.

The time ordered products presented in Eq. (5.20) are only Λ/Q down from the class-I T amplitudes. Therefore, they give the dominant contribution to the color-suppressed and W-exchange amplitudes in the limit of an energetic pion ($\Lambda/Q \ll 1$). This is a new result, not noticed previously in the literature. The power counting of "factorizable" F_0 type contributions are indeed suppressed by Λ^2/Q^2 in our analysis in agreement with the literature. However, these terms do not give the dominant contribution.

5.1.6 Phenomenology

A factorization theorem for color-suppressed $\bar{B}^0 \to D^0 M^0$ decays was proven in Section 5.1.3 and extended to decays to kaons in Section 5.1.4. The amplitudes at leading order in $\Lambda_{\rm QCD}/Q$ with $Q = \{m_b, m_c, E_\pi\}$ have the form

$$\begin{aligned} A_{00} &= A(\bar{B}^0 \to D^{(*)0} M^0) \\ &= N_0^M \int_0^1 dx\, dz \int dk_1^+ dk_2^+ \sum_{i=0,8} \left[C_L^{(i)}(z)\, S_L^{(i)}(k_j^+) \pm C_R^{(i)}(z)\, S_R^{(i)}(k_j^+) \right] J^{(i)}(z, x, k_j^+)\, \phi_M(x) \\ &\quad + A_{\rm long}^{D^{(*)}M}, \end{aligned} \tag{5.54}$$

where the sign $\pm$ corresponds to a D^0 or D^{*0} meson in the final state, respectively. In this section the implications of Eq. (5.54) for the phenomenology of color suppressed decays are discussed. One class of predictions follow without any assumptions about the form of J:

- Heavy quark symmetry relates the nonperturbative soft matrix elements appearing in the $\bar{B}^0 \to D^0 M^0$ and $\bar{B}^0 \to D^{*0} M^0$ decays with the same light meson at leading order in $\alpha_s(Q)/\pi$. This implies relations among their branching fractions and equal strong phases in their isospin triangles.

These relations are encoded in the ratios R_0^M in Eq. (5.12). A second class of predictions depend on using a perturbative expansion of J in $\alpha_s(\mu_0)$ for $\mu_0^2 \sim E_M \Lambda$:

- Using a perturbative description of J the amplitudes and strong phases for decays to different light mesons M can be related at leading order in $\alpha_s(\mu_0)/\pi$.

These predictions are encoded in the ratios $R_0^{M/M'}$, R_c, and strong phase ϕ in R_I, as defined in Eq. (5.12). We consider the two classes of predictions in turn.

First, consider relations between color-suppressed $\bar{B} \to DM$ and $\bar{B} \to D^* M$ decays with the same light meson. At tree level in the matching at the hard scale $\mu \simeq Q$, two of the Wilson coefficients vanish $C_R^{(0,8)} = 0$. Therefore both amplitudes for D and D^* contain only the soft functions $S_L^{(0,8)}(k_j^+)$ appearing in the same linear combination. This implies model-independent predictions, which can be made even in

the absence of any information about the jet functions $J^{(i)}$ and the non-perturbative functions $S_L^{(i)}$, ϕ_M, and without knowing $A_{\rm long}^{D^{(*)}M}$. For $M = \pi^0, \rho^0$, we have $A_{\rm long}^{D^{(*)}M} = 0$ so Eq. (5.54) gives

$$R_0^\pi \equiv \frac{A(\bar{B}^0 \to D^{*0}\pi^0)}{A(\bar{B}^0 \to D^0\pi^0)} = 1\,, \qquad R_0^\rho \equiv \frac{A(\bar{B}^0 \to D^{*0}\rho^0)}{A(\bar{B}^0 \to D^0\rho^0)} = 1\,. \tag{5.55}$$

For decays to $D_s^{(*)}K^-$, $D_s^{(*)}K_{||}^{*-}$, $D^{(*)0}\bar{K}^0$, and $D^{(*)0}\bar{K}_{||}^{*0}$ it was shown that $A_{\rm long}^{DM} = A_{\rm long}^{D^*M}$ and so

$$\begin{aligned} R_0^{K^-} &= \frac{A(\bar{B}^0 \to D_s^* K^-)}{A(\bar{B}^0 \to D_s K^-)} = 1\,, \qquad R_0^{K_{||}^{*-}} = \frac{A(\bar{B}^0 \to D_s^* K_{||}^{*-})}{A(\bar{B}^0 \to D_s K_{||}^{*-})} = 1\,, \\ R_0^{K^0} &= \frac{A(\bar{B}^0 \to D^* \bar{K}^0)}{A(\bar{B}^0 \to D \bar{K}^0)} = 1\,, \qquad R_0^{K_{||}^{*0}} = \frac{A(\bar{B}^0 \to D^* \bar{K}_{||}^{*0})}{A(\bar{B}^0 \to D \bar{K}_{||}^{*0})} = 1\,. \end{aligned} \tag{5.56}$$

The ratios in Eqs. (5.55) and (5.56) have calculable corrections of order $\alpha_s(Q)/\pi$ and power corrections[10] of order Λ/Q, which can be expected to be $\sim 20\%$.

These amplitude relations imply the equality of the branching fractions. They also imply the equality of the non-perturbative strong phases between isospin amplitudes, namely the phases $\delta^{D^{(*)}M}$ in the ratios $R_I^{D^{(*)}M}$ as shown in Fig. 5-6. Thus for each of $M = \pi^0, \rho^0, K^0, K_{||}^{*0}$

$$Br(\bar{B}^0 \to D^{*0}M^0) = Br(\bar{B}^0 \to D^0 M^0)\,, \qquad \delta^{D^{*0}M^0} = \delta^{D^0 M^0}\,, \tag{5.57}$$

and for $M = K^-, K_{||}^{*-}$

$$Br(\bar{B}^0 \to D_s^* M) = Br(\bar{B}^0 \to D_s M)\,, \qquad \delta^{D_s^* M} = \delta^{D_s M}\,. \tag{5.58}$$

The predictions in Eqs. (5.55,5.57) agree well with the data for $D^{(*)}\pi$ in Table 5.1, which give

$$|R_0^\pi|^{\rm exp} = 0.94 \pm 0.21\,, \qquad \delta^{D\pi} = 30.3^\circ {}^{+7.8}_{-13.8}\,, \qquad \delta^{D^*\pi} = 30.1^\circ \pm 6.1^\circ\,. \tag{5.59}$$

[10]Note that using the observed D and D^* masses $R_0^M = N_0^*/N_0 = 1.04$. This small difference corresponds to keeping an incomplete set of higher order corrections.

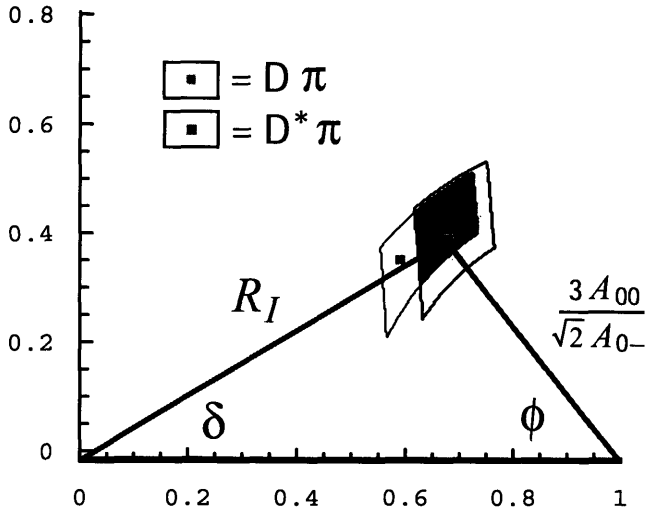

Figure 5-6: The ratio of isospin amplitudes $R_I = A_{1/2}/(\sqrt{2}A_{3/2})$ and strong phases δ and ϕ in $\bar{B} \to D\pi$ and $\bar{B} \to D^*\pi$. The central values following from the D and D^* data in Table I are denoted by squares, and the shaded regions are the 1σ ranges computed from the branching ratios. The overlap of the D and D^* regions show that the two predictions embodied in Eq. (5.55) work well.

This agreement is represented graphically by the overlap of the 1σ regions in Fig. 5-6, with small squares indicating the central values. The dominant contribution to the phase δ is generated by the $(C - E)$ amplitudes which have complex phases from $J^{(i)}\, S_L^{(0,8)}$ in Eq. (5.54). Since the phases in $S_L^{(0,8)}$ are non-perturbative and can be large it is expected that they will dominate. Note that with this choice of triangle the power suppressed side in Fig. 5-6 is enlarged by a isospin prefactor of $3/\sqrt{2} = 2.1$.

For $\bar{B}^0$ decays to $D^{(*)0}\rho^0$, $D^{(*)0}\bar{K}^0$, $D^{(*)0}\bar{K}^{*0}_{||}$, $D_s^{(*)}K^-$ and $D_s^{(*)}K^{*-}_{||}$ only upper bounds on the branching ratios exist, so our relation between D and D^* triangles has not yet be tested. For each of these channels similar triangles to the one in Fig. 5-6 can be constructed once data becomes available.

The results in Eqs. (5.55) and (5.56) can be contrasted with the absence of a definite prediction in the large N_c limit as in Eq. (5.6). Even when only the F_0 term is included (naive factorization), R_π is given by a ratio of $B \to \pi$ form factors, which for generic $m_{b,c}$ are not related by heavy quark symmetry. Thus, one does not expect a relation between the branching fractions or strong phases unless the $1/Q$ expansion is used.

Next consider the second class of predictions, which follow from the perturbative expansion of the jet function in Eq. (5.54). We now assume that $\alpha_s(\mu_0)$ is perturbative, and focus on $M = \pi, \rho$ since the kaons are contaminated by contributions from $A_{\rm long}^{D^{(*)}M}$. The tree level result for J is given in Eq. (5.41), and was used to define the nonperturbative parameters $s^{(0,8)}$ through convolutions with the soft distribution functions $S_L^{(0,8)}(k_i^+)$ as in Eq. (5.43). It is convenient to introduce an effective moment parameter,

$$s_{\rm eff} = -s^{(0)} + \frac{1}{2N_c C_F}\frac{C_L^{(8)}}{C_L^{(0)}} s^{(8)} = |s_{\rm eff}| e^{-i\phi} \,. \tag{5.60}$$

In terms of the effective moment the result in Eq. (5.54) at lowest order in $\alpha_s(Q)$ and $\alpha_s(\mu_0)$ becomes

$$A(\bar{B}^0 \to D^{(*)0} M^0) \;=\; N_0^M \, C_L^{(0)} \, \frac{16\pi\alpha_s(\mu_0)}{9} \, s_{\rm eff}(\mu_0) \, \langle x^{-1} \rangle_M \,, \tag{5.61}$$

where N_0^M is defined in Eq. (5.35). Since $s_{\rm eff}$ is independent of $M = \pi, \rho$ the same phase ϕ is predicted for these two light mesons.

At leading order in $1/Q$ the type-I amplitude $A_{0-} = A(B^- \to D^0\pi^-)$ factors as in Eq. (5.7) giving the product of a form factor and decay constant, both of which are real (with the usual phase conventions for the states, and neglecting tiny $\alpha_s(m_b)$ strong phases ($\sim 2°$) generated by the coefficients $C_{L,R}^{(0)}$ at one-loop [29]). Therefore the amplitude A_{0-} is real at leading order in $1/Q$, up to calculable corrections of order $\alpha_s(Q)$. Choosing the orientation of the triangle so that A_{0-} lies on the real axis, the phase ϕ can be directly extracted as one of the angles in the isospin triangle

$$\sqrt{2}A_{00} + A_{+-} = A_{0-} \,. \tag{5.62}$$

This is shown in Fig. 5-7 where we divide by A_{0-} to normalize the base. The data on $\bar{B}^0 \to D^0\rho^0$ is not yet sensitive enough to test the prediction that ϕ is the same for π^0 and ρ^0.

Using Eqs. (5.7) and (5.61) it is possible to make a prediction for the ratio R_c in Eq. (5.12) at NLO in the power expansion. Since $R_c = A_{+-}/A_{0-}$ contains only charged light mesons it is easier to measure than neutral pion channels. Data is available for all four of the $D^{(*)}\pi$ and $D^{(*)}\rho$ channels. Using the triangle relation in Eq. (5.62) one finds for the ratio of any two such modes [$M = \pi, \rho$]

$$R_c^{D^{(*)}M} = 1 - \sqrt{2}\frac{A_{00}}{A_{0-}} = 1 - \frac{16\pi\alpha_s(\mu_0) m_{D^{(*)}}}{9\, E_M (m_B + m_{D^{(*)}})} \frac{s_{\rm eff}(\mu_0)}{\xi(w_0,\mu_0)} \langle x^{-1}\rangle_M \,. \tag{5.63}$$

It is easy to see that the ratio of amplitudes on the right-hand side is common to final states containing a D or D^*, and has only a mild dependence on the light meson, introduced through the inverse moment $\langle x^{-1}\rangle_M$. In particular we note that there is no dependence on the decay constant f_M on the RHS of Eq. (5.63), since it cancels in the ratio A_{00}/A_{0-}. This implies that the ratios R_c are comparable for all four channels $D^{(*)}\pi$ and $D^{(*)}\rho$, up to corrections introduced by $\langle x^{-1}\rangle_\pi \neq \langle x^{-1}\rangle_\rho$. These corrections can be smaller than the correction one might expect from the ratio of decay constants $f_\rho/f_\pi \simeq 1.6$ (which appear in the naive a_2 factorization). The experimental values of these ratios can be extracted from Table I and are in good agreement with a quasi-universal prediction

$$\begin{aligned}
|R_c^{(D\pi)}| &= \frac{|A(\bar B^0 \to D^+\pi^-)|}{|A(\bar B^- \to D^0\pi^-)|} = 0.77 \pm 0.05\,, \\
|R_c^{(D^*\pi)}| &= \frac{|A(\bar B^0 \to D^{*+}\pi^-)|}{|A(\bar B^- \to D^{*0}\pi^-)|} = 0.81 \pm 0.05\,, \\
|R_c^{(D\rho)}| &= \frac{|A(\bar B^0 \to D^+\rho^-)|}{|A(\bar B^- \to D^0\rho^-)|} = 0.80 \pm 0.09\,, \\
|R_c^{(D^*_L\rho_L)}| &= \frac{|A(\bar B^0 \to D^{*+}\rho^-)|}{|A(\bar B^- \to D^{*0}\rho^-)|} = 0.86 \pm 0.10\,.
\end{aligned} \tag{5.64}$$

This lends support to our prediction for the universality of the strong phase ϕ in $\bar B \to D^{(*)}\pi$ and $\bar B \to D^{(*)}\rho$ decays from the $s_{\rm eff}$ in Eq. (5.63). The central values of $R_c \simeq 0.8$ are well described by an $s_{\rm eff}$ of the expected size ($\sim \Lambda_{\rm QCD}$) as discussed in the fit to the isospin triangle below. Further data on these channels may expose other interesting questions, such as whether $R_c^{(D^*M)}$ is closer to $R_c^{(DM)}$ than $R_c^{(D^{(*)}\pi)}$

is to $R_c^{(D^{(*)}\rho)}$.

An alternative use of Eq. (5.63) and the R_c amplitude ratios is to give us a method for extracting the ratio of ρ and π moments. Using the $D\pi$ and $D\rho$ measurements which have smaller errors than for D^*, we find

$$\frac{\langle x^{-1}\rangle_\rho}{\langle x^{-1}\rangle_\pi} = \frac{|R_c^{(D\rho)}| - 1}{|R_c^{(D\pi)}| - 1} = 0.87 \pm 0.42\,. \tag{5.65}$$

where only the experimental uncertainty is shown. The extraction in Eq. (5.65) is smaller, but still in agreement with the ratio extracted from light-cone QCD sum rules. The best fit from the $\gamma^*\gamma \to \pi^0$ data performed in Ref. [11] gives $\langle x^{-1}\rangle_\pi = 3.2 \pm 0.4$ in agreement with sum rule estimates of the moment. The QCD sum-rule result $\langle x^{-1}\rangle_\rho = 3.48 \pm 0.27$ [12], then implies

$$\left.\frac{\langle x^{-1}\rangle_\rho}{\langle x^{-1}\rangle_\pi}\right|_{\rm SR} = 1.10 \pm 0.16\,. \tag{5.66}$$

The result that this ratio is close to unity is consistent with the universality of the data in Eq. (5.64). This data can be contrasted with cases where the single light meson is replaced by a multibody state such as [52]

$$\frac{Br(\bar{B}^0 \to D^{*+}\pi^-\pi^-\pi^+\pi^0)}{Br(\bar{B}^- \to D^{*0}\pi^+\pi^-\pi^-\pi^0)} = 1.02 \pm 0.27\,, \tag{5.67}$$

For the four pion final state our proof of the factorization theorem does not work, since for many events one or more of the pions will be slow. We therefore would expect less universality in branching ratios involving more than one light meson. (For these decays a different type of factorization involving large N_c works well for the q^2 spectrum [83].)

The result in Eq. (5.61) also leads to predictions for the ratios of color-suppressed decay amplitudes to final states containing different light mesons $M^0 = \pi^0, \rho^0$. We find

$$R_0^{\rho/\pi} \equiv \frac{|A(\bar{B}^0 \to D^0\rho^0)|}{|A(\bar{B}^0 \to D^0\pi^0)|} = \frac{f_\rho}{f_\pi}\,\frac{\langle x^{-1}\rangle_\rho}{\langle x^{-1}\rangle_\pi} = 1.40 \pm 0.77\,, \tag{5.68}$$

where we used $f_{\pi^\pm} = 130.7 \pm 0.4$ MeV, and $f_{\rho^\pm} = 210 \pm 10$ MeV, and inserted the result in Eq. (5.65) for the moments. This can be compared with the experimental result $(R_{\rho/\pi})^{\rm exp} = 1.02 \pm 0.21$. The large uncertainty in the ratio of moments in Eq. (5.65) dominates the error in Eq. (5.68). With the QCD sum rule result in Eq. (5.66) we find $R_{\rho/\pi} = 1.64 \pm 0.35$, a result whose central value is farther from the experimental data, but still consistent with it.

In contrast to the first class of predictions, the predictions for the ratios in Eqs. (5.63), (5.65), and (5.68) and the prediction for the universality of ϕ can receive corrections from neglected $[\alpha_s(\mu_0)^2/\pi]$ terms in J. The dominant theoretical corrections to this extraction are expected to come again from these perturbative corrections to J or from power corrections, which we estimate may be at the $\sim 30\%$ level. A future study of the perturbative corrections is possible within the framework of our factorization theorem and SCET.

The result in Eq. (5.61) and the data on $B \to D\pi$ and $B \to D^*\pi$ decays can be used to extract values of the moment parameters $|s_{\rm eff}|$ and strong phase ϕ. We present in Fig. 5-7 the constraints on the parameter $s_{\rm eff}$ in the complex plane, obtained from $D\pi$ (light shaded region) and $D^*\pi$ data (darker shaded area). We used in this determination $\mu_0 = E_\pi = 2.31\,{\rm GeV}$, and leading order running which gives $\alpha_s(\mu_0) = 0.25$, $C_1(\mu = \mu_0) = 1.15$, and $C_2(\mu = \mu_0) = -0.32$. The good agreement between the $D\pi$ and $D^*\pi$ 1σ regions marks a quantitative success of our factorization relation in Eq. (5.54). Averaging over the $D\pi$ and $D^*\pi$ results, we find the following values for the soft parameters at $\mu = \mu_0$

$$\begin{aligned} |s_{\rm eff}| &= \left(428 \pm 48 \pm 100\ {\rm MeV}\right) \left(\frac{0.26}{C_L(\mu_0)\alpha_s(\mu_0)}\right) \left(\frac{3.2}{\langle x^{-1}\rangle_\pi}\right), \\ \phi &= 44.0^\circ \pm 6.5^\circ . \end{aligned} \tag{5.69}$$

In this determination the inverse moment of the pion wave function was taken from the best fit to the $\gamma^*\gamma \to \pi^0$ data [11], $\langle x^{-1}\rangle_\pi = 3.2 \pm 0.4$. For $|s_{\rm eff}|$ the first error is experimental, while the second is our estimate of the theoretical uncertainty in the extraction from varying μ_0 from $E_\pi/2$ to $2E_\pi$. At the order we are working the

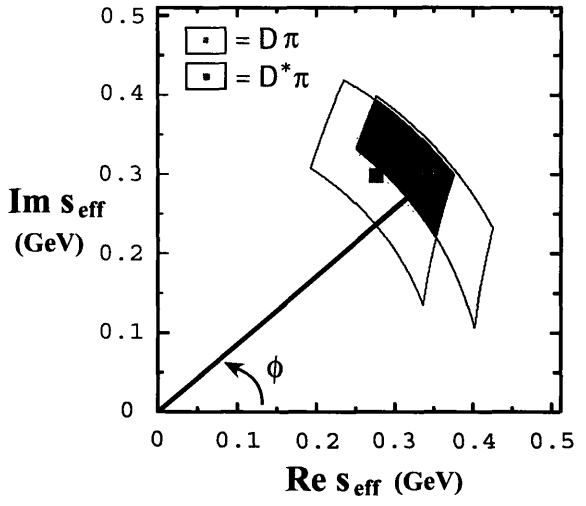

Figure 5-7: Fit to the soft parameter $s_{\rm eff}$ defined in the text, represented in the complex plane with the convention that A_{0-} is real. The regions are derived by scanning the 1σ errors on the branching fractions (which may slightly overestimate the uncertainty). The light grey area gives the constraint from $\bar{B} \to D\pi$ and the dark grey area gives the constraint from $\bar{B} \to D^*\pi$.

extraction of the phase ϕ is independent of the scale, since the prefactor $\alpha_s(\mu_0)\langle x^{-1}\rangle_\pi$ drops out. The result in Eq. (5.69) agrees well with the dimensional analysis estimates $s_{\rm eff} \sim s^{(0,8)} \sim \Lambda_{\rm QCD}$. Since ϕ is non-perturbative its value is unconstrained, and a large value of this phase is allowed.

The recent $\bar{B}^0 \to D^0\rho^0$ data from Belle allows us to extract $|s_{\rm eff}|$ and ϕ in a manner independent of the above determination. Keeping only experimental errors we find

$$\begin{aligned} |s_{\rm eff}| &= \left(259 \pm 124 \text{ MeV}\right)\left(\frac{0.26}{C_L(\mu_0)\alpha_s(\mu_0)}\right)\left(\frac{3.5}{\langle x^{-1}\rangle_\rho}\right), \\ \phi &= 17^\circ \pm 70^\circ . \end{aligned} \tag{5.70}$$

The results agree with Eq. (5.69) within 1σ, but currently have errors that are too large to significantly test the factorization prediction of equality on the 20-30% level of the parameters extracted from $D\rho$ and $D\pi$.

The $\bar{B}^0 \to D_s^{(*)+}K^-$ channels proceed exclusively through the W-exchange graph and have been the object of recent theoretical work [85]. For the result analogous to

Eq. (5.61) we would have [$M = K, K^*$]

$$A(\bar{B}^0 \to D_s^{(*)} M) \;=\; \sqrt{2} N_0^M \, C_L^{(0)} \, \frac{16\pi\alpha_s(\mu_0)}{9} \, s_{\rm eff}^E(\mu_0) \, \langle x_s^{-1} \rangle_M + A_{\rm long}^{D_s^{(*)} M} \,. \quad (5.71)$$

Both the $\bar{B}^0 \to D_s^{(*)+} K^-$ modes and the Cabibbo-suppressed decays $\bar{B} \to D^{(*)} \bar{K}^{(*)}$ receive this additional contribution from $A_{\rm long}^{D^{(*)} M}$. This makes the factorization theorem less predictive, and so we do not attempt an analysis of ratios $R_c^{D^{(*)} K^{(*)}}$, $R_0^{M/M'}$, or the universal phases ϕ_E and ϕ_C that are analogous to the ϕ in Eq. (5.60).

On the experimental side both the Babar and Belle Collaborations [7] recently observed the $\bar{B}^0 \to D_s^+ K^-$ decay, and set an upper limit on the branching ratio of $\bar{B}^0 \to D_s^{*+} K^-$

$$\begin{aligned} B(\bar{B}^0 \to D_s^+ K^-) &= [3.2 \pm 1.0 \text{ (stat)} \pm 1.0 \text{ (sys)}\,] \times 10^{-5} && \text{(Babar)} \quad (5.72) \\ &= [4.6^{+1.2}_{-1.1} \text{ (stat)} \pm 1.3 \text{ (sys)}\,] \times 10^{-5} && \text{(Belle)} \\ B(\bar{B}^0 \to D_s^{*+} K^-) &\le 2.5 \times 10^{-5} \, (90\%\text{CL}) && \text{(Babar)}\,. \end{aligned}$$

The branching fraction for $\bar{B}^0 \to D_s^+ K^-$ is an order of magnitude smaller than that for $\bar{B}^0 \to D^0 \pi^0$. This indicates that the W-exchange amplitude $E^{D_s K^-}$ is suppressed relative to $(C - E)^{D\pi}$ and $(V_{ud}/\sqrt{2} V_{us}) \, C^{D^0 \bar{K}^0}$. In SCET the SU(3) breaking between $\phi_\pi(x)$ and $\phi_K(x)$ is generated by masses in the collinear quark Lagrangian [79]. This causes an asymmetry in the light-cone kaon wavefunction. This SU(3) violation can be expected to be at most a canonical $\sim$ 20-30% effect, which would not account for the observed suppression.

However, there is one important source of potentially larger SU(3) breaking from an enhancement in moments of the light-cone kaon wavefunction which appear in the short distance amplitude. This may account for the observed suppression. Basically strange quark mass effects imply a larger SU(3) violation for inverse moments than expected for ϕ_π versus ϕ_K alone, and implies that $\langle x_s^{-1} \rangle_K < \langle x_d^{-1} \rangle_K$. Using the result from QCD sum rules the ratio of moments [12] is $\langle x_d^{-1} \rangle_K / \langle x_s^{-1} \rangle_K \sim 1.4$. Furthermore, we anticipate a similar large effect from the moments that appear in the soft matrix

elements which again differ by factors of $(k_d^+)^{-1}$ versus $(k_s^+)^{-1}$, and appear in a way that suppresses D_sK^-. The combination of these two suppression factors might accommodate the observed factor of three suppression in the D_sK^- amplitudes.[11] The long distance amplitude also involves two inverse momentum fractions through $\overline{J}^{(0,8)}$ in Eq. (5.25), although admittedly much less is known about the non-perturbative functions $\Psi_M^{(0,8)}$ and $\Phi_{L,R}^{(0,8)}$. Thus, we find that the suppression of $E^{D_sK^-}$ may not imply much about the relative size of $C^{D\pi}$ and $E^{D\pi}$. Finally, we note that the suppression mechanism for $s\bar{s}$ creation that we have identified is particular to problems involving large energies where light-cone wavefunctions arise.

Further information on the relative size of the short and long distance contributions to the kaon factorization theorem is clearly desirable. In section 5.1.4 it was noted that in type-II decays transverse K^*'s are produced only by the long distance contribution at this order in $\Lambda_{\rm QCD}/Q$. Therefore, measuring the polarization of the K^* in both the $\bar{B}^0 \to D_s^* K^{*-}$ and $\bar{B}^0 \to D^{*0}K^{*0}$ decays can give us a direct handle on whether there might be additional dynamical suppression of either the long or short distance contributions, or whether they are similar in size as one might expect apriori from the power counting.

5.1.7 Discussion of results

We presented a model-independent analysis of color-suppressed $\bar{B}^0 \to D^{0(*)}M^0$ decays, in the limit of an energetic light meson M^0. The soft-collinear effective theory (SCET) was used to prove a factorization theorem for these decay amplitudes at leading order in $\Lambda_{\rm QCD}/Q$, where $Q = \{m_b, m_c, E_M\}$. Compared with decays into a charged pion these decays are suppressed by a factor $\Lambda_{\rm QCD}/Q$. Therefore, in the effective theory they are produced exclusively by subleading operators.[12]

[11] In general this argument gives a dynamic explanation for the suppression of $s\bar{s}$-popping at large energies which could be tested elsewhere. The production of an $s\bar{s}$ pair which end up in different strange hadrons is likely to be accompanied by a suppression from inverse momentum fractions that arise from the gluon propagator that produced these quarks. This enhances the SU(3) violation in a well defined direction so that less $s\bar{s}$ pairs are produced. A factor of 3 suppression of $s\bar{s}$ popping is implemented in JETSET [106].

[12] In type-I decays, other subleading operators can compete with the time ordered products we have identified at the same order in Λ/Q. This makes a complete analysis of power corrections to

We have identified the complete set of subleading operators which contribute to $\bar{B}^0 \to D^{0(*)}M^0$ decays with $M = \pi, \rho, K, K^*$, as well as for the decays $\bar{B}^0 \to D_s^{(*)}K^{(*)-}$. After hard-soft-collinear factorization, their matrix elements are given by i) a short distance contribution involving a jet function convoluted with nonperturbative soft distribution functions, and the non-perturbative light-cone meson wave function, and ii) a long distance contribution involving another jet function and additional $x_\perp$ dependent nonperturbative functions for the soft B, D and collinear M. The long distance contributions were shown to vanish for $M = \pi, \rho$ at lowest order in $\alpha_s(Q)/\pi$.

The factorization formula is given in Eqs. (5.34) and (5.36). It may seem surprising that the type-II decays factor into a pion light-cone wave function and a $B \to D^{(*)}$ soft distribution function rather than being like the naive a_2 factorization in Eq. (5.2). Our results indicate that factorization for type-II decays is similar to factorization for type-I decays (albeit with new non-perturbative soft functions and additional long distance contributions for kaons). To derive Eq. (5.34), QCD was first matched onto SCET_I at the scale $\mu^2 = Q^2$. In SCET_I it is still possible for gluons to redistribute the quarks. This intermediate theory provides a mechanism for connecting the soft spectator quark in the B to a quark in the pion, and for connecting the energetic quark produced by the four-quark operator with the soft spectator in the D (see Fig. 6-2). This process is achieved by the power suppressed time ordered products given in Eq. (5.20). SCET_I is then matched onto SCET_II at a scale $\mu_0^2 = E_M\Lambda$. In SCET_II the collinear quarks and gluons are non-perturbative and bind together to make the light meson M. This second stage of matching introduces a new coefficient function (jet functions) as in Eq. (5.23). The jet function J contains the information about the SCET I graphs that move the spectator quarks into the pion. The physics at various scales is neatly encoded in Eq. (5.34). The Wilson coefficient $C(z)$ from matching QCD onto SCET I depends on physics at the scale Q^2, the jet functions $J, \overline{J}$ from matching SCET I onto SCET II depends on $Q\Lambda$ physics which is where quark redistribution occurs, and finally the soft distribution functions S, Φ and the pion

type-I decays more complicated than our analysis of type-II decays.

light cone wavefunction ϕ_M, Ψ_M depend on non-perturbative physics at Λ^2 which is where the binding of hadrons occur.

The soft functions S are complex, and encode information about strong rescattering phases. This information is introduced through Wilson lines along the light meson direction of motion, which exchange soft gluons with the final state meson $D^{(*)}$. They provide a new mechanism which generates non-perturbative strong phases. In the literature other mechanisms which generate perturbative strong phases have been proposed. In particular in Ref. [13, 29] a method for identifying perturbative strong phases with an expansion in $\alpha_s(Q^2)$ was developed. In Ref. [70, 68] it was pointed out that strong phases can also be generated perturbatively at the intermediate scale $\alpha_s(E_M\Lambda)$. In the language of our factorization theorem in Eq. (5.34) these phases roughly correspond to imaginary parts in the hard coefficients $C_{L,R}^{(0,8)}$ and jet functions J respectively. These phases exist, but for the $B \to D\pi$ channels they only show up at next-to-leading order in the $\alpha_s(m_b)$ or $\alpha_s(\mu_0)$ expansion. (In type-I $B \to D^{(*)}\pi$ decays the hard strong phase is very small, $\sim 2^\circ$ [29]). In contrast, our new source of strong phases is entirely non-perturbative in origin and can produce unconstrained phases. For the case of $B \to D^{(*)}M$ these phases show up in the power suppressed class-II amplitudes.

The factorization theorem proven in this section leads to predictions which were tested against existing experimental data on color-suppressed decays. We derived two model independent relations, which related

- the $\bar{B}^0 \to D^0 M^0$ and $\bar{B}^0 \to D^{*0} M^0$ decay branching fractions and
- the $\bar{B} \to DM$ and $\bar{B} \to D^* M$ strong phases.

Here $M = \pi, \rho, K, K^*_\parallel$, and these relations are true to all orders in the strong coupling at the collinear scale. The same predictions are also obtained for $\bar{B}^0 \to D_s^{(*)} K^-$ and $\bar{B}^0 \to D_s^{(*)} K^{*-}_\parallel$. The good numerical agreement observed between the strong phases and branching fractions in the $D\pi$ and $D^*\pi$ channels gives strong backing to our results. This prediction can be tested further since the equality of the strong phases for the ρ, K, and $K^*_\parallel$ channels have not yet been tested experimentally.

Additional predictions followed from the factorization theorem by using a perturbative expansion for the jet function, including $[M = \pi, \rho]$

- the ratios $|R_c| = |A(\bar{B}^0 \to D^{(*)+} M^-)/A(B^- \to D^{(*)0} M^-)|$ to subleading order
- the ratios $|R_0^{\rho/\pi}| = |A(\bar{B}^0 \to D^{(*)0}\rho^0)/A(\bar{B}^0 \to D^{(*)0}\pi^0)|$ to subleading order
- universal parameters $\{|s_{\rm eff}|, \phi\}$ which appear for both $D^{(*)}\pi$ and $D^{(*)}\rho$, and
- a mechanism for enhanced $SU(3)$ violation in $s\bar{s}$ production for the short distance amplitude which might explain the suppression of the $\bar{B}^0 \to D_s^{(*)} K^-$ rates relative to $\bar{B}^0 \to D^0\pi^0$.

For $|R_c|$ taking different values of M with the same isospin the power corrections only differ by the moments $\langle x^{-1}\rangle_M$, giving an explanation for the observed quasi-universality of these ratios. The isospin triangles for these M's are predicted to involve a universal angle ϕ. The ratio of neutral modes $|R_0^{\rho/\pi}|$ are determined by inverse moments of the light-cone wavefunctions and decay constants. Finally extractions of the non-perturbative soft moment parameter $s_{\rm eff}$ agrees with the $\sim \Lambda_{\rm QCD}$ size estimated by dimensional analysis.

In the case of $\bar{B}^0 \to D_s^{(*)} K^{(*)-}$ an additional suppression mechanism was identified, which arises from enhanced SU(3) violation due to the asymmetry of non-perturbative distributions involving strange versus down quarks. The inverse moments that appear in the factorization theorem enhances this difference, and can lead to a dynamic suppression of $s\bar{s}$-popping. Further information on the size of the short and long distance amplitudes would help in clarifying this observation.

A more detailed experimental study of the channels in Tables I and II is crucial to further test the accuracy of the factorization theorem and improve our understanding of the structure of power corrections.

Chapter 6

Isosinglets

6.1 Isosinglets

6.1.1 SCET Analysis and Data

We now consider the case when the final state light meson is an isosinglet. The Belle and BaBar Collaborations have recently reported measurements of the color suppressed decay channels $\bar{B}^0 \to D^{(*)0}\eta$, $\bar{B}^0 \to D^0\eta'$, and $\bar{B}^0 \to D^{(*)0}\omega$ which have an isosinglet meson M in the final state [10, 1, 9]. A summary of the data is given in Table 6.1. By now it is well understood that naive factorization [108] fails for these color-suppressed decays. A rigorous framework for discussing them in QCD is provided by the factorization theorem derived in the last section. The presence of isosinglet mesons enriches the structure of the decays due to η–η' and ω–ϕ mixing effects and gluon production mechanisms [56, 73, 34]. In this section, we generalize the SCET analysis of the last section to include isosinglets. We also construct a test of SU(3) flavor symmetry in color suppressed decays, using our results to include the $\eta - \eta'$ mixing.

The quark level weak Hamiltonian is the same as in Eq. (5.1). For color-suppressed decay channels with isosinglets, it gives rise to three flavor amplitudes denoted C, E, and G in Fig. 6-1, which take on a precise meaning in terms of operators in the SCET analysis at leading order in Λ_{QCD}/Q. Here Q is a hard scale on the order of the heavy

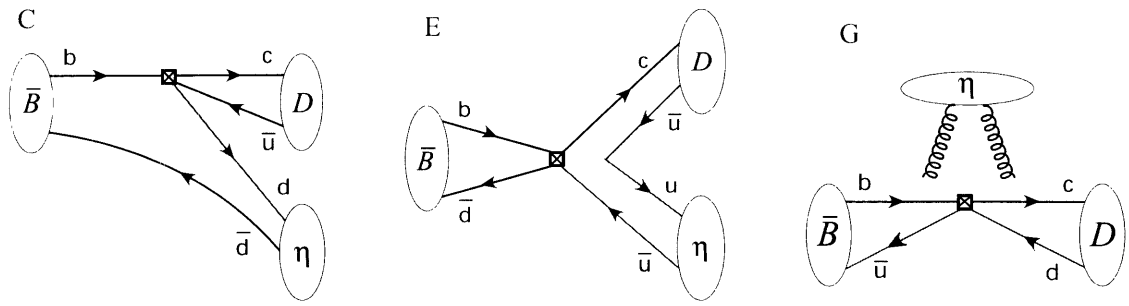

Figure 6-1: Flavor diagrams for $\bar{B} \to D\eta$ decays, referred to as color-suppressed (C), W-exchange (E), and gluon production (G). These amplitudes denote classes of Feynman diagrams where the remaining terms in a class are generated by adding any number of gluons as well as light-quark loops to the pictures.

quark masses m_b, m_c or the isosinglet meson energy E_M. The gluon G amplitude is unique to isosinglet mesons. We will show however that for $B \to D^{(*)}M$ decays the G amplitude is suppressed by $\alpha_s(\sqrt{E\Lambda})$ relative to the C, E contributions.

For color suppressed decays to isosinglet mesons $M = \{\eta, \eta', \omega, \phi\}$ we will show that the factorization theorem for the amplitudes $A_M^{(*)} = \langle D^{(*)0} M | H_W | \bar{B}^0 \rangle$ is

$$A^{(*)M} = A^{(*)M}_{\rm short} + A^{(*)M}_{\rm glue} + A^{(*)M}_{\rm long} \pm (L \leftrightarrow R)\,, \tag{6.1}$$

Decay	Br(10^{-4}) (BaBar)	Br(10^{-4}) (Belle)	Br(10^{-4}) (Avg.)	$\|A\|$ (10^{-4} MeV)
$\bar{B}^0 \to D^0\eta$	$2.5 \pm 0.2 \pm 0.3$	$1.83 \pm 0.15 \pm 0.27$	2.1 ± 0.2	1.67 ± 0.09
$\bar{B}^0 \to D^{*0}\eta$	$2.6 \pm 0.4 \pm 0.4$	–	2.6 ± 0.6	1.87 ± 0.22
$\bar{B}^0 \to D^0\eta'$	$1.7 \pm 0.4 \pm 0.2$	$1.14 \pm 0.20 \pm 0.11$	1.3 ± 0.2	1.31 ± 0.11
$\bar{B}^0 \to D^{*0}\eta'$	$1.3 \pm 0.7 \pm 0.2$	$1.26 \pm 0.35 \pm 0.25$	1.3 ± 0.4	1.33 ± 0.19
$\bar{B}^0 \to D^0\omega$	$3.0 \pm 0.3 \pm 0.4$	$2.25 \pm 0.21 \pm 0.28$	2.5 ± 0.3	1.83 ± 0.11
$\bar{B}^0 \to D^{*0}\omega$	$4.2 \pm 0.7 \pm 0.9$	–	4.2 ± 1.1	2.40 ± 0.31
$\bar{B}^0 \to D^{(*)0}\phi$	–	–	–	–
$\bar{B}^0 \to D^0\pi^0$	$2.9 \pm 0.2 \pm 0.3$	$2.31 \pm 0.12 \pm 0.23$	2.5 ± 0.2	1.81 ± 0.08
$\bar{B}^0 \to D^{*0}\pi^0$	–	–	2.8 ± 0.5	1.95 ± 0.18
$\bar{B}^0 \to D^0\bar{K}^0$	$0.62 \pm 0.12 \pm 0.04$	$0.50^{+0.13}_{-0.12} \pm 0.06$	0.44 ± 0.06	0.76 ± 0.06
$\bar{B}^0 \to D^{*0}\bar{K}^0$	$0.45 \pm 0.19 \pm 0.05$	< 0.66	0.36 ± 0.10	0.69 ± 0.10
$\bar{B}^0 \to D_s^+ K^-$	$0.32 \pm 0.10 \pm 0.10$	$0.293 \pm 0.055 \pm 0.079$	0.30 ± 0.08	0.64 ± 0.08

Table 6.1: Data on $B \to D$ and $B \to D^*$ decays with isosinglet light mesons and the weighted average. The BaBar data is from Ref. [10] and the Belle data is from Refs. [1].

where the $\pm$ refers to the cases DM, D^*M and the three amplitudes at LO are

$$
\begin{aligned}
A_{\rm short}^{(*)M} &= N_q^M \sum_{i=0,8} \int_0^1 dx\, dz \int dk_1^+ dk_2^+\, C_L^{(i)}(z)\, J_q^{(i)}(z,x,k_1^+,k_2^+)\, S_L^{(i)}(k_1^+,k_2^+)\, \phi_q^M(x)\,, \qquad (6.2)\\
A_{\rm glue}^{(*)M} &= N_g^M \sum_{i=0,8} \int_0^1 dx\, dz \int dk_1^+ dk_2^+\, C_L^{(i)}(z)\, J_g^{(i)}(z,x,k_1^+,k_2^+)\, S_L^{(i)}(k_1^+,k_2^+)\, \overline{\phi}_g^M(x)\,,\\
A_{\rm long}^{(*)M} &= N_q^M \sum_{i=0,8} \int_0^1 dz \int dk^+ d\omega \int d^2x_\perp C_L^{(i)}(z)\, \bar{J}^{(i)}(\omega k^+)\, \Phi_L^{(i)}(k^+,x_\perp,\varepsilon_{D^*}^*) \Psi_M^{(i)}(z,\omega,x_\perp,\varepsilon_M^*),
\end{aligned}
$$

where $i = 0, 8$ are for two different color structures. Here $A_{\rm short}^{(*)M}$ and $A_{\rm long}^{(*)M}$ are very similar to the results derived for non-singlet mesons the last section, and each contains a flavor-singlet subset of the sum of C and E graphs. The amplitude $A_{\rm glue}^{(*)M}$ contains the additional gluon contributions. The $S_L^{(0,8)}$ are universal generalized distribution functions for the $B \to D^{(*)}$ transition. The $\phi_{q,g}^M$ are meson distribution functions, and [1]

$$
N_q^M = \frac{1}{2} f_q^M G_F V_{cb} V_{ud}^* \sqrt{m_B m_{D^{(*)}}}\,, \qquad N_g^M = \sqrt{\frac{8}{3}} f_1^M\, G_F V_{cb} V_{ud}^* \sqrt{m_B m_{D^{(*)}}}\,. \quad (6.3)
$$

The $\Phi_L^{(i)}$ and $\Psi_M^{(i)}$ are long distance analogs of $S_L^{(i)}$ and ϕ^M where the $x_\perp$ dependence does not factorize. At lowest order in the perturbative expansion, $C_L^{(0)} = C_1 + C_2/3$ and $C_L^{(8)} = 2C_2$ and are independent of the parameter z. The $(L \leftrightarrow R)$ terms in Eq. (6.1) have small coefficients $C_R^{(0,8)} \sim \mathcal{O}(\alpha_s(Q))$ and will be neglected in our phenomenological analysis. Finally, the jet functions $J_q^{(i)}$, $J_g^{(i)}$, and $\bar{J}^{(i)}$ are responsible for rearranging the quarks in the decay process; they can be computed in perturbation theory and are discussed further below.

The derivation of Eq. (6.2) involves subsequently integrating out the scales $Q = \{m_b, m_c, E_M\}$ and then $\sqrt{E_M \Lambda_{\rm QCD}}$ by matching onto effective field theories, QCD $\to$ SCET$_{\rm I}$ $\to$ SCET$_{\rm II}$ as for the case of non-singlet mesons. Here we only give the reader a sense of the procedure, and discuss additions needed for the isosinglet case. In SCET$_{\rm I}$ the same time ordered product of Eq. (5.20) appears. However, this time additional Wick contractions corresponding to the gluon production mechanism or

[1] For Cabbibo suppressed channels we replace $V_{ud}^* \to V_{us}^*$ in N_q^M and N_g^M.

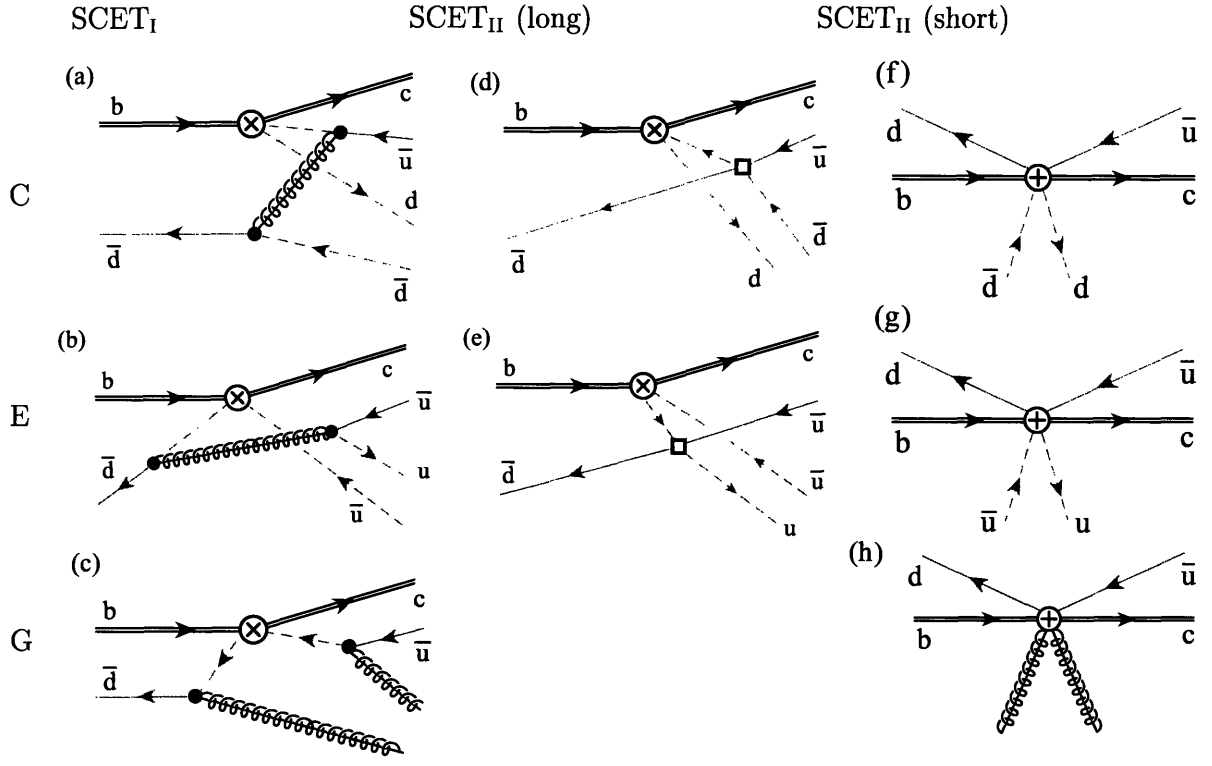

Figure 6-2: Graphs for the tree level matching calculation from SCET$_{\rm I}$ (a,b,c) onto SCET$_{\rm II}$ (d,e,f,g,h). The dashed lines are collinear quark propagators and the spring with a line is a collinear gluon. Solid lines are quarks with momenta $p^\mu \sim \Lambda$. The $\otimes$ denotes an insertion of the weak operator in the appropriate theory. The solid dots in (a,b,c) denote insertions of the mixed usoft-collinear quark action $\mathcal{L}^{(1)}_{\xi q}$. The boxes in (d,e) denote the SCET$_{\rm II}$ operator $\mathcal{L}^{(1)}_{\xi\xi qq}$ from Ref. [93].

the G topology are possible. Once again, the power suppression from the two $\mathcal{L}^{(1)}_{\xi q}$'s makes the amplitudes for color suppressed decays smaller by Λ/Q from those for color allowed decays. The C, E, and G diagrams in Fig. 6-1 are different contractions of the terms in $T^{(0,8)}_{L,R}$, and at tree level are given by Figs. 6-2(a), 6-2(b), and 6-2(c) respectively. The propagators in these figures are offshell by $p^2 \sim E_M\Lambda$. In SCET$_{\rm II}$ all lines are offshell by $\sim \Lambda^2$, so the propagators either collapse to a point as shown in Figs. 6-2(f), 6-2(g), and 6-2(h), or the quark propagator remains long distance as denoted in Figs. 6-2(d) and 6-2(e). For the terms in the factorization theorem in Eq. (6.2), Figs. 6-2(f,g) contribute to $A_{\rm short}$, Fig. 6-2(h) contributes to $A_{\rm glue}$, and Figs. 6-2(d,e) contributes to $A_{\rm long}$. A notable feature is the absence of a long distance gluon contribution. Momentum conservation at the $\mathcal{L}^{(1)}_{\xi q}$ vertex forbids

the quark propagators in Fig. 6-2(c) from having a long distance component (or more generally there does not exist an appropriate analog of the shaded box operator in Figs. 6-2(d,e) that takes a soft $\bar{d}$ to a soft $\bar{u}$).

The diagrams in Fig. 6-2(f,g) have isosinglet and isotriplet components. The corresponding isosinglet operators in $\mathrm{SCET_{II}}$ are [93]

$$\begin{aligned} O_j^{(0)}(k_i^+,\omega_k) &= \Big[\bar{h}_{v'}^{(c)}\Gamma_j^h\, h_v^{(b)}\,(\bar{d}\,S)_{k_1^+}\not{n}P_L\,(S^\dagger u)_{k_2^+}\Big]\Big[(\bar{\xi}_n^{(q)}W)_{\omega_1}\Gamma_c(W^\dagger\xi_n^{(q)})_{\omega_2}\Big]\,, \\ O_j^{(8)}(k_i^+,\omega_k) &= \Big[(\bar{h}_{v'}^{(c)}S)\Gamma_j^h\,T^a\,(S^\dagger h_v^{(b)})\,(\bar{d}\,S)_{k_1^+}\not{n}P_L T^a(S^\dagger u)_{k_2^+}\Big]\Big[(\bar{\xi}_n^{(q)}W)_{\omega_1}\Gamma_c(W^\dagger\xi_n^{(q)})_{\omega_2}\Big]\,, \end{aligned} \tag{6.4}$$

where h_v and $h_{v'}$ are Heavy Quark Effective Theory (HQET) fields for the bottom and charm quarks, the index $j = L, R$ refers to the Dirac structures $\Gamma_L^h = \not{n}P_L$ or $\Gamma_R^h = \not{n}P_R$, $\Gamma_c = (\not{n}P_L)/2$, $\xi_n^{(q)}$ are collinear quark fields and we sum over the $q = u, d$ flavors. Note that no collinear strange quarks appear. In Eq. (6.4) the factors of W and S are Wilson lines required for gauge invariance and the momenta subscripts $(\cdots)_{\omega_i}$ and $(\cdots)_{k_i^+}$ refer to the momentum carried by the product of fields in the brackets. The matrix element of the soft fields in $O_L^{(0,8)}$ gives the $S_L^{(0,8)}(k_1^+,k_2^+)$ distribution functions, for example

$$\frac{\langle D^{(*)0}(v')|(\bar{h}_{v'}^{(c)}S)\not{n}P_L(S^\dagger h_v^{(b)})(\bar{d}S)_{k_1^+}\not{n}P_L(S^\dagger u)_{k_2^+}|\bar{B}^0(v)\rangle}{\sqrt{m_B m_D}} = A^{D^{(*)}}\,S_L^{(0)}(k_1^+,k_2^+)\,, \tag{6.5}$$

where $A^D = 1$ and $A^{D^*} = n\cdot\varepsilon^*/n\cdot v' = 1$ (since the polarization is longitudinal). The matrix element of the collinear operator gives the LO light-cone distribution functions. We work in the isospin limit and use the $(u\bar{u}+d\bar{d})$, $s\bar{s}$ basis for our quark operators. For $M = \eta, \eta'$ we have

$$\begin{aligned} \langle M(p)|\sum_{q=u,d}(\bar{\xi}_n^{(q)}W)_{\omega_1}\frac{\bar{n}\!\!\!/\gamma_5}{\sqrt{2}}(W^\dagger\xi_n^{(q)})_{\omega_2}|0\rangle &= -i\,\bar{n}\cdot p\,f_q^M\,\phi_q^M(\mu,x)\,, \\ \langle M(p)|(\bar{\xi}_n^{(s)}W)_{\omega_1}\bar{n}\!\!\!/\gamma_5(W^\dagger\xi_n^{(s)})_{\omega_2}|0\rangle &= -i\,\bar{n}\cdot p\,f_s^M\,\phi_s^M(\mu,x)\,, \end{aligned} \tag{6.6}$$

while for vector mesons $M = \omega, \phi$ we simplify the dependence on the polarization

using $m_V\,\bar{n}\cdot\varepsilon^* = \bar{n}\cdot p$ and then have

$$\begin{aligned}\langle M(p,\varepsilon^*)|\sum_{q=u,d}(\bar{\xi}_n^{(q)}W)_{\omega_1}\frac{\bar{n}\!\!\!/}{\sqrt{2}}(W^\dagger\xi_n^{(q)})_{\omega_2}|0\rangle &= i\,\bar{n}\cdot p\,f_q^M\,\phi_q^M(\mu,x)\,, \\ \langle M(p,\varepsilon^*)|(\bar{\xi}_n^{(s)}W)_{\omega_1}\bar{n}\!\!\!/(W^\dagger\xi_n^{(s)})_{\omega_2}|0\rangle &= i\,\bar{n}\cdot p\,f_s^M\,\phi_s^M(\mu,x)\,.\end{aligned} \tag{6.7}$$

In both Eq. (6.6) and (6.7) we have suppressed a prefactor for the ϕ^M's on the RHS:

$$\int_0^1 dx\,\delta(\omega_1 - x\,\bar{n}\cdot p)\,\delta(\omega_2 + (1-x)\bar{n}\cdot p)\,. \tag{6.8}$$

Note that these definitions make no assumption about η-η' or ω-ϕ mixing. The SCET operators in Eq. (6.4) only give rise to the ϕ_q^M terms. By charge conjugation $\phi_q^M(1-x) = \phi_q^M(x)$ and $\phi_s^M(1-x) = \phi_s^M(x)$ for both the isosinglet pseudoscalars and isosinglet vectors. Our definitions agree with those in Ref. [73].

Now consider the graph emitting collinear gluons, Fig. 6-2(c). and integrate out the hard-collinear quark propagators to match onto Fig. 6-2(h). Writing the result of computing this Feynman diagram in terms of an operator gives a factor of $[\bar{h}_{v'}^{(c)}\Gamma_j^h\{1,T^c\}h_v^{(b)}]$ times

$$[\bar{d}T^a\gamma_\perp^\mu P_L\{1,T^c\}\frac{\bar{n}\!\!\!/}{2}\gamma_\perp^\nu T^b\,u](ig\mathcal{B}_\perp^{\mu\,a})(ig\mathcal{B}_\perp^{\nu\,b})\,\frac{-\bar{n}\cdot p_2}{-\bar{n}\cdot p_2 n\cdot k_2 + i\epsilon}\,\frac{\bar{n}\cdot p_1}{\bar{n}\cdot p_1 n\cdot k_1 + i\epsilon}\,, \tag{6.9}$$

where $ig\mathcal{B}_{\perp\omega}^{\mu\,b}T^b = [1/\bar{\mathcal{P}}\;W^\dagger[i\bar{n}\cdot D_c\,, iD_{c\perp}^\mu]W]_\omega$ is a LO gauge invariant combination with the gluon field strength. The Dirac structure can be simplified: $\gamma_\perp^\mu P_L\bar{n}\!\!\!/\gamma_\perp^\nu = -\bar{n}\!\!\!/\,P_L(g_\perp^{\mu\nu}+i\epsilon_\perp^{\mu\nu})$ where $\epsilon_{12}^\perp = +1$. Furthermore we only need to keep operators that are collinear color singlets, since others give vanishing contributions at this order. These simplifications hold at any order in perturbation theory in $\mathrm{SCET_I}$, so the matching gives only two $\mathrm{SCET_{II}}$ operators

$$\begin{aligned}G_j^{(0)}(k_i^+,\omega_k) &= \left[\bar{h}_{v'}^{(c)}\Gamma_j^h\,h_v^{(b)}\,(\bar{d}\,S)_{k_1^+}\bar{n}\!\!\!/P_L\,(S^\dagger u)_{k_2^+}\right]\left[(g_{\mu\nu}^\perp+i\epsilon_{\mu\nu}^\perp)\,\mathcal{B}_{\perp\omega_1}^{\mu\,b}\mathcal{B}_{\perp\omega_2}^{\nu\,b}\right], \\ G_j^{(8)}(k_i^+,\omega_k) &= \left[\bar{h}_{v'}^{(c)}\Gamma_j^h T^a\,h_v^{(b)}\,(\bar{d}\,S)_{k_1^+}\bar{n}\!\!\!/P_L T^a(S^\dagger u)_{k_2^+}\right]\left[(g_{\mu\nu}^\perp+i\epsilon_{\mu\nu}^\perp)\,\mathcal{B}_{\perp\omega_1}^{\mu\,b}\mathcal{B}_{\perp\omega_2}^{\nu\,b}\right].\end{aligned} \tag{6.10}$$

The operators in Eq. (6.10) appear as products of soft and collinear fields allowing us

to factorize the amplitude into soft and collinear matrix elements. We immediately notice that the soft fields in Eq. (6.10) and Eq. (6.4) are identical. Thus, the same non-perturbative $B \to D^{(*)}$ distribution functions $S_L^{(0,8)}$ occur in the factorization theorem for the gluon and quark contributions (cf. Eq. (6.2)). The matrix elements of the collinear fields give

$$\begin{aligned} M = \eta, \eta' : \quad \langle M(p)| i\epsilon_{\mu\nu}^{\perp} \mathcal{B}_{\perp,-\omega_1}^{\mu\, b} \mathcal{B}_{\perp,\omega_2}^{\nu\, b} |0\rangle &= \frac{i}{2} \sqrt{C_F} f_1^M \, \overline{\phi}_M^g(\mu, x) \,, \\ M = \phi, \omega : \quad \langle M(p)| g_{\mu\nu}^{\perp} \mathcal{B}_{\perp,-\omega_1}^{\mu\, b} \mathcal{B}_{\perp,\omega_2}^{\nu\, b} |0\rangle &= \frac{i}{2} \sqrt{C_F} f_1^M \, \overline{\phi}_M^g(\mu, x) \,, \end{aligned} \tag{6.11}$$

where

$$\overline{\phi}_g^M(x,\mu) = \frac{\phi_g^M(x,\mu)}{x(1-x)} , \tag{6.12}$$

$C_F = (N_c^2 - 1)/(2N_c) = 4/3$, and $f_1^M = \sqrt{2/3}\, f_q^M + \sqrt{1/3}\, f_s^M$. (We again suppressed a prefactor on the RHS of Eq. (6.11) which is given in Eq. (6.8).) Our ϕ_g^η and $\phi_g^{\eta'}$ are the same as the ones defined in Ref. [73], where they were used to analyze the γ-η and γ-η' form factors. Charge conjugation implies

$$\phi_g^M(1-x) = -\phi_g^M(x) \,. \tag{6.13}$$

At tree level using Eq. (6.9) to match onto the gluon operators $G_j^{(0,8)}$ gives

$$J_g^{(0)} = \frac{\pi\alpha_s(\mu_0)}{N_c(n\cdot k_2 - i\epsilon)(n\cdot k_1 + i\epsilon)} , \qquad J_g^{(8)} = \frac{\pi\alpha_s(\mu_0)}{(-N_c^3 + N_c)(n\cdot k_2 - i\epsilon)(n\cdot k_1 + i\epsilon)} \tag{6.14}$$

where more generally $J_g^{(0,8)} = J_g^{(0,8)}(z, x, k_1^+, k_2^+)$. Thus, the jet functions are even under $x \to 1-x$ while the gluon distributions are odd, and the convolution in Eq. (6.2) for $A_{\rm glue}^{(*)M}$ vanishes. Thus, $A_{\rm glue}^{(*)M}$ starts at $\mathcal{O}[\alpha_s^2(\sqrt{E\Lambda})]$ from one-loop corrections to the gluon jet function.

The remaining contributions to the amplitude come from the isosinglet component of the long distance operators shown in Figs. 6-2(d,e). These operators take the form

of a T-ordered product in $\mathrm{SCET_{II}}$

$$\overline{O}_j^{(0,8)}(\omega_i, k^+, \omega, \mu) \;=\; \int \mathrm{d}^4x\, T\, \mathcal{Q}_j^{(0,8)}(\omega_i, x=0)\; iL^{(0,8)}(\omega, k^+, x)\,. \qquad (6.15)$$

where $L^{(0,8)}(\omega, k^+, x)$ [93] are four quark operators in $\mathrm{SCET_{II}}$ denoted by the shaded boxes in Figs. 6-2(d,e). The matrix element of these long distance operators give the contribution $A_{long}^{(*)M}$ in Eq. (6.2) where the collinear and soft functions $\Psi_M^{(0,8)}$ and $\Phi_L^{(0,8)}$ are defined as

$$\begin{aligned}
&\Big\langle M^0(p_M,\epsilon_M)\Big|\Big[(\bar\xi_n^{(d)}W)_{\omega_1}\bar n\!\!\!/ P_L(W^\dagger\xi_n^{(u)})_{\omega_2}\Big](0_\perp)\Big[(\bar\xi_n^{(u)}W)_{\omega}\bar n\!\!\!/ P_L(W^\dagger\xi_n^{(d)})_{\omega}\Big](x_\perp)\Big|0\Big\rangle \\
&\quad = if^M/\sqrt{2}\,\Psi_M^{(0)}(z,\omega,x_\perp,\varepsilon_M^*)\,, \\
&\Big\langle D^{(*)0}(v',\epsilon_{D^*})\Big|\Big[(\bar h_{v'}^{(c)}S)\bar n\!\!\!/ P_L^h(S^\dagger h_v^{(b)})\Big](0_\perp)\Big[(\bar dS)_{k^+}\bar n\!\!\!/ P_L(S^\dagger u)_{k^+}\Big](x_\perp)\Big|\bar B^0\Big\rangle \\
&\quad = \sqrt{m_B m_{D^{(*)}}}\;\Phi_L^{(0)}(k^+,x_\perp,\varepsilon_{D^*}^*)\,, \qquad (6.16)
\end{aligned}$$

and at tree level the jet functions are $\overline{J}^{(0)}(\omega k^+) = -4/3\,\overline{J}^{(8)}(\omega k^+) = -8\pi\alpha_s(\mu)/(9\omega k^+)$.

Eqs. (6.5,6.6,6.11,6.16) combined with Eq. (6.2) completely define the amplitude for color suppressed decays to leading nonvanishing order in Λ_{QCD}/Q. We are now in a position to make phenomenological predictions. We will neglect perturbative corrections at the hard scale, $\alpha_s(Q)$. For heavy quark symmetry predictions we will work to all orders in $\alpha_s(\sqrt{E\Lambda})$, while for relating the η and η' amplitudes we will work to leading order in $\alpha_s(\sqrt{E\Lambda})$.

6.1.2 Phenemenology

The first class of predictions that we address make use of heavy quark symmetry to relate the D and D^* amplitudes. The factorization theorem in SCET, Eq. (6.2), moves the energetic light meson into a separate matrix element. This allows us to use the formalism of HQET in the soft sector to relate the $\bar B \to D$ and $\bar B \to D^*$ matrix elements in Eqs. (6.5) and (6.16). For A_{short}^M, the contribution is the same for the D and D^* channels with identical soft functions $S_L^{(i)}$ as a consequence of heavy quark symmetry. The same is true for the soft matrix element in A_{glue} which also gives $S_L^{(i)}$.

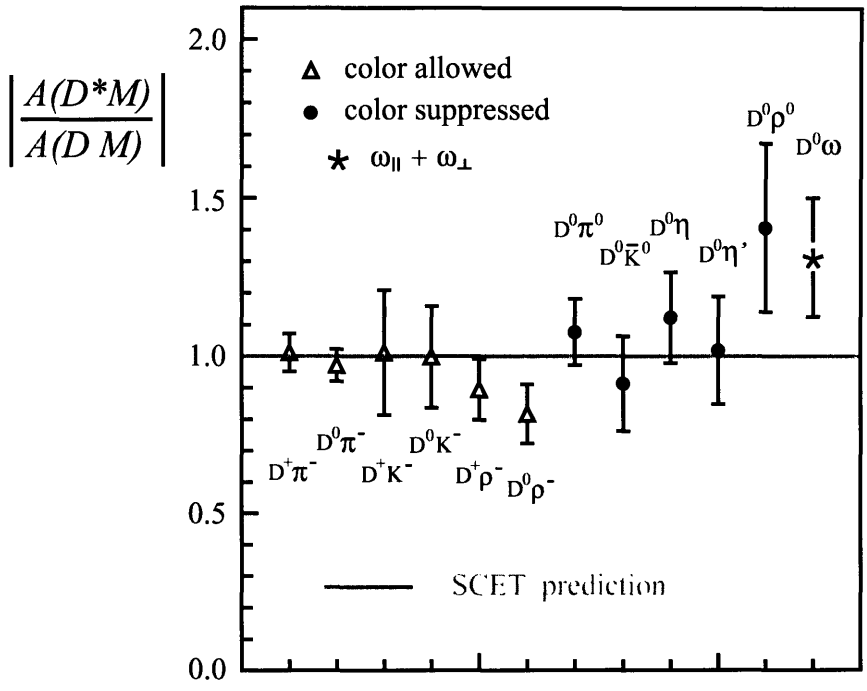

Figure 6-3: Comparison of the absolute value of the ratio of the amplitude for $B \to D^* M$ divided by the amplitude for $B \to DM$ versus data from different channels. This ratio of amplitudes is predicted to be one at leading order in SCET. For ω's this prediction only holds for the longitudinal component, and the data shown is for longitudinal plus transverse.

For the long distance contribution A^M_{long}, in addition to a dependence on powers of $x_\perp^2$, the soft function $\Phi_L^{(i)}(k^+, x_\perp, \varepsilon^*_{D^*})$ can have terms proportional to $x_\perp \cdot \epsilon^*_{D^*}$ in the D^* channel while the collinear function $\Psi_M^{(i)}(z, \omega, x_\perp, \varepsilon^*_M)$ can have terms proportional to $x_\perp \cdot \epsilon^*_M$ in the case of vector mesons. In the convolution over $x_\perp$ in A^M_{long}, the term in the integrand proportional to the product $(x_\perp \cdot \epsilon^*_{D^*})(x_\perp \cdot \epsilon^*_M)$ can be non-vanishing in the D^* channel with a vector meson. Such terms do not appear in the D channel making the D and D^* amplitudes unrelated in general. However, if we restrict ourselves to longitudinal polarizations, such terms in the D^* channel vanish and the long distance contributions in the two channels become identical. Finally, note that the $\mathrm{SCET_I}$ jet functions, and the other collinear matrix elements in $\mathrm{SCET_{II}}$ are identical for the two channels. Thus, at leading order in $\alpha_s(Q)$ and Λ_{QCD}/Q the D and D^* channels are

related as

$$\frac{Br(\bar{B} \to D^* \eta)}{Br(\bar{B} \to D \eta)} = \frac{Br(\bar{B} \to D^* \eta')}{Br(\bar{B} \to D \eta')} = \frac{Br(\bar{B} \to D^* \omega_{\|})}{Br(\bar{B} \to D \omega)} = 1 \,. \tag{6.17}$$

For the decay to ϕ's we also have

$$\frac{Br(\bar{B} \to D^* \phi_{\|})}{Br(\bar{B} \to D \phi)} = 1 \,, \tag{6.18}$$

however in this case the prediction assumes that the $\alpha_s^2(\sqrt{E\Lambda})$ contribution from $A_{\rm glue}$ dominates over power corrections. Note that we are expanding in m_M/E_M so one might expect the predictions to get worse for heavier states. Fig. (6-3) summarizes the heavy quark symmetry predictions for cases where data is available. In Fig. (6-3) we have included the results from section 5.1.6 for non-singlet mesons as well as the results for the color allowed modes [**?**]. We show the ratio of amplitudes because our power expansion was for the amplitudes making it easier to estimate the uncertainty. There is remarkable agreement in the color allowed channel where the error bars are smaller and good agreement in the color suppressed channels as well.

So far our parameterization of the mixing between isosinglets in the factorization theorem has been kept completely general, and we have not used the known experimental mixing properties of η-η' and ϕ-ω. For the next set of predictions we use the flavor structure of the SCET_{II} operators and the isosinglet mixing properties to a) relate the η and η' channels and b) show that decays to ϕ's are suppressed. Our discussion of mixing parameters follows that in Refs. [81, 57, 66, 55]. In general for a given isospin symmetric basis there are two light quark operators and two states (say η and η') so there are four independent decay constants. These can be traded for two decay constants and two mixing angles. In an SU(3) motivated singlet/octet operator basis, $\{(\bar{u}u+\bar{d}d+\bar{s}s)/\sqrt{3}, (\bar{u}u+\bar{d}d-2\bar{s}s)/\sqrt{6}\}$, we have

$$f_1^\eta = -f_1 \sin\theta_1 \,, \quad f_1^{\eta'} = f_1 \cos\theta_1 \,, \quad f_8^\eta = f_8 \cos\theta_8 \,, \quad f_8^{\eta'} = f_8 \sin\theta_8 \,. \tag{6.19}$$

An alternative is the flavor basis used in Eq. (6.2) , $\{O_q, O_s\} \sim \{(\bar{u}u+\bar{d}d)/\sqrt{2},\ \bar{s}s\}$.

Here

$$f_q^\eta = f_q \cos\theta_q\,, \quad f_q^{\eta'} = f_q \sin\theta_q\,, \quad f_s^\eta = -f_s \sin\theta_s\,, \quad f_s^{\eta'} = f_s \cos\theta_s\,. \tag{6.20}$$

Phenomenologically, $(\theta_8-\theta_1)/(\theta_8+\theta_1) \simeq 0.4$ which can be attributed to sizeable SU(3) violating effects, whereas $(\theta_q - \theta_s)/(\theta_q + \theta_s) \simeq 0.06$ where a non-zero value would be due to OZI violating effects [56]. We therefore adopt the FKS mixing scheme [55, 56] where OZI violating effects are neglected and the mixing is solely due to the anomaly. Here one finds experimentally

$$\theta_q \simeq \theta_s \simeq \theta = 39.3^\circ \pm 1.0^\circ\,. \tag{6.21}$$

Thus it is useful to introduce the approximately orthogonal linear combinations

$$|\eta_q\rangle = \cos\theta\,|\eta\rangle + \sin\theta\,|\eta'\rangle\,, \qquad |\eta_s\rangle = -\sin\theta\,|\eta\rangle + \cos\theta\,|\eta'\rangle\,, \tag{6.22}$$

since neglecting OZI effects the offdiagonal terms $\langle 0|O_q|\eta_s\rangle$ and $\langle 0|O_q|\eta_s\rangle$ are zero. Since this is true regardless of whether these operators are local or non-local, the matrix elements in Eqs. (6.6,6.16) must obey the same pattern of mixing as in Eq. (6.20) [$f_q^\eta \phi_q^\eta(x) = f_q \phi_q(x)\,\cos\theta_q$, etc.] and so

$$\phi_q^\eta(x) = \phi_q^{\eta'}(x) = \phi_q(x)\,, \qquad \phi_s^\eta(x) = \phi_s^{\eta'}(x) = \phi_s(x)\,, \qquad \Psi_\eta^{(0,8)} = \Psi_{\eta'}^{(0,8)} = \Psi_q^{(0,8)} \tag{6.23}$$

The $\mathrm{SCET_{II}}$ operators of Eq. (6.10) which contribute to $A_{glue}^{(*)M}$ can produce both the η_q and η_s components of the isosinglet mesons. However, recall that at LO in $\alpha_s(\sqrt{E\Lambda})$ the convolution over the momentum fractions in $A_{glue}^{(*)M}$ vanishes allowing us to ignore this contribution. The remaining contributions from $A_{short}^{(*)M}$ and $A_{long}^{(*)M}$ involve operators that can only produce the η_q component of the isosinglet mesons as seen by the flavor structure of the operators in Eqs. (6.4) and (6.16). We can now

write the amplitude for the $\eta^{(\prime)}$ channels in the form

$$A^{(*)\eta} = \cos\theta\,[A^{(*)\eta_q}_{\rm short} + A^{(*)\eta_q}_{\rm long}]\,, \qquad A^{(*)\eta'} = \sin\theta\,[A^{(*)\eta_q}_{\rm short} + A^{(*)\eta_q}_{\rm long}]. \tag{6.24}$$

This leads to a prediction for the relative rates with SCET

$$\frac{Br(\bar{B}\to D\eta')}{Br(\bar{B}\to D\eta)} = \frac{Br(\bar{B}\to D^*\eta')}{Br(\bar{B}\to D^*\eta)} = \tan^2(\theta) = 0.67\,, \tag{6.25}$$

with uncertainties from $\alpha_s(\sqrt{E\Lambda})$ that could be at the $\sim 35\%$ level. Experimentally the results in Table 6.1 imply

$$\frac{Br(\bar{B}\to D\eta')}{Br(\bar{B}\to D\eta)} = 0.61\pm 0.12\,, \qquad \frac{Br(\bar{B}\to D^*\eta')}{Br(\bar{B}\to D^*\eta)} = 0.51\pm 0.18\,, \tag{6.26}$$

which agree with Eq. (6.25) within the 1-σ uncertainties.

For the isosinglet vector mesons we adopt maximal mixing which is a very good approximation (meaning minimal mixing in the FKS basis), and is consistent with the anomaly having a minimal effect on these states and with neglecting OZI effects. In this case only $\langle 0|O_q|\omega\rangle$ and $\langle 0|O_s|\phi\rangle$ are non-zero. Thus only $A^{(*)\omega}_{short}$ and $A^{(*)\omega}_{long}$ are non-zero and we predict that ϕ production is suppressed

$$\frac{Br(\bar{B}^0\to D^{(*)0}\phi)}{Br(\bar{B}^0\to D^{(*)0}\omega)} = \mathcal{O}\Big(\alpha_s^2(\sqrt{E\Lambda}), \alpha_s(\sqrt{E\Lambda})\frac{\Lambda_{\rm QCD}}{Q}, \frac{\Lambda^2_{\rm QCD}}{Q^2}\Big) \simeq 0.2\,, \tag{6.27}$$

possibly explaining why it has not yet been observed. Interestingly a measurement of $\bar{B}\to D\phi$ or $\bar{B}\to D^*\phi$ may give us a direct handle on the size of these expansion parameters.

Just using the original form of the electroweak Hamiltonian in Eq. (5.1) there is an SU(3) flavor symmetry relation among the color suppressed decays [104]

$$\begin{aligned} R_{\rm SU(3)} &= \frac{Br(\bar{B}^0\to D_s^+K^-)}{Br(\bar{B}\to D^0\pi^0)} + \left|\frac{V_{ud}}{V_{us}}\right|^2\frac{Br(\bar{B}^0\to D^0\bar{K}^0)}{Br(\bar{B}\to D^0\pi^0)} - \frac{3Br(\bar{B}^0\to D^0\eta_8)}{Br(\bar{B}\to D^0\pi^0)} = 1\,,\\ R^*_{\rm SU(3)} &= \frac{Br(\bar{B}^0\to D_s^{*+}K^-)}{Br(\bar{B}\to D^{*0}\pi^0)} + \left|\frac{V_{ud}}{V_{us}}\right|^2\frac{Br(\bar{B}^0\to D^{*0}\bar{K}^0)}{Br(\bar{B}\to D^{*0}\pi^0)} - \frac{3Br(\bar{B}^0\to D^{*0}\eta_8)}{Br(\bar{B}\to D^{*0}\pi^0)} = 1\,, \end{aligned} \tag{6.28}$$

where η_8 is the SU(3) octet component of the η. In the SU(3) limit the $\eta - \eta'$ mixing vanishes and we can take $\eta_8 = \eta$. Away from this limit there is SU(3) violation from the mixing as well as from other sources, and it is the latter that we would like to study. To get an idea about the effect of mixing we set $|\eta_8\rangle = \cos\vartheta|\eta\rangle + \sin\vartheta|\eta'\rangle$, which from Eq. (6.22) can then be written in terms of $|\eta_q\rangle$ and $|\eta_s\rangle$, and vary ϑ between $-10°$ and $-23°$. From the flavor structure of the leading order SCET operators for $B \to DM$ decays we then find

$$\frac{Br(\bar{B}^0 \to D\eta_8)}{Br(\bar{B}^0 \to D\eta)} = \frac{Br(\bar{B}^0 \to D^*\eta_8)}{Br(\bar{B}^0 \to D^*\eta)} = \frac{\cos^2(\theta - \vartheta)}{\cos^2(\theta)}, \tag{6.29}$$

where ϑ is the η-η' state mixing angle in the flavor octet-singlet basis and θ is the FKS mixing angle. In the SU(3) limit $\vartheta = \theta_1 = \theta_8 = 0$, however phenomenologically $\vartheta \simeq -10°$ to $-23°$. Experimentally taking $|V_{us}/V_{ud}| = 0.226$ and using Table 6.1 gives

$$R_{\rm SU(3)} = \begin{cases} 1.00 \pm 0.59 & [\vartheta = 0°] \\ 1.75 \pm 0.57 & [\vartheta = -10°] \\ 2.64 \pm 0.56 & [\vartheta = -23°] \end{cases}, \quad R^*_{\rm SU(3)} = \begin{cases} -0.22 \pm 0.97 & [\vartheta = 0°] \\ 0.59 \pm 0.88 & [\vartheta = -10°] \\ 1.57 \pm 0.83 & [\vartheta = -23°] \end{cases} \tag{6.30}$$

In all but one case the central values indicate large SU(3) violation, however the experimental uncertainty is still large. It would be interesting to compute the uncertainties by properly accounting for correlations between the data rather than assuming these correlations are zero as we have done. At 1-σ the errors accommodate $R^*_{\rm SU(3)} = 1$ except if $\vartheta = 0°$, and only accommodate $R_{\rm SU(3)} = 1$ if $\vartheta = 0°$. Note that the heavy quark symmetry prediction, $R^*_{\rm SU(3)} = R_{\rm SU(3)}$, is still accommodated within the error bars.

In the pQCD approach predictions for color suppressed decays to isosinglets have been given in Refs. [69, 84], where they treat the charm as light and expand in m_c/m_b. With such an expansion there is no reason to expect simple relationships between decays to D and D^* mesons because heavy quark symmetry requires a heavy charm. In Ref. [84] predictions for η and η' were given dropping possible gluon contributions.

Our analysis shows that this is justified and predicts a simple relationship between these decays, given above in Eq. (6.25).

Chapter 7

Excited charmed Mesons

7.1 Excited Charmed Mesons

We now turn to nonleptonic decays where the final state charmed meson is in an orbitally excited state such as the D_1 and D_2^*(see Table 7.1) collectively referred to as D^{**}. $\bar{B} \to D^{**}K$ decays have been recently proposed [105] as candidates for a theoretically clean extraction of the CKM angle γ making such decays all the more interesting to study. These decays also raise interesting questions regarding the power counting scheme used to make quantitative phenomenological predictions. Based on analysis of semileptonic decays [77] near zero recoil, the leading order contributions are expected to be suppressed due to heavy quark symmetry constraints. This suggests that subleading contributions could have a significant effect on leading order predictions in $\bar{B} \to D^{**}M$ type processes. We will address these issues on power counting and provide a resolution. On another note, the $\bar{B}^0 \to D^{(*)0}\rho^0$ rates are more difficult to extract cleanly from experimental data due to background contributions from intermediate D^{**} states. In particular, in the D^{*0} channel only an upper bound on the branching fraction has been measured [52] and the errors in the D^0 channel are still fairly large [103]. This has made it difficult to test the SCET prediction [94] relating the D and D^* amplitudes. With the ρ^0 meson primarily decaying to $\pi^+\pi^-$ and the excited D^{**+} mesons decaying to $D^{(*)0}\pi^+$ the same final state is observed for $\bar{B}^0 \to D^{**+}\pi^-$ and $\bar{B}^0 \to D^{(*)0}\rho^0$. Thus, a precise extraction of the $\bar{B}^0 \to D^{(*)0}\rho^0$

Mesons	$s_l^{\pi_l}$	J^P	$\bar{m}$(GeV)
(D, D^*)	$\frac{1}{2}^-$	$(0^-, 1^-)$	1.971
(D_0^*, D_1^*)	$\frac{1}{2}^+$	$(0^+, 1^+)$	2.40
(D_1, D_2^*)	$\frac{3}{2}^+$	$(1^+, 2^+)$	2.445

Table 7.1: The HQS doublets are labeled by $s_l^{\pi_l}$. Here s_l denotes the spin of the light degrees of freedom and π_l the parity. The D, D^* mesons are $L = 0$ negative parity mesons. The D_0^*, D_1^* and D_1, D_2^* are excited mesons with $L = 1$ and positive parity. $\bar{m}$ refers to the average mass of the HQS doublet weighted by the number of helicity states [77].

rates requires us to better understand B decays to excited charmed mesons.

The $\bar{B} \to (D^{(*)}, D^{**})\pi$ type decays proceed via three possible topologies shown in Fig. 5-1 but with the D meson replaced by the orbitally excited state D^{**}. The color suppressed modes which proceed exclusively through C and E topologies and will be shown to be suppressed relative to the color allowed modes that are dominated by the T topology.

As explained in chapter 3, there exists a tower of HQS doublets for the charmed mesons where (D, D^*) sits at the base. The first three HQS doublets are listed in Table 7.1. In this section we extend the analysis to the case where the final state charmed mesons are D_1 or D_2^* which sit in the third HQS doublet. A similar analysis can be done for the (D_0^*, D_1^*) doublet but these are difficult to observe due to their relatively broad width [91]. For this reason, we restrict our analysis to the (D_1, D_2^*) doublet. The most recent measurements in the color allowed sector giving the ratio

$$\frac{Br(B^- \to D_2^{*0}\pi^-)}{Br(B^- \to D_1^0\pi^-)} = 0.79 \pm 0.11, \tag{7.1}$$

obtained after averaging the Belle [3] and Babar [8] data. In this section, we shed light on this ratio and also make predictions in the color suppressed sector.

In extending the analysis to include excited charmed mesons, the constraint of HQS introduces possible complications in the power counting scheme. HQS requires the matrix elements of the weak current between B and (D_1, D_2^*) to vanish at zero recoil [65]. This requires that they be proportional to some positive power of $(\omega - 1)$

at leading order in Λ_{QCD}/Q. Here $\omega = v \cdot v'$ where v and v' are the velocities of the bottom and charm quarks respectively and $v^2 = v'^2 = 1$. For semileptonic decays this means that HQS breaking Λ_{QCD}/Q corrections can compete with the leading order prediction [77, 78]. For example, if the amplitude were to have the generic form

$$A(\omega) \sim (\omega - 1)[1 + \Lambda_{QCD}/Q + \cdots] + [0 + \Lambda_{QCD}/Q + \cdots], \tag{7.2}$$

and $(\omega - 1) \sim \Lambda_{QCD}/Q$, then the subleading Λ_{QCD}/Q terms in the second square bracket are of the same order as the leading order terms in the first square bracket. The effect of the subleading corrections is especially important near zero recoil where $\omega \to 1$. The two body decays $\bar{B} \to (D_1, D_2^*)M$ occur at maximum recoil where $(\omega_0 - 1) \sim 0.3$ which is numerically of the same order as Λ_{QCD}/Q. One is thus forced to consider the role of subleading corrections and how they compare with the leading order predictions. However, we will see that maximum recoil is a special kinematic point at which the constraint of HQS enters in a very specific manner so as to preserve the Λ_{QCD}/Q power counting scheme. The main results of this paper are

- At leading order, the ideas of factorization, generation of non-perturbative strong phases, and the relative Λ_{QCD}/Q suppression of the color suppressed modes are the same for B-decays to excited charmed mesons $\bar{B} \to D^{**}M$ and to ground state charmed mesons $\bar{B} \to D^{(*)}M$.

- The constraint of HQS takes on a different character at maximum recoil compared to expectations from the analysis of semileptonic decays near zero recoil. In particular, at maximum recoil there is no suppression of the leading order contribution due to HQS. Thus, the SCET/HQET power counting scheme remains intact and allows us to rely on leading order predictions up to corrections suppressed by at least Λ_{QCD}/Q. We verify this explicitly for subleading corrections to the semileptonic form factors at maximum recoil.

- At leading order, factorization combined with HQS predicts the equality of the $\bar{B} \to D_1 M$ and $\bar{B} \to D_2^* M$ branching fractions and their strong phases. In

the color suppressed sector, this prediction is quite non-trivial from the point of naive factorization since the tensor meson D_2^* cannot be created via a V-A current.

- Recent data [3, 8] reports a 20% deviation of the ratio of branching fractions from unity in the color allowed sector. The subleading corrections of order Λ_{QCD}/Q are expected to be of this same size and could explain this deviation from unity.

Eqs. (5.7) and (5.34) are the main results of the analysis for the $B \to D^{(*)}M$ decays. The analysis for decays with excited charmed mesons $B \to D^{**}M$ will proceed in exactly the same manner. Any difference in results will show up only at the non-perturbative scale i.e. in SCET_{II} . In other words, the doublets (D, D^*) and (D_1, D_2^*) have the same quark content and any difference between them arises only from non-perturbative effects responsible for their binding. The physics at the scales $\mu^2 \sim m_W^2$, Q^2, and $Q\Lambda_{QCD}$ or in the theories SM, H_W, and SCET_{I} is the same leaving the perturbative functions $C_{1,2}$, $C_{L,R}^{(0,8)}$, and $J^{(0,8)}$ unchanged (see Fig. 5-2). The light cone wave function ϕ_M will also remain unchanged since the same final state light meson appears. At leading order, the only change will be in the soft functions $S_{L,R}^{(i)}$ and ξ since the matrix elements will now involve different non-perturbative final states namely (D_1, D_2^*). We will denote the modified functions as $Q_{L,R}^{(i)}$ and τ corresponding to $S_{L,R}^{(i)}$ and ξ respectively.

7.1.1 SCET Analysis: Leading Order

We now begin our analysis for the excited charmed states. We start by obtaining the modified soft functions τ and $Q_{L,R}^{(i)}$ and then carry over results for the perturbative functions and the non-perturbative collinear sector from the previous section to obtain the analog of Eqs. (5.7) and (5.34).

Color Allowed Modes

We first analyze the soft functions for the color allowed modes $\bar{B}^0 \to (D_1^+, D_2^{*+})M^-$ and $B^- \to (D_1^0, D_2^{*0})M^-$. As before, the leading contribution to these modes comes from the T topology which is given by the matrix elements of the effective $\mathrm{SCET_{II}}$ operators $\mathcal{Q}_{L,R}^{(0,8)}$ of Eq. (5.19). These matrix elements factorize into soft and collinear sectors. Using the formalism of HQET, the soft part of the matrix element can be expressed in general form as a trace

$$\frac{\langle D_2^*, D_1(v')|\bar{h}_{v'}^{(c)}\Gamma_{L,R}^h h_v^{(b)}|\bar{B}^0(v)\rangle}{\sqrt{m_B m_D}} = \tau(\omega)\mathrm{Tr}\left[v_\sigma \overline{F}_{v'}^{(c)\sigma}\Gamma H_v^{(b)}\right], \tag{7.3}$$

where $\tau(\omega)$ is a new Isgur-Wise function analogous to $\xi(\omega)$. As in the case of ground state charmed mesons, the operators $\mathcal{Q}_{L,R}^{(8)}$ give vanishing contribution. $H_v^{(b)}$ and $F_{v'}^{(c)\sigma}$ in Eq. (7.3) are the superfields for the heavy meson doublets $(\bar{B}, \bar{B}^*)$ and (D_1, D_2^*) respectively [53]

$$\begin{aligned} H_v &= \frac{1+\not{v}}{2}(P_v^{*\mu}\gamma_\mu + P_v\gamma_5) \\ F_v^\sigma &= \frac{1+\not{v}}{2}(D_2^{*\sigma\nu}\gamma_\nu - \sqrt{\frac{3}{2}}D_1^\nu\gamma_5[g_\nu^\sigma - \frac{1}{3}\gamma_\nu(\gamma^\sigma - v^\sigma)]) . \end{aligned} \tag{7.4}$$

As mentioned in the introduction, the matrix element in Eq. (7.3) which also appears in the case of semileptonic decays must vanish in the limit of zero recoil. This condition is manifest in the right hand side of Eq. (7.3) through the property $v'_\sigma \overline{F}_{v'}^{(c)\sigma} = 0$. Thus, we expect the leading order amplitude to be proportional to some positive power of $(\omega - 1)$. At maximum recoil $(\omega_0 - 1) \sim 0.3 \sim \Lambda_{QCD}/Q$ putting $(\omega_0 - 1)$ and Λ_{QCD}/Q on the same footing in the power counting scheme. In addition, maximum recoil is a special kinematic point where the heavy meson masses are related to ω_0 through $(\omega_0 - 1) = \frac{(m_B - m_D)^2}{2m_B m_D}$. We must keep this relation in mind to make the power counting manifest and so it becomes convenient to express $(m_B - m_D)$ in terms of $(\omega_0 - 1)$.

Computing the trace in Eq. (7.3) we arrive at the result

$$\begin{aligned}
\frac{\langle D_1(v')|\bar{h}^{(c)}_{v'}\Gamma^h_{L,R}h^{(b)}_v|\bar{B}^0(v)\rangle}{\sqrt{m_B m_D}} &= \tau(\omega)\sqrt{\frac{m_B(\omega+1)}{3m_D}}\epsilon^*\cdot v \\
\frac{\langle D_2^*(v')|\bar{h}^{(c)}_{v'}\Gamma^h_{L,R}h^{(b)}_v|\bar{B}^0(v)\rangle}{\sqrt{m_B m_D}} &= \pm\tau(\omega)\sqrt{\frac{m_B}{2m_D(\omega-1)}}\epsilon^{*\sigma\nu}v_\sigma v_\nu,
\end{aligned} \tag{7.5}$$

where the $\pm$ for the D_2^* refer to the choice of Γ^h_L and Γ^h_R Dirac structures respectively. ϵ^μ and $\epsilon^{\mu\nu}$ are the polarizations for D_1 and D_2^* respectively. Combining this result for the soft sector with the hard and collinear parts from the previous section we obtain the final result

$$\begin{aligned}
A(B\to D_1M) &= N^{D1}E_M\sqrt{\frac{m_B(\omega_0+1)}{3m_D}}\epsilon^*\cdot v\,\tau(w_0,\mu) \\
&\times \int_0^1 dx\, T^{D_1}(x,m_c/m_b,\mu)\,\phi_M(x,\mu) \\
A(B\to D_2^*M) &= N^{D2*}E_M\sqrt{\frac{m_B}{2m_D(\omega_0-1)}}\epsilon^{*\sigma\nu}v_\sigma v_\nu\,\tau(w_0,\mu) \\
&\times \int_0^1 dx\, T^{D_2^*}(x,m_c/m_b,\mu)\,\phi_M(x,\mu)\,,
\end{aligned} \tag{7.6}$$

where the normalizations are given by

$$N^{D1} = \frac{G_F V_{cb}V_{ud}^*}{\sqrt{2}} f_M\sqrt{m_B m_{D1}}, \qquad N^{D2*} = \frac{G_F V_{cb}V_{ud}^*}{\sqrt{2}} f_M\sqrt{m_B m_{D2*}} \tag{7.7}$$

and the hard kernels $T^{(D_1,D_2^*)}(x,\mu)$ are the same as those appearing in Eq. (5.7) $T^{(D_1,D_2^*)}(x,\mu) = T^{(*)}(x,\mu)$. Using the properties of the polarization sums

$$\sum_{pol}|\epsilon^*\cdot v|^2 = (\omega+1)(\omega-1)\,, \qquad \sum_{pol}|\epsilon^{*\sigma\nu}v_\sigma v_\nu|^2 = \frac{2}{3}(\omega+1)^2(\omega-1)^2, \tag{7.8}$$

the unpolarized amplitude squared is given by

$$\begin{aligned}
\sum_{pol}|A(B\to(D_1,D_2^*)M)|^2 &= |N^{(D1,D2*)}\int_0^1 dx\, T^{(D1,D_2^*)}(x,m_c/m_b,\mu)\,\phi_M(x,\mu)|^2 \\
&\times \frac{m_B\tau^2(\omega,\mu)}{3m_D}(\omega_0+1)^2(\omega_0-1).
\end{aligned} \tag{7.9}$$

At leading order in $\Lambda_{QCD}/m_{b,c}$ the masses in the heavy quark doublet (D_1, D_2^*) are degenerate giving the relation $N^{(D_1)} = N^{(D_2*)}$. In addition at leading order in $\alpha_s(Q)$, $T^{(D_1)} = T^{(D_2*)}$ allowing us to make a prediction for the unpolarized color allowed branching ratios:

$$\frac{Br(\bar{B}^0 \to D_2^{*+} M^-)}{Br(\bar{B}^0 \to D_1^+ M^-)} = \frac{Br(B^- \to D_2^{*0} M^-)}{Br(B^- \to D_1^0 M^-)} = 1\,. \tag{7.10}$$

The same result was derived in ref. [77] at lowest order in $1/m_{b,c}$ by evaluating their results for semileptonic decays at the maximum recoil point and replacing the $e\bar{\nu}$ pair with a massless pion. Recently, a theoretical prediction of 0.91 for the above ratio was made in the covariant light front model [44].

Color Suppressed Modes

Now we look at the color suppressed modes $\bar{B}^0 \to (D_1^0, D_2^{*0}) M^0$. The leading contributions are from the C and E topologies which are given by matrix elements of the $\mathrm{SCET_{II}}$ operators $O_j^{(0,8)}(k_i^+, \omega_k)$ of Eq. (5.27). Once again, the result factorizes and using the formalism of HQET, the soft part of the matrix element can be expressed as a trace

$$\frac{\langle D_2^{(*)0}, D_1^0(v') | (\bar{h}_{v'}^{(c)} S) \Gamma_j^h \, (S^\dagger h_v^{(b)}) \, (\bar{d} S)_{k_1^+} \not{n} P_L \, (S^\dagger u)_{k_2^+} | \bar{B}^0(v) \rangle}{\sqrt{m_B m_D}} = \mathrm{Tr}\,[\overline{F}_{v'}^{(c)\sigma} \Gamma_j^h H_v^{(b)} X_\sigma^{(0)}] \tag{7.11}$$

with similar expressions for the $O_j^{(8)}(k_i^+, \omega_k)$ operators. The Dirac structure $X_\sigma^{(0,8)}$ is of the most general form allowed by the symmetries of QCD and involves eight form factors

$$\begin{aligned} X_\sigma^{(0,8)} &= v_\sigma (a_1^{(0,8)} \not{n} P_L + a_2^{(0,8)} \not{n} P_R + a_3^{(0,8)} P_L + a_4^{(0,8)} P_R) \\ &\quad + n_\sigma (a_5^{(0,8)} \not{n} P_L + a_6^{(0,8)} \not{n} P_R + a_7^{(0,8)} P_L + a_8^{(0,8)} P_R) \end{aligned} \tag{7.12}$$

Computing the trace in Eq. (7.11), the soft matrix elements are given by

$$\begin{aligned}
\frac{\langle D_2^{*0}(v')|(\bar{h}_{v'}^{(c)} S)\Gamma_{L,R}^h (S^\dagger h_v^{(b)})\,(\bar{d}\,S)_{k_1^+} \not{n} P_L\,(S^\dagger u)_{k_2^+}|\bar{B}^0(v)\rangle}{\sqrt{m_B m_D}} &= \frac{(\mp \epsilon^{*\sigma\nu} v_\sigma v_\nu) Q_{L,R}^{(0)}}{4(\omega+1)(\omega-1)} \\
\frac{\langle D_1^0(v')|(\bar{h}_{v'}^{(c)} S)\Gamma_{L,R}^h (S^\dagger h_v^{(b)})\,(\bar{d}\,S)_{k_1^+} \not{n} P_L\,(S^\dagger u)_{k_2^+}|\bar{B}^0(v)\rangle}{\sqrt{m_B m_D}} &= \frac{(\epsilon^* \cdot v) Q_{L,R}^{(0)}}{\sqrt{24(\omega+1)(\omega-1)}}
\end{aligned} \tag{7.13}$$

where,

$$\begin{aligned}
Q_L^{(0)} &= \frac{-1}{m_B^2 m_D^2}[2m_B m_D(2a_1^{(0)} m_B^2 - a_3^{(0)} m_B^2 - a_4^{(0)} m_B m_D)\sqrt{(\omega+1)(\omega-1)} \\
&+ 4a_5^{(0)} m_B^4 - 2a_7^{(0)} m_B^4 - 2a_8^{(0)} m_D m_B^3] \\
Q_R^{(0)} &= \frac{-1}{m_B^2 m_D^2}[2m_B m_D(2a_2^{(0)} m_B^2 - a_3^{(0)} m_B m_D - a_4^{(0)} m_B^2)\sqrt{(\omega+1)(\omega-1)} \\
&+ 4a_6^{(0)} m_B^4 - 2a_7^{(0)} m_D m_B^3 - 2a_8^{(0)} m_B^4],
\end{aligned} \tag{7.14}$$

with similar expressions for $Q_{L,R}^{(8)}$. Here the soft functions $Q_{L,R}^{(0,8)}$ are the analog of $S_{L,R}^{(0,8)}$ in Eq. (5.34). It was shown [94] that these soft functions generate a non-perturbative strong phase. We note that in both the D_1 and D_2^* decay channels, since the same moments of the non-perturbative functions $Q_{L,R}^{(0,8)}$ appear, their strong phases are predicted to be equal

$$\phi_{D_1 M} = \phi_{D_2^* M}. \tag{7.15}$$

The analogous strong phase ϕ for $\bar{B}^0 \to D^{(*)0}\pi^0$ is shown in Fig. 5-6. Since the strong phases ϕ and $\phi_{D_1\pi, D_2^*\pi}$ are determined by different non-perturbative functions $S_{L,R}^{(0,8)}$ and $Q_{L,R}^{(0,8)}$ respectively, we do not expect them to be related.

Keeping in mind that the perturbative functions $C_{L,R}^{(i)}$ and $J^{(i)}$ remain unchanged, we can combine the result in Eq. (7.13) for soft sector with the collinear and hard parts of the amplitude to arrive at the result

$$\begin{aligned}
A_{00}^{(D1)} &= \frac{-N^{D_1}\epsilon^* \cdot v}{\sqrt{24(\omega_0+1)(\omega_0-1)}} \int_0^1 dx\, dz \int dk_1^+ dk_2^+ \left[C_L^{(i)}(z)\, J^{(i)}(z,x,k_1^+,k_2^+)\, Q_L^{(i)}(k_1^+,k_2^+)\, \phi_M(x)\right. \\
&\left. - C_R^{(i)}(z)\, J^{(i)}(z,x,k_1^+,k_2^+)\, Q_R^{(i)}(k_1^+,k_2^+)\, \phi_M(x)\right]
\end{aligned}$$

$$A_{00}^{(D2*)} = \frac{N^{D_2^*}\epsilon^{*\sigma\nu}v_\sigma v_\nu}{4(\omega_0+1)(\omega_0-1)}\int_0^1 dx\,dz\int dk_1^+ dk_2^+ \left[C_L^{(i)}(z)\,J^{(i)}(z,x,k_1^+,k_2^+)\,Q_L^{(i)}(k_1^+,k_2^+)\,\phi_M(x)\right.$$
$$\left.+C_R^{(i)}(z)\,J^{(i)}(z,x,k_1^+,k_2^+)\,Q_R^{(i)}(k_1^+,k_2^+)\,\phi_M(x)\right]. \quad (7.16)$$

Once again the vanishing of $C_R^{(0,8)}$ in Eq. (7.16) at leading order in $\alpha_s(Q)$ and using the polarization sums in Eq. (7.8) gives the unpolarized amplitude squared

$$\sum_{pol}|A_{00}^{(D_1,D_2*)}|^2 = \frac{1}{24}\Big|N^{(D_1,D_2^*)}\int_0^1 dx\,dz\int dk_1^+ dk_2^+ \left[C_L^{(i)}(z)\,J^{(i)}(z,x,k_1^+,k_2^+)\right.$$
$$\left.\times\; Q_L^{(i)}(k_1^+,k_2^+)\,\phi_M(x)\right]\Big|^2. \quad (7.17)$$

Since $N^{D_1} = N^{D_2*}$, at leading order in Λ_{QCD}/m_Q we can make a prediction for the unpolarized branching ratios

$$\frac{Br(\bar{B}^0 \to D_2^{*0}M^0)}{Br(\bar{B}^0 \to D_1^0 M^0)} = 1, \quad (7.18)$$

which is one of the main results of this paper. Note that from the point of view of naive factorization, this result is quite unexpected since the tensor meson D_2^* cannot be produced by a V-A current.

7.1.2 SCET Analysis: Power Counting at Subleading Order

Color Allowed Modes

We see that as required by HQS, the unpolarized amplitude in Eq. (7.9) is proportional to $(\omega_0 - 1)$ which is expected to provide a suppression of this leading order result. However, it is also accompanied by a factor of $(\omega_0 + 1)^2$. At maximum recoil ω_0 is related to the energy of the light meson and the mass of the charmed meson through

$$\sqrt{(\omega_0+1)(\omega_0-1)} = \frac{E_M}{m_D}. \quad (7.19)$$

Thus, in the SCET power counting scheme the quantity $\sqrt{(\omega_0+1)(\omega_0-1)}$ is of order one. It is now clear from Eq. (7.9) and the above relation that despite the constraint of

HQS there is no suppression of the leading order result and the subleading corrections of order Λ_{QCD}/Q are not dangerous to the leading order result. This allows us to rely on the leading order predictions up to corrections supressed by Λ_{QCD}/Q.

To illustrate the above ideas, in this section we will compute some of the subleading corrections and compare their sizes relative to the leading order predictions. The leading order operators in Eqs. (5.19) and (5.27) are products of soft and collinear operators $O = O_s * O_c$. Subleading corrections can arise in four possible ways

- corrections in the soft sector to O_s and from T-products(see Fig. 7-1a) with O_s.
- corrections in the collinear sector to O_c and from T-products(see for example Fig. 7-1b) with O_c.
- corrections from subleading mixed collinear-soft operators and their T-products.
- Beyond the heavy quark limit, s_l is no longer a good quantum number. From table 7.1, we see that it implies mixing between D_1 and D_1^*. Thus, the physical D_1 state will have a small admixture of the D_1^* state beyond the heavy quark limit which will play a role in subleading corrections.

We will only focus on subleading corrections in the soft sector from HQET as in Fig. 7-1a in order to illustrate the power counting. These corrections give precisely the subleading semileptonic form factors which were computed in Ref. [77]. The analysis for the remaining subleading corrections will follow in a similar manner and we leave it as possible future work.

The HQET and QCD fields are related to eachother through

$$Q(x) = e^{-im_Q v\cdot x}[1 + \frac{i\not{D}}{2m_Q} + \ldots]h_v^{(Q)}, \tag{7.20}$$

where the ellipses denote terms suppressed by higher orders of Λ_{QCD}/m_Q and $Q = b, c$. Including the Λ_{QCD}/m_Q corrections, the QCD current is now matched onto

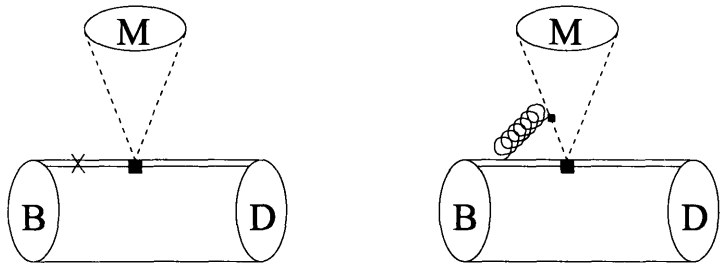

(a) (b)

Figure 7-1: Contributions to the color allowed sector from T-ordered products of the effective weak vertex in $\mathrm{SCET_I}$ with subleading kinetic and chromomagnetic HQET operators (a) and with the subleading SCET operators(b). In this section, to illustrate through examples the relative suppression the subleading contributions by at least Λ_{QCD}/Q, we only consider T-ordered products of type (a). The analysis for type (b) contributions will proceed in a similar manner.

$$\bar{c}\Gamma b \to \bar{h}_{v'}^{(c)}(\Gamma - \frac{i}{2m_c}\not{D}\Gamma + \frac{i}{2m_b}\Gamma\not{\vec{D}})h_v^{(b)}. \tag{7.21}$$

Then there are subleading corrections from T-ordered products of the leading order current with order Λ_{QCD}/Q terms in the HQET Lagrangian:

$$\delta L_{HQET} = \frac{1}{2m_Q}[O_{kin,v}^{(Q)} + O_{mag,v}^{(Q)}] \tag{7.22}$$

where $O_{kin,v}^{(Q)}$ and $O_{mag,v}^{(Q)}$ are the kinetic and chromomagnetic operators

$$O_{kin,v}^{(Q)} = \bar{h}_v^{(Q)}(iD)^2 h_v^{(Q)}, \qquad O_{mag,v}^{(Q)} = \bar{h}_v^{(Q)}\frac{g_s}{2}\sigma_{\alpha\beta}G^{\alpha\beta}h_v^{(Q)}. \tag{7.23}$$

We employ the trace formalism to compute these subleading corrections to the soft matrix element from corrections to the matching in Eq. (7.21)

$$\begin{aligned}\bar{h}_{v'}^{(c)} i\overleftarrow{D}_\lambda\gamma^\lambda\Gamma h_v^{(b)} &= Tr[S_{\sigma\lambda}^{(c)}\bar{F}_{v'}^{\sigma(c)}\gamma^\lambda\Gamma H_v^{(b)}] \\ \bar{h}_{v'}^{(c)}\Gamma\gamma^\lambda i\vec{D}_\lambda h_v^{(b)} &= Tr[S_{\sigma\lambda}^{(b)}\bar{F}_{v'}^{\sigma(c)}\Gamma\gamma^\lambda H_v^{(b)}],\end{aligned} \tag{7.24}$$

and from T-ordered products with δL_{HQET}

$$
\begin{aligned}
i\int d^4x T(O^{(c)}_{mag,v'}(x)[\bar{h}^{(c)}_{v'}\Gamma h^{(b)}_{v}](0)) &= Tr[R^{(c)}_{\sigma\alpha\beta}\bar{F}^{\sigma(c)}_{v'} i\sigma^{\alpha\beta}\frac{1+\not{v}'}{2}\Gamma H^{(b)}_{v}] \\
i\int d^4x T(O^{(b)}_{mag,v}(x)[\bar{h}^{(c)}_{v'}\Gamma h^{(b)}_{v}](0)) &= Tr[R^{(b)}_{\sigma\alpha\beta}\bar{F}^{\sigma(c)}_{v'}\Gamma\frac{1+\not{v}}{2} i\sigma^{\alpha\beta}H^{(b)}_{v}] \qquad (7.25)
\end{aligned}
$$

where the structures $S^{(Q)}_{\sigma\lambda}$ and $R^{(Q)}$ are parametrized as

$$
\begin{aligned}
S^{(Q)}_{\sigma\lambda} &= v_\sigma[\tau^{(Q)}_1 v_\lambda + \tau^{(Q)}_2 v'_\lambda + \tau^{(Q)}_3\gamma_\lambda] + \tau^{(Q)}_4 g_{\sigma\lambda} \\
R^{(c)}_{\sigma\alpha\beta} &= n^{(c)}_1 v_\sigma\gamma_\alpha\gamma_\beta + n^{(c)}_2 v_\sigma v_\alpha\gamma_\beta + n^{(c)}_3 g_{\sigma\alpha}v_\beta, \\
R^{(b)}_{\sigma\alpha\beta} &= n^{(b)}_1 v_\sigma\gamma_\alpha\gamma_\beta + n^{(b)}_2 v_\sigma v'_\alpha\gamma_\beta + n^{(b)}_3 g_{\sigma\alpha}v'_\beta. \qquad (7.26)
\end{aligned}
$$

The T-ordered products with the kinetic energy operator $O^{(Q)}_{kin,v}$ do not violate spin symmetry and simply provide Λ_{QCD}/m_Q corrections to the form factor in Eq. (7.3) $\tau \to \tilde{\tau} = \tau + \frac{\eta^c_{ke}}{2m_c} + \frac{\eta^b_{ke}}{2m_b}$. The form factors appearing in $S^{(Q)}_{\sigma\lambda}$ are not all independent and are related [77] through

$$
\begin{aligned}
\omega\tau^{(c)}_1 + \tau^{(c)}_2 - \tau^{(c)}_3 &= 0 \\
\tau^{(b)}_1 + \omega\tau^{(b)}_2 - \tau^{(b)}_3 + \tau^{(b)}_4 &= 0 \\
\tau^{(c)}_1 + \tau^{(b)}_1 &= \bar{\Lambda}\tau \\
\tau^{(c)}_2 + \tau^{(b)}_2 &= -\bar{\Lambda}'\tau \\
\tau^{(c)}_3 + \tau^{(b)}_3 &= 0 \\
\tau^{(c)}_4 + \tau^{(b)}_4 &= 0, \qquad (7.27)
\end{aligned}
$$

where $\bar{\Lambda}$ and $\bar{\Lambda}'$ are the energies of the light degrees of freedom in the $m_{b,c} \to \infty$ limit for the $(\bar{B}, \bar{B}^*)$ and (D_1, D_2^*) HQS doublets respectively. Using these relations we can express our results in terms of the τ, $\tau^{(c)}_1$, and $\tau^{(c)}_2$ form factors. Combining the subleading contributions from Eqs. (7.24) and (7.25) with the leading order result in Eq. (7.3) and using constraints from Eq. (7.27) we can write the soft matrix element

as

$$
\begin{aligned}
S_{D1,D2*} &= \tilde{\tau}(\omega_0)\mathrm{Tr}\,[v_\sigma \overline{F}_{v'}^{(c)\sigma}\Gamma H_v^{(b)}] - \frac{1}{2m_c}Tr[S_{\sigma\lambda}^{(c)}\bar{F}_{v'}^{\sigma(c)}\gamma^\lambda\Gamma H_v^{(b)}] - \frac{1}{2m_b}Tr[S_{\sigma\lambda}^{(c)}\bar{F}_{v'}^{\sigma(c)}\Gamma\gamma^\lambda H_v^{(b)}] \\
&+ \frac{\tau(\omega)}{2m_b}Tr[(\bar{\Lambda}v_\lambda - \bar{\Lambda}'v'_\lambda)v_\sigma\bar{F}_{v'}^{\sigma(c)}\Gamma\gamma^\lambda H_v^{(b)}] + \frac{1}{2m_c}Tr[R_{\sigma\alpha\beta}^{(c)}\bar{F}_{v'}^{\sigma(c)}i\sigma^{\alpha\beta}\frac{1+\not{v}'}{2}\Gamma H_v^{(b)}] \\
&+ \frac{1}{2m_b}Tr[R_{\sigma\alpha\beta}^{(b)}\bar{F}_{v'}^{\sigma(c)}\Gamma\frac{1+\not{v}}{2}i\sigma^{\alpha\beta}H_v^{(b)}] + \cdots, \qquad (7.28)
\end{aligned}
$$

where the ellipses denote contributions from other subleading operators that we have not considered. Computing the above traces and combining the results for the hard and collinear parts from section II, the amplitudes can be brought into the final form

$$
\begin{aligned}
A(B \to D_1 M) &= N^{D1} f^{BD1}\epsilon^* \cdot v \int_0^1 dx\, T^{D_1}(x, m_c/m_b, \mu)\,\phi_M(x,\mu) \\
A(B \to D_2^* M) &= N^{D2*} f^{BD2*}\epsilon^{*\sigma\nu}v_\sigma v_\nu \int_0^1 dx\, T^{D_2*}(x, m_c/m_b, \mu)\,\phi_M(x,\mu), \qquad (7.29)
\end{aligned}
$$

where $f^{(BD1,BD2*)}$ are functions of the form factors $\tilde{\tau}, \tau_1^{(c)}, \tau_2^{(c)}, \eta_{1,2,3}^{(c,b)}$. For the D_1 channel, f^{BD1} is given by

$$
\begin{aligned}
\sum_{pol}|\epsilon^*\cdot v\bar{f}^{BD1}|^2 &= \frac{m_B(\omega_0+1)}{12m_D} \\
&\times \Big[\Big(2\tilde{\tau} + \frac{6\eta_1^{(c)}}{m_c} - \frac{2\eta_2^{(c)}}{m_c} - \frac{\eta_3^{(c)}}{m_c} + \frac{6\eta_1^{(b)}}{m_b} + \frac{\eta_2^{(b)}}{m_b} + \frac{\eta_3^{(b)}}{m_b} \\
&+ \Big(\frac{m_B}{m_D} + \frac{m_D}{m_B}\Big)\frac{\eta_2^{(c)}}{m_c} - \Big(\frac{m_B}{m_D} + \frac{m_D}{m_B} - 1\Big)\frac{\eta_2^{(b)}}{m_b}\Big)\sqrt{(\omega_0+1)(\omega_0-1)} \qquad (7.30) \\
&- \Big(\frac{m_B^2}{m_D^2} + \frac{m_D^2}{m_B^2}\Big)\frac{\tau_1^{(c)}}{2m_c} + \Big(\frac{\tau_2^{(c)}}{m_c} - \frac{2\bar{\Lambda}\tau}{m_c}\Big) + \Big(\frac{m_B}{m_D} + \frac{m_D}{m_B}\Big)\Big(\frac{\bar{\Lambda}'\tau}{m_c} + \frac{\tau_1^{(c)}}{2m_c} - \frac{\tau_2^{(c)}}{2m_c}\Big) \\
&+ \Big(\frac{m_B}{m_D} + \frac{m_D}{m_B} + 1\Big)\frac{\tau_1^{(c)}}{m_b}\sqrt{(\omega_0-1)} + \Big(\frac{\tau_2^{(c)}}{m_b} - \frac{\bar{\Lambda}\tau}{m_b} - \frac{\bar{\Lambda}'\tau}{m_b}\Big)(\omega_0-1) + \cdots\Big]^2,
\end{aligned}
$$

and for the D_2 channel, f^{BD2} is given by

$$
\begin{aligned}
\sum_{pol}|\epsilon^{*\sigma\nu}v_\sigma v_\nu \bar{f}^{BD2*}|^2 &= \frac{m_B(\omega_0+1)}{12m_D} \\
&\times \Big[\Big(2\tilde{\tau} - \frac{2\eta_1^{(c)}}{m_c} + \frac{\eta_2^{(c)}}{m_c} + \frac{\eta_3^{(c)}}{m_c} - \frac{\tau_2^{(c)}}{m_c} + \frac{6\eta_1^{(b)}}{m_b} + \frac{\eta_2^{(b)}}{m_b} + \frac{\eta_3^{(b)}}{m_b}
\end{aligned}
$$

$$+ \quad (\frac{m_B}{m_D} + \frac{m_D}{m_B} - 1)(\frac{\tau_1^{(c)}}{m_c} - \frac{\eta_2^{(b)}}{m_b})\Big)\sqrt{(\omega_0+1)(\omega_0-1)} \tag{7.31}$$

$$- \quad \Big((\bar{\Lambda}+\bar{\Lambda}')\frac{\tau}{m_b} - \frac{\tau_2^{(c)}}{m_b} - (\frac{m_B}{m_D} + \frac{m_D}{m_B} + 1)(\frac{\eta_2^{(c)}}{m_c} - \frac{\tau_1^{(c)}}{m_b})\Big)(\omega_0 - 1) + \cdots\Big]^2.$$

The above expressions are written in a way to make the power counting manifest. The ratio $\frac{m_B}{m_D}$ is of order one, $(\omega_o - 1)$ is numerically of order Λ_{QCD}/Q, and as discussed in Eq. (7.19) the quantity $\sqrt{(\omega_0-1)(\omega_0+1)}$ is of order one. We see that the leading order contribution inside the square brackets in Eqs. (7.30) and (7.31) is proportional to $\tau\sqrt{(\omega_0-1)(\omega_0+1)}$ and is the same for the D_1 and D_2^* channels. More importantly, there is no suppression of the leading order term due to HQS since $\sqrt{(\omega_0-1)(\omega_0+1)}$ is of order one. On the other hand, the subleading corrections in the square brackets are of size either Λ_{QCD}/m_Q, $(\omega_0-1)\Lambda_{QCD}/m_Q$, $\sqrt{(\omega_0-1)}\Lambda_{QCD}/m_Q$, or $\sqrt{(\omega_0-1)(\omega_0+1)}\Lambda_{QCD}/m_Q$ and hence are suppressed by at least Λ_{QCD}/m_Q relative to the leading order prediction. Thus, we see that the constraints of HQS enter in a very specific manner so as to preserve the power counting scheme of SCET allowing us to ignore the subleading corrections near maximum recoil. It was the maximum recoil relation in Eq. (7.19) that ensured no suppression of the leading order result. The predictions of Eq. (7.10) remain intact with these subleading corrections suppressed by at least Λ_{QCD}/Q.

Color Suppressed Modes

In the case of color suppressed decays which are mediated by operators that are not conserved currents, there is no reason to expect the soft matrix element to vanish at zero recoil by HQS and thus no reason to expect a suppression at maximum recoil. In fact the non-trivial dependence of the soft matrix elements in Eq. (7.11) on the light cone vector n_μ makes it difficult to make a comparison with the zero recoil limit. The soft functions $Q_{L,R}^{(0,8)}$ will depend on the light cone vector n^μ through the arguments $(n\cdot v, n\cdot v', n\cdot k_1, n\cdot k_2)$ and it is not obvious how to extrapolate such a function away

from maximum recoil. At maximum recoil v, v' and n are related through

$$m_B v^\mu = m_D v'^\mu + E_M n^\mu. \tag{7.32}$$

The light cone vector has the special property $n^2 = 0$ and is a reflection of the onshell condition of the pion $p_\pi^2 = (E_\pi n)^2 = 0$. Away from maximum recoil, $E_M n^\mu$ is to be replaced by q^μ which is offshell $q^2 \neq 0$, inconsistent with the $n^2 = 0$ property of the light cone vector. So, Eq. (7.32) can no longer be used to determine n^μ in terms of v^μ and v'^μ and thus more care is required in extrapolating away from maximum recoil.

From Eqs. (7.16), (7.14), and (7.19) and the power counting scheme discussed earlier we see that there is in fact no suppression of the leading order color suppressed amplitude. The leading order predictions of Eq. (7.18) remain intact with corrections suppressed by at least Λ_{QCD}/Q. We leave the analysis of subleading corrections in the color suppressed sector as possible future work.

7.1.3 Phenomenology

In the color allowed sector, based on an analysis of semileptonic decays and an expansion in powers of $(\omega_0 - 1)$, the ratio in Eq. (7.10) was previously predicted to be in the range $0.1 - 1.3$ in Ref. [77] and 0.35 in Ref. [95]. In this paper, with the new power counting introduced at maximum recoil, we have shown the ratio to be one at leading order. In fact we have obtained the same result even for the color suppressed channel. The main results of this paper at leading order are the equality of branching fractions and strong phases

$$\frac{Br(\bar{B} \to D_2^* M)}{Br(\bar{B} \to D_1 M)} = 1\,, \qquad \phi^{D_2^* M} = \phi^{D_1 M}\,, \tag{7.33}$$

where $M = \pi, \rho, K, K^*$ in the color allowed channel and $M = \pi, \rho, K, K_{||}^*$ in the color suppressed channel. This result in the color suppressed channel is quite unexpected from the point of view of naive factorization. In the color suppressed channel the long distance operators in Fig. 6-2c,d give non-vanishing contributions for kaons at

leading order in $\alpha_s(Q)$ unlike the case of $M = \pi, \rho$. However, based on the same arguments [94] given for the case of B-decays to ground state charmed mesons the long distance contributions to the color suppressed decays $\bar{B}^0 \to D_1^0 \bar{K}^0$ and $\bar{B}^0 \to D_2^{0*} \bar{K}^0$ are equal and the result still holds. For K^*'s the long distance contributions are equal only when they are longitudinally polarized.

Once data is available for the color suppressed channel we can construct isospin triangles analogous to Fig. (5-6). With A_{0-} chosen as real, the strong phase ϕ^{D**M} generated by the color suppressed channel A_{00} through the soft functions $Q_{L,R}^{(0,8)}$ in Eq. (7.14), is identical for D_1 and D_2^*. The isospin angle δ which is related to ϕ through Eq. (5.62) is also the same for D_1 and D_2^*. Thus, at leading order we predict the isospin triangles for D_1 and D_2^* to identically overlap.

Recent data [3, 8] reports the ratio of branching fractions in the color allowed channel

$$\frac{Br(B^- \to D_2^{*0}\pi^-)}{Br(B^- \to D_1^0\pi^-)} = 0.79 \pm 0.11. \tag{7.34}$$

The deviation of this ratio from one, which will cause the isospin triangles to no longer overlap, can be attributed to subleading effects. The subleading effects shown to be suppressed by Λ_{QCD}/Q are expected to give a 20% correction, enough to bring agreement with current data. Thus, our claim that subleading corrections are suppressed Λ_{QCD}/Q is in agreement with current data.

Chapter 8

Conclusions

We have applied effective field theory techniques to gain control over strong interaction effects in nonleptonic electroweak decays of $\bar{B}$ mesons into a charmed meson and an energetic light meson of energy E. A typical decay of this type is $\bar{B} \to D^{(*)}\pi$. There are several relevant energy scales involved each contributing important effects to the decay process. The quark level $b \to c$ transitions are determined by electroweak scale physics $\mu \sim M_W$, the characteristic energy scale for the decay process is determined by the bottom quark mass $\mu \sim m_b$, typical energies involved in soft-collinear transitions are of order $\mu \sim \sqrt{E\Lambda_{QCD}}$, and the non-perturbative physics that goes into binding quarks into hadrons occurs at the confinement scale $\mu \sim \Lambda_{QCD}$. We dealt with the large range of energies involved through a sequence of appropriate effective field theories between the electroweak and QCD confinement scales

$$\text{Standard Model} \longrightarrow \text{Fermi Theory} \longrightarrow \text{SCET}_{\text{I}} \longrightarrow \text{SCET}_{\text{II}} \ .$$

The major focus of this thesis was Soft Collinear Effective Theory(SCET) which deals with the physics of the two lowest energy scales in the above sequence. SCET formulates the problem of studying $\bar{B} \to D^{(*)}\pi$ type decays as an expansion in powers of $\Lambda_{QCD}/\{m_b, m_c, E\}$. An introduction to SCET was given in chapter 4.

In our journey from the electroweak scale towards the confinement scale, addi-

tional approximate symmetries were made manifest by the effective field theories encountered along the way. We found Heavy Quark Symmetry(HQS) as an approximate low energy symmetry in SCET and used it to derive a host of phenemenological relations in chapter 5. HQS first appeared in the context of Heavy Quark Effective Theory(HQET), an effective theory for the interactions of a heavy quark with soft gluons, and was discussed in chapter 3. Making HQS manifest in SCET was a rather non-trivial task. It required proving a factorization theorem that decouples the energetic degrees of freedom associated with the light meson responsible for breaking HQS and was the subject of chapter 5.

The main results of this thesis have to do with factorization, heavy quark symmetry relations, generation of non-perturbative strong phases, and power counting. Factorization, proven at leading order in SCET, was of two types. The first was a factorization of effects from the different energy scales involved and the second achieved a decoupling of the energetic modes associated with the light meson. Factorization of the amplitude was proven for color suppressed modes which involve interactions of spectator quarks making the proof all the more non-trivial. With the factorization theorem at hand, we were able to derive heavy quark symmetry relations. A typical result was the equality of the branching fractions for the color suppressed modes $\bar{B}^0 \to D^0\pi^0$ and $\bar{B}^0 \to D^{0*}\pi^0$. Similar relations were derived for $\bar{B} \to D^{(*)}\eta$ and $\bar{B} \to D^{**}\pi$ type decays with an isosinglet meson and excited charmed meson in the final state respectively. A new mechanism for the generation of non-perturbative strong phases was shown within the framework of factorization. Heavy quark symmetry relations were derived for these strong phases as well. A typical leading order result was $\delta^{D\pi} = \delta^{D^*\pi}$ for the above mentioned color suppressed decays. A certain degree of universality was shown for the strong phases through their independence of the final state light meson. A typical univeraslity relation was of the type $\delta^{D\pi} = \delta^{D\rho}$ corresponding to an equality of strong phases for $\bar{B}^0 \to D^0\pi^0$ and $\bar{B}^0 \to D^0\rho^0$. Finally, color suppressed decays of the type $\bar{B}^0 \to D^0\pi^0$ were shown to suppressed relative to the color allowed decays of the type $\bar{B}^- \to D^0\pi^-$ by one power of $\sim \Lambda_{QCD}/\{m_b, m_c, E\}$. All of the results obtained are in good agreement

with available data.

Chapter 9

Appendix

9.1 Long Distance contributions for π and ρ

The factorization theorem derived in Sec. 5.1.3 for the color-suppressed $B^0 \to D^0 M^0$ amplitude contains both short- and long-distance contributions. In this Appendix we show that, working at lowest order in the Wilson coefficients at the hard scale Q, the long-distance amplitude vanishes for the case of an isotriplet light mesons $M = \pi, \rho$.

We start by recalling the factorized form of the long-distance amplitude, which is given by SCET_{II} time ordered products $\bar{T}^{(0,8)}_{L,R}$

$$\begin{aligned} A^{D^{(*)}M}_{\text{long}} &= \int_0^1 dz \int dk^+ d\omega \int d^2x_\perp \Big[C_L^{(i)}(z)\, \bar{J}^{(i)}(\omega k^+)\, \Phi_L^{(i)}(k^+, x_\perp, \varepsilon^*_{D^*}) \Psi_M^{(i)}(z, \omega, x_\perp, \varepsilon^*_M) \\ &\quad \pm C_R^{(i)}(z)\, \bar{J}^{(i)}(\omega k^+)\, \Phi_R^{(i)}(k^+, x_\perp, \varepsilon^*_{D^*}) \Psi_M^{(i)}(z, \omega, x_\perp, \varepsilon^*_M) \Big] . \end{aligned} \tag{9.1}$$

The functions $\Psi_M^{(i)}$ and $\Phi_{L,R}^{(i)}$ are SCET_{II} matrix elements of collinear and soft fields, respectively, and their precise definitions are given in Eqs. (6.16). The jet functions $\bar{J}^{(i)}(\omega k^+)$ appear in the definition of the subleading soft-collinear Lagrangian $\mathcal{L}^{(1)}_{\xi\xi qq}$ and their lowest order expressions are given in Eq. (5.25).

In the following we derive a few general properties of the functions $\Psi_M^{(i)}$ and $\overline{J}^{(0,8)}$ following from isospin, charge conjugation, parity and time-reversal. The collinear

function $\Psi_M^{(i)}(z,\omega,x_\perp,\varepsilon_M^*)$ is defined as the matrix element

$$\Big\langle M^0(\varepsilon)\Big|\Big[(\bar\xi_n^{(d)}W)_{\tau_1}\bar n\!\!\!/ P_L(W^\dagger\xi_n^{(u)})_{\tau_2}\Big](0_\perp)\Big[(\bar\xi_n^{(u)}W)_\omega \bar n\!\!\!/ P_L(W^\dagger\xi_n^{(d)})_\omega\Big](x_\perp)\Big|0\Big\rangle\,. \qquad (9.2)$$

We will prove that $\Psi_{M=\pi,\rho}$ is even under $\omega\to-\omega$ and $z\to 1-z$. As motivation consider the first bilinear in Eq. (9.2), which creates a $d\bar u$ collinear quark pair. The second bilinear in Eq. (9.2) must act at some point along the collinear quark lines: it either takes a $d\to u$ (for $\omega>0$) or takes a $\bar u\to\bar d$ (for $\omega<0$). Examination of lowest order graphs contributing to Ψ_M shows that these two types of contributions always appear in pairs, such that the projection of Ψ_M onto an isotriplet state is even under $\omega\to-\omega$. This suggests the existence of a symmetry argument, valid to all orders in perturbation theory.

We will prove that $\Psi_M^{(0,8)}$ is even, as a consequence of G-parity. This is defined as usual by $G=C\exp(-i\pi I_2)$ where C is charge conjugation and I_2 is the isospin generator, and is a symmetry of the collinear Lagrangian in the limit $m_{u,d}\ll\Lambda_{\rm QCD}$. Its action on the collinear operators in Eq. (9.2) can be worked out from that of its components C and I_2 (cf. Ref. [17]) and is given by

$$\begin{aligned} G\,(\bar\xi_n^{(d)}W)_{\tau_1}\bar n\!\!\!/ P_L(W^\dagger\xi_n^{(u)})_{\tau_2}\,G^\dagger &= (\bar\xi_n^{(d)}W)_{-\tau_2}\bar n\!\!\!/ P_R(W^\dagger\xi_n^{(u)})_{-\tau_1}\,, \qquad (9.3)\\ G\,(\bar\xi_n^{(u)}W)_{\omega}\bar n\!\!\!/ P_L(W^\dagger\xi_n^{(d)})_{\omega}\,G^\dagger &= (\bar\xi_n^{(u)}W)_{-\omega}\bar n\!\!\!/ P_R(W^\dagger\xi_n^{(d)})_{-\omega}\,. \end{aligned}$$

Taking into account the G-parity of the states, Eq. (9.2) is equal to

$$\pm\Big\langle M^0(\varepsilon)\Big|\Big[(\bar\xi_n^{(d)}W)_{-\tau_2}\bar n\!\!\!/ P_R(W^\dagger\xi_n^{(u)})_{-\tau_1}\Big](0_\perp)\Big[(\bar\xi_n^{(u)}W)_{-\omega}\bar n\!\!\!/ P_R(W^\dagger\xi_n^{(d)})_{-\omega}\Big](x_\perp)\Big|0\Big\rangle\,, \qquad (9.4)$$

where the $\pm$ refer to the ρ^0 and π^0 respectively. Next we apply parity in the matrix element followed by switching our basis vectors $n\leftrightarrow\bar n$. Acting on Eq. (9.4) this gives

$$\Big\langle M^0(\varepsilon_P^*)\Big|\Big[(\bar\xi_n^{(d)}W)_{-\tau_2}\bar n\!\!\!/ P_L(W^\dagger\xi_n^{(u)})_{-\tau_1}\Big](0_\perp)\Big[(\bar\xi_n^{(u)}W)_{-\omega}\bar n\!\!\!/ P_L(W^\dagger\xi_n^{(d)})_{-\omega}\Big](-x_\perp)\Big|0\Big\rangle\,, \qquad (9.5)$$

where the overall sign is now the same for $M=\rho,\pi$. Now since $\Psi_M^{(0,8)}$ is a scalar

function the only allowed perpendicular dot products are $(-x_\perp)^2 = x_\perp^2$ and $-x_\perp \cdot \varepsilon_P^* = x_\perp \cdot \varepsilon^*$. Finally we note that the change in $\tau_{1,2}$ from Eqs. (9.2) to (9.5) is equivalent $z \to 1-z$. Thus the invariance of $\mathrm{SCET_{II}}$ under G-parity and regular parity has allowed us to prove that

$$\Psi^{(i)}_{\pi,\rho}(z,\omega,x_\perp,\varepsilon^*) = \Psi^{(i)}_{\pi,\rho}(1-z,-\omega,x_\perp,\varepsilon^*)\,. \tag{9.6}$$

Next we prove that $\overline{J}^{(0,8)}(\omega k^+)$ is odd under $\omega \to -\omega$. By reparameterization invariance type-III [42] only the product ωk^+ will appear. Consider applying time reversal plus the interchange $(n \leftrightarrow \bar{n})$ to the $\mathrm{SCET_{II}}$ Lagrangian. Since this Lagrangian does not have coefficients that encode decays to highly virtual offshell states it should be invariant under this transformation. Acting on Eq. (5.24) this implies that $\overline{J}^{(0,8)}$ must be real,

$$[\overline{J}^{(0,8)}(\omega k^+)]^* = \overline{J}^{(0,8)}(\omega k^+). \tag{9.7}$$

At tree level this implies that we should drop the $i\epsilon$ in the collinear gluon propagator in matching onto this operator. This was done in arriving at the odd functions $J^{(0,8)} \propto 1/(\omega k^+)$ in Eq. (5.25). The imaginary part would give a $\delta(\omega k^+)$ and corresponds to cases where the $\mathrm{SCET_I}$ T-product is reproduced by a purely collinear $\mathrm{SCET_{II}}$ T-product ($k^+ = 0$), or a purely soft $\mathrm{SCET_{II}}$ T-product ($\omega = 0$). Thus dropping the $i\epsilon$ also saves us from double counting.

Now consider what functions can be generated by computing loop corrections to $\overline{J}^{(0,8)}$. By dimensional analysis $\overline{J}^{(0,8)}$ must be proportional to $1/(\omega k^+)$ times a dimensionless function of $\omega k^+/\mu^2$. Since at any order in perturbation theory the matching calculation will involve only massless quarks we can only generate logarithms. Therefore, we must study functions of the form

$$\frac{1}{\omega k^+} \ln^n\Big(\frac{\omega k^+ \pm i\epsilon}{\mu^2}\Big)\,. \tag{9.8}$$

To demand that only the real part of these functions match onto $\overline{J}^{(0,8)}$ we average

them with their conjugates. It is straightforward to check that only terms odd in $\omega \to -\omega$ survive. Thus, all the terms that can correct the form of $\overline{J}^{(0,8)}$ at higher orders in α_s are odd under $\omega \to -\omega$.

Now in Eq. (9.1) the integration over ω is from $-\infty$ to ∞, while z varies from 0 to 1. Consider the change of variable $\omega \to -\omega$ and $z \to 1-z$. If $C^{(i)}_{L,R}(z) = C^{(i)}_{L,R}(1-z)$ then under this interchange one of the functions in the integrand is odd ($\overline{J}$) and the other two are even ($C^{(i)}_{L,R}$ and $\Psi^{(i)}_{\pi,\rho}$), so the integral would vanish.

Now if $C^{(i)}_{L,R}(z)$ are kept only to leading order then they are independent of z and thus unchanged under $z \to 1-z$. So at this order in the $\alpha_s(Q)/\pi$ expansion of $C^{(i)}_{L,R}(z)$ we find $A^{D^{(*)}M}_{\text{long}} = 0$. This completes the proof of the assertion about the vanishing of the long distance contributions for $M = \pi, \rho$.

9.2 Helicity Symmetry and Jet functions

In this appendix we discuss the general structure of the jet functions $J^{(0,8)}(z, x, k_j^+)$ in Eq. (5.34), which are generated by matching SCET_I and SCET_II at any order in $\alpha_s(\mu_0)$. In Fig. 6-2a,b this means adding additional collinear gluons which generate loops by attaching to the collinear lines already present (as well as vacuum polarization type collinear quark, gluon, and ghost loops). Additional collinear loops should also be added to Figs. 6-2c,d,e, and the difference at lowest order in λ gives J. Throughout this appendix we continue to drop isosinglet combinations of $\bar{\xi}_n \cdots \xi_n$. These will also have additional contributions from topologies where the outgoing collinear quarks are replaced by outgoing gluons (through $B^\mu_\perp$ operators).

The leading order collinear Lagrangian has a U(1) helicity spin symmetry for the quarks, see reference 2 in [16]. It is defined by a generator h_n that has the quark spin projection along the n direction, which is different from usual definition of helicity as the projection of the spin along its momentum. Unlike QCD, the collinear fields in SCET only allow quarks and antiquarks that move in the n direction. For h_n we

have

$$h_n = \frac{1}{4}\,\epsilon_\perp^{\mu\nu}\sigma_{\mu\nu}\,, \qquad h_n^2 = 1\,, \qquad [h_n, \not{n}] = [h_n, \not{\bar{n}}] = 0\,, \qquad \{h_n, \gamma_\perp^\sigma\} = 0\,. \tag{9.9}$$

After making a field redefinition [22] to decouple ultrasoft gluons the leading order collinear quark Lagrangian is

$$\mathcal{L}_{\xi\xi}^{(0)} = \bar{\xi}_{n,p'}\left\{in\cdot D_c + i\not{D}_c^\perp \frac{1}{i\bar{n}\cdot D_c} i\not{D}_c^\perp\right\}\frac{\not{\bar{n}}}{2}\,\xi_{n,p}, \tag{9.10}$$

where iD_c^μ contains only collinear $A_{n,q}^\mu$ gluons. $\mathcal{L}_{\xi\xi}^{(0)}$ is invariant under the transformation $\xi_n \to \exp(i\theta h_n)\xi_n$, $\bar{\xi}_n \to \bar{\xi}_n \exp(-i\theta h_n)$. This means that any number of leading order collinear quark interactions preserve the quark helicity h_n. The collinear gluon interactions take $u_n(\uparrow) \to u_n(\uparrow)$, $u_n(\downarrow) \to u_n(\downarrow)$, $v_n(\uparrow) \to v_n(\uparrow)$, $v_n(\downarrow) \to v_n(\downarrow)$, and can also produce or annihilate the quark-antiquark combinations $u_n(\uparrow)\,v_n(\downarrow)$ or $u_n(\downarrow)\,v_n(\uparrow)$ (the arrows refer to the helicity of the antiparticles themselves rather than their spinors). For this reason we refer to $\mathcal{L}_{\xi\xi}^{(0)}$ as a $\Delta h_n = 0$ operator.

The leading order $\mathrm{SCET_I}$ operators in Eq. (5.17) are also unchanged by the h_n-transformation and therefore does not change collinear quark helicity. In contrast the operators $\mathcal{L}_{\xi q}^{(1)}$ do generate or annihilate a collinear quark giving $\Delta h_n = \pm 1/2$. However, at tree level we showed in Section 5.1.3 that the two graphs in Figs. 6-2a,b match onto an overall $\Delta h_n = 0$ operator in $\mathrm{SCET_{II}}$ as given in Eqs. (5.27). Since at higher orders the $\mathcal{L}_{\xi\xi}^{(0)}$ will not cause a change in the helicity they also match onto these same operators, so the structure $\not{\bar{n}}\gamma_\perp^\nu$ will not occur. At tree level only the structure $\not{n}P_L \otimes \not{\bar{n}}P_L$ appeared in Eq. (5.27). To rule out the appearance of P_R beyond tree level we note that the weak operator projects onto left handed collinear fermions, and for the jet function the conservation of helicity in $\mathcal{L}_{\xi\xi}^{(0)}$ implies a conservation of chirality. This leaves us with the desired result.

It is perhaps illustrative to see this more explicitly by looking at the spin structure of the loop graphs. We begin by noting that the spin and color structure in $\bar{h}_{v'}^{(c)} \cdots h_v^{(b)}$ is unaffected by this second stage of matching. Adding additional collinear attach-

ments only can affect the spin and color structure generated in putting the collinear quark fields and light ultrasoft quark fields together.

Consider how additional gluon attachments effect the spin structures that appear in Figs. 6-2a,b. The leading order collinear quark Lagrangian is $\mathcal{L}^{(0)}_{\xi\xi}$ in Eq. (9.10). Each attachment of a collinear gluon to a collinear quark lines in the figures generates a $\bar{n}\!\!\!//2$ from the vertex and a $n\!\!\!//2$ from the quark propagator. These combine to a projector which can be eliminated by commuting them to the right or left to act on the collinear quark spinors, via $(n\!\!\!/\bar{n}\!\!\!/)/4\ \xi_n = \xi_n$. Therefore, at most we have additional pairs of $\gamma_\perp$'s that appear between the light quark spinors. The aim is to show that just like the tree level calculation in Eq. (5.41) the resulting operators have spin structure $(\bar{d}\bar{n}\!\!\!/P_L u)\ (\bar{\xi}_n n\!\!\!/P_L \xi_n)$.

For the contraction of $T_j^{(0,8)}$ which gives the C topology the spin structure is

$$\begin{aligned}&\Big[\bar{u}_n^{(d)}\gamma_\perp^{\mu_1}\gamma_\perp^{\mu_2}\cdots\gamma_\perp^{\mu_{2k-1}}\gamma_\perp^{\mu_{2k}}\Big(\frac{\bar{n}\!\!\!/}{2}P_L\Big)\gamma_\perp^{\nu_1}\cdots\gamma_\perp^{\nu_{2\ell}}\Big(\frac{n\!\!\!/}{2}\gamma_\perp^{\alpha}\Big)u_s^{(u)}\Big]\ \Big[\bar{u}_s^{(d)}\Big(\gamma_\perp^{\beta}\Big)\gamma_\perp^{\lambda_1}\cdots\gamma_\perp^{\lambda_{2j}}u_n^{(d)}\Big]\\ &=[\bar{u}_n^{(d)}\gamma_\perp^{\mu_1}\cdots\gamma_\perp^{\mu_{2k'}}\gamma_\perp^{\alpha}P_L u_s^{(u)}]\ [\bar{u}_s^{(d)}\gamma_\perp^{\beta}\gamma_\perp^{\lambda_1}\cdots\gamma_\perp^{\lambda_{2j}}u_n^{(d)}]\,.\end{aligned}\tag{9.11}$$

In the first line $(\frac{\bar{n}\!\!\!/}{2}P_L)$ comes from $\mathcal{Q}^{(0,8)}_{L,R}$, the $\gamma_\perp^\alpha$ and $\gamma_\perp^\beta$ are terms generated by the $\mathcal{L}^{(1)}_{\xi q}$ insertions and the $n\!\!\!//2$ is from the extra collinear quark propagator. In the second line the P_L projector was moved next to $u_s^{(u)}$ without a change of sign (for anticommuting γ_5), and the remaining $\bar{n}\!\!\!/$ and $n\!\!\!/$ were then moved next to the $\bar{u}_n^{(d)}$ and canceled. The remaining free $\perp$ indices in the second line are contracted with each other in some manner. Fierzing the set of γ matrices in Eq. (9.11) by inserting $1\otimes 1$ next to the collinear spinors gives

$$[\bar{u}_n^{(d)}\,\Gamma_1\,u_n^{(d)}]\ [\bar{u}_s^{(d)}\gamma_\perp^{\beta}\gamma_\perp^{\lambda_1}\cdots\gamma_\perp^{\lambda_{2j}}\,\Gamma_1'\,\gamma_\perp^{\mu_1}\cdots\gamma_\perp^{\mu_{2k'}}\gamma_\perp^{\alpha}P_L u_s^{(u)}]\,,\tag{9.12}$$

where

$$\begin{aligned}\Gamma_1\otimes\Gamma_1' &= \frac{\bar{n}\!\!\!/}{2}\otimes n\!\!\!/ - \frac{\bar{n}\!\!\!/\gamma_5}{2}\otimes n\!\!\!/\gamma_5 - \frac{\bar{n}\!\!\!/\gamma_\perp^\nu}{2}\otimes n\!\!\!/\gamma_\nu^\perp\\ &\to \frac{\bar{n}\!\!\!/}{2}(1-\gamma_5)\otimes n\!\!\!/ - \frac{\bar{n}\!\!\!/\gamma_\perp^\nu}{2}\otimes n\!\!\!/\gamma_\nu^\perp\,.\end{aligned}\tag{9.13}$$

In the second line of Eq. (9.13) we have used the fact that the γ_5 in the bracket with soft quark spinors can be eliminated by moving it next to the P_L. To eliminate the $\bar{n}\cdot\gamma_\perp^\nu$ Dirac structure we note that between the soft spinors in Eq. (9.12) there are an odd number of $\gamma_\perp$'s to the left and right of $\bar{n}\cdot\gamma_\nu^\perp$, and so at least one set of indices are contracted between the sets $\{\beta, \lambda_1, \ldots, \lambda_{2j}\}$ and $\{\mu_1, \ldots, \mu_{2k'}, \alpha\}$. The identity $\{\gamma_\perp^\sigma, \gamma_\perp^\tau\} = 2g_\perp^{\sigma\tau}$ can be used to move these matrices so that they sandwich $\gamma_\nu^\perp$, and this gives the product $\gamma_\perp^\mu \gamma_\nu^\perp \gamma_\mu^\perp = 0$. After these manipulations only the spin structure $(\bar{d}\bar{n}P_L u)\,(\bar{\xi}_n \bar{n} P_L \xi_n)$ remains. A similar argument can be applied to the E-topology with the same result.

In several places in the above argument we made use of Dirac algebra that is particular to 4-dimensions (anticommuting γ_5 and setting $\gamma_\perp^\mu \gamma_\nu^\perp \gamma_\mu^\perp = 0$). If the $\gamma_\perp$'s are taken in in full dimensional regulation then it is not apriori clear if the manipulations survive regulation. However, the original helicity symmetry argument shows that as long as the theory can be regulated in a way that preserves this symmetry this will indeed be the case.

9.3 Properties of Soft Distribution Functions

In this appendix we derive some useful properties of the soft functions $S^{(0,8)}$. In particular we show that these functions are complex. The imaginary parts have a direct interpretation as non-perturbative contributions to final state rescattering between the $D^{(*)}$ and final energetic meson as discussed in section 5.1.3.

To be definite we consider the function $S_L^{(0)}$, and suppress the index L. The manipulations for the remaining soft functions $S_R^{(0)}$ and $S_{L,R}^{(8)}$ are identical. The definition in Eq. (6.5) is

$$\langle D^0(v')|(\bar{h}_{v'}^{(c)} S)\bar{n}P_L(S^\dagger h_v^{(b)})(\bar{d}S)_{k_1^+}\bar{n}P_L(S^\dagger u)_{k_2^+}|\bar{B}^0(v)\rangle \;=\; S^{(0)}\,, \qquad (9.14)$$

where the Wilson lines are defined as

$$W = \Big[\sum_{\text{perms}} \exp\Big(-\frac{g}{\bar{\mathcal{P}}}\,\bar{n}\cdot A_{n,q}(x)\Big)\Big], \quad S = \Big[\sum_{\text{perms}} \exp\Big(-g\,\frac{1}{n\cdot\mathcal{P}}\,n\cdot A_{s,q}\Big)\Big] \tag{9.15}$$

In general $S^{(0)}$ is a dimensionless function of $v\!\cdot\!v'$, $n\!\cdot\!v$, $n\!\cdot\!v'$, $n\!\cdot\!k_1$, $n\!\cdot\!k_2$, $\Lambda_{\rm QCD}$, and μ. Since $(S^\dagger q)_{k_2^+} = \delta(k_2^+ - n\!\cdot\!\mathcal{P})(S^\dagger q)$ the LHS is invariant under a type-III reparameterization transformation [42] ($n \to e^\alpha n$, $\bar{n} \to e^{-\alpha}\bar{n}$). Therefore the RHS can only be a function of w, $t = n\!\cdot\!v/n\!\cdot\!v'$, $z = n\!\cdot\!k_1/n\!\cdot\!k_2$, $K/\mu = [n\!\cdot\!k_1\, n\!\cdot\!k_2/(n\!\cdot\!v\, n\!\cdot\!v'\mu^2)]^{1/2}$, and $\Lambda_{\rm QCD}/\mu$.

Rather than study the matrix element in Eq. (9.14) directly it is useful to instead consider

$$\begin{aligned}&\langle H_i(v')|(\bar{h}_{v'}S)\not{n}P_L(S^\dagger h_v)(\bar{q}S)_{k_1^+}\not{n}P_L\tau^a(S^\dagger q)_{k_2^+}|H_j(v)\rangle \\ &\quad = S^{(0)}\Big(t, z, v\!\cdot\!v', \frac{K}{\mu}, \frac{\Lambda_{\rm QCD}}{\mu}\Big)(\tau^a)_{ij}\,,\end{aligned} \tag{9.16}$$

where h_v are doublet fields under heavy quark flavor symmetry, and q and $|H_{i=1,2}(v)\rangle$ are isospin doublets of (u,d). The last three variables in Eq. (9.16) will not play a crucial role so we will suppress this dependence. Taking the complex conjugate of Eq. (9.16) gives

$$\begin{aligned}\langle H_j(v)|(\bar{h}_v S)\not{n}P_L(S^\dagger h_{v'})(\bar{q}S)_{k_2^+}\not{n}P_L\tau^a(S^\dagger q)_{k_1^+}|H_i(v')\rangle &= [S^{(0)}(t,z)]^*(\tau^a)_{ji} \\ &= S^{(0)}\Big(\frac{1}{t},\frac{1}{z}\Big)(\tau^a)_{ji}\end{aligned} \tag{9.17}$$

The dependence on w and K is unchanged since they are even under the interchange $v \leftrightarrow v'$, $n\!\cdot\!k_1 \leftrightarrow n\!\cdot\!k_2$. Next, decompose the functions $S^{(0)}$ in terms of even and odd functions under $t \to 1/t$, $z \to 1/z$:

$$S^{(0)} = S_E^{(0)} + S_O^{(0)}\,, \tag{9.18}$$

where $S_{E,O}^{(0)} = [S^{(0)}(t,z) \pm S^{(0)}(1/t,1/z)]/2$. Now Eq. (9.17) implies that

$$[S_E^{(0)}(t,z)]^* = S_E^{(0)}(t,z)\,, \qquad [S_O^{(0)}(t,z)]^* = -S_O^{(0)}(t,z) \tag{9.19}$$

so $S_E^{(0)}$ is real and $S_O^{(0)}$ is imaginary. An identical argument for $S^{(8)}$ implies that it too is a complex function.

For the above analysis it is important to note that $n \cdot v' = m_B/m_D$ is not 1 in the heavy quark limit where we have new spin and flavor symmetries. These symmetries arise from taking $m_B \gg \Lambda_{\rm QCD}$ and $m_D \gg \Lambda_{\rm QCD}$, not from having $m_B = m_D$.

Bibliography

[1] K. Abe. Improved measurements of color-suppressed decays anti-B0 – ¿ D0 pi0, D0 eta and D0 omega. 2004.

[2] K. Abe et al. Observation of color-suppressed anti-B0 → D0 pi0, D*0 pi0, D0 eta and D0 omega decays. *Phys. Rev. Lett.*, 88:052002, 2002.

[3] K. Abe et al. Study of B- → D**0 pi- (D**0 → D(*)+ pi-) decays. *Phys. Rev.*, D69:112002, 2004.

[4] S. Ahmed et al. Measurement of B(B- → D0 pi-) and B(anti-B0 → D+ pi-) and isospin analysis of B → D pi decays. *Phys. Rev.*, D66:031101, 2002.

[5] Ahmed Ali, G. Kramer, and Cai-Dian Lu. Experimental tests of factorization in charmless non- leptonic two-body B decays. *Phys. Rev.*, D58:094009, 1998.

[6] M. Christian Arnesen, Ben Grinstein, Ira Z. Rothstein, and Iain W. Stewart. A precision model independent determination of —V(ub)— from B → pi e nu. 2005.

[7] B. Aubert et al. A study of the rare decays B0 → D/s(*)+ pi- and B0 → D/s(*)- K+. ((B)). *Phys. Rev. Lett.*, 90:181803, 2003.

[8] B. Aubert et al. Study of the decays B- → D(*)+ pi- pi-. 2003.

[9] B. Aubert et al. A study of anti-B0 → D(*)0 anti-K(*)0 decays. 2004.

[10] B. Aubert et al. Measurement of branching fractions of color-suppressed decays of the anti-B0 meson to D(*)0 pi0, D(*)0 eta, D(*)0 omega, and D0 eta'. *Phys. Rev.*, D69:032004, 2004.

[11] Alexander P. Bakulev, S. V. Mikhailov, and N. G. Stefanis. CLEO and E791 data: A smoking gun for the pion distribution amplitude? *Phys. Lett.*, B578:91–98, 2004.

[12] Patricia Ball and Vladimir M. Braun. Handbook of higher twist distribution amplitudes of vector mesons in QCD. 1998.

[13] Myron Bander, D. Silverman, and A. Soni. Cp noninvariance in the decays of heavy charged quark systems. *Phys. Rev. Lett.*, 43:242, 1979.

[14] C. W. Bauer, B. Grinstein, D. Pirjol, and I. W. Stewart. Testing factorization in B $\to$ D(*) X decays. *Phys. Rev.*, D67:014010, 2003.

[15] Christian W. Bauer, Matthew P. Dorsten, and Michael P. Salem. Infrared regulators and scet(ii). *Phys. Rev.*, D69:114011, 2004.

[16] Christian W. Bauer, Sean Fleming, and Michael E. Luke. Summing Sudakov logarithms in B $\to$ X/s gamma in effective field theory. *Phys. Rev.*, D63:014006, 2001.

[17] Christian W. Bauer, Sean Fleming, Dan Pirjol, Ira Z. Rothstein, and Iain W. Stewart. Hard scattering factorization from effective field theory. *Phys. Rev.*, D66:014017, 2002.

[18] Christian W. Bauer, Sean Fleming, Dan Pirjol, and Iain W. Stewart. An effective field theory for collinear and soft gluons: Heavy to light decays. *Phys. Rev.*, D63:114020, 2001.

[19] Christian W. Bauer, Sean Fleming, Dan Pirjol, and Iain W. Stewart. An effective field theory for collinear and soft gluons: Heavy to light decays. *Phys. Rev.*, D63:114020, 2001.

[20] Christian W. Bauer, Dan Pirjol, Ira Z. Rothstein, and Iain W. Stewart. B $\to$ M(1) M(2): Factorization, charming penguins, strong phases, and polarization. *Phys. Rev.*, D70:054015, 2004.

[21] Christian W. Bauer, Dan Pirjol, and Iain W. Stewart. A proof of factorization for B $\to$ D pi. *Phys. Rev. Lett.*, 87:201806, 2001.

[22] Christian W. Bauer, Dan Pirjol, and Iain W. Stewart. Soft-collinear factorization in effective field theory. *Phys. Rev.*, D65:054022, 2002.

[23] Christian W. Bauer, Dan Pirjol, and Iain W. Stewart. Factorization and endpoint singularities in heavy-to-light decays. *Phys. Rev.*, D67:071502, 2003.

[24] Christian W. Bauer, Dan Pirjol, and Iain W. Stewart. On power suppressed operators and gauge invariance in scet. *Phys. Rev.*, D68:034021, 2003.

[25] Christian W. Bauer, Dan Pirjol, and Iain W. Stewart. On power suppressed operators and gauge invariance in scet. *Phys. Rev.*, D68:034021, 2003.

[26] Christian W. Bauer and Iain W. Stewart. Invariant operators in collinear effective theory. *Phys. Lett.*, B516:134–142, 2001.

[27] Manfred Bauer, B. Stech, and M. Wirbel. EXCLUSIVE NONLEPTONIC DECAYS OF D, D(S), and B MESONS. *Z. Phys.*, C34:103, 1987.

[28] Thomas Becher, Richard J. Hill, and Matthias Neubert. Soft-collinear messengers: A new mode in soft-collinear effective theory. *Phys. Rev.*, D69:054017, 2004.

[29] M. Beneke, G. Buchalla, M. Neubert, and Christopher T. Sachrajda. QCD factorization for exclusive, non-leptonic B meson decays: General arguments and the case of heavy-light final states. *Nucl. Phys.*, B591:313–418, 2000.

[30] M. Beneke, A. P. Chapovsky, M. Diehl, and T. Feldmann. Soft-collinear effective theory and heavy-to-light currents beyond leading power. *Nucl. Phys.*, B643:431–476, 2002.

[31] M. Beneke, A. P. Chapovsky, M. Diehl, and T. Feldmann. Soft-collinear effective theory and heavy-to-light currents beyond leading power. *Nucl. Phys.*, B643:431–476, 2002.

[32] M. Beneke and T. Feldmann. Multipole-expanded soft-collinear effective theory with non-abelian gauge symmetry. *Phys. Lett.*, B553:267–276, 2003.

[33] M. Beneke and T. Feldmann. Factorization of heavy-to-light form factors in soft- collinear effective theory. *Nucl. Phys.*, B685:249–296, 2004.

[34] Martin Beneke and Matthias Neubert. Flavor-singlet B decay amplitudes in QCD factorization. *Nucl. Phys.*, B651:225–248, 2003.

[35] G. Bertsch, Stanley J. Brodsky, A. S. Goldhaber, and J. F. Gunion. Diffractive excitation in QCD. *Phys. Rev. Lett.*, 47:297, 1981.

[36] B. Blok and Mikhail A. Shifman. Nonfactorizable amplitudes in weak nonleptonic decays of heavy mesons. *Nucl. Phys.*, B389:534–548, 1993.

[37] Nora Brambilla, Antonio Pineda, Joan Soto, and Antonio Vairo. Potential nrQCD: An effective theory for heavy quarkonium. *Nucl. Phys.*, B566:275, 2000.

[38] Stanley J. Brodsky, Dae Sung Hwang, and Ivan Schmidt. Final-state interactions and single-spin asymmetries in semi-inclusive deep inelastic scattering. *Phys. Lett.*, B530:99–107, 2002.

[39] Gerhard Buchalla, Andrzej J. Buras, and Markus E. Lautenbacher. Weak decays beyond leading logarithms. *Rev. Mod. Phys.*, 68:1125–1144, 1996.

[40] Gerhard Buchalla, Andrzej J. Buras, and Markus E. Lautenbacher. Weak decays beyond leading logarithms. *Rev. Mod. Phys.*, 68:1125–1144, 1996.

[41] Andrzej J. Buras and Luca Silvestrini. Non-leptonic two-body B decays beyond factorization. *Nucl. Phys.*, B569:3–52, 2000.

[42] Junegone Chay and Chul Kim. Collinear effective theory at subleading order and its application to heavy-light currents. *Phys. Rev.*, D65:114016, 2002.

[43] Junegone Chay, Chul Kim, Yeong Gyun Kim, and Jong-Phil Lee. Soft wilson lines in soft-collinear effective theory. *Phys. Rev.*, D71:056001, 2005.

[44] Hai-Yang Cheng, Chun-Khiang Chua, and Chien-Wen Hwang. Covariant light-front approach for s-wave and p-wave mesons: Its application to decay constants and form factors. *Phys. Rev.*, D69:074025, 2004.

[45] Hai-Yang Cheng and B. Tseng. Nonfactorizable effects in spectator and penguin amplitudes of hadronic charmless B decays. *Phys. Rev.*, D58:094005, 1998.

[46] T. P. Cheng and L. F. Li. Gauge theory of elementary particle physics. Oxford, Uk: Clarendon (1984) 536 P. (Oxford Science Publications).

[47] Cheng-Wei Chiang and Jonathan L. Rosner. Final-state phases in B $\to$ D pi, D* pi, and D rho decays. *Phys. Rev.*, D67:074013, 2003.

[48] T. E. Coan et al. Observation of anti-B0 $\to$ D0 pi0 and anti-B0 $\to$ D*0 pi0. *Phys. Rev. Lett.*, 88:062001, 2002.

[49] S. E. Csorna et al. Measurements of the branching fractions and helicity amplitudes in B $\to$ D* rho decays. *Phys. Rev.*, D67:112002, 2003.

[50] Michael J. Dugan and Benjamin Grinstein. QCD basis for factorization in decays of heavy mesons. *Phys. Lett.*, B255:583–588, 1991.

[51] Estia Eichten and Brian Hill. An effective field theory for the calculation of matrix elements involving heavy quarks. *Phys. Lett.*, B234:511, 1990.

[52] S. Eidelman et al. Review of particle physics. *Phys. Lett.*, B592:1, 2004.

[53] Adam F. Falk, Howard Georgi, Benjamin Grinstein, and Mark B. Wise. Heavy meson form-factors from QCD. *Nucl. Phys.*, B343:1–13, 1990.

[54] Edward Farhi and Leonard Susskind. Technicolor. *Phys. Rept.*, 74:277, 1981.

[55] T. Feldmann, P. Kroll, and B. Stech. Mixing and decay constants of pseudoscalar mesons. *Phys. Rev.*, D58:114006, 1998.

[56] Thorsten Feldmann. Quark structure of pseudoscalar mesons. *Int. J. Mod. Phys.*, A15:159–207, 2000.

[57] Thorsten Feldmann and Peter Kroll. Flavor symmetry breaking and mixing effects in the eta gamma and eta' gamma transition form factors. *Eur. Phys. J.*, C5:327–335, 1998.

[58] H. Georgi. Effective field theory. *Ann. Rev. Nucl. Part. Sci.*, 43:209–252, 1993.

[59] Howard Georgi. An effective field theory for heavy quarks at low- energies. *Phys. Lett.*, B240:447–450, 1990.

[60] Benjamin Grinstein. The static quark effective theory. *Nucl. Phys.*, B339:253–268, 1990.

[61] Igor E. Halperin. Soft gluon suppression of 1/N(c) contributions in color suppressed heavy meson decays. *Phys. Lett.*, B349:548–554, 1995.

[62] (ed.) Hewett, J. and (ed.) Hitlin, D. G. The discovery potential of a Super B Factory. Proceedings, SLAC Workshops, Stanford, USA, 2003. 2004.

[63] Richard J. Hill and Matthias Neubert. Spectator interactions in soft-collinear effective theory. ((u)). *Nucl. Phys.*, B657:229–256, 2003.

[64] Nathan Isgur and Mark B. Wise. Weak transition form-factors between heavy mesons. *Phys. Lett.*, B237:527, 1990.

[65] Nathan Isgur and Mark B. Wise. Spectroscopy with heavy quark symmetry. *Phys. Rev. Lett.*, 66:1130–1133, 1991.

[66] Roland Kaiser and H. Leutwyler. Pseudoscalar decay constants at large N(c). 1998.

[67] B. Kayser, F. Gibrat-Debu, and F. Perrier. The physics of massive neutrinos. *World Sci. Lect. Notes Phys.*, 25:1–117, 1989.

[68] Yong-Yeon Keum, T. Kurimoto, Hsiang Nan Li, Cai-Dan Lu, and A. I. Sanda. Nonfactorizable contributions to B $\rightarrow$ D(*) M decays. *Phys. Rev.*, D69:094018, 2004.

[69] Yong-Yeon Keum, T. Kurimoto, Hsiang Nan Li, Cai-Dan Lu, and A. I. Sanda. Nonfactorizable contributions to B $\rightarrow$ D(*) M decays. *Phys. Rev.*, D69:094018, 2004.

[70] Yong-Yeon Keum, Hsiang-nan Li, and A. I. Sanda. Fat penguins and imaginary penguins in perturbative QCD. *Phys. Lett.*, B504:6–14, 2001.

[71] G. P. Korchemsky and A. V. Radyushkin. Infrared factorization, wilson lines and the heavy quark limit. *Phys. Lett.*, B279:359–366, 1992.

[72] P. Krokovnz et al. Observation of anti-B0 $\rightarrow$ D0 anti-K0 and anti-B0 $\rightarrow$ D0 anti-K*0 decays. *Phys. Rev. Lett.*, 90:141802, 2003.

[73] Peter Kroll and Kornelija Passek-Kumericki. The two-gluon components of the eta and eta' mesons to leading-twist accuracy. *Phys. Rev.*, D67:054017, 2003.

[74] Bjorn O Lange. Soft-collinear factorization and sudakov resummation of heavy meson decay amplitudes with effective field theories. 2004.

[75] Bjorn O. Lange, Matthias Neubert, and Gil Paz. Theory of charmless inclusive B decays and the extraction of V(ub). 2005.

[76] Keith S. M. Lee and Iain W. Stewart. Factorization for power corrections to B $\rightarrow$ X/s gamma and B $\rightarrow$ X/u l anti-nu. 2004.

[77] Adam K. Leibovich, Zoltan Ligeti, Iain W. Stewart, and Mark B. Wise. Semileptonic B decays to excited charmed mesons. *Phys. Rev.*, D57:308–330, 1998.

[78] Adam K. Leibovich, Zoltan Ligeti, Iain W. Stewart, and Mark B. Wise. Predictions for nonleptonic Lambda/b and Theta/b decays. *Phys. Lett.*, B586:337–344, 2004.

[79] Adam K. Leibovich, Zoltan Ligeti, and Mark B. Wise. Comment on quark masses in scet. *Phys. Lett.*, B564:231–234, 2003.

[80] G. Peter Lepage and Stanley J. Brodsky. Exclusive processes in perturbative quantum chromodynamics. *Phys. Rev.*, D22:2157, 1980.

[81] H. Leutwyler. On the 1/N-expansion in chiral perturbation theory. *Nucl. Phys. Proc. Suppl.*, 64:223–231, 1998.

[82] Hsiang-nan Li. QCD aspects of exclusive b meson decays. *Czech. J. Phys.*, 53:657–666, 2003.

[83] Zoltan Ligeti, Michael E. Luke, and Mark B. Wise. Comment on studying the corrections to factorization in B - -¿ D(*) X. *Phys. Lett.*, B507:142–146, 2001.

[84] Cai-Dian Lu. Study of color suppressed modes B0 → anti-D(*)0 eta('). *Phys. Rev.*, D68:097502, 2003.

[85] Cai-Dian Lu and Kazumasa Ukai. Branching ratios of B → D/s K decays in perturbative QCD approach. ((U)). *Eur. Phys. J.*, C28:305–312, 2003.

[86] Michael E. Luke, Aneesh V. Manohar, and Ira Z. Rothstein. Renormalization group scaling in nonrelativistic QCD. *Phys. Rev.*, D61:074025, 2000.

[87] Michael E. Luke and Martin J. Savage. Power counting in dimensionally regularized nrQCD. *Phys. Rev.*, D57:413–423, 1998.

[88] Aneesh V. Manohar. The hqet/nrQCD lagrangian to order alpha/m**3. *Phys. Rev.*, D56:230–237, 1997.

[89] Aneesh V. Manohar. Deep inelastic scattering as x → 1 using soft-collinear effective theory. *Phys. Rev.*, D68:114019, 2003.

[90] Aneesh V. Manohar, Thomas Mehen, Dan Pirjol, and Iain W. Stewart. Reparameterization invariance for collinear operators. *Phys. Lett.*, B539:59–66, 2002.

[91] Aneesh V. Manohar and Mark B. Wise. Heavy quark physics. *Camb. Monogr. Part. Phys. Nucl. Phys. Cosmol.*, 10:1–191, 2000.

[92] Aneesh V. Manohar and Mark B. Wise. Heavy quark physics. *Camb. Monogr. Part. Phys. Nucl. Phys. Cosmol.*, 10:1–191, 2000.

[93] Sonny Mantry, Dan Pirjol, and Iain W. Stewart. Strong phases and factorization for color suppressed decays. *Phys. Rev.*, D68:114009, 2003.

[94] Sonny Mantry, Dan Pirjol, and Iain W. Stewart. Strong phases and factorization for color suppressed decays. *Phys. Rev.*, D68:114009, 2003.

[95] M. Neubert. Theoretical analysis of anti-B $\to$ D** pi decays. *Phys. Lett.*, B418:173–180, 1998.

[96] Matthias Neubert and Alexey A. Petrov. Comments on color suppressed hadronic B decays. *Phys. Lett.*, B519:50–56, 2001.

[97] Matthias Neubert and Berthold Stech. Non-leptonic weak decays of B mesons. *Adv. Ser. Direct. High Energy Phys.*, 15:294–344, 1998.

[98] Michael E. Peskin and D. V. Schroeder. An introduction to quantum field theory. Reading, USA: Addison-Wesley (1995) 842 p.

[99] A. Pineda and J. Soto. Effective field theory for ultrasoft momenta in nrQCD and nrqed. *Nucl. Phys. Proc. Suppl.*, 64:428–432, 1998.

[100] Dan Pirjol and Iain W. Stewart. A complete basis for power suppressed collinear-ultrasoft operators. *Phys. Rev.*, D67:094005, 2003.

[101] H. David Politzer and Mark B. Wise. Perturbative corrections to factorization in anti-B decay. *Phys. Lett.*, B257:399–402, 1991.

[102] Ira Z. Rothstein. Tasi lectures on effective field theories. 2003.

[103] A. Satpathy et al. Study of anti-B0 $\rightarrow$ D(*)0 pi+ pi- decays. *Phys. Lett.*, B553:159–166, 2003.

[104] Martin J. Savage and Mark B. Wise. SU(3) PREDICTIONS FOR NONLEPTONIC B MESON DECAYS. *Phys. Rev.*, D39:3346, 1989.

[105] Nita Sinha. Determining gamma using B $\rightarrow$ D** K. *Phys. Rev.*, D70:097501, 2004.

[106] Torbjorn Sjostrand. High-energy physics event generation with pythia 5.7 and jetset 7.4. *Comput. Phys. Commun.*, 82:74–90, 1994.

[107] Scott Willenbrock. Symmetries of the standard model. 2004.

[108] M. Wirbel, B. Stech, and Manfred Bauer. Exclusive semileptonic decays of heavy mesons. *Z. Phys.*, C29:637, 1985.

[109] Zhi-zhong Xing. Determining the factorization parameter and strong phase differences in B $\rightarrow$ D(*) pi decays. *High Energy Phys. Nucl. Phys.*, 26:100–103, 2002.

[110] Zhi-zhong Xing. Final-state rescattering and SU(3) symmetry breaking in B $\rightarrow$ D K and B $\rightarrow$ D K* decays. *Eur. Phys. J.*, C28:63–69, 2003.